UNIVERSITÀ DEGLI STUDI DI CAMERINO

School of Advanced Studies

Doctoral Course in

Chemical and Pharmaceutical Sciences and Biotechnology – Pharmaceutical Sciences

Cycle XXXI

Searching for effective natural products against Human African Trypanosomiasis (HAT) with special reference to African natural resources

PhD Candidate

Stephane Landry Ngahang Kamte

Supervisors

Prof. Riccardo Petrelli

Prof.ssa Loredana Cappellacci

Coordinator

Prof. Sauro Vittori

2015-2018

Table of contents

LIST OF PUBLICATIONS

This thesis is based on the following publications, which are appropriately adapted in every Chapter:

1. Orsomando, G., Agostinelli, S., Bramucci, M., Cappellacci, L., Damiano, S., Lupidi, G., Maggi, F., **Ngahang Kamte, S.L.**, Biapa Nya, P.C., Papa, F., Petrelli, D., Quassinti, L., Sorci, L., Vitali, L.A., Petrelli, R. (**2016**). Mexican sunflower (*Tithonia diversifolia*, Asteraceae) volatile oil as a selective inhibitor of Staphylococcus aureus nicotinate mononucleotide adenylyltransferase (NadD) *Ind*.*Crop*.*Prod*. *85*, 181-189.

2. Petrelli, R., Ranjbarian, F., Dall'Acqua, S., Papa, F. Iannarelli, R., **Ngahang Kamte, S.L.**, Vittori, S., Benelli, G., Maggi, F., Hofer, A., Cappellacci, L. (**2017**). An overlooked orticultural crop, *Smyrnium olusatrum*, as a potential source of compounds effective against African trypanosomiasis. *Parasitol*. *Int*. *66*, 146-151.

3. **Ngahang Kamte, S.L.**, Ranjbarian, F., Campagnaro, G.D., Biapa Nya, P.C. Mbuntcha, H., Woguem,V., Womeni, H.M., Azefack Tapondjou, L., Giordani, C., Barboni, L., Benelli, G., Cappellacci, L., Hofer, A., Petrelli, R., Maggi, F. (**2017**). *Trypanosoma brucei* inhibition by essential oils from medicinal and aromatic plants traditionally used in Cameroon (Azadirachta indica, Aframomum melegueta, Aframomum daniellii, Clausena anisata, Dichrostachys cinerea and Echinops giganteus). *Int*. *J*. *Environ*. *Res*. *Public Health 74*, 1-16.

4. Sut, S., Dall'Acqua, S., Baldan, V., **Ngahang Kamte, S.L.**, Ranjbarian, F., Biapa Nya, P.C., Vittori, S., Benelli, G., Maggi, F., Cappellacci, L., Hofer, A., Petrelli, R. (**2018**). Identification of tagitinin C from Tithonia diversifolia as antitrypanosomal compound using bioactive-guided fractionation. *Fitoterapia 124*, 145-151.

5. Pavela, R., Dall'Acqua, S., Sut, S., Baldan, V. **Ngahang Kamte, S.L.**, Biapa Nya, P.C., Cappellacci, L., Petrelli, R., Nicoletti, M., Canale, A., Maggi, F., Benelli, G. (**2018**). Oviposition inhibitory activity of the Mexican sunflower Tithonia diversifolia (Asteraceae) polar extracts against the two-spotted spider mite Tetranychus urticae (Tetranychidae). *Physiol*. *Mol*. *Plant Pathol*. *101*, 85-92.

6. **Ngahang Kamte, S.L.**, Ranjbarianb, F., Cianfaglione, K., Sut, S., Bruno, M., Afshar, F.H., Iannarelli, R., Benelli, G., Cappellacci, L., Hofer, A., Maggi, F., Petrelli, R. (**2018**). Identification of highly effective antitrypanosomal compounds in essential oils from the Apiaceae family. *Ecotoxicol*. *Environ*. *Saf*. *156*, 154-165.

Comments on contribution

1. Collected the plant material and performed the hydrodistillation. Conducted test for antitrypanosomal activity.

2. Collected the plant material, performed the hydrodistillation and the chemical and gas-chromatography analysis. Conducted test for antitrypanosomal activity.

3. Collected the plant material and performed the hydrodistillation. Took part in all data analysis and was one of the main contributors to writing the manuscript.

4. Collected the plant material and performed the fractionation of the extracts. Performed and analysed all of the IC_{50} determinations on *T. brucei* and mammalian cells.

5. Collected the plant material and performed the preparation of the crude extracts and the isolation of sesquiterpene lactones. Contributed to writing the manuscript.

6. Collected part of the plant material and performed the hydrodistillation and chemical analysis of essential oils. Performed and analysed all of the IC_{50} determinations on *T. brucei* and mammalian cells. Contributed to writing the manuscript.

Publications not included in the thesis

1. Pavela, R., Maggi, F., **Ngahang Kamte, S.L.,** Rakotosaona, R., Rasoanaivo P., Nicoletti, M., Canale, A., Benelli, G. (**2017**). Chemical composition of Cinnamosma madagascariensis (Cannelaceae) essential oil and its larvicidal potential against the filariasis vector Culex quinquefasciatus Say. *S. Afr. J. Bot. 108*, 359-363.

2. Benelli, G., Pavela, R., Lupidi, G., Nabissi, M. Petrelli, R., **Ngahang Kamte, S.L.,** Cappellacci, L., Fiorini, D., Sut, S., Dall'Acqua, S., Maggi, F. (**2018**). The crop-residue of fiber hemp *cv* Futura 75: from a waste product to a source of botanical insecticides against Culex quinquefasciatus, Spodoptera littoralis and Musca domestica. *Environ. Sci. Poll. Res. 25*, 1-11.

ABSTRACT

For centuries, African natives have been facing various infectious tropical illnesses, among which African trypanosomiases are some of the most frequent relevant parasitic diseases. African trypanosomiases, commonly called sleeping sickness in humans (HAT; Human African Trypanosomiasis) and Nagana in domestic livestock, affect a huge number of people living in poverty in 36 sub-Saharan countries, resulting in a key socioeconomic impact. After a century of outbreaks, due to political instability and lack of funding, around 70 million people and 50 million cattle are still at risk of exposure in Africa. Trypanosomiasis is transmitted by the bite of insects from the *Glossina* spp (Glossinidae) and is fatal in humans, if untreated. While taking a blood meal, infected *Glossina* flies can spread extracellular protozoans from the species *Trypanosoma brucei*. There are three morphologically indistinguishable subspecies of *T. brucei*. The subspecies *T. b. gambiense* is responsible for a chronic form of the human disease, while *T. b. rhodesiense* causes an acute form, which more rapidly leads to death. Both subspecies are infective to humans, whereas *T. b. brucei* is only infective to animals. During the early stage of the disease or hemolymphatic phase, the parasite is restricted to the blood and lymph and after months or years it invades the central nervous system resulting in various neurological symptoms including sleeping disturbance. As for other neglected tropical diseases, the chemotherapeutical arsenal against HAT is based on limited, expensive and often toxic medicines that are administered parentally in a context of poverty and lack of qualified personnell in healthcare centers. The few drugs that are available are pentamidine and suramin for the early stage disease and eflornithine (also in combination with nifurtimox) and melarsoprol for the late stage when the parasite infects the brain. Overall, the situation described above highlights the critical nature of this phenomena and the urgent need to explore new sources of potentially effective and safe compounds for therapy. In this scenario the naturally-occurring products may play a crucial role as source of bioactive drug candidates.

With this vision in mind, in **Chapter 2** I performed a complete phytochemical analysis on both polar and volatile compounds of *T. diversifolia* collected from a geographically isolated population living in Dschang, Cameroon and I assessed their biological activities (antitrypanosomal and amtimicrobial activities). The main secondary metabolites occurring in the *T. diversifolia* methanolic extract were isolated by column chromatography and structurally elucidated by MS and NMR techniques. Tagitinins C emerged as the most active compound against *T. brucei* (TC221) with an IC_{50} value of 0.0042 μg/mL. This activity was 4.5 times better than that of the reference drug suramin. Then I analysed the chemical composition and the antimicrobial effects of the essential oil (EO) hydrodistilled from inflorescences of *T. diversifolia*. Results showed that *T. diversifolia* EO was mostly active against *Staphylococcus aureus* and selectively inhibited *in vitro*

the NAD biosynthetic enzyme NadD from *S. aureus* (IC_{50} of ~60 μg/mL). Besides its extensive utilizations in the traditional medicine, the plant is believed to have a great potential in agriculture. For this reason, I decided to evaluate the *T. diversifolia* polar extracts against the two-spotted spider mite *Tetranychus urticae* (Tetranychidae), which is one of the most economically important arthropod pests worldwide. The ethyl acetate extract resulted as the most active oviposition inhibitor, with an ED_{50} value of 44.3 $\mu g.cm^{-3}$ and an ED_{90} of 121.5 $\mu g.cm^{-3}$.

In **Chapter 3**, I investigated a lipophilic extract of *Onosma visianii* roots containing 12% of shikonin derivatives. The phytochemical investigation of the lipophilic extract resulted in the isolation of 12 naphtoquinone derivatives which were evaluated against *Trypanosoma brucei*. Isobutylshikonin and isovalerylshikonin emerged as the most active naphtoquinone derivatives, showing an IC_{50} of 3.3 and 2.7 μg/mL, respectively. Furthermore, isovalerylshikonin provided an inhibition of *Glossina palpalis* acetylcholinesterase (*gp*AChE) (IC_{50} = 7.1 μg/mL), stronger than isobutyrylshikonin (IC_{50} = 91.3 μg/mL), with a significant tse-tse fly *versus* human selectivity (SI = 7.2).

In **Chapter 4**, I oriented my attention to the Apiaceae family, which is a class of aromatic plants rich of EOs. Four out of nine Apiaceae EOs resulted active against *T. brucei* showing an IC_{50} in the range 2.7-10.7 μg/mL. Terpinolene, one the major isolated component of these oils, was particularly active with an IC_{50} value of 0.035 μg/mL (0.26 μM) and a selectivity index (SI) of 180.

As part of the extended family of naturally-occurring products, sesquiterpenes hold promising inhibitory effects against the bloodstream forms of *T. brucei*. For this reason, in **Chapter 5**, I decided to explore the potential of *Smyrnium olusatrum* EOs obtained and its main oxygenated sesquiterpenes, namely germacrone, isofuranodiene, and β-acetoxyfuranoeudesm-4(15)-ene, as potential inhibitors of *T. brucei*. The EOs obtained efficiently inhibited the growth of parasite with IC_{50} ranging from 1.9 to 4.0 μg/mL. Among the isolated main EOs components, isofuranodiene exhibited a significant and selective inhibitory activity against *T. brucei* (IC_{50} = 0.6 μg/mL, SI = 30).

In **Chapter 6**, I finally selected six medicinal and aromatic plants traditionally used in Cameroon to treat several disorders, including infections and parasitic diseases. Then I evaluated the activity of their EOs against *T. brucei* TC221 and their selectivity against Balb/3T3 cells, used as counter-screen for cytotoxicity. The most relevant outcomes showed that the EOs from *A. indica, A. daniellii* and *E. giganteus* were the most active ones, with IC_{50} values of 15.21, 7.65 and 10.50 μg/mL, respectively.

Overall, the results of my PhD thesis provided new insights into the potential of naturally-occurring compounds as valuable sources for the development of innovative trypanocidal drugs or botanical insecticides.

CHAPTER 1.

Searching for effective natural products against Human African Trypanosomiasis (HAT) with special reference to African natural resources

"*The forest not only hides man's enemies*

but it is full of man's medicine,

healing power and food."

African proverb

Chapter 1 Outline

Abbreviation

BBB = Blood brain barrier

CATT = Card agglutination trypanosomiasis test

CNS = Central nervous system

CPDD = Consortium for parasitic drug developement

CSF = Cerebrospinal fluid

CTC = Capillary tube centrifugation

DFMO = DL-α-difluoromethylornithine

DMC = Dichloretamethane

DNDi = Drug for neglected disease initiative

ES = Ectoperitrophic space

GAPDH = Glyceraldeyde-3-phosphate dehydrogenase

gHAT = Gambiense human african trypanosomiasis

HAT = Human african trypanosomiasis

L6 cells = Rat skeletal myoblast cells

MAECT = Mini anion exchange centrifugation

MIC = Minimum inhibitory concentration

MRC-S =

NECT = Nifurtimox eflornithine combination therapy

ODC = Ornithine decarboxylase

OAU = Organisation of African Unity

PATTEC = Pan African tsetse and trypanosomiasis eradication campaign

PF = Procyclic form

PM = Peritropic matrix

QBC = Quantitative buffy coat

RDT = Rapid diagnostic tests

rHAT = Rhodiesiense human african trypanosomiasis

TPP = Target product profile

VSG = Variant surface glycoproteins

1.1 Epidemiology of Human African Trypanosomiasis (HAT)

The protozoal parasite trypanosomes are grouped in the order "kinetoplastida" because of the presence of a kinetoplast. The genus *Trypanosoma* is divided in two main groups based on the mode of transmission by their insect vectors: Stercoraria and Salivaria (Figure 1). The infection to the vertebrate of Stercoraria parasites is *via* feces. The causative agent of Chagas' disease, *Trypanosoma cruzi*, is a representative example of this group. On the other hand, in the Salivarian parasites the infection of the vertebrate occurs *via* saliva when the vector bites the host's skin.

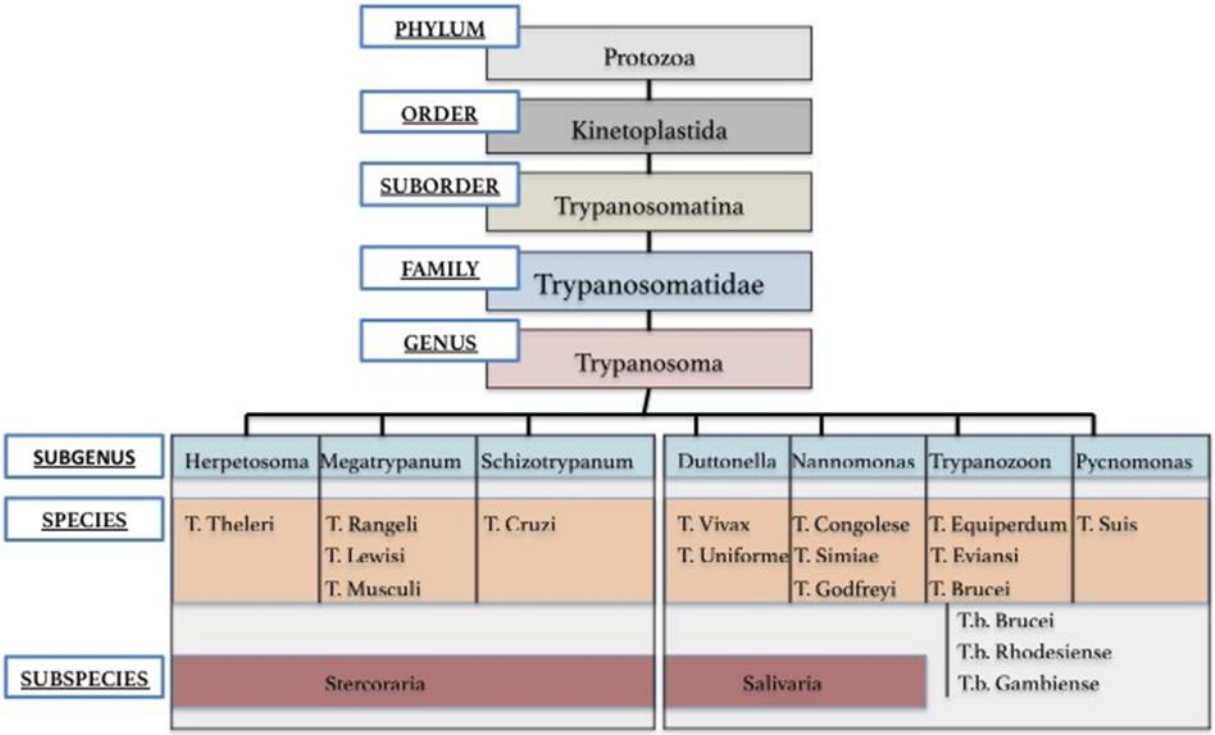

Fig. 1. Classification of trypanosomes.

Human African Trypanosomiasis (HAT) also known as sleeping sickness is a vector borne neglected tropical disease caused by two parasites from the genus *Trypanosoma* and the specie *T. brucei* namely *Trypanosoma brucei gambiense* (*T.b. gambiense*) and *Trypanosoma brucei rhodesiense* (*T.b. rhodesiense*). *T.b. gambiense* is considered the slow-progressing form and is endemic in western and central Africa, whereas *T.b. rhodesiense* is the faster progressing form found in eastern and southern Africa (Simarro *et al*., 2010). Both forms are classically transmitted by the bite of blood-sucking vector tsetse flies (Diptera, genus Glossina). *T.b. gambiense* can also be transmitted by other routes which are poorly documented, one of them is congenitally (Lestrade-Carluer De Kyvon, 2016).

T.b. *gambiense* is also called Gambian HAT (Figure 2) and it is considered a chronic illness that can take years or decades before fatality (Checchi *et al*., 2008). It is an anthroponotic disease with a minor incidence for animals (livestock and wildlife) and it is responsible for 98% of HAT cases reported in the last few decade (Franco *et al*., 2014).

T.b. *rhodesiense*, also called Rhodesian HAT (Figure 2), is an acute zoonotic disease, causing death within weeks or months upon infection, mainly affecting livestock and game animals (Odiit *et al*., 1997). Humans represent the main reservoir host for *T.b*. *gambiense*, whereas domestic cattle and wild animals are considered the main animal reservoir of *T.b*. *rhodesiense*.

Animal African Trypanosomiasis (AAT, also called Nagana, from the Zulu word 'N'gana' which means 'powerless/useless'), is caused by trypanosome species *T*. *vivax*, *T*. *congolense*, and *T*. *brucei brucei*. Nagana is widespread in sub-Saharan Africa and it is cyclically transmitted by the same vector responsible of human-infective trypanosomes, the tsetse fly. Trypanosomes can be also transmitted mechanically when the flies begin a blood meal on an infected host and they end it on another one. The time between the two meals is short enough to ensure the survival of parasites in the insect mouth. This distinctive feature (mechanical transmission) has allowed *T*. *vivax* to be spread outside the limits of the "African tsetse fly belt" and the parasite is now present in 13 South American countries where it is considered an emerging disease (especially on cattle farming). Unlike other trypanosomes, *T*. *vivax* completes its short life cycle in the insect proboscis and this is the reason why can also be transmitted mechanically (Moloo *et al*. 2000). Furthermore, among African trypanosomes, *T*. *vivax* is the most phylogenetically distinct species as shown in Figure 3.

Historically, the impact of AAT has been so deep, that it has influenced the migration routes of cattle-owning tribes that avoided the "tsetse fly belt" (Figure 4), as well as the movements of early European and Arab colonizers who depended on horses and oxen in Africa.

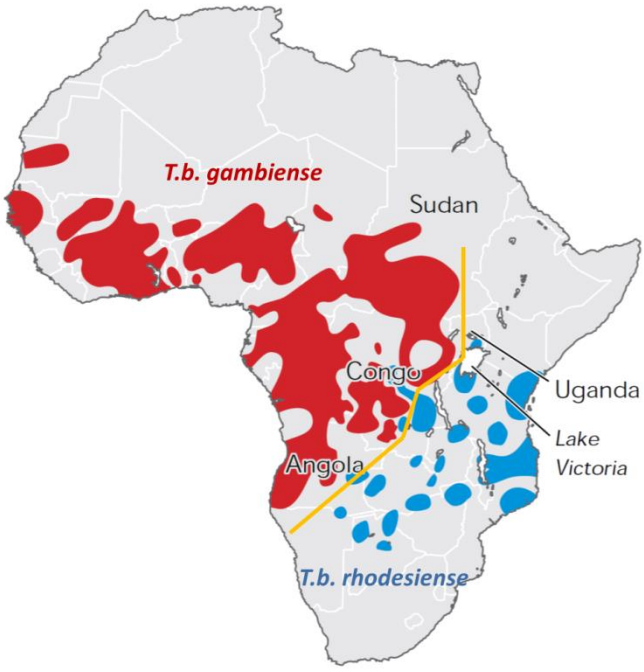

Fig. 2. Distribution of the main foci of the two forms of HAT in sub-Saharan Africa with incidences and risk for travelers. The yellow line divides the areas in which *T.b. gambiense* prevails and those in which *T.b. rhodesiense* predominates.

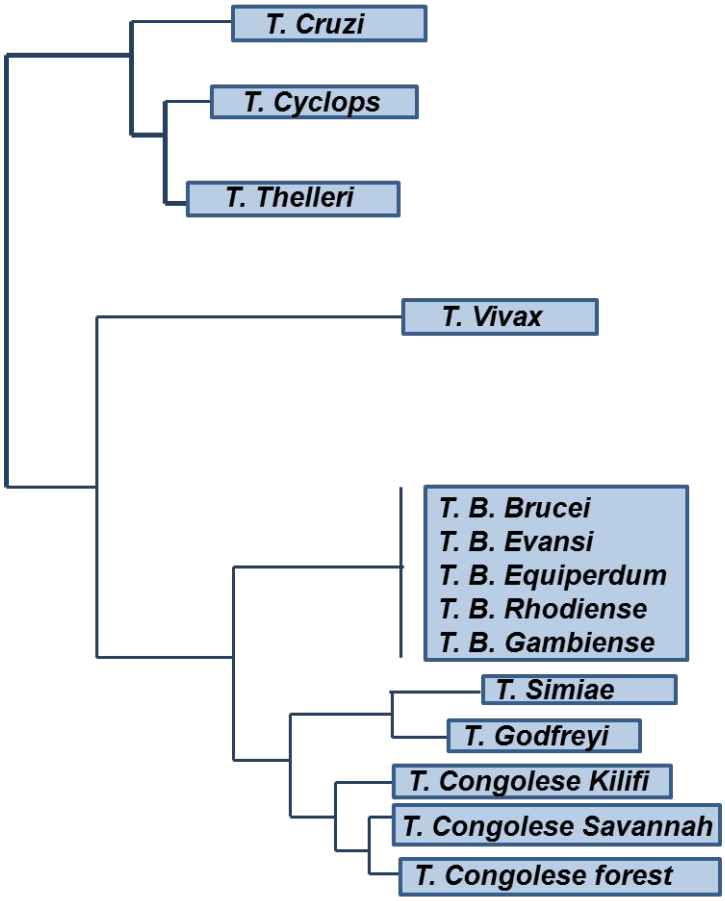

Fig. 3. Phylogenetic tree based on SSU rRNA sequences from trypanosome species. Adapted from (Cortez *et al*. 2006).

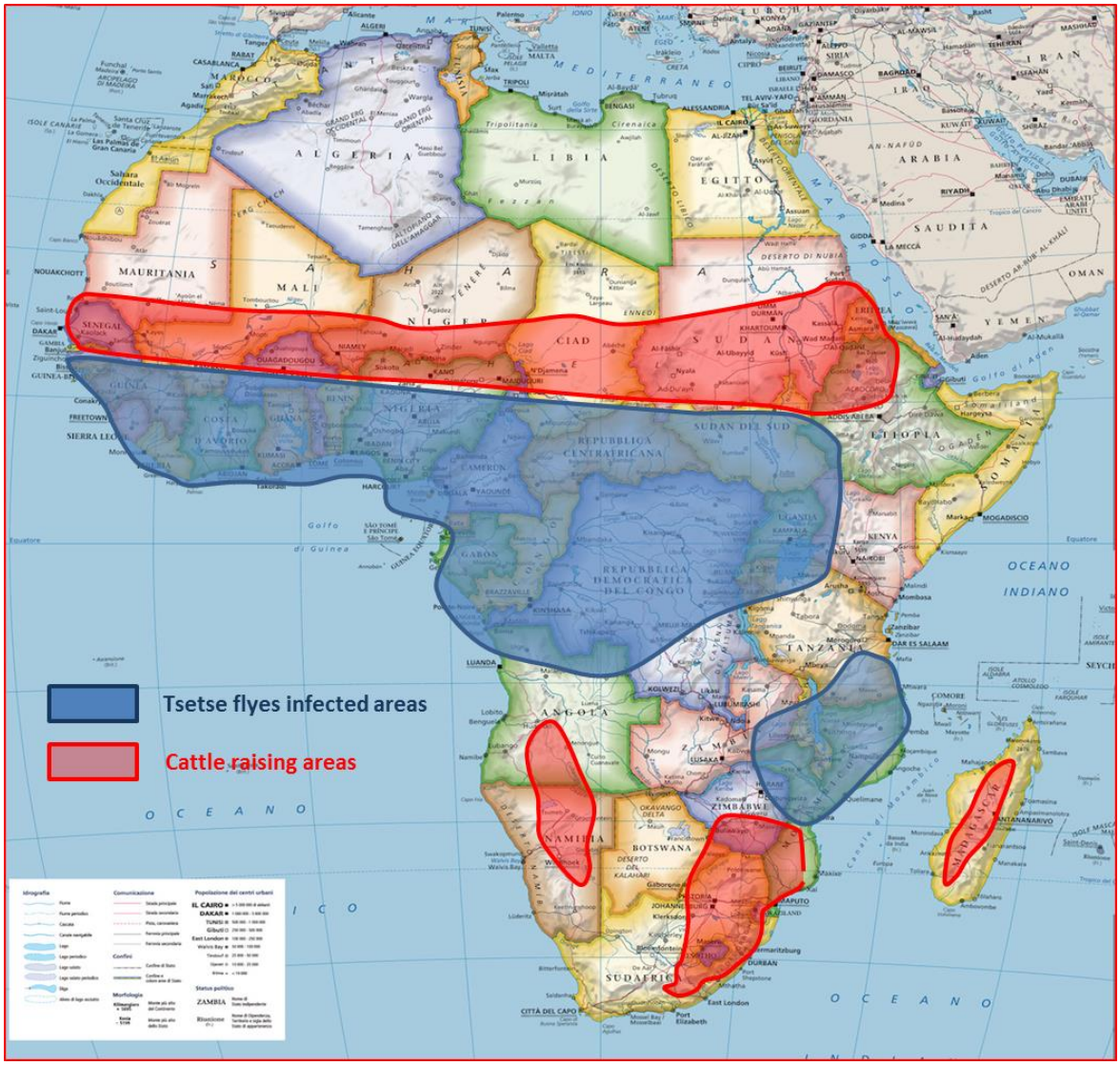

Fig. 4. The "flies belt" : distribution of tsetse and cattle raising area in Africa.

According to WHO reports (WHO 2013), if we take into the accounts the Disability Adjusted Life Year (DALY) guidance (i.e., loss of healthy life, premature mortality and disability) HAT can be considered the third most important contributor to the global burden of the parasitic diseases after schistosomiasis and malaria. The distribution of the disease overlaps with the presence of the vector. It occurs in 36 sub-Saharan countries (where is endemic) on an area of 1,55 million Km^2 between 14°N and 20°S latitude (Simarro *et al*., 2012) (Figure 5). The disease is mostly present in rural area with suitable environment for tsetse flies development. It is estimated that 69 million persons are at risk of HAT (of which 57 million are exposed to *T.b*. *gambiense*) as well as 50 million head of cattle (Keating *et al*., 2015; WHO 2013) (Figure 6). In 2015, WHO reported 2733 cases due to *T.b*. *gambiense* mostly in western and central Africa. Although the infection is present in 24 countries, the highest number of cases was found in democratic republic of Congo (86%), central African republic and Chad (5% and 2%, respectively). On the same year, only 71

cases were caused by *T.b. rhodesiense* mostly in eastern and southern Africa with Malawi and Uganda hosting more than 80% of the cases (Büscher *et al*., 2017). Thanks to the public private partnership established in 2000, the number of cases was reduced by 73% in little more than a decade reversing the epidemiological trend (WHO 2013). The prevalence of the disease is higher in the adult population and there is a relationship with the type of activity. For example fishermen which are in close contact with the vector appeared to be more prone to infection (Büscher *et al*., 2017). Cases are detected either by a passive case detection in which the patients report themselves to the healthcare services or by active screening carried by health professionals in remote areas with mobile teams.

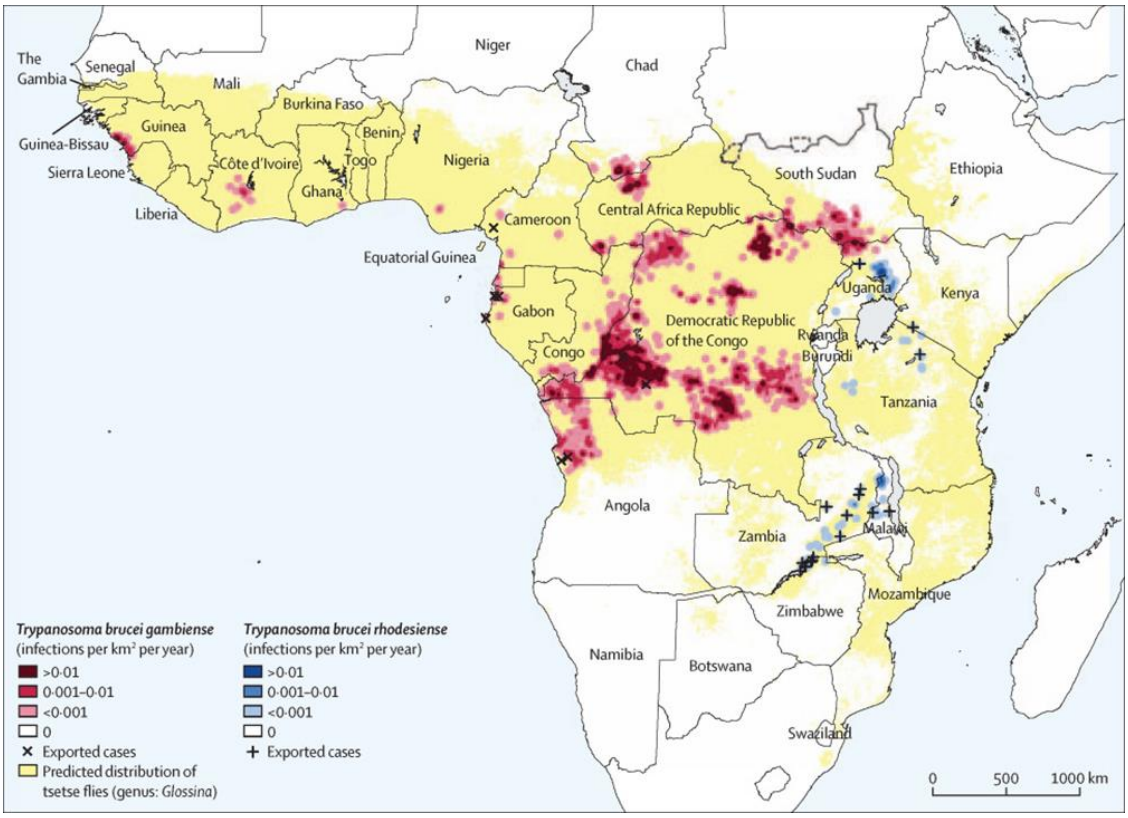

Fig. 5. Geographic distribution of HAT cases reported in the period 2010–2014 (Büscher *et al*., 2017).

According to WHO reports, the number of HAT cases reported globally decreased from 37,991 in 1998 to 7216 cases in 2012 (five folds). Encouraged by this important decrease linked to the intensified control efforts, HAT has been included in the WHO NTD roadmap, a program targeted for elimination of HAT as a public health problem by the year 2020 and zero transmission by the year 2030 (WHO 2013) (Figure 7). The successes of this ambitious approach will rely on commitment of both international players and the national control programs of endemic countries. However, active case detection through mass community screening and related trends should be

interpreted carefully, as the number of cases are strictly related to the intensity and the quality of screening efforts.

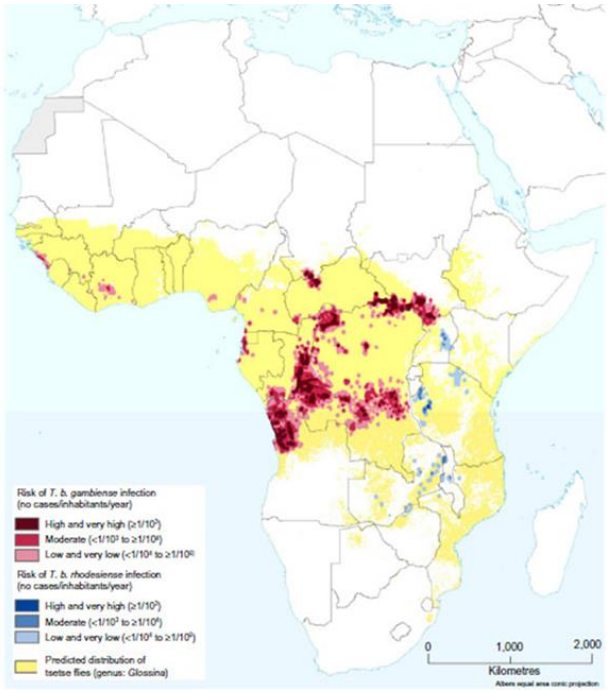

Fig. 6. Persons at risk for HAT (Simarro *et al*. 2012).

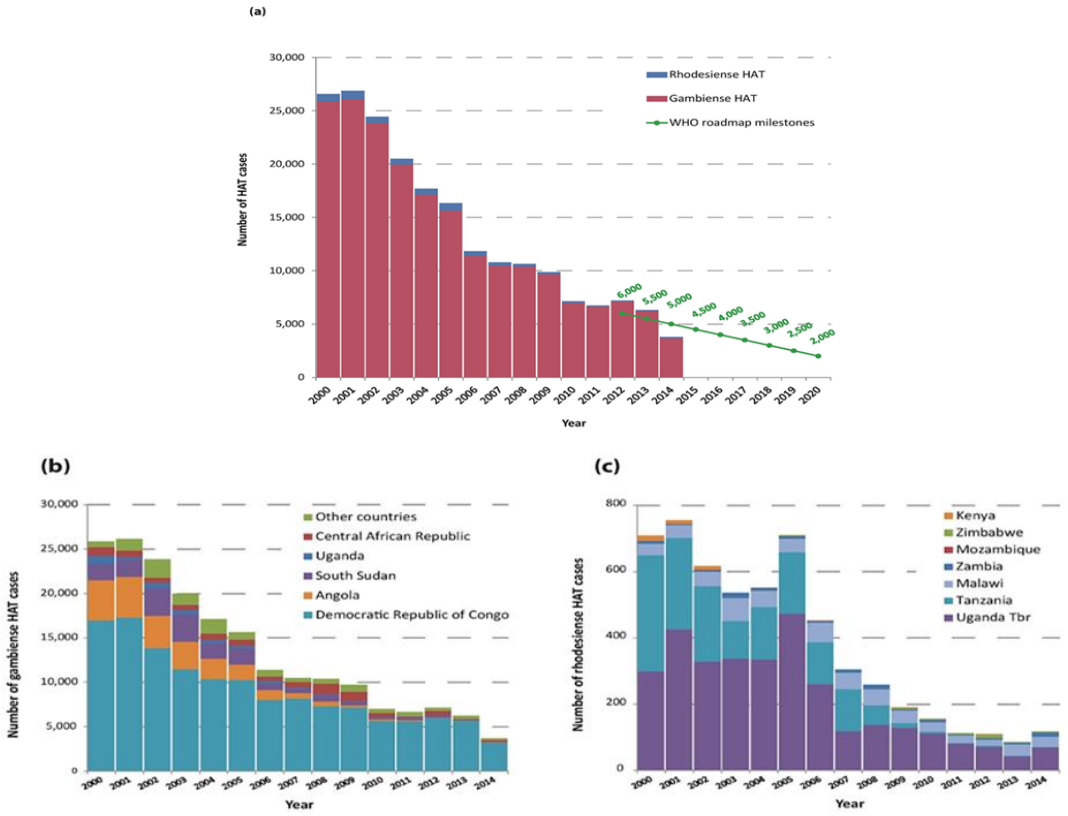

Fig. 7. (a) Total number of reported cases of HAT (*gambiense* and *rhodesiense*) per year. The green line shows the milestones set in WHO Roadmap for HAT elimination (b) Number of reported cases of *gambiense* HAT per year and per country. (c) Number of reported cases of *rhodesiense* HAT per year and per country.

1.1.1 Economic burden and public health impact in Africa

According to the Global Burden of Disease the estimates of "years lived with disability" (YLDs) for HAT, range from 2,000 to 25,000 per year (Sutherland *et al*., 2015). However, the decreasing trend in HAT case numbers is reflected in the recent Global Burden of Disease estimates. In 2010 the HAT-related burden was estimated to cause a loss of 560,000 DALYs per year, with a 72.5 % reduction from the 1990 DALY estimate (Murray 2012). Although the global HAT elimination appears to be on track, sleeping sickness remains a major public health problem in rural poor communities. For example, in the Democratic Republic of Congo (DRC), one of the most affected country, the number of years of life lost (YLL) per death caused by HAT was estimated at 27 years (Lutumba *et al*. 2007).

A recent study showed that HAT resulted in exorbitant indirect health care costs (ranging from US$ 60–170) for people already living on less than US$1 per day (Bukachi *et al*., 2017). Morbidity from HAT temporarily removes adults from their regular employment, causing shifting of their household roles. This phenomena negatively impact on children which are forced to be absent from school to provide household work. In addition, the socio-economic effects of HAT are exacerbated by coping strategies with negative consequences on people. For this reason, continuous sensitization about HAT risks at all the community levels is critical in making progress towards the goal of HAT elimination by 2020.

1.2 Historical perspective on African Trypanosomiasis: the journey so far

The economic and cultural development of sub-Saharan African has been severely repressed by African trypanosomiasis. Different parameters including climate, environmental and socio-economic changes have influenced the spread of the disease through history. History has also demonstrated that African trypanosomiasis prevented the introduction of stock farming in endemic areas and the problem is still present today. A consequence of this is that much of sub-Saharan Africa has not been converted yet into grassland for cattle breeding, since the disease can be controlled but can't be completely eradicated. The disease affecting cattle, Nagana, has been recognized since antiquity and interestingly, humans are resistant to these species of trypanosomes such as *T. congolense*, *T.vivax*, and *T. brucei brucei*. The trypanosome lytic factors circulating in human blood, which brings attention to the long evolution of humans in the presence of these parasites in Africa, are responsible of this resistance. On the other hand, HAT is a relatively recent event in human evolution and the infectivity of *T. brucei rhodesiense* to humans is due to a serum-resistance associated (SRA) gene. After this event, the mutate gene has been spread through sub-Saharian Africa by genetic exchange (Gibson, 2005).

This chapter examines the contribution of these parameters to our understanding of the epidemiology and history of human sleeping sickness in sub-Saharan Africa.

1.2.1 Prehistory

Phylogenetic reconstruction research suggests that Salivarian trypanosomes emerged 300 million years ago and then probably became a gut parasite of some early insects (Haag *et al*., 1998). The bloodsucking insect tsetse fly emerged 35 million years ago and transmitted the trypanosome to mammals, which evolved 180 million years ago.

The long coexistence of both tsetse flies and wild animals may explain why most African wildlife species are tolerant of trypanosomiasis. In contrast, domestic animals have yet been incapable to develop tolerance or resistance to trypanosome infections.

Around 1.8. million years ago, concomitantly with serious climate changes, the hominids moved from the rainforest to the savannah (open plains of East Africa) and came into close contact with large game animals and trypanosome-carrying tsetse flies. At the first time the serum sensitivity of *T.b. brucei* protected them from infection. As soon as they became big-game hunters and they increased their exposure to tsetse flies, the *T.b. brucei* mutated and lost its serum sensitivity allowing the new *T.b. rhodesiense* to survive in humans.

1.2.2 Antiquity

As shown in Figure 8, a four thousand years old veterinary papyrus describes a disease similar to nagana (animal trypanosomiasis) infecting cattle in ancient Egypt (Steverding *et al*., 2008). It is also reported that an ointment made from the fat of particular birds was used as treatment against the bite of flies. This suggests the presence of sleeping sickness in that region meanwhile in the sub-Saharan region, the spread of trypanosomiasis was unintentionally slowed as the border of the villages were cleared from vegetation as a protection from foreign invasion and as adjustment of the stream course of the Nile River. This gradual eradication of the tsetse fly allowed the ancient Egyptians to raise pure breeds of zebu cattle. However, the failure in horse breeding, introduced in Egypt after the 16th century BC, may be also due to trypanosome infections.

Fig. 8. A section of a damaged veterinary papyrus about a cattle disease from the 2nd millennium BC. The papyrus explains the different symptoms of the animal trypanosomiasis called ushau.

1.2.3 Middle Ages

There are only a few reports on the occurrence of trypanosomiasis in Africa during the Middle Ages and most of them are from the Arabs. For trade purposes, the Arabs made relations with West African kingdoms like Benin, Mali, Ghana and Songhai.

The first case of sleeping sickness report comes from the Arabian geographer Abu Abdallah Yakut, who describes a devastating outbreak in Sudan (at the turn of the 12th century). Then, the famous Arabian writer Ibn Khaldun (around 1373) describes the death of the emperor of Mali, King

Mari Jata, who died of an illness which corresponds to the description of human trypanosomiasis. Both are considered as the first written reports on sleeping sickness (Steverding *et al*., 2008).

1.2.4 Modern Times

In early Modern Times, the history of HAT is closely linked to the slave trade and the first accounts of sleeping sickness came from ship doctors and slave-trade companies. Since HAT caused increasing losses in slaves, slave-traders pushed their ship doctor to investigate this disease. In 1734, John Aktins published the first accurate medical report on HAT, describing only the neurological symptoms of the late stage of the disease (Cox, 2004). Although in the 19th century HAT became a well-accepted disease, no one had any clue about the nature of the illness (Bruce, 1895). It was the Scottish explorer David Livingston, in 1852, who first suggested that "Nagana" is caused by the bite of tsetse flies. However, it took another 50 years until trypanosomes were identified as the causative agents of Nagana and sleeping sickness, and in 1895 the microbiologist David Bruce discovered *T*. *brucei* as the factor for cattle trypanosomiasis (cattle Nagana).

Colonial authorities played an important role to give scientific evidence on the existence of the disease. Physicians were sent in the endemic areas to study the cause of swollen lymph nodes on the neck of some autochthones and the occurrence of neurological symptoms. These studies allowed making a relationship between the distribution of the tsetse fly and the cases of sleeping sickness. It is in 1901 that the British surgeon Robert Forde observed trypanosomes in human blood (Forde, 1902). The colony where it was observed (the Gambia) inspired the name of the species *Trypanosoma gambiense* (Dutton, 1902). In the meantime, the two other animal pathogenic trypanosome species *T*. *congolense* and *T*. *vivax* were discovered in 1904 and 1905 by Alphonse Broden (Broden, 1904) and Hans Ziemann (Ziemann, 1905), respectively. Subsequently, the second human pathogenic trypanosome species, *T*. *rhodesiense* (now *T.b*. rhodesiense), was uncovered in 1910 by the two parasitologists John William Watson Stephens and Harold Benjamin Fantham (Stephens *et al*., 1910).

These discoveries opened the way for a better understanding of the pathology, the life cycle of the parasite and for the exploration of possible chemotherapy. In fact, after the huge wave of sleeping sickness epidemics that killed around half of million people in central and West Africa at the beginning of the last century, the arsenical drug atoxyl was developed and showed encouraging results on some patients (Johnston, 1908). The drug atoxyl was then found to be harmful to patients causing optic nerve atrophy.

In the 20th century, Africa have been plagued by three major sleeping sickness. The first epidemic at the turn of the 20th century, killed about 300 000−500 000 people in the Congo basin, Uganda, and Kenya. In 1916 a small team of chemists in collaboration with the pharmaceutical company Bayer developed the first effective drug (Bayern 205, later named suramin) for the treatment of sleeping sickness. Suramin is still in use in therapy for the treatment of the first phase of *T.b*. *rhodesiense* infections, alone or in combination with other drugs (Steverding *et al*., 2008).

A year earlier, the organo-arsenical tryparsamide was discovered and it was considered the first drug for the treatment of late-stage of HAT. Later on, a third drug, named pentamidine, was introduced into the market by the English chemist Ewins for the treatment of late-stage of HAT. Pentamidine is still regarded as the only effective drug for late stage *T.b*. *rhodesiense* sleeping sickness. The second major epidemic occurred between about 1920 and 1940, and as a consequences to these epidemics, severe control measures were introduced (e.g. fly traps, brush clearing, and game destruction).

Since the 1950s, several drugs have become available for chemotherapy of animal trypanosomiasis and these included: the phenanthridine derivatives homidium bromide (Ethidium®, Novidium®) and isometamidium chloride (Samorin®, Trypamidium®), the aminoquinaldine derivative quinapyramine (Anthrycid®) and the aromatic diamidine diminazene aceturate (Berenil®). Vector control and employment of chemotherapy, led to a drastic reduction in the incidence of sleeping sickness at the beginning of the 1960s.

The third major HAT epidemic occurred following the departure of colonial powers (exacerbated by the banning of DDT in the 1970s). By the mid of the 1960s, most of the trypanosomiasis-endemic countries became independent (decolonized) and experienced economic crisis and political instability with negative consequences on their health systems. After that, the control of trypanosomiasis was no longer a priority and specific screening programs were stopped. As result, by the mid of 1970s, there has been a substantial increase in the number of reported cases of sleeping sickness (Figure 9). This was the beginning of the third and most recent sleeping sickness epidemic in the 20th century, mainly affecting Congo, Angola, Sudan, and the West Nile district of Uganda. The scenario remained unchanged until eflornithine (DL-α-difluoromethylornithine, DFMO), a drug initially developed for the treatment of cancer by the Merrell Research Institute in Strasbourg (Meyeskens *et al*., 1999), was introduced into the clinic for the treatment of late stage *T.b*. *gambiense* HAT.

In 2001, a new initiative has been launched by the Organisation of African Unity (OAU) a new initiative, named Pan African Tsetse and Trypanosomiasis Eradication Campaign (PATTEC),

aimed to eliminate the tsetse fly from Africa. It has been proposed to use odour-baited traps, insecticide-treated targets and aerial spraying insecticides in order to eradicate the tsetse fly population. However, in contrast to the Zanzibar project (an island infested with only one tsetse fly species), the PATTEC campaign dealt with a vast expanse of untamed territory (sub-Saharan Africa is ~10 million km^2) populated by 7 different Glossina species accepted as vectors for transmission of sleeping sickness.

Since in the past a similar eradication campaign already failed, the scientific community was considerable skeptical about its feasibility, because the tsetse fly infested areas could not be isolated. Furthermore, the huge costs associated with the eradication projects were also matter of concern.

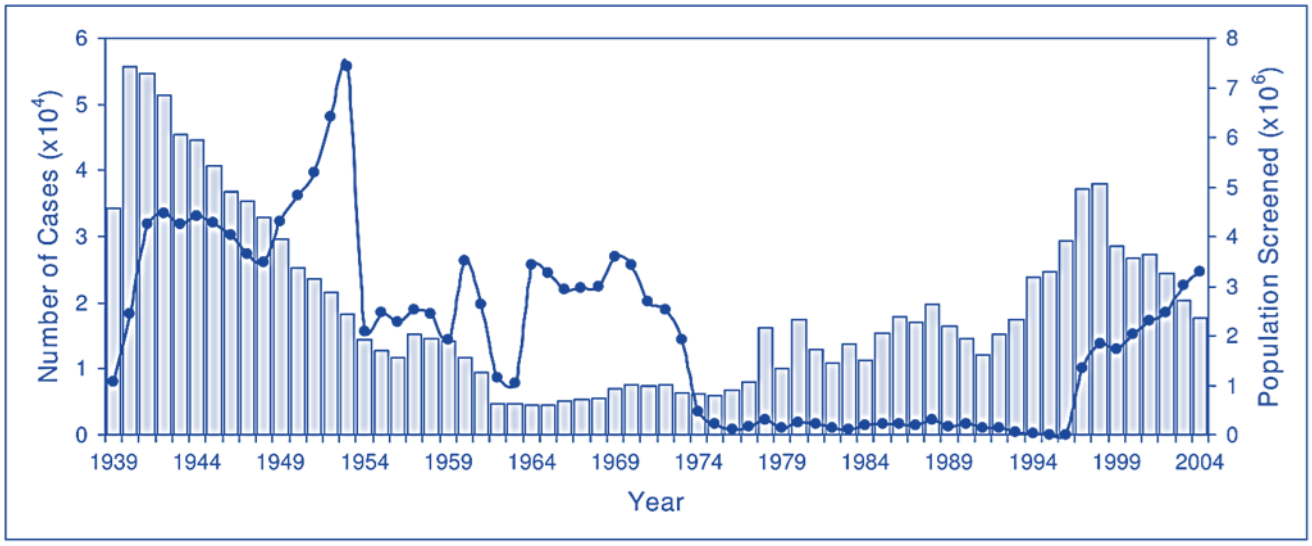

Fig. 9. Number of reported cases of sleeping sickness and population screened, 1939–2004. Light blue columns, number of reported cases; blue circles, population screened. Figure derived from (Steverding *et al*., 2008).

1.3 Biology

The Vector and Parasite Life Cycle

1.3.1 The Vector

The commonly called Tsetse fly belongs to the order of *Diptera* and based on its reproduction through adenotropic viviparity, tsetse fly is categorized as member of the superfamily *Hippoboscidea*, the family of *Glossinidae* and genus of *Glossina*. Tsetse fly includes 31 species classified in three species groups (or subgenera): *palpalis* group (Nemorhina), *morsitans* group (Glossina) and *fusca* group (Austenina) (Franco *et al*., 2014) (Figure 10). The 31 tsetse flies species can be also classified as forest, riverine, or savannah, based on their morphological differences and habitat preference (Cecchi *et al*., 2008).

Overall, the species of the *fusca* and the *palpalis* groups are mainly implicated in the transmission of *T.b. gambiense*, while species of the *morsitans* group are involved in the transmission of *T.b. rhodesiense* (Geiger *et al*., 2004). The most important species involved are *G. palpalis gambiensis*, *G. palpalis palpalis*, *G. fuscipes quanzensis*, *G. tachinoides*, *G. fuscipes fuscipes* and *G. fuscipes martini*. *G. fuscipes fuscipes* is considered the major vector of both forms of HAT in Uganda.

Fig. 10. The figure showed the principal vectors of HAT: *Glossina morsitans* on the left and *Glossina palpalis* on the right.

The insect is characterized by a recognizable proboscis, antenna with branched arista hairs and wings that fold and have a characteristic “hatchet” cell (Figure 11).

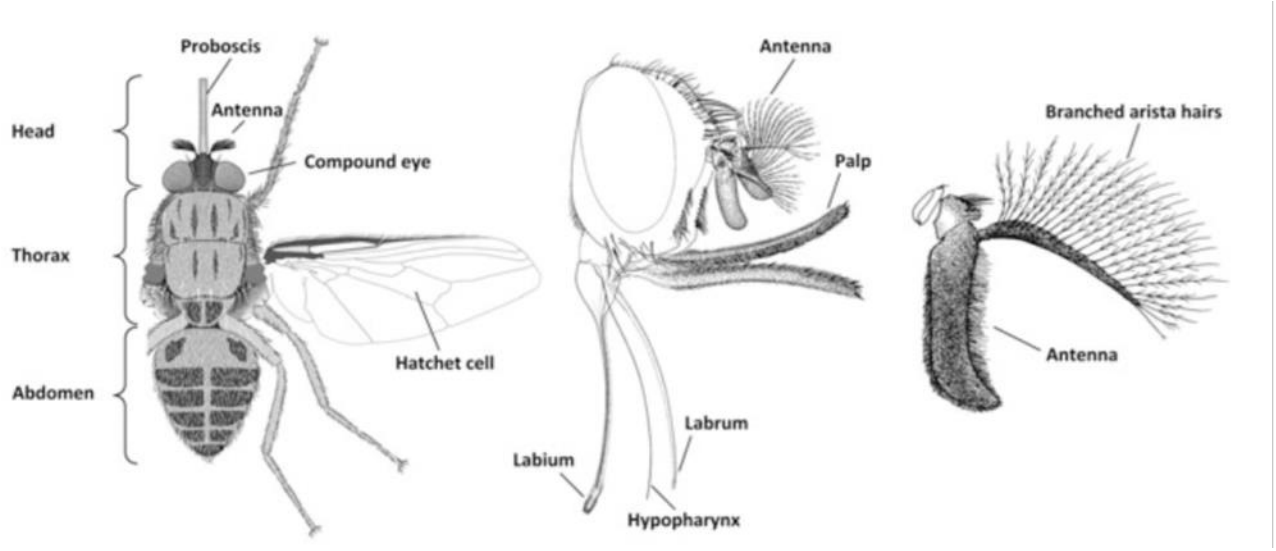

Fig. 11. Anatomy of the tsetse fly.

Tsetse flies of both sexes are hematophagous (blood-feeding) and can transmit trypanosomes, which relay on the insect for their cyclical transmission. The insects are viviparous and have a particular reproductive cycle. The female deposits a fully developed larva in humid soil instead of lays eggs (Figure 12). After 20-80 days the larva turns up as an adult. A female fly will only produce three to five such larvae during her 2-3 months lifespan (2 months for males) (Figure 13). Consequently, the growth rate of tsetse populations is fairly low.

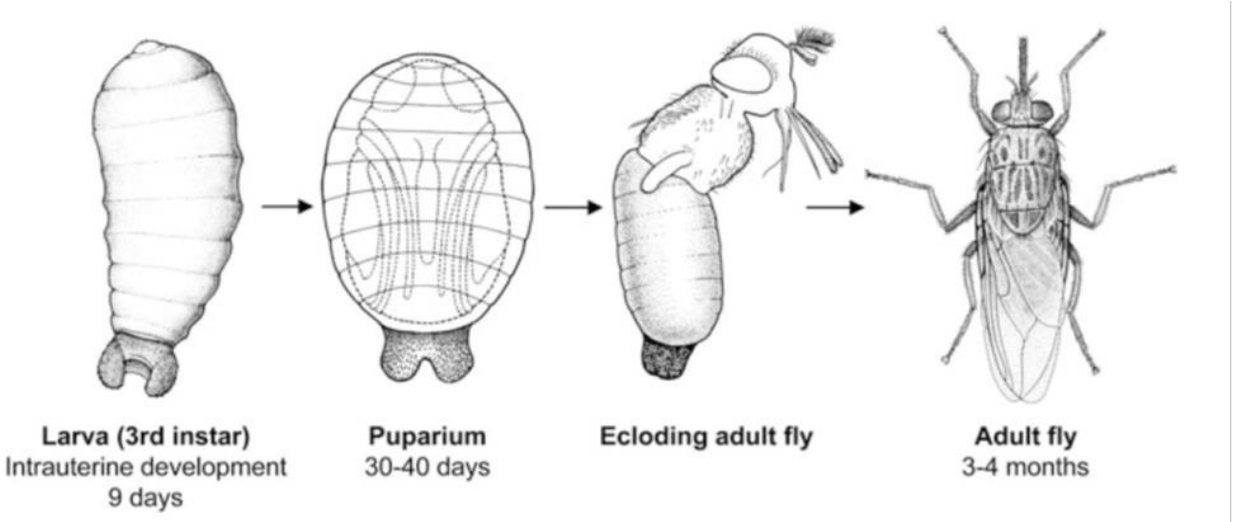

Fig. 12. The *Glossina* life cycle illustrating the development from a larva into an adult fly.

Fig. 13. On the left: Tsetse fly female laying larva. On the right: Adult tsetse fly.

Tsetse flies are infected with *T. brucei* when they ingest trypanosomes in the blood or in the skin of mammals. Once ingested, the "*short stumpy*" trypanosomes reach the salivary glands of the insects and develop into the human-infective metacyclic forms.

In a normal tsetse flies population, only a small proportion (about 0.01%) carries the metacyclic trypanosomes in their salivary glands, as detected by parasitological methods (dissection and microscopy). The classical dissection/microscopy technique is the only tool available to determine infection rates in the field (Abdi *et al*., 2017; Wamwiri *et al*., 2016). However, a tsetse fly feeds every 3 days and can infect several people during its lifetime. Based on this, eliminating the flies (by aerial spraying and installation of impregnated traps) or reducing the contact between them and humans can be considered as effective approaches to block the transmission of *T. brucei*.

1.3.2 The parasite life cycle

The trypanosomes represent the excellent examples of organisms that display an extreme adaptation to their environment, mostly because they must avoid the immune response of the host. The parasite's life cycle involves tsetse flies and mammalians and the trypanosomes undergo many morphological changes (Figure 14). Mammalians get infected after the bite of infected blood-sucker insects from the Glossina genus. During a blood meal on the mammalian host, an infected tsetse fly releases in the intradermal tissue the metacyclic trypanosomes. The parasites enter the lymphatic system and pass into the bloodstream (phase 1). Inside the host, they transform into bloodstream trypomastigotes (phase 2), which are carried to other sites throughout the body, and reach other blood fluids (e.g., lymph, spinal fluid). The bloodstream trypanosomes then replicate by binary fission (phases 3 and 4) and get into the insect midgut after another blood meal (phase 5). In the fly's midgut, the trypanosomes transform in procyclic trypomastigotes, multiply by binary fission

(phase 6) and reach the salivary glands as epimastigotes (phase 7). The epimastigotes will also divide in the salivary glands and transform into metacyclic trypomastigotes responsible for new infection (phase 8).

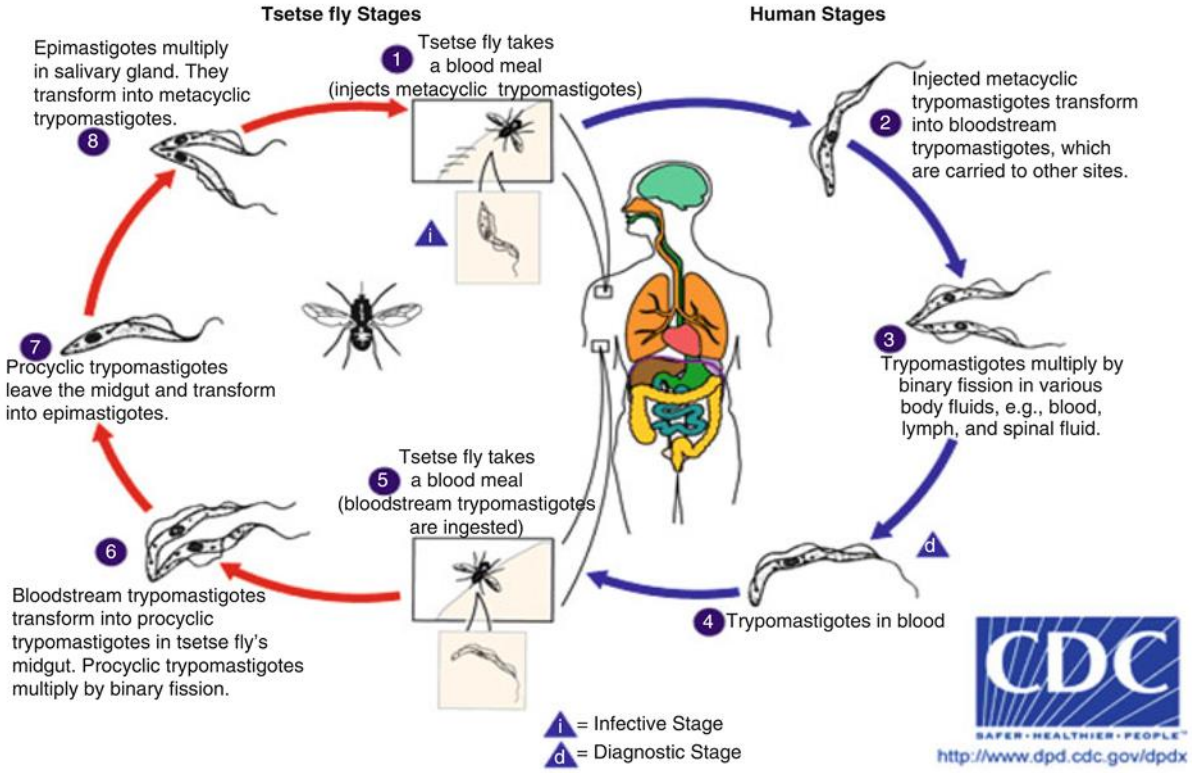

Fig. 14. Life cycle of *Trypanosoma spp*. (CDC, 2015).

Injected into human skin, the trypanosome parasites will first proliferate at the site of the tsetse fly bite and divide by binary fission in the interstitial spaces. The local inflammation reaction generated by the buildup of metabolic wastes and cell debris also leads to the formation of a trypanosomal "chancre" (called 'trypanome') and some local lymphadenopathy.

Another important factor to taking into the consideration is that in many laboratory experiments used as infection models, is extremely evident that there is a fine tuning between the ability of the tsetse to eliminate the infection and the capacity of the parasite to evade the hostile environment of the fly. That means that tsetse infection by trypanosomes is likely to be a strongly contested process. In the Figure 15 are represented the major bottlenecks affecting the transmission of *T. brucei* through the tsetse fly midgut. *T. brucei* long and proliferative slender (LS) and short stumpy (ST) blood forms are ingested with blood. In the tsetse midgut, ST forms transform into the proliferative procyclic forms (PFs), whereas LS forms die. Three to six days post-infection (dpi) procyclic forms (PFs) cross the peritrophic matrix (PM) and proliferate in the ectoperitrophic space

(ES). Both survival and establishment of a parasite infection in the midgut are major bottlenecks as highlighted by the arrow at the bottom of the Figure 15. Even in successful midgut colonizations, parasite survival ranges from 1% to 0.013–0.027% by 3 dpi.

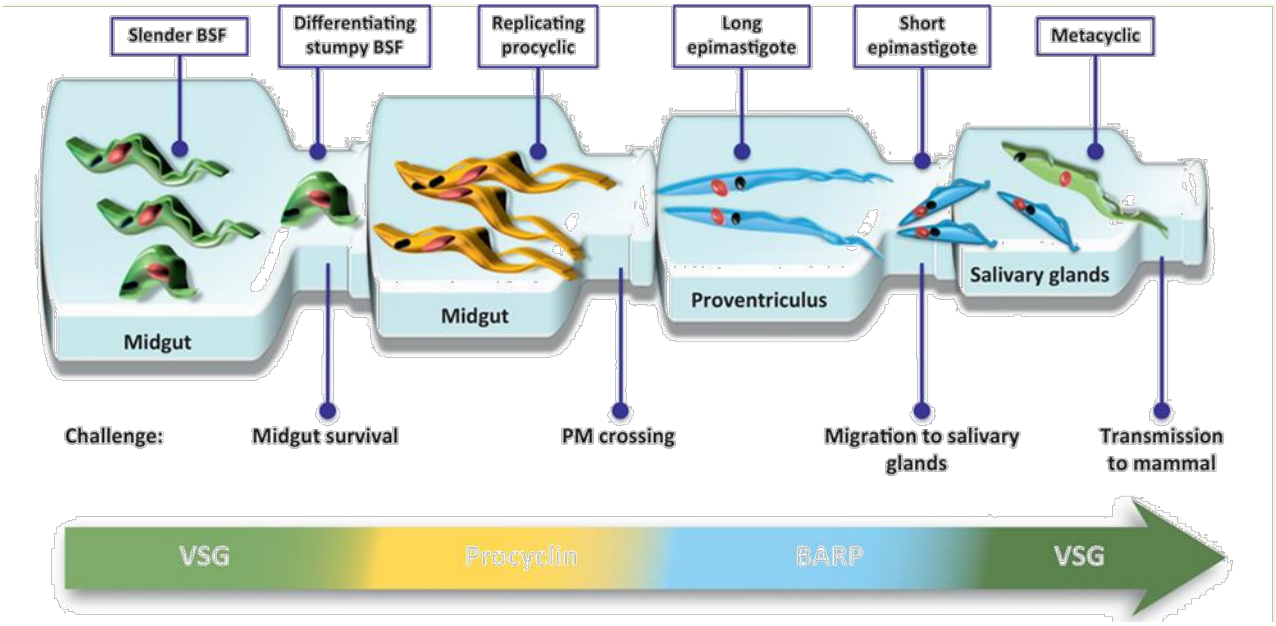

Fig. 15. Bottlenecks affecting the transmission of *T. brucei* through the tsetse fly. The parasite nuclei and kinetoplasts are represented in red and black.

1.3.3 The parasite architecture (morphology)

Trypanosomes are among the most ancient eukaryotes. The cell is elongated and shaped by the presence of a microtubules network following the longitudinal axis of the parasite (Mc Kean, 2003). The major organelles are present, such as mitochondria, the nucleus, the golgi apparatus and endoplasmic reticulum. The nucleus is located in the central region of the cell and contains 11 diploid pairs of megabase chromosomes, and approximately100 minichromosomes (Akiyoshi *et al*., 2013). The kinetoplast (mitochondrial genome) is located at the posterior end of the cell and is linked to the flagellum basal body. The flagellum rises up from the cell and is attached to the cell body along most of its length.

As part of kinetoplastids, trypanosomes possess a mitochondrial DNA which is organized in a large structure also known as kinetoplast. The presence of the flagellum is essential for the parasite motility and is attached to the trypanosome body (Figure 16).

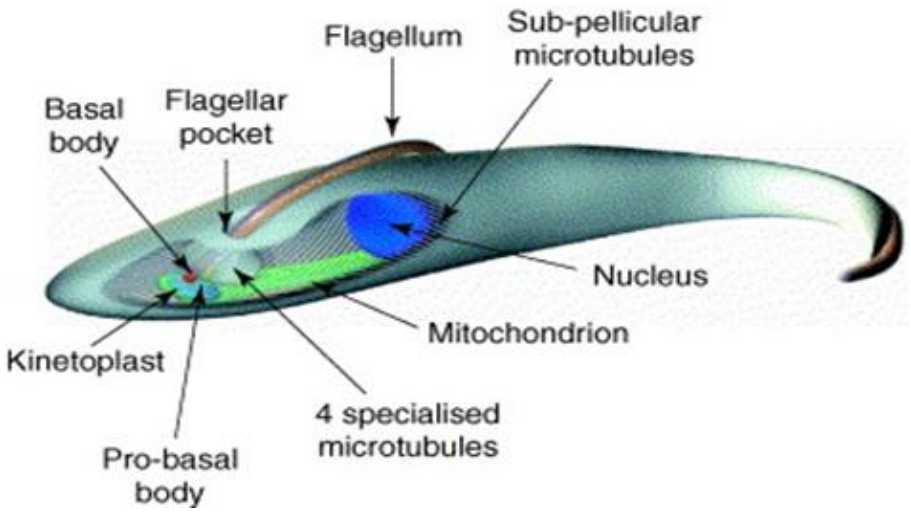

Fig. 16. Schematic representation of procyclic *T. brucei* on the basis of electron microscopy studies (Mc Kean, 2003)

1.3.4 The Variant Surface Glycoproteins (VSG)

Some trypanosome species are not infective to human and are infective only to animals. This is due to the presence in the human serum of the trypanolytic factors (TNF1 and TNF2) that provide innate protection. The species responsible for HAT, *T.b. gambiense* and *T.b. rhodesiense*, are not sensitive to these factors (Molina-Portela *et al*., 2008). Another very important feature of the parasite is the presence of the Variant Surface Glycoproteins that start to be expressed on the metacyclic form. These molecules are densely packed glycoproteins from 55 to 65 KDa (Dubois *et al*., 2005). The invasion of the host by trypanosomes triggers a humoral immune response. The VSG is the only antigen that can be targeted by the human's immune system and only one species is present on the trypanosome surface coat. The parasite escapes the immune response by a continuous change of the VSG coat through an antigenic variation. This phenomenon of antigenic variation renders the development of an effective vaccine improbable (Magez *et al*., 2010).

1.4 Mode of trasmission

T.b. *rhodesiense* HAT is a zoonosis and its transmission is predominantly maintained in an animal reservoir (cattle and wildlife). In countries where the reservoir is mainly wildlife, sporadic transmission can happen to tourists visiting National Parks. Some countries like Malawi, Tanzania, and Zambia have National Park areas within HAT endemic regions. Such "promiscuous" environment makes impossible the eradication of *T.b*. *rhodesiense* HAT. On the other hand, in Uganda, all recognised HAT endemic regions are outside National Parks areas, which makes effective control more feasible.

Due to the exponential growth of the African population, most wild animals living outside "Wildlife preserve" have been decimated by hunting and domestic animals represent nowadays the most important reservoirs of the disease. A recent study run in Busoga has shown that *T.b*. *rhodesiense* HAT can be transmitted five/six times more likely through a cattle-fly-human cycle than by a human-fly-human cycle (Hide *et al*., 2007) (Figure 17).

Fig. 17. Cattle chronically infected with *T.brucei* exhibit the same symptoms to those of late stage HAT.

On the contrary, *T.b*. *gambiense* HAT is sustained by the human-tsetse fly-human cycle, whereas the role of an animal reservoir is debated. Infrequently, the parasite is transmitted across the placenta or by blood transfusion.

Recently studies using modern molecular tools have confirmed the presence of *T.b. gambiense* in pigs in Cameroon and Ivory Coast (Jamonneau *et al*., 2004; Nkinin *et al*., 2002), and the infection was also detected in several primates.

Eight out of 24 different wild animal species (e.g. monkeys, ungulates and carnivores) were infected with *T.b. gambiense* in an HAT focus in Cameroon. Even though *T.b. gambiense* is commonly maintained by the human reservoir, this does not exclude that in some foci of Gambian HAT both reservoirs may coexist (WHO, 2013).

1.5 Clinical features of HAT disease

Many factors as the parasite subspecies, the host immune response and the stage of the disease can influence the clinical features of HAT (Büscher *et al*., 2017). *Gambiense* HAT (gHAT) leads to a chronic infection while *rhodesiense* HAT (rHAT) is acute. However, both are fatal if untreated or inadequately treated. The fast progression of rHAT to death is complete from few weeks to 6 months; on the other hand, it will take at least 3 years for gHAT to be fatal (Büscher *et al*., 2017).

Five-fifthteen days after the tsetse bite, a 3-4 cm local skin reaction called trypanosomal chancre, (Figure 18) coupled to the presence of enlarged posterior cervical lymphadenopathy, indicates the beginning of the disease (Sitch *et al*., 2002; Büscher *et al*., 2017). The dermal reaction occurs mostly in rHAT cases and is rare on patients with *T.b. gambiense* disease. Microscopic examination of the aspirate or palpation of enlarged neck glands in positive cases is generally used for HAT diagnosis (Lutumba *et al*., 2007).

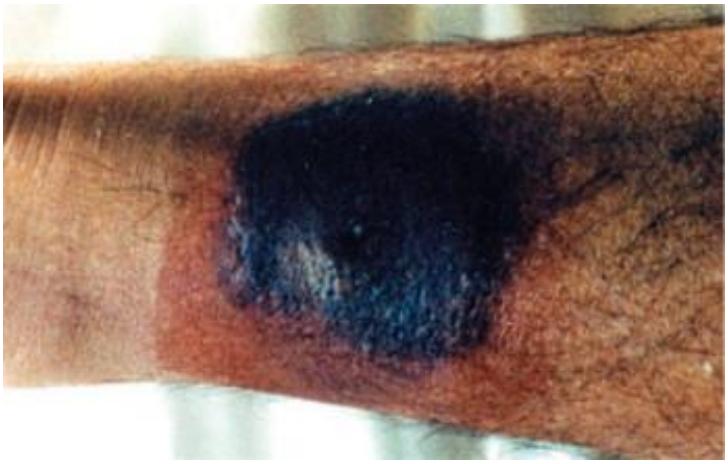

Fig. 18. Trypanosomal chancre on the dorsal side of the right ankle of a patient with *gambiense* HAT (Malvy D. *et al*., 2011).

The disease affects mainly the lymphoid system, heart, lungs, and brain and evolves in two stages. The first stage or early stage (haemolymphatic stage) is haemato-lymphatic and the parasite is present in the blood and in the lymphatic system. The parasitaemia is generally low (less than 100 parasites per ml of blood) and fluctuating. In the second or late stage (meningo-encephalic stage) parasites will penetrate the blood-brain barrier (BBB). The parasites invade perivascular areas with subsequent infiltration in the white and grey matter of the brain.

The most common symptom in the hemolymphatic phase is fever lasting one day to several weeks. Its irregular or intermittent pattern can be explained by the continuous waves of parasites in the blood (Sitch *et al*.,2002; Büscher *et al*., 2017). Other symptoms include headache, pruritus, hepatosplenomegaly and posterior cervical lymphadenopathy. Some endocrine dysfunctions like impotence, infertility and amenorrhea are also noticed (Figure 19).

The second phase occurs within weeks in the rHAT and months in the *gambiense* form following the invasion of the central nervous system (CNS) by the parasites. Some studies suggest that a high concentration of the parasites in the blood allows the cross of the BBB in an immune mediated way (Mogk *et al*., 2014). A chronic encephalopathy and sleep-pattern disturbances, with dysregulation of the circadian rhythm, represent the principal manifestations of the second stage and lend HAT its common name "sleeping sickness". Fever becomes less present and patients can experience mental changes and psychiatric disorders, painful peripheral sensory disturbances, tone and mobility disorders, and difficulties to concentrate. Cardiac disorders are also noticed with electrocardiogram abnormalities like perimyocarditis (Büscher *et al*., 2017).

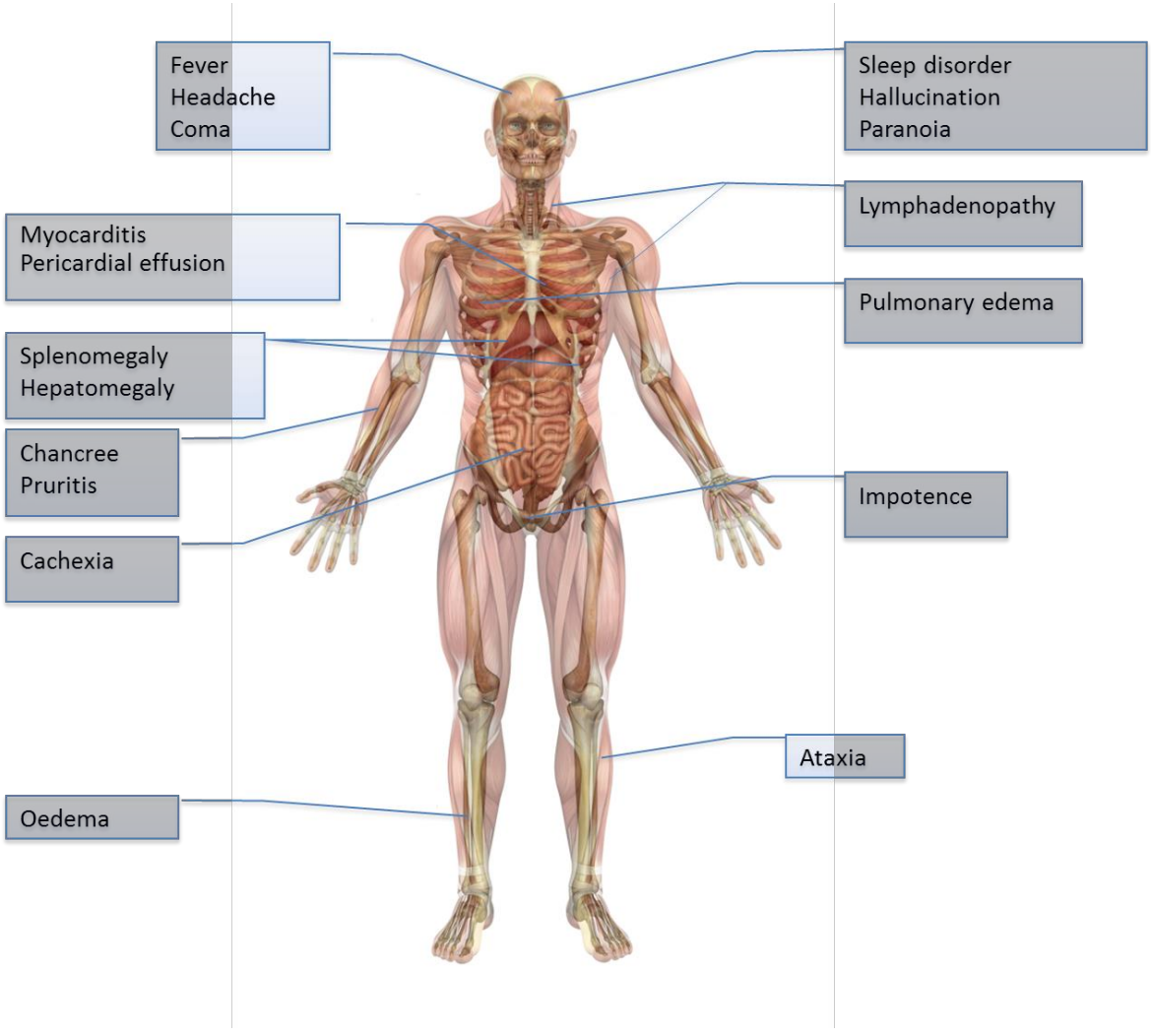

Fig. 19. Symptoms of HAT

1.6 Diagnosis

Symptoms for HAT are nonspecific and can easily be confused with other diseases, for this reason HAT diagnosis is based on laboratory tests. Early diagnosis is very important to increase the perspective of a cure. In fact, targeting the parasite before it get into the central nervous system necessitates a less complex therapy with relatively safer drugs. However, exhaustive screenings require major investment in hospital specialized personnel and material resources. In poor countries like Africa such resources are often limited, especially in rural and remote areas where the disease is most common. As a result, many infected people may die before diagnosis or treatment.

The differentiation between the two stages is done through examination of the cerebrospinal fluid (CSF). Staging is an important factor for HAT case management since drugs like Melarsoprol used for the second stage can cause reactive encephalopathy on patients (Checkley *et al*., 2007).The detection of the trypanosome parasites and the number of white blood cell (WBC) per µL are the criteria that allow to discriminate stage I and stage II. WHO recommends to consider the presence of trypanosome in the CSF or a count of more than 5 WBC/µL or both as a diagnostic criteria for second stage (Bonnet *et al*., 2015). The sensitivity and specificity of the criteria are debated due to the possibility of a low number of parasites present in the CSF making them undetectable. In addition, the presence of WBC in the CSF is not specific to HAT, but it is common in other diseases like meningitis. The most widely used screening test in *Gambiense* HAT is Card-Agglutination trypanosomiasis test (CATT), which was developed almost 40 years ago and still played an important role on the fight against the disease (Büscher *et al*., 2017) (Figures 20 and 21). The test is based on antigen type LiTat 1.3 (Bonnet *et al*., 2015) and its sensitivity and specificity vary between 68.8–100 and 83.5–99.3. Although its cost is affordable, limitation factors are represented by: cold chain storage, the 50-dose format that leads to loss of non-used doses and the availability of power sources. The test is carried on blood collected by finger prick and also on plasma or serum. Despite the high sensitivity, some false-positive results are noticed, especially for patients infected with malaria and filariasis. During the last 5 years, rapid diagnostic tests (RDT) were developed based on the antigens LiTat 1.3 and 1.5 and Second- generation RDTs based on recombinant antigens are now in clinical development (Sternberg *et al*., 2014).

The HAT Sero-K-Set and the SD bioline 1.0 were recently developed. These are rapid test made for gambiense HAT diagnostic. They are better than CATT and more suitable for population screening.

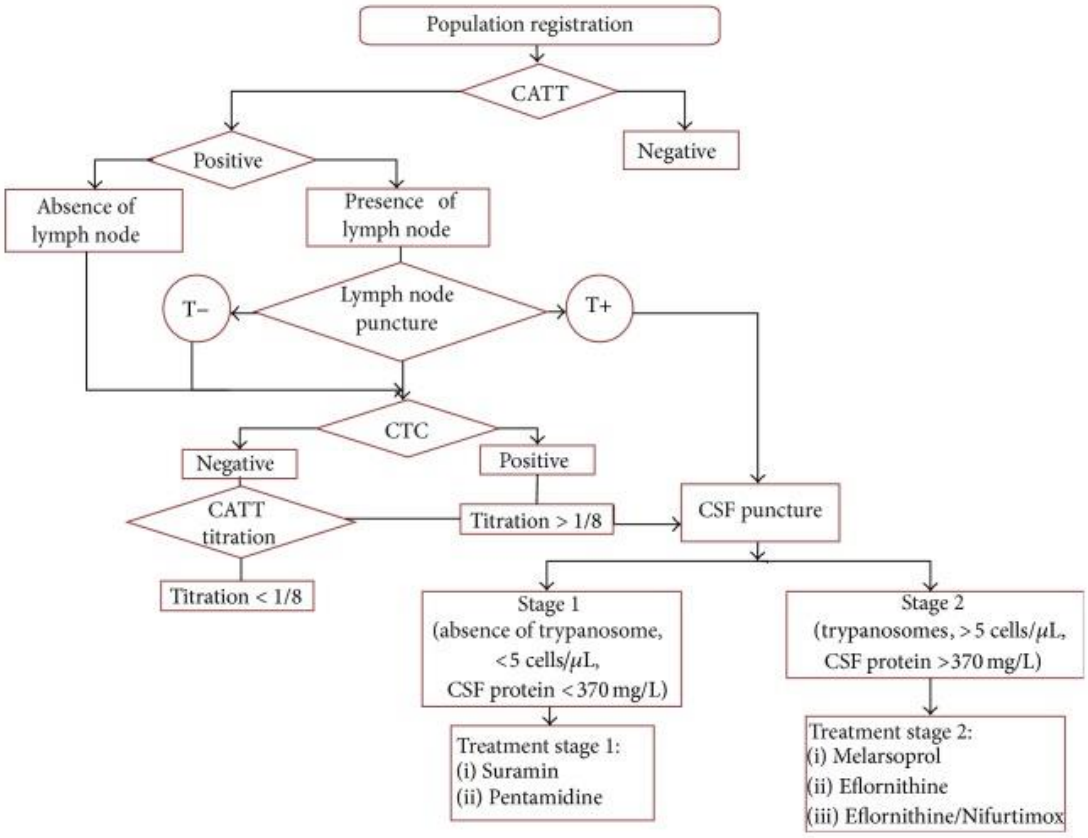

Fig. 20. Decision tree of HAT stage diagnosis (Bonnet *et al*., 2015). CTC (Capillary Tube Centrifugation); cerebrospinal fluid (CSF).

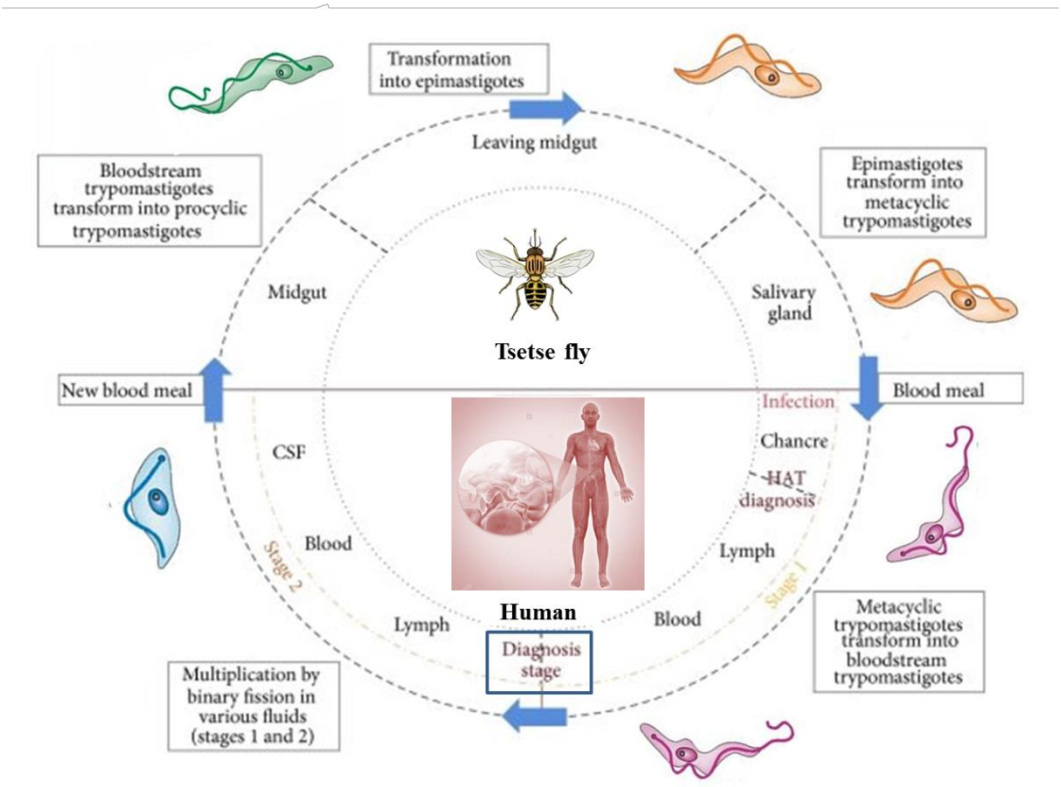

Fig. 21. Parasite life cycle and HAT stage diagnosis.

All HAT confirmatory tests are based on microscopic examination for the visualisation of parasites. However, there is no single confirmatory test that has a satisfactory sensitivity, and in practice combinations of several are used. These include: lymphnode aspirates in suspects with cervical adenopathy, capillary tube centrifugation (CTC), quantitative buffy coat (QBC) or the mini anion exchange centrifugation technique (mAECT). The most sensitive test is mAECT that isolates the parasites from venous blood using anion exchange mini columns by anion exchange and concentrate them. Patient blood cells are negatively charged, while trypanosomes remain neutral, so that they can be separated by anion-exchange chromatography at pH 8.

In confirmed HAT patients, an examination of CST by a lumbar puncture, helps to establish the stage of the disease and subsequently to determine the most appropriate treatment. When parasites are visualized in the cerebrospinal fluid, the patient is considered to be in the late stage of the disease. The WHO diagnostic criteria, which are the most widely used guidelines for diagnosing late stages of the disease, required the presence of trypanosomes in the CSF of more than 5 cells per μL (WHO, 2013). However, the detection of trypanosomes in CSF by microscopy alone has limited sensitivity and may generate false negative results.

Another potential parameter which may assist with late stage diagnosis is the measurement of CSF IgM concentrations, which are increased early when there is CNS involvement.

1.7 Chemotherapy for HAT

Since the development of a preventive vaccine would be an ideal approach to this devastating disease but, unfortunately, trypanosomes are able to evade the host immune system, chemotherapy remains the only available treatment option for fighting the infection.

Current treatments for HAT depend on the stage of the disease but also on the different parasite subspecies. Nowadays, there are four drugs and one drug combination available: pentamidine, suramin, melarsoprol, eflornithine and the nifurtimox-eflornithine combination therapy (NECT) (Figure 22 and Table 1). Three out of the four drugs available (**1**-**3**) were developed over 60 years ago and exhibit severe drawbacks.

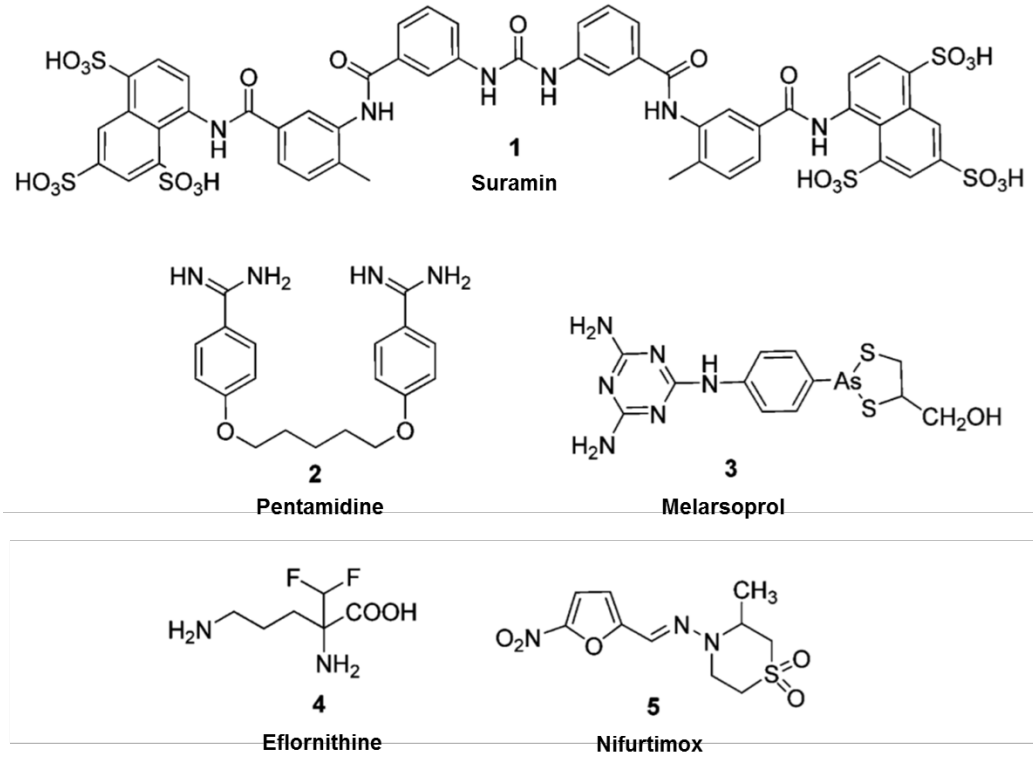

Fig. 22. Current drugs used for the treatment of HAT

Table 1. Drugs for treating HAT

Disease	Stage	Drug	Year of Introduction	Route of administration	Shortcomings
Gambiense HAT	Early	Pentamidine	1941	IM or IV	No oral formulation
		Eflornithine	1981	IV	Expensive
		Melarsoprol	1949	IV	Arsenical (toxic encephalopathy)
	Late	NECT	2009	IV + PO	Expensive
Rhodesiense HAT	Early	Suramin	1922	IV	No oral formulation
	Late	Melarsoprol	1949	IV	Arsenical (toxic encephalopathy)

1.7.1 Chemotherapy for first or early stage of HAT

1.7.1.1 Pentamidine

Pentamidine isethionate (**2**, Figure 22) is an aromatic diamine drug discovered in 1941. It is recommended by WHO as the first-line treatment for first stage *gambiense* infection and has been used as such for seven decades. It is also used against antimony-resistant leishmaniasis and against *Pneumocystis jiroveci* in AIDS patients (Soeiro *et al*., 2005).

Pentamidine efficacy against *T.b. gambiense* is very high, around 90-95%, while it is very limited for *rhodesiense* infection treatment (Büscher *et al*., 2017). Although the mechanism of action is unclear, the diamine structure is thought to be responsible for the antiparasitic activity trough parasite's DNA binding (Wilson *et al*., 2005). A recent study suggests that pentamidine uptake is by endocytosis with the specific aquaglyceroporin TbAQP2 acting as a high affinity receptor (Song *et al*., 2016).

It is administered once daily for 7 days intramuscularly or as an intravenous infusion in saline over 2h (Malvy *et al*., 2011). To avoid the hypoglycemia provoked by this drug, the administration is preceded by the ingestion of sugar, and supine position must be maintained for 1-2 h to avoid hypotension. The intramuscular administration is less suitable for developing countries with lack of healthcare facilities. To make the administration more convenient for patients, a new strategy based on three injections is on the way and comparative clinical trials have been launched.

Pentamidine is generally well tolerated but some adverse effects can be noticed and include pain at the site of injection, hypoglycemia, hypotension, abdominal pain and leucopenia. Resistance to pentamidine has been generated in laboratory strains but is not reported to be a widespread problem in the field (Barrett *et al*., 2011). The limitation of pentamidine use is the parenteral

administration because of the non-oral bioavailability due to the positively charged amidine group. For decades, researcher have focus their attention on the discovery of new diamines with a better efficacy, oral bioavailability and blood brain barrier penetration. Furamidine (Figure 23) showed a poor oral bioavailability despite good *in vitro* and *in vivo* activities on *Trypanosoma spp*. (Midgley *et al*., 2007; Wenzler *et al*., 2009). The selective and rapid uptake of furamidine allows an increase in the concentration in several pathogens including *Plasmodium falciparum*, *Leishmania spp*., *Gardia intestinalis* and *P*. *jiroveci*.

To increase the oral availability, furamidine prodrugs were synthesized. In 2000, the methamidoxime prodrug, parafuramidine (Figure 23), was selected by the consortium for parasitic drug development (CPDD) for clinical development. The first phase of clinical trials, conducted in 2000 on healthy patients for 21 days, was successful. The second lasted 6 years and was conducted on patients at the first stage of the disease. The third phase conducted in collaboration with the Food and drug administration (FDA) aimed to assess the efficacy and safety of parafuramide compared to pentamidine maleate for treatment of first stage sleeping sickness. Unfortunately, there were no significant difference in term of efficacy. Parafuramidine had a better safety profile but some renal post treatment toxicities have led to widespread concerns (Pohlig *et al*., 2015). For this reason the development was halted in 2008.

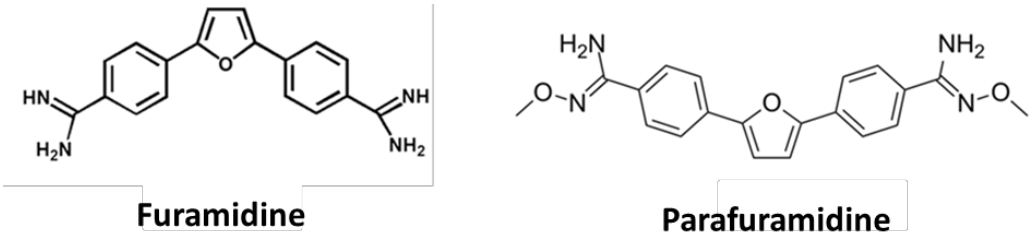

Fig. 23. Chemical structures of Furamide and Parafuramide.

1.7.1.2 Suramin

Suramin (**1**, Figure 22) was first used in 1922 for HAT treatment but developed few years earlier by Bayer chemists from azo dyes, trypan red and trypan blue. It is a polysulphonated naphtylamine-based compound used for the first stage of *T*. *b*. *rhodesiense*. It is also active on *T.b*. *gambiense* form of the disease but not used in therapy because of the high risk of co-infection with onchocerchiasis in endemic areas that could lead to allergic reactions due to rapid killing of the microfilariae (Büscher *et al*., 2017). Pentamidine administration is preferred for such cases since it is easier to administrate. In fact, the suramin therapy involves five slow intravenous injections of 20 mg/kg every 3-7 days for 4 weeks. A test dose is recommended to avoid hypersentivity reactions.

Intravenous administration is the best way of administration, because suramin is poorly absorbed orally and causes serious irritation after intramuscular injections (Babokhov *et al*., 2013).

Due to its high affinity with serum proteins (99.7%) it has a long half-life of around 44-54 days. Low-density lipoprotein (LDL) are uptaken through endocytosis as a sterols source for bloodstream forms and suramin can then enter *T.b*. *rhodesiense* (Babokhov *et al*., 2013).

Suramin targets include specific inhibition of *T*. *brucei* glycolytic enzymes. Thanks to its negative charge, it can specifically target the trypanosomal enzyme which has a higher isoelectric points than its mammalian counterpart (Bacchi *et al*., 2009). Other targets include dihydrofolate reductase, thymidine kinase and pentose phosphate pathway enzymes. The multiple targets aspect of suramin's mechanism of action may help to explain the low development of resistance. However, a study published in 2018 has revealed the involvement of VSG in the development of resistance to suramin (Wiedemar *et al*., 2018).

Suramin cannot cross the blood brain barrier probably due to its large size, the presence of tights junctions near the endothelial membrane and the absence of transport vesicles. All these factors contribute to limit the concentration of suramin in the CSF (around 1%) compared to the serum. Suramin is then not effective for second stage disease but can be used in synergy with second stage HAT drugs because of its ability to inhibit the P-glycoprotein leading to the limitation of second stage drug expulsion from CNS (Sanderson *et al*., 2007). The side effects due to suramin administration include fatigue, neuropathy, renal problems, anaemia and nausea.

1.7.2 Chemotherapy for second or late stage of HAT

1.7.2.1 Melarsoprol

Melarsoprol (**3**, Figure 22) is an arsenical compound introduced in 1949 and produced by Sanofi-Aventis. Melarsoprol has been also donated, free of charge, to WHO. It is derived from the toxic melamine arsenical called melarsen and was synthesized by the Swiss chemist Friedheim. To increase the antitrypanosomal activity of the molecule, some modifications from melarsen were performed and in 1939 an analogue of melarsen named melarsen oxide was synthesized (Figure 24).

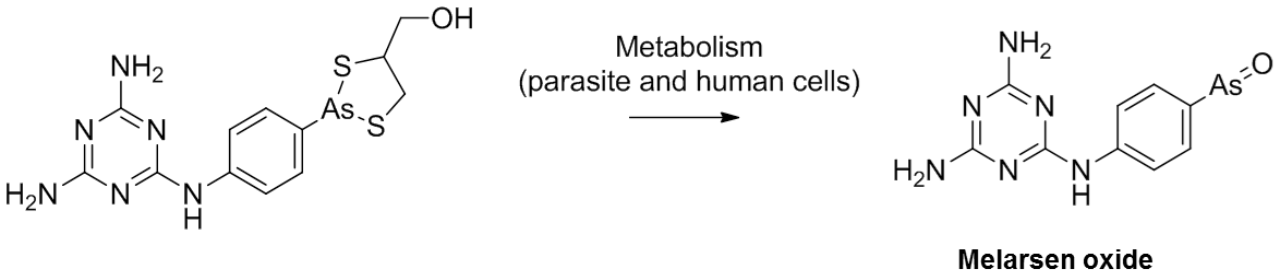

Fig. 24. Chemical structure of Melarsen oxide.

Unfortunately, the increase of activity also led to an increase in toxicity and melarsen oxide could not be used for therapy. The adding of dimercaprol (British Anti-Lewisite), a disulfide chelating agent, significantly reduced the toxicity and the resulting compound was named melarsoprol (Steverding *et al*., 2008). This latter has been for several decades the only option for second stage HAT treatment for both East and West African forms. After the introduction of eflornithine, melarsoprol is nowadays only recommended for treatment of late stage East African trypanosomiasis caused by *T. b. rhodesiense* thanks to its ability to cross the blood brain barrier.

The mechanism of action remains unclear but some studies suggest an inhibition of the trypanosomal enzymes pyruvate kinase, phosphofructokinase, fructose-2,6-bisphosphatase and trypanothione reductase (Denise *et al*., 1999). Arsenical interaction with glycerol-3-phosphate dehydrogenase has been studied and it has been shown that the enzyme binds specifically Cymelarsan, a melarsoprol analogue, used for animal trypanosomiasis (Denise *et al*., 1999). In addition, the bloodstream forms of trypanosomes are highly dependent on glycolytic and redox processes and any dysregulation of these factors may lead to cell lysis due to lack of ATP. Other studies report that melarsoprol uptake is done through the purine nucleotide transporter P2 and arsenical-resistant trypanosomes lack those transporters (Carter *et al*., 1993).

Melarsoprol is administered intravenously after dissolution in propylene glycol because it is not soluble in water. Different variants are considered for melarsoprol administration, but the best regiment consists of 2.2 mg/kg per day over 10 days with a cure rate of 93.9% at the beginning and 86.2% after two years of follow-up (Babokhov *et al*., 2013).

Melarsoprol has a high number of side effects and the most important is the arsenical-induced reactive encephalopathy syndrome (fever, convulsion, neurological disorders, and coma) occurring in 10% of treated patients followed by the death of half cases within 2 days (Priotto *et al*., 2008). Co-administration with corticoids can reduce the immune reaction that causes the syndrome. Patients should be followed after the injections and any onset of fever or headache should be

considered as an alarm and the treatment should be stopped. The intravenous administration is painful due to the presence of propylene glycol that can destroy the veins.

1.7.2.2 Eflornithine

Eflornithine (α-difluoromethylornithine or DMFO, **4**, Figure 22) is the latest antitrypanosomal monotherapy introduced in 1990. It was first developed in the 1970s as an anticancer and ten years later, the scientist Cyrus Bacchi decided to assess its antitrypanosomal activity. He demonstrated that eflornithine was able to cure *T.b. brucei* infected mice with no signs of side effects. DFMO was then subjected to extensive human clinical trials in Africa.

For a typical-sized individual, the demanding regime is nearly a half-kilogram of drug administered while the patient is hospitalised. Through support from WHO, eflornithine kits for two full treatments weigh 40 kg and cost US$ 1420, and have been made available for distribution in disease endemic countries.

Between 2001 and 2002, 1055 patients (adults and children) diagnosed with second stage HAT received eflornithine for 14 days at different dosages, 400 mg/Kg/day and 600 mg/Kg/day for adults and children, respectively. The study concluded that eflornithine is effective. and relative safety when used as first line treatment for HAT (Priotto *et al*., 2008). No relapse was observed more than 12 months after the treatment and higher doses were well tolerated by children. The drug is an inhibitor of the enzyme ornithine decarboxylase (ODC) which is responsible for the synthesis of polyamines to facilitate cell division and proliferation. It binds irreversibly to ODC catalytic site. A study assessing the *in vivo* activity of Eflornithine on metabolism and morphology of *T.b. brucei* reveals that treated parasites have a short and broader form with multiple kinetoplasts (Bacchi *et al*., 2009). In addition, trypanosomal ODC activity is reduced by 99% in 12 hours and polyamine levels are significantly reduced. It is only effective on *T.b. brucei* and *T.b. gambiense* but not on the *T.b. rhodesiense* strains. The selectivity is due to the slow ODC turnover rate of *T. brucei gambiense* (19 hours) compared to the *T.b. rhodesiense* and mammalian counterparts with respectively 4.3 hours and 10-30 minutes (Babokhov *et al*., 2013).

Eflornithine is not a trypanocidal but a trypanostatic molecule which blocks the division of bloodstream trypanosomes and requires a functional immune system to get rid of the parasite. The co-infection with HIV-AIDS or other immuno-suppressant conditions can be a serious problem.

The standard administration of DMFO involves 56 intravenous infusions at 100 mg/kg for adults and 150 mg/kg for children every 6 hours for 7 days. An alternative regiment involving a reduced number of intravenous injections at 100 mg/kg every 6 hours over 7 days was studied in clinical trials as well as the oral administration of Eflornithine. Both studies showed reduced efficacy (Babokhov *et al*., 2013).

Eflornithine is as an alternative after melarsoprol relapse for *gambiense* infection treatment. The drug is in fact more effective against *T.b*. *gambiense* compared to melarsoprol but less fatal. The fatality rate for eflornithine is estimated to be around 1.4% versus 5% for melarsoprol and the cure rate is 94% for eflornithine and 84% for melarsoprol (Priotto *et al*., 2008). The side effects for eflornithine include diarrhea, headache, seizures, anemia, and leucopenia, typical of anticancer drugs. Resistance, due to mutations in a putative amino acid transporter, has been shown *in vitro*.

1.7.2.3 Nifurtimox-Eflornithine combination therapy (NECT)

An important recent advancement in HAT chemotherapy was the introduction of nifurtimox-eflornithine combination therapy (NECT), which is currently the first line of treatment for HAT.
The treatment is strongly recommended by WHO and has been included to the WHO Essential Medicine List in 2009. Kits for four full treatment courses weigh 36 kg and cost US$ 1440, and are being widely adopted in disease endemic countries.

Nifurtimox (**5**, Figure 22), also known as Lampit, is a nitrofuran derivative trypanocide. It was developed by Bayer in 1960 and used as treatment of Chagas disease (South American trypanosomiasis) caused by *Trypanosoma cruzi* since 1967. The company provides free of charge tablets to WHO and financial assistance to sustain endemic countries like Honduras and El Salvador. The mechanism of action of nifurtimox is unclear, but some studies report a metabolic conversion after enzymatic reduction of the nitro group leading to the production of free radicals. Nitroreductases (NTR) and trypanothione reductases are the enzymes involved in the free radical generation which interfere with parasite membrane, DNA and proteins. The impairment of type I nitroreductase in *T*. *cruzi* conferred a resistance to nifurtimox (Wilkinson *et al*., 2008). Its efficacy against *T*. *brucei* infections have been assessed and showed a limited activity against stage II HAT. The low concentration of nifurtimox in the CNS compared to the plasma and the point mutation of trypanosomal NTR could explain the treatment failures (Bisser *et al*., 2007).

Because of the high cost of Eflornithine treatment, “Medecin sans frontière” and DNDi (Drug for Neglected Disease initiative) conducted several clinical trials to find an alternative for a cheaper, safer and more compliant combination therapy. Nifurtimox + eflornithine, melarsoprol +

nifurtimox and eflornithine + melarsoprol combination were assessed. The Nifurtimox + eflornithine combination therapy consisting of nifurtimox 15 mg/Kg/day over 10 days orally and eflornithine 400 mg/Kg/day over 7 days IV was shown to be the most potent with 94% cure rate and low fatality rate (Priotto *et al*., 2008). From 56 intravenous administration of eflornithine monotherapy, the combination allowed a reduction to 14, which makes it easier to administer and less expensive. In rural areas characterized by poverty and a lack of healthcare personnel, it is a huge advancement since it requires less hospitalization and allows a better compliance for patients who can take nifurtimox at home. The side effects for NECT replicates those of eflornithine and nifurtimox but it is generally well tolerated. This includes abdominal pain, vomiting and headache.

Despite this positive advancement with the HAT therapy, the high costs of distribution coupled with intravenous route of administration, makes the therapy way far from ideal chemotherapy. For this reason, DNDi has proposed a target product profile (TPP) for getting a better drug for HAT. The ideal drug would be orally administered, effective against both early- and late-stage disease, safe for children and pregnant women, without drawbacks and inexpensive (less than 30 euros per course). Due to the large distance between the ideal HAT drug and the state-of-art of currently used HAT drugs, there is still much work to be done as drug discovery. Recent advancements and new discoveries that will be discussed in the next chapters fill us with optimism that these goals are achievable in the foreseeable future.

1.8. Drug candidates in clinical trials for HAT

1.8.1 Fexinidazole

Fexinidazole (Figure 25) is a 2-substituted 5-nitroimidazole that was identified as a promising drug candidate for HAT after a screening of around 700 nitroheterocyclic compounds from diverse sources conducted by the DNDi. Fexinidazole (1-methyl-2-((p-methylthio)phenoxy)methyl)-5-nitroimidazole was first developed by Hoechst AG (now Sanofi-Aventis) as a broad spectrum antimicrobial agent in the 1970's.

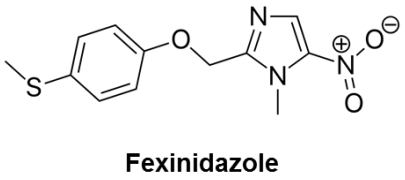

Fig. 25. Chemical structure of Fexinidazole.

In 2010, Torreele *et al*. conducted a study to assess the *in vitro* and *in vivo* antitrypanosomal activities of fexinidazole and its metabolites fexinidazole sulphoxide and fexinidazole sulphone (Torreele *et al*., 2010) (Figure 26).

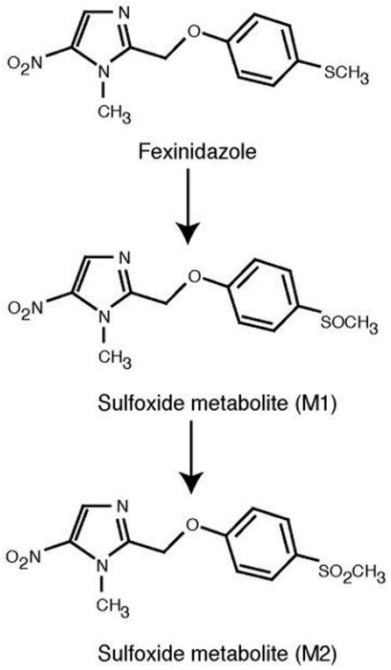

Fig. 26. Chemical structure of Fexinidazole and its main metabolites.

Fexinidazole and its metabolites showed moderate activities *in vitro* against *T.b.gambiense* and *T.b*. *rhodesiense* with an IC_{50} value ranging from 0.16 and 0.93 µg/ml. They also showed no cytotoxicity on L-6 rat myoblast cells with $IC_{50} > 90$ µg/ml and a selectivity index always above 97. Fexinidazole showed an almost similar activity of eflornithine and nifurtimox but was less active compared to reference drugs melarsoprol and pentamidine (IC_{50} = 0.003 µg/ml). The good absorption of fexinidazole was demonstrated with absolute oral bioavailability of 41, 30 and 10% in mice, rats, and dogs, respectively. In addition, fexinidazole cured mice with chronic and acute infection after oral administration of 200 mg/Kg/day and 100 mg/Kg/day for 5 and 4 days respectively (Torreele *et al*., 2010).

In 2011, a phase I clinical trials was done (clinical trial number NCT00982904) and the selected dose for further studies was 1800 mg/day for the first 4 days and 1200 mg/day for 6 other days. Based on these results, the randomized phase II/III, open label, non-inferiority trials started in 2012 on stage II *gambiense* HAT patients (NCT01685827), where it is being compared to NECT.

Between October 2012 and November 2016, more than half a million people were screened to identify 419 patients who were pre-screened. Of these, ten (2%) patients were not eligible. Of the 409 eligible patients, 14 patients were not included because they did not meet all inclusion criteria Of the 395 patients included in the study, one committed suicide. Therefore, 394 patients were randomly assigned, 264 of whom were assigned to fexinidazole and 130 to nifurtimox eflornithine combination therapy. After 18 months of observation, fexinidazole was 7% less successful than the NECT (91% *vs* 98%). However, the result it is not significant since it was inferior to the margin of difference in success rate defined as 13% (Mesu *et al*., 2018). The difference in the proportion of patients who experienced treatment-related adverse events (81% in the fexinidazole group *vs* 79% in the nifurtimox eflornithine combination therapy group), was quite similar. The study has demonstrated that fexinidazole is safe and effective against late stage *gambiense* infection.

Given the good results of the phase II/III conducted (NCT03025789). in Democratic Republic of Congo and Central Republic published one year ago (Mesu *et al*., 2018), the next step was to submit the dossier to the regulatory agency. At the beginning of the year 2018, Sanofi and the drug for neglected disease initiative (DNDi) asked the European Medicines Agency (EMA) to review fexinidazole for HAT treatment. Since the drug is intended to be used in endemic countries (Africa), fexinidazole was subjected to a special procedure called “Article 58”allowing the EMA in co-operation with WHO to evaluate products that are supposed to be used outside the European Union (DNDi, 2018). On November 2018, EMA recommended fexinidazole as the first oral treatment for HAT. The oral drug could be distributed in endemic countries in 2019 and will help to bypass the lack of health logistics in African countries (DNDi, 2018). Despite fexinidazole can help

to eradicate HAT in poor areas since it can be used for both stages and is active against gambiense and rhodesiense forms, it still holds some critical drawbacks (e.g. toxicity) making it even present the need for safer drugs.

1.8.2 Oxaborole (SCYX-7158)

The orally active benzoxaborole SCYX-7158 (Figure 27) has been identified as a promising trypanocide after a library screening of benzoxaborole 6-carboxamides from Anacor Pharmaceuticals. A lead-optimization program conducted at Scynexis led to SCYX-7158. The compounds showed *in vitro* growth inhibition against *T. brucei* as low as 0.02 µg/ml and *in vivo* efficacy in acute murine infection models after oral administration of doses as low as 12.5 mg/Kg x7 days (Jacobs *et al*., 2011). In addition, SCYX-7158 has a good tissue distribution and a low intravenous plasma clearance. The compound has been shown to be highly orally bioavailable in rodents and non-human primates.

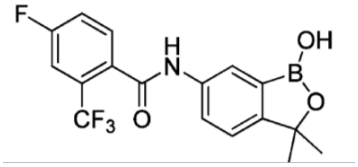

Oxaborole
(SCYX-7158)

Fig. 27. Chemical structure of Oxaborole (SCYX-7158).

The concentration in the CNS was maintained for 20 hours above the minimum inhibitory concentration (MIC) with a high brain exposure suggesting a BBB permeability and favorable conditions for late stage HAT therapy (Jacobs *et al*., 2011). Seketee and coworkers. proposed the perturbation of *T. brucei* S-adenosyl-L-methionine metabolism as a likely mechanism of action of benzoxaborole treatment (Seketee *et al*., 2018). First-in-man studies were conducted from 2012 to 2015 to assess the safety and tolerability of SCYX-7158 in France on 128 healthy human volunteers from sub-Saharan origin. The DNDi announced the successful completion of the study with a therapeutic dose determined at 960 mg administered once as three tablets. The drug showed a good safety profile and also a long half-life, around 400 hours (News-medical, 2018). Phase IIb/III trials are being carried out in the Democratic Republic of the Congo. If successful, SCXY-7158 will have the advantage to be administered orally as a single dose.

1.9 Natural products as a source of trypanocidal compounds

Nature's diversity offers a wide range of molecules with different scaffolds and pharmacological activities. Local population around the globe has been exploiting that potential for thousands of years and exclusively relied on traditional medicine for healing. In fact, records written on clays tablets in cuneiform from Mesopotamia around 4000 years ago can testify the central role played by natural products in the treatment and prevention of diseases (Gurib-Fakim, 2006). Some treatments based on natural products developed centuries ago are still practiced nowadays. According to WHO, 80% of people in developing countries use medicinal plants products for primary health care. In some countries, the medicinal herbs and phytomedicines can even be found in pharmacies and supermarkets. In the US, particularly, the sector is growing very fast and it is estimated that 20% of Americans use medicinal herbs. In addition, natural products represent 25% of the prescribed drugs while another 25% derive from a natural product modified structure (Seke Etet *et al*., 2011).

Natural products are a reservoir for bioactive compounds but also for template molecules of new drugs. In fact, some molecules isolated from medicinal herbs can serve as starting material for chemistry process. An important feature of medicinal herbs therapy is the synergistic activity of the phytocomplex as a result of the simultaneous action on different targets. This feature can sometimes increase the activity of the whole plant extract compared to the single isolated compound and the multi-target approach makes difficult the emergence of resistance and side effects. It is noteworthy that an antagonistic effect can also occur and the procedure then requires the isolation of the most active compound. The attraction towards natural products stands on the widespread belief that they are completely safe compared to the so-called "western drugs". This can be explained by the delayed occurrence of side effects that reduces the possibility to match the side effects to the causal event. However, it has been reported in several papers including ours that important cytotoxicity on mammalian cells is exhibited by phytocompounds like the Tagitinins A and C isolated from *Tithonia diversifolia* with IC_{50} of 1.27 and 0.036 µM (Sut *et al*., 2017).

The affordability and availability of natural products in poor areas are very important factors as people can have it cheaper or even grow it their selves. The dosage for natural product-based treatments is a critical issue as the concentration of the plant components can vary depending on the period of the year.

1.9.1 Antiparasitic drugs from natural origin

As already pointed out in the previous paragraph, natural products are secondary metabolites produced by organisms in order to provide an evolutionary benefit over the other competing organisms. Often it takes place by synthetizing chemical compounds that result toxic for the surrounding organisms. Secondary metabolites can be products by various biosynthetic pathways such as: the shikimate pathway, the mevalonate pathway, and polyketide synthases. Due to the nature of their biosynthesis, natural products and their naturally-occurring drug derivatives typically have lower hydrophobicity and higher stereochemical centers than synthetic compounds. These structural features are extremely important and beneficial in terms of pharmacokinetic parameters and structural diversity of compounds. For this reason, natural products have been a source of inspiration for a great number of current treatments targeting many diseases.

A recent review based on drugs introduced in the market between 1981 and 2014 reports that 49% of new drugs are natural based-products or structural derivatives (Newman *et al*., 2014). This observation places the natural products as promising candidates for the identification of new trypanocidal drugs, by utilizing common scaffolds observed in trypanocidal natural products, and chemically modifying them in order to acquire the required pharmacokinetic parameters to be effective.

Among the naturally-occurring drugs, artemisinin and quinine are considered the most famous anti-parasitic compounds used to treat malaria (Figure 28).

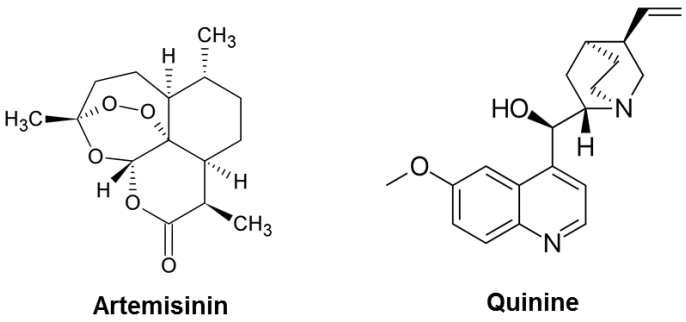

Fig. 28. Chemical structures of Artemisinin and Quinine.

The alkaloid quinine was isolated from the *Cinchona* species bark two centuries ago by the French pharmacists Caventou and Pelletier. The bark was introduced in Europe in the 1600s for malaria treatment but was previously used by autochthones of the Amazon region for diverse ailments including fever (Gurib-Fakim, 2006). Quinine and its derivatives including chloroquine,

amodiaquine, primaquine, and mefloquine were used as curative agents for malaria. Quinine continues to play a significant role because 31 African countries recommend it as second-line treatment for uncomplicated malaria and in other countries it is even used as a monotherapy, in contrast to the WHO recommendations (Achan *et al*., 2011). The recommended regimen for the malaria treatment according to the WHO is a combination therapy based on artemisinin derivatives.

Artemisinin is a sesquiterpene lactone isolated in 1971 from the Chinese traditional herb *Artemisia annua* (Asteraceae). This was the result of a screening of almost 2000 Chinese herbs used for fever treatment as the government launched a huge project against malaria called "project 523" in 1967 (Muangphrom *et al*., 2016). The research group led by the professor Tu Youyou noted an important activity of the water extract of *Artemisia annua* and the active compound was extracted from the leaves. The discovery represented one of the major breakthroughs for the fight against tropical diseases. In 2015, Tu Youyou was awarded the Nobel Prize in physiology or medicine.

1.9.2 Screening of natural product for antitrypanosomal activity

An extensive literature search revealed several natural based-product classes of antitrypanosomal compounds albeit very few have been advanced to *in vivo* evaluation while none have been clinically studied. For this reason, we decided to restrict in scope this paragraph, emphasizing only those natural products or plant extracts that have exhibited significant potency *in vitro* (IC_{50} < 5 μM) against trypanosomes responsible for HAT (Table 2).

Two sesquiterpene lactones named 15-acetoxy-8β-[(2-methylbutyryloxy)]-14-oxo-4,5-cis-acanthospermolide (**6**) and 9α-acetoxy-15-hydroxy-8β-(2-methylbutyryloxy)-14-oxo-4,5-trans-ancanthospermolide (**7**) were isolated from the areal part of *Acanthospermum hispidum* (Asteraceae) and were reported by Ganfon and coworkers (Ganfon *et al*., 2012) (Figures 29 and 30). The extract was prepared by maceration for 24 hours with water and sulfuric acid 0.5% to simulate the traditional preparation done with lemon juice in Benin. Both sesquiterpernes isolated after fractionation were tested against a panel of protozoans including *T.b. brucei* as well as against human fibroblast cell line (WI38) as a counter screen for toxicity. The acidic crude extract was not active but the two sesquiterpene lactones were active against *T.b. brucei* with IC_{50} values of 2.45 and 6.36 μM, respectively. The SI were 5.75 and 6.48, respectively. The activity of **6** and **7** can be explained by the presence in their structure of α-methylene γ-lactone moiety which is responsible for many biological activities of sesquiterpene lactones. The high reactivity of the moiety with thiol groups present in several enzymes like trypanothione can lead to cell death.

Fig. 29. *Acanthospermum hispidum* (Asteraceae).

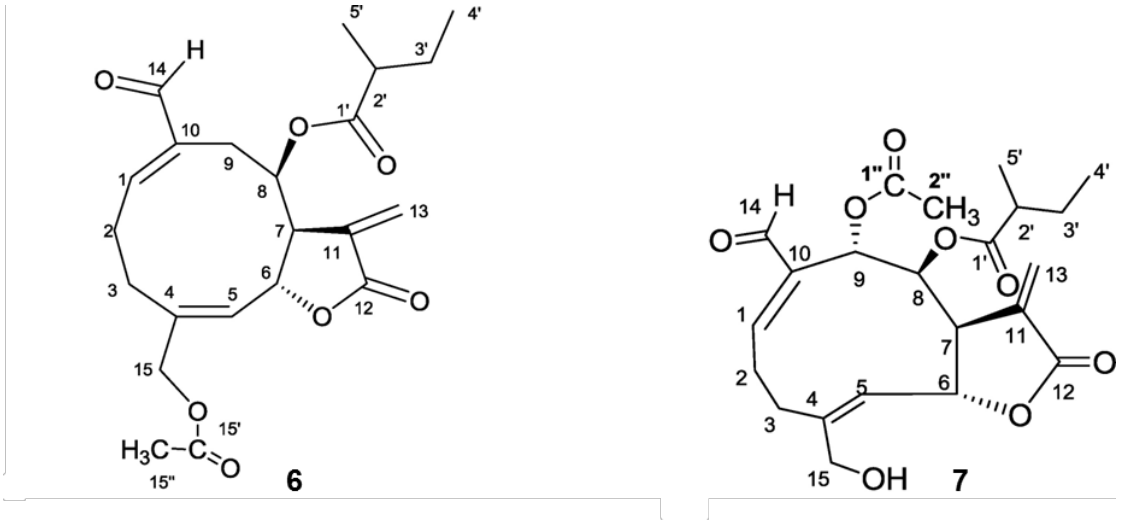

Fig. 30. Chemical structures of compound **6**: 15-acetoxy-8β-[(2-methylbutyryloxy)]-14-oxo-4.5-cis-acanthospermolide and compound **7**: 9α-acetoxy-15-hydroxy-8β-(2-methylbutyryloxy)-14-oxo-4.5-trans-acanthospermolide.

Among the class of phenolic derivatives two arylnaphthalide lignans, justicidin B (**8**) and its hydroxylated derivative, piscatorin (**9**, Figure 30), have been identified. The bioactivity-guided fractionation of the dichloromethane extract of *Phyllanthus piscatorum* (Figure 31), led to the isolation of the two compounds. When tested on the bloodstream trypomastigotes of *T.b. rhodesiense*, compound **8** exhibited strong inhibition with submicromolar activity (IC_{50} = 0.2 µg/mL) albeit cytotoxic on mammalian cell lines. The hydroxylated derivative **9** was found to be 11-fold less potent than the parent compound **8** (IC_{50} = 2.3 µg/mL) (Gertsch *et al*., 2003).

A chalcone-flavone dimer, cissampeloflavone (**10**, Figure 30), has been reported by Ramírez and coworkers and has been isolated from the aerial parts of *Cissampelos pareira*

(Menispermaceae) (Ramírez *et al*., 2003). Compound **10** exhibited good potency on the *T.b. rhodesiense* bloodstream stage (IC_{50} = 0.61 µg/ml). Encouragingly, the compound had a low cytotoxicity to the human KB cell line (IC_{50} = 106 µg/ml).

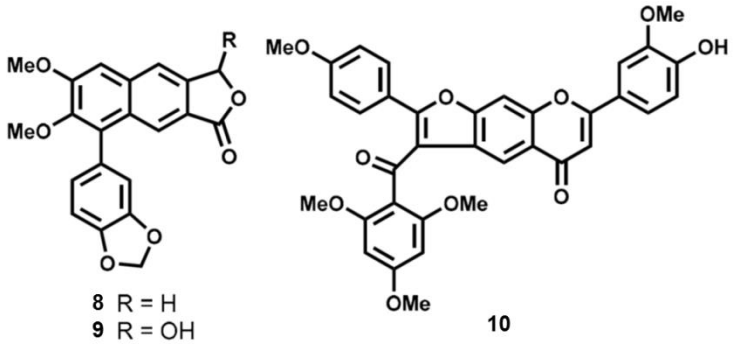

Fig. 30. Chemical structures of trypanocidal phenolic derivatives.

Fig. 31. *Phyllanthus piscatorum* Kunth (Euphorbiaceae).

Fig. 32. *Cissampelos pareira* (Menispermaceae).

Methoxylated flavonoids were isolated from the dichloromethane (DCM) extract of the aerial parts of *Ageratum conyzoides* L. (Asteraceae) (Figure 33) collected in Sudan. The five methoxylated flavonoids have been identified as 5,6,7,8,5'-pentamethoxy-3',4'-methylenedioxyflavone (**11,** eupalestin), 5,6,7,5'-tetramethoxy-3',4'-methylenedioxyflavone (**12**), 5,6,7,8,3',4',5'-heptamethoxyflavone (**13**), 5,6,7,3',4',5'-hexamethoxyflavone (**14**) and 4'-hydroxy-5,6,7,3',5'-pentamethoxyflavone (**15**). Beside all these flavonoids, the chromene derivative encecalol methyl ether (**16**) was also isolated (Nour *et al*., 2010) (Figure 34).

The crude extract and the isolated compounds were tested against *T*. *b*. *rhodesiense* and L6 rat skeletal myoblast cell line. The DCM extract was very active against *T*. *b*. *rhodesiense* (IC_{50} = 0.78 µg/mL, SI = 47). The chromene was inactive and all the flavonoids showed moderate activity. Among the isolated compounds the compound **15** was the most active with an IC_{50} value of 3.1 µg/mL and SI > 30. In comparison, the reference drug melarsoprol showed an IC_{50} of 0.003 µM.

Fig. 33. *Ageratum conyzoides L.* (Asteraceae).

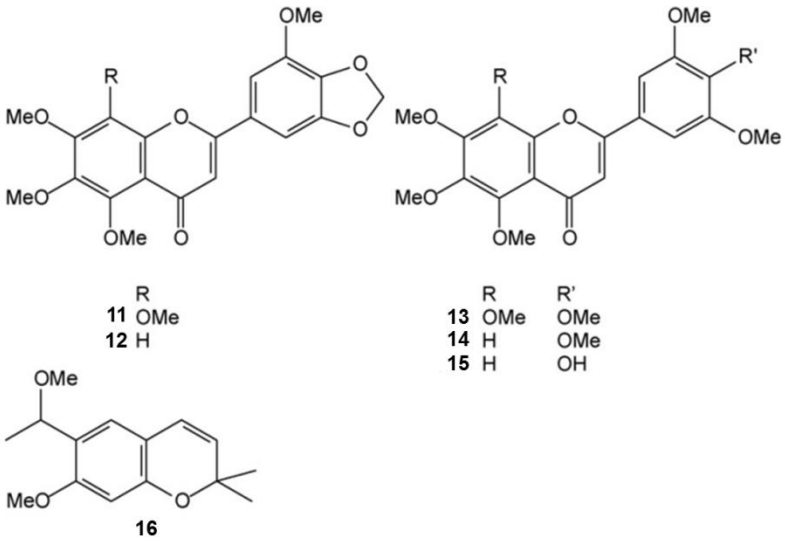

Fig. 34. Structures of the isolated constituents of *Ageratum conyzoides*.

The aqueous and 80% methanol extract of different parts of *Alstonia congensis* (Apocynaceae) (Figure 35) harvested in Congo were assessed against *T.b*. *brucei* and MRC-5 cells (human lung fibroblasts). In addition, a series of fractions and subfractions from the leaves, root bark and stem were also assessed. An ethnopharmacological and ethnobotanical study reveals that the plant is traditionally used for the treatment of parasitic diseases such as malaria (Kambu, 1990). The phytochemical screening revealed the presence of alkaloids, phenolic compounds, terpenes and steroids. The fractions from the stem bark were more active against *T.b*. *brucei* and one of the fractions showed an IC_{50} of 2.02 µg/ml and SI of 16 (Lumpu *et al*., 2013).

Fig. 35. *Alstonia congensis* (Apocynaceae).

Alkamides were isolated from the plant *Anacyclus pyrethrum* L. (Asteraceae) (Figure 36). The plant is known since the ancient times for the treatment of ailments like fever. From the DCM extract, were isolated the alkamides tetradeca-2E,4E-dien-8,10-diynoic acid isobutylamide (**17**), deca-2E,4E-dienoic acid isobutylamide (**18**), deca-2E,4E,9-trienoic acid isobutylamide (**19**), deca-2E,4E-dienoic acid 2-phenylethylamide (**20**), undeca-2E,4E,9-trienoic acid isobutylamide (**21**), tetradeca-2E,4E,12Z-trien-8-diynoic acid isobutylamide (**22**) and dodeca-2E,4E-dien acid-4-hydroxy-2-phenylethylamide (**23**) (Figure 37). An inseparable mixture of undeca-2E,4E-dien-8,10-diyonic acid 2-phenylethylamide and deca-2E,4E-dienoic acid 4-hydroxy-2-phenylethylamide was also isolated (**24** and **25**). The crude extract and the isolated compounds were assessed against the *T.b*. *rhodesiense* parasite and the L6 rat skeletal myoblasts. The crude extract displayed an $IC_{50} > 10$ µg/ml against the parasite and the most active compound **23** displayed an IC_{50} value of 2.26 µg/ml (7.17 µM) but was not selective (SI = 0.1). On the other hand, the mixture displayed an important activity toward *T.b*. *rhodesiense* but was also toxic (SI = 1.5). The reference drug melarsoprol displayed an IC_{50} value of 0.003 µg/ml (0.008 µM). The trypanocidal and cytotoxic activities of the compound **14** can be explained by the presence of a p-hydroxy-substituted phenylethyl amide moiety based on the structure-activity relationship (Althaus *et al*., 2017).

Fig. 36. *Anacyclus pyrethrum L.* (Asteraceae).

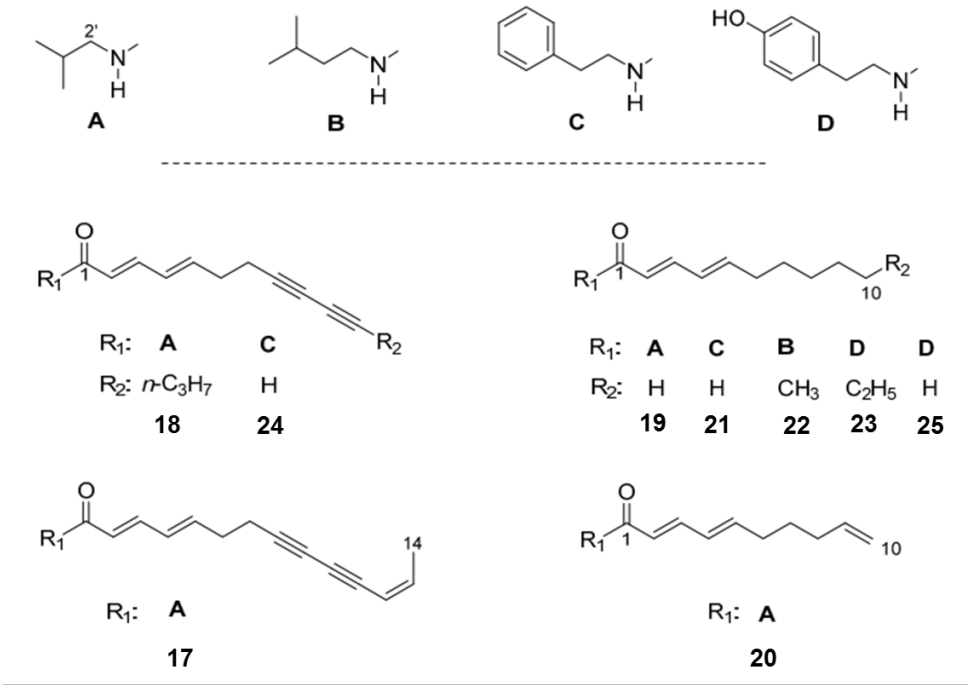

Fig. 37. Structures of the isolated alkamides from *A. pyrethrum*.

Protoberberin and aporphine alkaloids were isolated from the methanol leaves extract of the Tanzanian plant *Annickia kummeriae* (Annonaceae) (Figure 38). The plant is used widely for the treatment of malaria and other ailments. The methanol extract was assessed on the *T.b. rhodesiense* as well as against the rat skeletal myoblast (L-6).

It exhibited a good activity towards *T.b. rhodesiense* with an IC_{50} of 2.5 µg/ml (SI =12). Bioassay-guided chromatographic fractionation was used to isolate the antitrypanosomal compounds. This yielded pure alkaloids: lysicamine, trivalvone, palmatine, jatrorrhizine, columbamine and (-)-tetrahydropalmatine. The isolated alkaloids exhibited an IC_{50} ranging from 3.2 to 14.3 µg/ml with palmatine as the most active compound. Indeed, palmatine (**26**) displayed a IC_{50} of 3.2 µg/ml and a good selectivity with a SI of 28 (Figure 39). Trivalvone was the less active compound (IC_{50} = 14.3 µg/ml).

The antiprotozoal activity displayed by protoberberine alkaloids can be explained by the oxygenation of C-2, C-3 (ring A) and C-9, C-10 (ring D) together with the presence of quaternary nitrogen atom in position 7 (Malebo *et al*., 2013).

Fig. 38. *Annickia kummeriae* (Annonaceae).

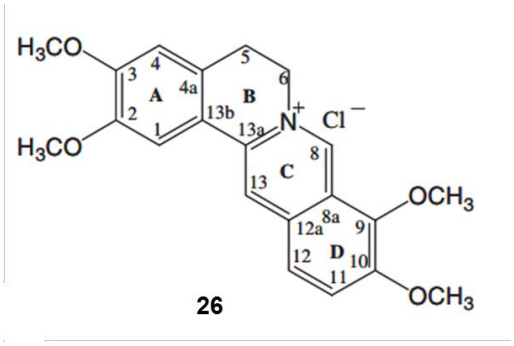

Fig. 39. Chemical structure of Palmatine (**26**) isolated from *Annickia kummeriae*.

The plants from *Artemisia* spp (Figure 40) are known for their antiplasmodial activities, even though some of them can also display antitrypanosomal activities. Efferth and co-workers prepared methanol and dichloromethane extracts of six different *Artemisia annua* (Asteraceae) samples from different origin to assess their activity against *T.b. brucei* cells (TC221). The dichloromethane extracts showed better activity (range of IC_{50}: 1.8-14.4 µg/ml) compared to the methanol extracts (range of IC_{50} 10.8-77.5 µg/ml) (Efferth *et al*., 2011). The phytochemistry analysis of extracts revealed the presence of artemisinin, arteanuine B and scopoletin in different amounts depending on the origin of the plant. Another study published in 2007 reports the activity of artemisinin derivative against *T.b. rhodesiense*. Artemisinin exhibited a moderate activity with an IC_{50} of 20.4 µM and was less active than 4-fluorophenyl-artemisinin which had the best activity with an IC_{50} of 15.7 µM (Mishina *et al*., 2007).

Fig. 40. *Artemisia annua* (Asteraceae).

Ceasalpinia benthamiana (Fabiaciae) (Figure 41) is a well-known plant in the Guinean traditional medicine. It is used for the treatment of diseases like malaria and it has been demonstrated to be active against the malaria parasite *Plasmodium falciparum* with an IC_{50} of 5.8 µg/ml (Traore *et al*., 2013). The methanol extract of *C*. *benthamiana* was tested against the parasite *T.b*. *brucei* and the human cell line MRC-5 (Loua *et al*., 2017). The methanol extract displayed a moderate activity toward the parasite with an IC_{50} of 13 µg/ml (SI = 2.5) and the aqueous extract was less active with an IC_{50} of 32 µg/ml.

A bioassay-guided fractionation of the methanol extract yielded seven fractions and the first three fractions exhibited the best activities against *T.b*. *brucei* with IC_{50} of 32, 35, and 33 µg/ml respectively, all of them being less active than the mother extract. The phytochemical investigation of the 70% ethanol leaf extract revealed the presence of flavonoids, saponins, terpenoids and tannins.

Other studies describe the presence of mezobenthamic acids A and B and neocaesalpin H (terpenoids), kaempferol and quercetin (flavonoids), resveratrol, gallic acid, β-sitosterol glucoside and 13β-hydroxypheophorbide (Jansen *et al*., 2017).

Fig. 41. *Ceasalpinia benthamiana* (Fabiaciae).

Greenwaydendron suaveolens (Annonaceae) is a 35-40 m high tree used by the Nkundo people in Democratic Republic of Congo (DRC) alone or as a mixture for the treatment of parasitic diseases including malaria and helminthiasis (Mato, 2005) (Figure 42). Different parts of the plant collected in the Salonga national park were used to prepare crude extracts from with different solvents. The extract was tested against a panel of protozoan parasites including *T.b*. *brucei* as well as MRC-5 cells as a counter screen for toxicity. The root bark dichloromethane extract rich in alkaloids showed the best activity with an IC_{50} of 0.5 µg/ml and a very good selectivity (SI > 100) (Musuyu Muganza *et al*., 2016).

The stem bark ethanol and methanol extracts also exhibited a good activity against *T.b*. *brucei* with IC_{50} of 2.01 µg/ml (SI = 17.85) and 2.20 µg/ml (SI = 3.4) respectively. To isolate the compounds responsible for the activity, the root bark dichloromethane extract was subjected to fractionation by successive open column chromatography on silica gel.

Four compounds were obtained: the triterpenes polycarpol and dihydropolycarpol and the alkaloids polyalthenol and *N*-acetyl-polyveoline. Excepted *N*-acetyl-polyveoline which showed no activity, the other three isolated compounds showed a moderate activity with IC_{50} around 8 µM and a very low selectivity (SI $\simeq$ 2). The isolated compounds were less active than the crude extracts, this may be due to a synergistic effect of the constituents.

Fig. 42. *Greenwaydendron suaveolens* (Annonaceae).

Holarrhena africana (Apocynaceae) (Figure 43) is a tree distributed in tropical countries like Nigeria where its leaves are traditionally used for the treatment of convulsion, fever and malaria. Extracts from the leaves and bark were investigated for their activity against the bloodstream form of *T.b. rhodesiense* as well as against L6 cells to assess the toxicity. The crude extract and alkaloid-rich fraction were prepared.

The crude extract and the alkaloid-rich fraction exhibited an interesting activity against *T.b. rhodesiense* with IC_{50} of 4.7 µg/ml (SI = 18.6) and 0.9 µg/ml (SI = 48.4), respectively (Okeke Nnadi *et al*., 2017). The bioactivity-guided fractionation of the alkaloid-rich fraction resulted in the isolation of 17 steroid alkaloids, one nitrogen-free steroid and one alkaloid-like non-steroid. Eight of the isolated compounds displayed a very strong activity against *T.b. rhodesiense* (IC_{50}, SI): 3β-holaphyllamine (0.4 µM, 12.6), 3α-holaphyllamine (0.37 µM, 42.9), 3β-dihydroholaphyllamine (0.67 µM, 25.8), N-methylholaphyllamine (0.08 µM, 33.2), conessimine (0.17 µM, 302), conessine (0.42 µM, 146), isoconessimine (0.17 µM, 168) and holarrhesine (0.12 µM, 121).

In comparison, the reference drug melarsoprol exhibited an IC_{50} of 0.002 µM. The basic amino group of the pregn-5-ene steroid nucleus has been demonstrated to be a requirement for the antitrypanosomal activity.

Fig. 43. *Holarrhena africana* (Apocynaceae).

Senna spectabilis (Fabaceae) (Figure 44) is a wooden plant native from Central and South America. It is also present in Africa and Asia as an ornamental plant. In Brazil, it is traditionally used as anti-inflammatory, analgesic, laxative, purgative, anti-microbial. In Africa the plant is used for the treatment of parasitic diseases like malaria. Methanol leaves extract and fractions from *S. spectabilis* harvested in Malaysia were tested against the *T.b. rhodesiense* parasite and also against L6 cells to assess toxicity.

Fig. 44. *Senna spectabilis* (Fabaceae).

Methanol leaves extract showed a potent inhibitory activity against *T.b. rhodesiense* with an IC_{50} of 1.54 µg/ml (SI = 32.7). The dichloromethane and ethyl acetate fractions obtained after a partition of the methanol extract displayed an IC_{50} of 0.45 (SI = 144.8) and 1.14 µg/ml (SI = 77.17) respectively. A bioguided-assay fractionation was performed on the DCM extract and yielded two compounds: (+)-spectaline (**27**) and iso-6-spectaline (**28**) (Figure 45) (Lim *et al*., 2018). Both isolated compounds displayed potent antitrypanosomal activities on *T.b. rhodesiense* with an IC_{50} of 0.13 µg/ml (0.41 µM) for (+)-spectaline and 0.23 µg/ml (0.71 µM) for iso-6-spectaline without toxic effect on L6 cells (SI of 134.9 and 123.7, respectively). In comparison, the standard drug pentamidine exhibited an IC_{50} of 1.59 nM with SI > 185.

The alteration of trypanosomes ultrastructures by the isolated compounds was revealed by electron microscopy and led to programmed cell death. The alterations included disorganization of the kinetoplast, swelling of the mitochondria, formation of autophagic vacuoles which suggest an autophagic cell death.

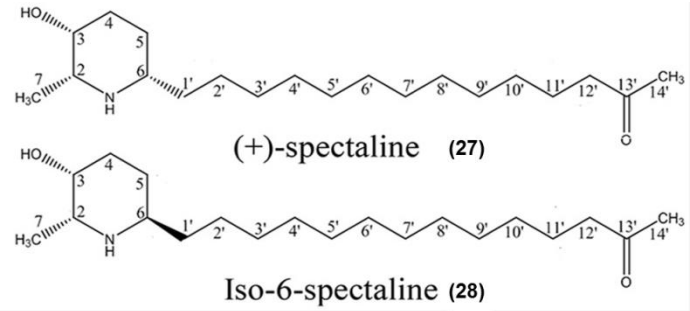

Fig. 45. Chemical structure of (+)-spectaline (**27**) and iso-6-spectaline (**28**).

Tabernaemontana longipes (Apocynaceae) (Figure 46) is a tropical plant found in Latin American countries like Nicaragua, Colombia, Ecuador and Costa Rica. *T. longipes* leaves were harvested in Costa Rica and a chloroform extract was prepared. A fractionation of the extract on silica gel yielded 49 fractions, which were then pooled together in nine super-fractions. Those fractions were tested for their inhibition of *T. brucei* strain 427 growth. To assess the cytotoxicity, the fractions were also tested on the human hepatocarcinoma cell line (Hep G2). The second fraction exhibited an interesting antitrypanosomal activity with 76% growth inhibition at 10 µg/ml. It was subsequently subjected to further separation for the isolation of the active compounds (Carothers *et al*., 2018). The pentacyclic triterpenoid bauerenol acetate (**29**) was purified and showed an IC_{50} of 3.1 µM on *T. brucei* with a low cytotoxicity on Hep G2 (IC_{50} > 80 µM). To improve the solubility of the acetate in DMSO during the biological test, the acetate was transformed through hydrolysis into bauerenol (**30**), its alcohol derivative (Figure 47). Bauerenol

displayed a better activity on *T*. *brucei* with an IC_{50} of 2.7 µM and low cytotoxicity on Hep G2 (IC_{50} > 80 µM). The reference drug suramin exhibited an IC_{50} of 0.04 µM. To understand the mechanism of action of bauerenol, a primary metabolic profiling assay was performed. *T*. *brucei* cells were exposed to 0.15 and 5 µM of bauerenol for 4h and the metabolites analyzed by GC-TOFMS. The metabolites that showed concentration-dependent changes compared to the control were cholesterol, arachidic acid, phosphoenolpyruvate, myristic acid and adenine. This suggests an interference of the triterpenoid with sterol metabolism.

Fig. 46. *Tabernaemontana longipes* (Apocynaceae).

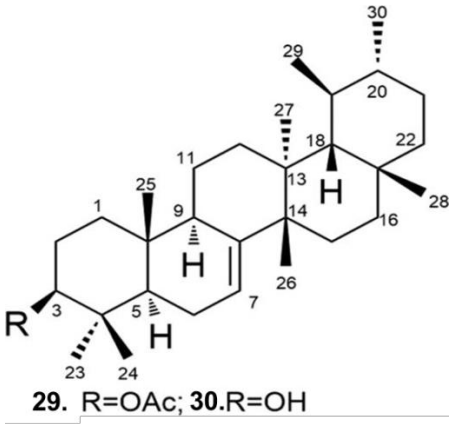

29. R=OAc; **30.**R=OH

Fig. 47. Chemical structures of bauerenol acetate (**29**) and bauerenol (**30**).

Vernonia cinerascens (Asteraceae) (Figure 48) is a highly branched annual herb of around 0.3-2 m tall. It is native to Africa and India. It is traditionally used for ulcer, constipation and urinary tract infections. The dichloromethane extract of leaves from *V*. *cinerascens* harvested in Narok (Kenya) was prepared for *in vitro* antitrypanosomal assays (*T*. *b*. *rhodesiense*) and for cytotoxicity assays against mammalian cell line L6 (Kimani *et al*. 2018). The extracted exhibited a

potent activity toward *T.b. rhodesiense* with an IC_{50} of 0.24 µg/ml and a moderate toxicity on L6 cell line (IC_{50} = 6.1 µg/ml). The dichloromethane extract was fractionated by silica gel and yielded nine fractions. The fractions were also tested for their antitrypanosomal and cytotoxic activities. The most active fraction showed IC_{50} value of 0.17 µg/ml. The separation of that fraction yielded the sesquiterpene lactones: vernodalin (**31**, Figure 49), 11β,13-dihydrovernodalin, 11β,13-dihydrovernolide; hydroxyvernolide, 11β,13-dihydrohydroxyvernolide, and vernocinerascolide. Vernodalol was not isolated but was identified as one of the compounds. All sesquiterpene lactones were tested and vernodalin was the most active with an IC_{50} of 0.16 µM (SI = 35). The reduction of the activity of the 11β,13-dihydro derivative of vernodalin (IC_{50} = 1.1 µM) may be due to the loss of one of the Micheal acceptor systems. In fact, as explained previously, the Micheal acceptors α,β-unsaturated carbonyl groups can alkylate biological macromolecules such as enzymes thus inhibiting their functions.

Fig. 48. *Vernonia cinerascens* (Asteraceae).

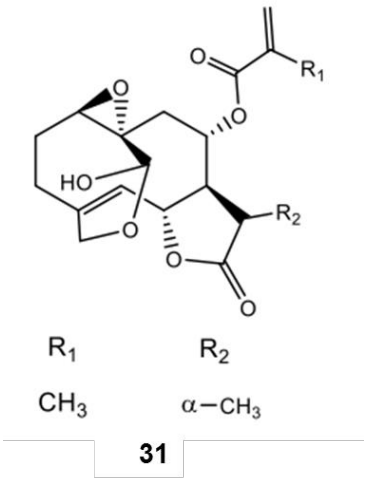

Fig. 49. Chemical structure of vernodalin (**31**).

Keetia leucantha (Rubiaceae) (Figure 50) is a West African tree traditionally used in the treatment of parasitic diseases. The essential oil obtained by hydrodistillation of the leaves and its constituents were assessed for their activity against both bloodstream and procyclic forms (i.e. the insect form) of *T.b. brucei* parasite (Bero *et al*., 2013). Characterization of the essential oil allowed the identification of 42 constituents representing 89.57% of the oil. The most abundant components were n-hexadecanoic acid (43.5%), oleic acid (9.5%) and phytol (5.7%). The essential oil displayed an IC_{50} of 20.9 µg/ml on the *T.b. brucei* bloodstream form but was not active on the procyclic form . Some commercially available compounds were tested against the *T.b. brucei* bloodstream form. The most abundant components n-hexadecanoic acid and oleic acid were not active with IC_{50} >100 µg/ml and 64µg/ml, respectively. The most active compounds were ursolic acid, oleanolic acid and β-ionone with IC_{50} of 2.5, 7.3 and 10.5 µg/ml respectively (Figure 51). The reference drug suramin exhibited an IC_{50} of 0.11 µg/ml.

The most promising compounds were tested for their inhibitory activity on a glycolytic enzyme of *T. brucei* called glyceraldehyde-3-phosphate dehydrogenase (GAPDH). GAPDH catalyses the phosphorylation of glyceraldehyde-3-phosphate to 1,3-bisphosphoglycerate with NAD^+ and inorganic phosphate. The compound oleanolic showed the best enzyme inhibition with 72.6% at 20 µg/ml, followed by β-ionone and ursolic acid with around 30% of inhibition at the same concentration.

The GAPDH inhibition alone cannot explain the antitrypanosomal activity and the authors suggested to study the effect of those pentacyclic triterpenoids on trypanosomal topoisomerases since they have been shown to inhibit the human topoisomerase I and II.

Fig. 50. *Keetia leucantha* (Rubiaceae).

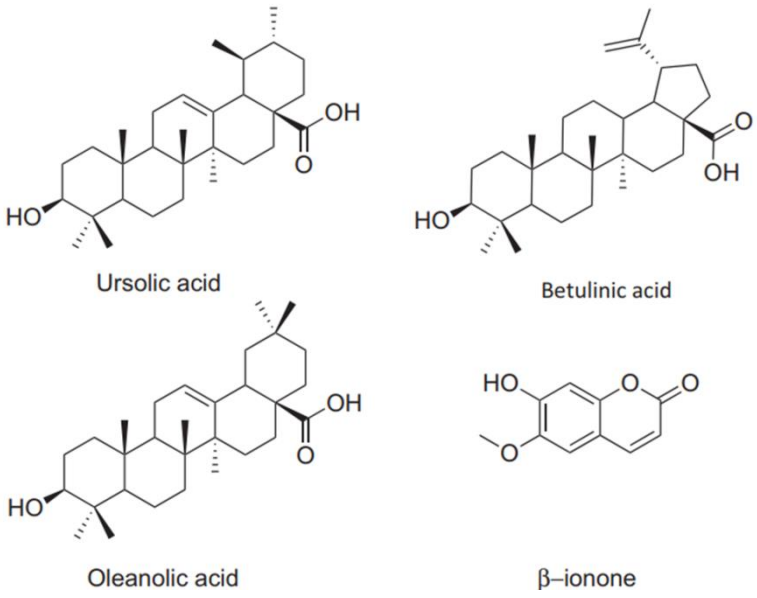

Fig. 51. Chemical structures of ursolic acid, betulinic acid, oleanolic acid and β-ionone.

Table 2. Selection of plants with antitrypanosomal activity

Name	Family	Active components	Trypanosoma species	Results	Ref.
Acanthospermum hispidum	Asteraceae	Sesquiterpene lactones (**6**) and (**7**)	*T.b. brucei*	(**6**) IC_{50} = 2.45 µM (SI = 5.75) (**7**) IC_{50} = 6.36 µM (SI = 6.48)	Ganfon *et al*., 2012
Ageratum conyzoides L.	Asteraceae	Dichloromethane extract	*T.b. rhodesiense*	IC_{50} = 0.78 µg/ml (SI= 47)	Nour *et al*., 2010
Alstonia congensis	Apocynaceae	Stem, root, bark, leaves methanol extracts.	*T.b. brucei*	stem bark IC_{50} = 2.02 µg/ml (SI = 16)	Lumpu *et al*., 2013
Anacyclus pyrethrum L.	Asteraceae	Dichloromethane extract Alkamide derivate (**23**)	*T. b. rhodesiense*	IC_{50} > 10 µg/ml (**23**) IC_{50} = 2.26 µg/ml	Althaus *et al*., 2017
Annickia Kummeriae	Annonaceae	Methanol extract Palmatine (**26**)	*T. b. rhodesiense*	IC_{50} = 2.5 µg/ml (SI = 12) (**26**) IC_{50} = 3.2 µg/ml (SI = 28)	Malebo *et al*., 2013
Artemisia annua	Asteraceae	Dichloromethane extract	*T.b. brucei*	IC_{50} = 1.8 µg/mL	Efferth *et al*., 2011
Ceasalpinia benthamiana	Fabiaciae	Methanol extract	*T.b. brucei*	IC_{50} = 13 µg/ml (SI = 2.5)	Loua *et al*., 2017
Cissampelos pareira	Menispermaceae	Cissampeloflavone (**10**)	*T.b. rhodesiense*	IC_{50} = 0.61 µg/mL	Ramírez *et al*., 2003
Greenwaydendron suaveolens	Annonaceae	Dichloromethane extract	*T.b. brucei*	IC_{50} = 0.5 µg/ml (SI = > 100)	Musuyu Muganza, *et al*., 2016
Holarrhena africana	Apocynaceae	Alkaloid-rich fraction	*T.b.rhodesiense*	IC_{50} = 0.9 µg/ml (SI = 48.4)	Okeke Nnadi *et al*., 2017
Phyllanthus piscatorum	Euphorbiaceae	Justicidin B (**8**) Piscatorin (**9**)	*T.b. rhodesiense*	(**8**) IC_{50} = 0.2 µg/mL (**9**) IC_{50} = 2.3 µg/mL	Gertsch *et al*., 2003

Senna spectabilis	Fabaceae	Dichloromethane extract (+)-spectaline (**27**) iso-6-spectaline (**28**)	*T.b.rhodesiense*	IC_{50} = 0.45 µg/ml (SI = 144) (**27**) IC_{50} = 0.13 µg/ml (SI = 135) (**28**) IC_{50} = 0.23 µg/ml (SI = 124)	Lim *et al*., 2018
Tabernaemontana longipes	Apocynaceae	Bauerenol acetate (**29**) Bauerenol (**30**)	*T.b. rhodesiense*	(**29**) IC_{50} = 3.1 µM (SI = > 40) (**30**) IC_{50} = 2.7 µM (SI = > 40)	Carothers *et al*., 2018
Vernonia cinerascens	Asteraceae	Dichloromethane extract Vernodalin (**31**)	*T.b. rhodesiense*	IC_{50} = 0.24 µg/ml (SI = 30) (**31**) IC_{50} = 0.16 µg/ml (SI = 35)	Kimani *et al*. 2018

Essential oils (EOs) and pure compounds

Cymbopogon citratus	Poaceae	Aerial parts EO	*T.b. brucei*	IC_{50} = 3.2 µg/mL (SI = 9)	Costa *et al*., 2018
Erigeron floribundus	Asteraceae	Aerial parts EO Limonene	*T.b. brucei*	IC_{50} = 33.5 µg/mL (SI = >5.97) IC_{50} = 5.6 µg/mL (SI = >17.85)	Petrelli *et al*., 2016
Juniperus oxycedrus	Cupressaceae	Aerial parts EO	*T.b. brucei*	IC_{50} = 0.9 µg/ml (SI = 64)	Costa *et al*., 2018
Keetia leucantha	Rubiaceae	Aerial parts EO Ursolic acid	*T.b. brucei*	IC_{50} = 20.9 µg/mL IC_{50} = 2.5 µg/mL	Bero *et al*., 2013
Lavandula luisieri	Lamiaceae	Influorescence EO	*T.b. brucei*	IC_{50} = 5.7 µg/ml (SI = 12)	Costa *et al*., 2018
Seseli tortuosum	Apiaceae	Aerial parts EO	*T.b. brucei*	IC_{50} = 10.4 µg/ml (SI = 2.2)	Costa *et al*., 2018
Syzygium aromaticum	Myrtaceae	Floral buttons EO	*T.b. brucei*	IC_{50} = 10.4 µg/ml (SI = 2.2)	Costa *et al*., 2018
Thymbra capitata	Lamiaceae	Aerial parts EO	*T.b. brucei*	IC_{50} = 14.2 µg/ml (SI = 6.1)	Costa *et al*., 2018

References

Abdi, R.D., Agga, G.E., Aregawi, W.G. (2017). A systematic review and meta-analysis of trypanosome prevalence in tsetse flies. *BMC Vet. Res.. 13*, 100.

Achan, J., Talisuna, A.O., Erhart, A. (2011). Quinine, an old anti-malarial drug in a modern world: role in the treatment of malaria. *Malar. J. 10*, 144.

Akiyoshi, B., Gull, K. (2013). Evolutionary cell biology of chromosome segregation: insights from trypanosomes. *Open Biol. 3*, 130023-133029.

Al Musayeib, N.M., Mothana, R.A., Gamal, A.A.E., Al-Massarani, S.M., Maes, L. (2013) *In Vitro* Antiprotozoal Activity of Triterpenoid Constituents of *Kleinia odora* Growing in Saudi Arabia. *Molecules 18*, 9207-9218.

Althaus, J.B., Malyszek, C., Kaiser, M.; Brun, R., Schmidt, T.J. (2017). Alkamides from *Anacyclus pyrethrum* L. and their in vitro Antiprotozoal Activity. *Molecules 22*, 796.

Althaus, J.B.; Kaiser, M.; Brun, R.; Schmidt, T.J. (2014) Antiprotozoal Activity of *Achillea ptarmica* (Asteraceae) and Its Main Alkamide Constituents. *Molecules 19*, 6428-6438.

Babokhov, P., Sanyaolu, A.O., Oyibo, W.A., Fagbenro-Beyioku, A.F., *et al*. (2013). A current analysis of chemotherapy strategies for the treatment of human African trypanosomiasis. *Pathog. Glob.Health 107*, 242-252.

Bacchi, C.J. (2009). Chemotherapy of Human African Trypanosomiasis. *Interdisciplinary Perspect.Infect. Dis. 2009*, 195040-195045.

Baral, T.N. (2010). Immunobiology of African trypanosomes: need of alternative interventions, *J. Biomed Biotechnol 2010*, 389153.

Barrett, M. P., Vincent, I. M., Burchmore, R. J., Kazibwe, A. J., et al. (2011). *Future Microbiol. 6*, 1037-1045.

Barry, J.D., McCulloch, R. (2001). Antigenic variation in trypanosomes: enhanced phenotypic variation in a eukaryotic parasite. *Adv. Parasitol. 49*, 1-70.

Bero, J., Beaufaya, C., Hannaert , V.,b, Hérent , M.-F., et al. (2013). Antitrypanosomal compounds from the essential oil and extracts of Keetia leucantha leaves with inhibitor activity on Trypanosoma brucei glyceraldehyde-3-phosphate dehydrogenase. *Phytomedicine 20*, 270–274.

Bisser, S., N'Siesi, F.X., Lejon, V., Preux, P.M., *et al*. (2007). Equivalence trial of melarsoprol and nifurtimox monotherapy and combination therapy for the treatment of second-stage *Trypanosoma brucei gambiense* sleeping sickness. *J Infect Dis. 195*, 322–329.

Bonnet, J.; Boudot, C.; Courtioux, B. (2015). Overview of the Diagnostic Methods Used in the Field for Human African Trypanosomiasis: What Could Change in the Next Years? *BioMed Res. Int.. 2015*, 583262.

Broden, A. (1904). Les infections à trypanosomes au Congo chez l'homme et les animaux (communication préliminaire). *Bull Soc d'Etudes Colon 11*,116-139.

Bruce, D. (1895). Preliminary report on the tsetse fly disease or nagana in Zululand Durban. Bull Soc d'Etudes Colon *6*, 128-142.

Bukachi, S.A., Wandibba, S., Nyamongo, I.K. (2017). The socio-economic burden of human African trypanosomiasis and the coping strategies of households in the South Western Kenya foci. *PLoS Negl. Trop. Dis. 11*, e0006002.

Büscher, P., Cecchi, G., Jamonneau, V., Priotto, G. (2017) Human African trypanosomiasis, *The Lancet* 390, 2397-2409.

Carothers, S.; Nyamwihura, R.; Collins, J.; Zhang, H.; Park, H.; Setzer, W.N.; Ogungbe, I.V. Bauerenol Acetate, the pentacyclic triterpenoid from *Tabernaemontana longipes*, is an antitrypanosomal agent. *Molecules*, **2018**, 23(2): doi:10.3390/molecules23020355.

Carter, N.S., Fairlamb, A.H. (1993). Arsenical-resistant trypanosomes lack an unusual adenosine transporter *Nature* 14, 173-176.

CDC. Life cycle of *Trypanosoma spp*. Available from: http://www.cdc.gov/dpdx/trypanosomiasisAfrican/index.html.

Cecchi, G., Mattioli, R.C., Slingenbergh, J., de La Rocque. S. (2008) Land cover and tsetse fly distributions in sub-Saharan Africa. *Med. Vet. Entomol. 22*, 364–73.

Chanie, M.; Adula, D.; Bogale, B. (2013) Socio-Economic Assessment of the Impacts of Trypanosomiasis on Cattle in Girja District, Southern Oromia Region, Southern Ethiopia. *Acta Parasitologica Globalis 4*, 80-85.

Checchi, F., Filipe, J.A., Haydon, D.T., Chandramohan, D., *et al*. (2008). Estimates of the duration of the early and late stage of gambiense sleeping sickness. *BMC Infect. Dis. 8*, 1.

Checkley, A.M., Pepin, J., Gibson, W.C., Taylor, M.N., *et al*. (2007) Human African trypanosomiasis: diagnosis, relapse and survival after severe melarsoprol-induced encephalopathy. *Roy. Soc. of Trop. Med. H. 5*, 523–526.

Cortez, A. P., Ventura, R.M., Rodrigues, A. C., Batista, J. S., *et al*. (2006). The taxonomic and phylogenetic relationships of Trypanosoma vivax from South America and Africa. *Parasitology 133*, 159–169.

Costa, S., Cavadas, C., Cavaleiro, C., Salgueiro, L. (2018). In vitro susceptibility of Trypanosoma brucei brucei to selected essential oils and their major components. *Exp Parasitol. 190*, 34-40.

Cox, F. (2004). History of sleeping sickness (African trypanosomiasis). *Infect Dis Clin N Am 18*, 231-245.

De Mieri, M., Monteleone, G., Ismajili, I., Kaiser, M., Hamburger, M. (2017). Antiprotozoal Activity-Based Profiling of a Dichloromethane Extract from Anthemis nobilis Flowers. *J. Nat. Prod. 80*, 459-470.

Denise, H., Giroud, C., Barrett, M.P., Baltz, T. (1999).Affinity chromatography using trypanocidal arsenical drugs identifies a specific interaction between glycerol-3-phosphate dehydrogenase from *Trypanosoma brucei* and Cymelarsan. *Eur. J. Biochem*, 259, 339-346.

DNDi. Sanofi, DNDi seek European Medicines Agency review for sleeping sickness treatment. Available from: https://www.dndi.org/2018/media-centre/press-releases/sanofi-dndi-seek-ema-review-for-sleeping-sickness-treatment/. Accessed November 26, 2018.

DNDi. European Medicines Agency recommends fexinidazole, the first oral treatment for sleeping sickness. Available from: https://www.dndi.org/2018/media-centre/press-releases/ema-recommends-fexinidazole-first-all-oral-treatment-sleeping-sickness/. Accessed November 26, 2018.

Dubois, M.E., Demick, K. P., Mansfield, J. M. (2005). Trypanosomes Expressing a Mosaic Variant Surface Glycoprotein Coat Escape Early Detection by the Immune System. *Infect*. *Imm*.*73*, 2690–2697.

Dutton, J.E. (1902). Preliminary note upon a trypanosome occurring in the blood of man. *Thompson Yates Lab Rep*., 4, 455–468.

Dyer, N.A., Rose, C,, Ejeh, N.O., Acosta-Serrano, A., et al. (2013). Flying tryps: survival and maturation of trypanosomes in tsetse flies. *Trends Parasitol*. *4*, 188-196.

Efferth, T., Herrmann, F., Tahrani, A., Wink, M. (2011). Cytotoxic activity of secondary metabolites derived from Artemisia annua L. towards cancer cells in comparison to its designated active constituent artemisinin. *Phytomedicine 18*, 959-969.

Forde, R.M. (1902) Some clinical notes on a European patient in whose blood a trypanosome was observed. *J Trop Med*. *5*, 261–263.

Franco, J.R., Cecchi, G., Priotto, G., Paone, M., *et al*. (2017) Monitoring the elimination of human African trypanosomiasis:Update to 2014. *PLoS Negl Trop Dis*. *1*, e0005585.

Franco, J.R., Simarro, P.P., Diarra, A.; Jannin, J.G. (2014) Epidemiology of human African trypanosomiasis. *Clinical Epidemiology 6*, 257-275.

Ganfon, H., Bero, J., Tchinda, A.T., Gbaguidi, F., *et al*. (2012). Antiparasitic activities of two sesquiterpenic lactones isolated from Acanthospermum hispidum D.C. *J*. *Ethnopharmacol*. *141*, 411-417.

Geiger, A., Cuny, G., Frutos, R. (2005) Two Tsetse Fly Species, *Glossina palpalis gambiensis* and *Glossina morsitans morsitans*, Carry Genetically Distinct Populations of the Secondary Symbiont *Sodalis glossinidius*. *Applied and Environmental Microbiology 71*, 8941-8943.

Gertsch, J., Tobler, T.R.; Brun, R.; Sticher, O., *et al*. (2003). Antifungal, Antiprotozoal, Cytotoxic and Piscicidal Properties of Justicidin B and a New Arylnaphthalide Lignan from Phyllanthus piscatorum. *Planta Med*. *69*, 420-424.

Gibson, W. C. (2005). The SRA gene: the key to understanding the nature of Trypanosoma brucei rhodesiense. *Parasitology 131*, 143-150.

Gurib-Fakim , A. (2006). Medicinal plants: traditions of yesterday and drugs of tomorrow. *Mol Aspects Med 27*, 1–93.

Haag, J., O'hUigin, C., Overath, P. (1998) The molecular phylogeny of trypanosomes: evidence for an early divergence of the Salivaria. *Mol Biochem Parasitol*. *91*, 37-49.

Hide, G., Tait, A,, Maudlin, I., Welburn, S.C. (2007) The origins, dynamics and generation of Trypanosoma brucei rhodesiense epidemics in East Africa. *Parasitology Today 12*, 50-55.

Jacobs, R. T., Nare, B., Wring, S. A., Orr, M. D., et al. (2011). SCYX-7158, an orally-active benzoxaborole for the treatment of stage 2 human African trypanosomiasis. PLoS Neglected Trop. Dis. 5, e1151.

Jamonneau, V., Ravel, S., Koffi, M., Kaba, D., *et al*. (2004). Mixed infections of trypanosomes in tsetse and pigs and their epidemiological significance in a sleeping sickness focus of Cote d'Ivoire. *Parasitology 129*, 693–702.

Jansen, O., Tchinda, A.T., Loua, J. *et al*. (2017). Antiplasmodial activity of Mezoneuron benthamianum leaves and identification of its active constituents. *Journal of Ethnopharmacology*, *203*, 20-26.

Johnston, T.A. (1908). A case of sleeping sickness treated with atoxyl; apparent recovery. *The Lancet 172*, 867-869.

Jordan, A.M. (1976). Tsetse flies as vectors of trypanosomes. *Veterinary Parasitology 2*, 143–152.

Kambu, K. (1990). Eléments de phytothérapie comparés, Plantes Médicinales Africaines. CRP-Kinshaza, Zaire.

Keating, J., Yukich, J.O., Sutherland, C.S., Woods, G., *et al*. (2015). Human African trypanosomiasis prevention, treatment and control costs: A systematic review. *Acta Trop*.*150*, 4-13.

Kimani, N.M., Matasyoh, J.C., Kaiser, M., Brun, R., *et al*. (2018). Sesquiterpene Lactones from *Vernonia cinerascens* Sch. Bip. and Their in Vitro Antitrypanosomal Activity. *Molecules 23*, 248.

Kimani, N.M., Matasyoh, J.C., Kaiser, M., Brun, R., *et al*. (2018). Antiprotozoal Sesquiterpene Lactones and Other Constituents from Tarchonanthus camphoratus and Schkuhria pinnata *Journal of Natural Products 81*, 124-130.

Kimani, N.M., Matasyoh, J.C., Kaiser, M., Brun, R., et al. (2017). Anti-Trypanosomatid Elemanolide Sesquiterpene Lactones from Vernonia lasiopus O. Hoffm. *Molecules 22*, 597.

Lestrade-Carluer De Kyvon MA, Maakaroun-Vermesse Z, Lanotte P, *et al*. (2016). Congenital trypanosomiasis in child born in France to African mother. *Em Inf Dis 22*, 935–937.

Lim, K.T., Amanah, A., Chear, N.J., Zahari, Z.; *et al*. (2018). Inhibitory effects of (+)-spectaline and iso-6-spectaline from Senna spectabilis on the growth and ultrastructure of human-infective species Trypanosoma brucei rhodesiense bloodstream form. *Experimental Parasitology*, *184*, 57-66.

Loua, J., Traore, M.S., Camara, A. *et al*. (2017). Biological and Phytochemical Investigations on *Caesalpinia benthamiana*, a Plant Traditionally Used as Antimalarial in Guinea. *Evidence-based Complem*. *Alternat*. *Med*. *: eCAM*. 2017, 9438607.

Lumpu, S.L., Kikueta, C.M., Tshodi, M.E., Mbenza, A.P., *et al*. (2013). Antiprotozoal screening and cytotoxicity of extracts and fractions from the leaves, stem bark and root bark of Alstonia congensis, *J*. *Ethnopharmacol*. *148*, 724-727.

Lutumba, P., Makieya, E., Shaw, A., Meheus, F., et al. (2007). Human African Trypanosomiasis in a rural community, Democratic Republic of Congo. *Emerg Infect Dis*.*13*, 248–254.

Magez, S., Caljon, G., Tran, T., Stijlemans, B., *et al*. (2010). Current status of vaccination against African trypanosomiasis. *Parasitology 137*, 2017–2027.

Malebo, H.M., Tanja, W., Cal, M., Swaleh, S.A.,et al. (2009). Antiplasmodial, anti-trypanosomal, anti-leishmanial and cytotoxicity of selected Tanzanian medicinal plants. *Tanzan*. *J*. *Health Res*. *11*, 226-234.

Malebo, H.M., Wenzler, T., Cal, M. *et al*. (2013). Anti-protozoal activity of aporphine and protoberberine alkaloids from *Annickia kummeriae* (Engl. & Diels) Setten & Maas (Annonaceae). *BMC Complem.Altern. Med. 13*, 48.

Malvy, D., Chappuis, F. (2011). Sleeping sickness. *Clin. Microbiol. Inf*. 17, 986-995.

Mamoon-Ur -Rashid Ali, S., Alamzeb, M., Igoli, J., Clements, C., *et al*. (2014). Phytochemical and antitrypanosomal investigation of the fractions and compounds isolated from *Artemisia elegantissima Pharm. Biol. 52*, 983-987.

Mato, K.B. (2005). Savoir-faire local dans la périphérie de la partie Sud-Ouest du parc national de la Salonga. Mémoire DEA Biologie, Université de Kinshasa, Kinshasa.

Mc Kean, P.G. (2003) Coordination of cell cycle and cytokinesis in Trypanosoma brucei. *Curr Opin Microbiol. 6*, 600-607.

Mesu,V.K.B.K., Kalonji, W.M., Bardonneau, C. *et al*. (2018). Oral fexinidazole for late-stage African *Trypanosoma brucei gambiense* trypanosomiasis: a pivotal multicentre, randomised, non-inferiority trial. *Lancet 391*,144-154.

Meyskens, F.L., Gerner, E.W. (1999). Development of difluoromethylornithine (DFMO) as a chemoprevention agent. *Clin Cancer Res 5*, 945-951.

Mishina, Y.V., Krishna, S., Haynes, R.K., Meade, J.C. (2007). Artemisinins Inhibit *Trypanosoma cruzi* and *Trypanosoma brucei rhodesiense* In Vitro Growth. *Antimicrobial Agents and Chemotherapy 51*, 1852-1854.

Mogk, S., Meiwes, A., Boßelmann, C.M., Wolburg, H., *et al*. (2014). The lane to the brain: how African trypanosomes invade the CNS. *Trends in Parasitology 30*, 470-477.

Molina-Portela, M..P., Samanovic, M., Raper, J. (2008). Distinct roles of apolipoprotein components within the trypanosome lytic factor complex revealed in a novel transgenic mouse model. *J Exp Med. 205*, 1721-1728.

Moloo, S. K., Kabata, J. M., Gitire, N. M. (2000). Study on the mechanical transmission by tsetse fly Glossina morsitans centralis of Trypanosoma vivax, T. congolense or T. brucei brucei to goats. *Acta Tropica 74*, 105–108.

Muangphrom, P.; Seki, H.; Fukushima, E.O.; Muranaka, T.(2016). Artemisinin-based antimalarial research: application of biotechnology to the production of artemisinin, its mode of action, and the mechanism of resistance of *Plasmodium* parasites. *J.Nat. Med. 70*, 318-334.

Murray, C.J. (2012). Disability-adjusted life years (DALYs) for 291 diseases and injuries in 21 Musuya Muganza, M. (2006).Contribution à la revue des plantes médicinales des Nkundo au Sud-Ouest du parc national de la Salonga. Mémoire DEA biologie. Université de Kinshasa, Kinshasa.

Musuyu Muganza, D., Fruth, B., Lami Nzunzu, J., Tuenter, E., *et al*. (2016). In vitro antiprotozoal activity and cytotoxicity of extracts and isolated constituents from Greenwayodendron suaveolens, *J.Ethnopharmacol. 193*, 510-516.

Musuyu Muganza, D., Fruth, B.I., Nzunzu Lami, J., Mesia, G.K., *et al*. (2012). In vitro antiprotozoal and cytotoxic activity of 33 ethonopharmacologically selected medicinal plants from Democratic Republic of Congo. *J.Ethnopharmacol. 141*, 301-308.

Newman, D.J., Cragg, G.M. (2014). Natural products as sources of new drugs over the last 30 years. *J Nat Prod*. *70*, 461–477.

News-medical. DNDi announces successful completion of SCYX-7158 Phase I study for treatment of sleeping sickness. (Accessed Sep 27, 2018).

Nkinin, S.W., Njiokou, F,, Penchenier, L., Grebaut, P., *et al*. (2002). Characterization of trypanosoma brucei s.l. subspecies by isoenzymes in domestic pigs from the Fontem sleeping sickness focus of Cameroon. *Acta Trop*. *81*, 225–232.

Nnadi, C.O., Nwodo, N.J., Kaiser, M., Brun, R., *et al*. (2017). Steroid Alkaloids from *Holarrhena africana* with Strong Activity against *Trypanosoma brucei rhodesiense*. *Molecules 22*, 1129.

Nogueira, M.S., Da Costa, F.B., Brun, R., Kaiser, M., *et al*. (2016). *ent*-Pimarane and *ent*-Kaurane Diterpenes from *Aldama discolor* (Asteraceae) and Their Antiprotozoal Activity. *Molecules 21*, 1237.

Nour, A.M.M., Khalid, S.A., Kaiser, M., Brun, R., *et al*. (2010). The antiprotozoal activity of methylated flavonoids from Ageratum conyzoides L. *J.Ethnopharmacol*. *129*, 127-130.

Odiit, M., Kansiime, F., Enyaru, J.C. (1997). Duration of symptoms and case fatality of sleeping sickness caused by Trypanosoma brucei rhodesiense in Tororo, Uganda. *East Afr*. *Med*. *J*. *74*, 792–795.

Okeke Nnadi, C., Nwodo, N.J., Kaiser, M., Brun, R. *et al*. (2017). Steroid Alkaloids from Holarrhena Africana with Strong Activity against Trypanosoma brucei rhodesiense. *Molecules 22*, 1129.

Ortiz, S., Dali-Yahia, K., Vasquez-Ocmin, P., Grougnet, R., *et al*. Heme-binding activity of methoxyflavones from Pentzia monodiana Maire (Asteraceae). *Fitoterapia 118*, 1-5.

Petrelli, R., Orsomando, G., Sorci, L., Maggi, F., *et al*. (2016). Biological Activities of the Essential Oil from *Erigeron floribundus*. *Molecules 21*, 1065.

Priotto, G., Pinoges, L., Fursa, I.B., Burke, B., *et al*. (2008). Safety and effectiveness of first line eflornithine for *Trypanosoma brucei gambiense* sleeping sickness in Sudan: cohort study. *BMJ 336*, 705-708.

Ramírez, I., Carabot, A., Meléndez, P., Carmona, J., *et al*. (2003). Cissampeloflavone, a chalcone-flavone dimer from Cissampelos pareira. *Phytochemistry 64*, 645–647.

Seke Etet, P.F., Fawzi Mahomoodally, M. (2012). New Insights in Staging and Chemotherapy of African Trypanosomiasis and Possible Contribution of Medicinal Plants. *The Scientific World Journal*. *2012*, 343652.

Silveira, N., Saar, J., Santos, A.D.C., Barison, A., *et al*. (2016). A New Alkamide with an Endoperoxide Structure from *Acmella ciliata* (Asteraceae) and Its *in Vitro* Antiplasmodial Activity. *Molecules 21*, 765.

Simarro, P.P., Cecchi, G,, Paone, M., Franco, J.R., *et al*. (2010). The atlas of human African trypanosomiasis: a contribution to global mapping of neglected tropical diseases. *Int J Health Geogr 9*, 57.

Simarro, P.P., Cecchi, G., Franco, J.R., Paone, M., *et al*. (2012). Estimating and Mapping the Population at Risk of Sleeping Sickness. *PLoS Negl Trop Dis*. *6*, e1859.

Skaf, J., Hamarsheh, O., Berninger, M., Balasubramanian, S., *et al*. (2018). Improving anti-trypanosomal activity of alkamides isolated from Achillea fragrantissima. *Fitoterapia 125*, 191-198.

Stephens, J.W.W., Fantham, H.B. (1910). On the peculiar morphology of a trypanosome from a case of sleeping sickness and the possibility of its being a new species (T. rhodesiense). *Proc R Soc Lond B 83*, 28-33.

Steketee, P.C., Vincent, I.M., Achcar, F., Giordani, F., *et al*. (2018). Benzoxaborole treatment perturbs S-adenosyl-L-methionine metabolism in Trypanosoma brucei. *PLoS Negl Trop Dis*. *12*, e0006450.

Sternberg, J.M., Gierlinski, M,, Bieler, S., Ferguson, M.A., *et al*. (2014). Evaluation of the diagnostic accuracy of prototype rapid tests for human African trypanosomiasis. *PLoS Negl Trop Dis 8*,e3373.

Steverding, D. (2008). The history of African trypanosomiasis. *Parasite Vector 1*, 3-11.

Stich, A., Abel, P.M., Krishna, S. (2002). Human African trypanosomiasis. *BMJ : British Medical Journal 325*, 203-206.

Sut, S., Dall'Acqua, S., Baldan, V., Ngahang Kamte, S.L., Ranjbarianb, F., *et al*. (2018). Identification of tagitinin C from Tithonia diversifolia as antitrypanosomal compound using bioactive-guided fractionation. *Fitoterapia*. *124*, 145-151.

Sutherland, C. S., Yukich, J., Goeree, R., Tediosi, F. (2015). A Literature Review of Economic Evaluations for a Neglected Tropical Disease: Human African Trypanosomiasis ("Sleeping Sickness"). *PLoS Negl.Trop*. *Dis*.*9*, e0003397.

Sutherland, C.S., Stone, C.M., Steinmann, P., Tanner, M., *et al*. (2017). Seeing beyond 2020: an economic evaluation of contemporary and emerging strategies for elimination of Trypanosoma brucei gambiense. *Lancet Glob Health 5*, e69-e79.

Torreele, E., Bourdin Trunz, B., Tweats, D., Kaiser, M., *et al*. (2010). Fexinidazole-a new oral nitroimidazole drug candidate entering clinical development for the treatment of sleeping sickness. *PLoS Negl Trop Dis*. *4*, e923.

Traore, M.S., Baldé, M.A., Dialo, A. *et al*. (2013). Ethnobotanical survey on medicinal plants used by Guinean traditional healers in the treatment of malaria. *J.Ethnopharmacol*. *150*, 1145-1153.

Tu, Y. (2011). The discovery of artemisinin (qinghaosu) and gifts from Chinese medicine. *Nat Med*. *17*,1217-1220.

Vásquez-Ocmín, P., Cojean,S.; Rengifo, E., Suyyagh-Albouz, S., *et al*. (2018). Antiprotozoal activity of medicinal plants used by Iquitos-Nauta road communities in Loreto (Peru), *J*. *Ethnopharmacol*. *210*,372-385.

Vieagas, C., Bolzani, V.D.S., Furlan, M., Barreiro, E.J., *et al*. (2004). Further bioactive piperidine alkaloids from the flowers and green fruits of Cassia spectabilis. *J*. *Nat*. *Prod*. *67*, 908-910.

Wamwiri, F.N., Changasi, R.E. (2016). Tsetse Flies (*Glossina*) as Vectors of Human African Trypanosomiasis: A Review. *BioMed Research International*. *2016*, 6201350.

WHO (2013). Control and surveillance of human African trypanosomiasis. *World Health Organ Tech Rep Ser 984,* 1-237.

Wiedemar, N., Graf, F. E., Zwyer, M.; Ndomba, E.,*et al*. (2018). Beyond immune escape: a variant surface glycoprotein causes suramin resistance in *Trypanosoma brucei*. *Molecular Microbiology*, *107*, 57-67.

Wilkinson, S.R., Taylor, M.C., Horn, D., Kelly, J.M., et al. (2008). A mechanism for cross-resistance to nifurtimox and benznidazole in trypanosomes. *Proc Natl Acad Sci U S A*. *105*,5022-5027.

Zahari,Z., Jani,N.A., Amanah, A., Latif, M.N., *et al*. (2014). Bioassay-guided isolation of a sesquiterpene lactone of deoxyelephantopin from Elephantopus scaber Linn. active on Trypanosome brucei rhodesience. *Phytomedicine 21*, 282-285.

Ziemann, H. (1905). Beitrag zur Trypanosomenfrage. Zentralbl Bakteriol Parasitenk Infektionskrankh, *Abt I Orig 38*, 307-314.

Zimmermann, S., Kaiser, M., Brun, R., Hamburger, M., *et al*. (2012). Cynapropicrin: the first plant natural product with in vivo activity against Trypanosoma brucei. *Planta*. *Med*. 78, 553-556.

CHAPTER 2.

Phytochemical analysis and bioactive constituents of the Mexican sunflower *Tithonia diversifolia* (Asteraceae)

"If you think you're too small to make a difference,

try going to bed with a mosquito or a tse-tse fly in the room"

Old African proverb

Chapter 2 Outline

Abbreviation

1D and 2D NMR = One and two-dimensional nuclear magnetic resonance

A375 = Human malignat melanoma cells

ABTS = 2,2'-Azino-bis(3-ethylbenzothiazoline-6-sulfonic acid)

BALB//3T3 = Mouse fibroblasts

CH_2Cl_2/MeOH = Methylene chloride/Methanol

DMSO = Dimethylsulfoxide

DPPH = 2,2-Diphenyl-1-picrilhydrayl

FRAP = Ferric reducing antioxidant power

HAT= Human African Trypanosomiasis

HCT116 = Human colon carcinoma cells

MDA-MB231 = Human breast adenocarcinoma cells

MTT = 3-(4,5-Dimethyl-2-thiazolyl)-2,5-diphenyl-2H-tetrazoliumbromide

NAD = Nicotinamide adenine dinucelotide

NadD = Nicotinate monucleotide adenylyltransferase

NaMN = Nicotinate mononucleotide

NMN = Nicotinamide mononucleotide

NTDs = Neglected tropical diseases

SAR = Structure-activity relationship

SI = Selectivity index

STLs = Sesquiterpene lactones

T. brucei = *Trypanosoma brucei*

T98G = Human glioblastoma multiforme cells

TC221 = *T. brucei* bloodstream-form parasites

TEAC = Tocopherol-equivalent antioxidant capacity

TLC: Thin layer chromatography

WHO = World Health Organization

Abstract

Tithonia diversifolia (Asteraceae), well-known as Mexican sunflower, is an invasive shrub growing in tropical areas of South America, Asia and Africa where is used as traditional medicine for the treatment of various diseases, including malaria, as ornamental plant and green biomass to improve soil fertility. Although numerous studies have assessed the antimalarial properties, nothing is known about the effect of *T. diversifolia* extracts on trypanosomiasis. In the first part of this Chapter the extracts of *T. diversifolia* aerial parts were evaluated for their bioactivity against *Trypanosoma brucei*. The activity was studied against bloodstream forms of *T. brucei* (TC221), as well as against mammalian cells (BALB/3T3 mouse fibroblasts), as a counter-screen for toxicity. Both methanolic and aqueous extracts showed significant effects with IC_{50} values of 1.1 and 2.2 μg/mL against *T. brucei* (TC221) and 5.2 and 3.7 μg/mL against BALB/3T3 cells, respectively. A bioassay-guided fractionation on the methanolic extract yielded in identification of active fractions (F8 and F9) with IC_{50} values of 0.41 and 0.43 μg/mL, respectively, against *T. brucei* (TC221) and 1.4 and 1.5 μg/mL, respectively, against BALB/3T3 cells. The phytochemical composition of the extracts and the purified fractions were investigated using HPLC-ESI-MS/MS and 1D and 2D NMR spectra showing the presence of sesquiterpene lactones that in turn were subjected to the isolation procedure. Tagitinins A and C were rather active but the latter presented a very strong inhibition on *T. brucei* (TC221) with an IC_{50} value of 0.0042 μg/mL. This activity was 4.5 times better than that of the reference drug suramin. The results of this study shed light on the antitrypanosomal effects of *T. diversifolia* extracts and highlighted tagitinin C as one of the possible responsible for this effect.

Given the traditional uses in the treatment of skin infections, in the second part of this Chapter we have analysed the chemical composition and the antimicrobial effects of the essential oil hydrodistilled from inflorescences of *T. diversifolia*. For the purpose the inhibition zones against a panel of pathogens were measured by the agar diffusion method. In addition, we evaluated the inhibitory effects on several NaMN/NMN adenylyltransferases, which are essential enzymes for NAD biosynthesis in most bacterial pathogens, and also tested the inhibition on the mammalian orthologue enzymes as a promising way to identify novel natural antibiotics. To complete the screening of biological effects, the antioxidant capacity and antiproliferative effects on human tumor cells were evaluated using the DPPH, ABTS, FRAP, and MTT methods. Results showed that *T. diversifolia* essential oil was mostly active against *Staphylococcus aureus* with a halo of 14 mm. The essential oil selectively inhibited *in vitro* the pure NAD biosynthetic enzyme NadD from *S. aureus* (IC_{50} of ~60 μg/mL), with basically none or only minor effects on mammalian orthologue

enzymes. Finally, the essential oil displayed significant cytotoxic effects on A375, MDA-MB231, HCT 116 and T98 G tumor cells with IC_{50} values of 3.02, 3.79, 3.46 and 12.82 μg/mL, respectively, and noticeable radical scavenging activity on DPPH and ABTS radicals, with IC_{50} values of 108.8 and 41.7 μg/mL, respectively.

Finally, in the last part of the Chapter we evaluated the potential of *T. diversifolia* against the two-spotted spider mite *Tetranychus urticae* (Tetranychidae), which is one of the most economically important arthropod pests worldwide. The leaf methanolic extract and its ethyl acetate fraction were tested for acute and chronic toxicity and for oviposition inhibitory effects. The chemical composition of the extracts was analysed by HPLC-MS^n and NMR and the main constituents resulted to be flavonoid derivatives, phenylpropanoids and sesquiterpene lactones (with tagitinins A and C as the more abundant compounds). In acute toxicity assays, mortality did not exceed 50% even for the highest tested dose of 150 $\mu g.cm^{-3}$. However, in chronic toxicity assays, on day 5 from application, the methanolic extract LD_{50} was 41.3 $\mu g.cm^{-3}$ while LD_{90} was 98.7 $\mu g.cm^{-3}$. Furthermore, both *T. diversifolia* extracts inhibited oviposition in *T. urticae*. The ethyl acetate extract was the most active oviposition inhibitor, with an ED_{50} value of 44.3 $\mu g.cm^{-3}$ and an ED_{90} of 121.5 $\mu g.cm^{-3}$. Overall, the good yield rate of the extract and the high crop yield highlighted good prospects of using the extract from this plant for the development of mite oviposition inhibitors.

2.1 Introduction

Tithonia diversifolia (Hemsl.) A. Gray (Asteraceae) also known as Mexican sunflower is a widespread plant native to lowlands of southeastern Mexico and Central America (Figure 1). It is nowadays spread globally and found in Africa, Asia, Central and South America (La Duke, 1982). *T. diversifolia* is the most studied plant from the genus *Tithonia* which includes 13 taxa distributed in 11 species and two sections, *Tithonia* and *Mirasola* (Chagas-Paula *et al*., 2012). The different sections have morphological and specific chemical features. Section *Tithonia* includes perennial and annual herbs and diverges from the ancestral stock (*T. fruticose, T. pedunculata, T. diversifolia, T. koelzi, T. bradypoda, T. rotundifolia, T. thurberi* and *T. tubaefornis*), whereas *T. auriculata, T. calva, T. horundurensis* and *T. longiradiata* are members of the *Mirasola* section, which includes only perennial taxa. Other well-studied plants from the genus are *T. rotundifolia* and *T. tabaeformis* (Chagas-Paula *et al*., 2012). The specific name *diversifolia*, which means separated leaves, is a mix of two different Latin words, "diversus" and "folium" meaning divergent and leaf, respectively. Other scientific names as *Helianthus quinquelobus Sessé Moc., Mirasolia diversifolia Hemsl*., *Tithonia diversifolia var. diversifolia, Urbanisol tagetiflora* can be used to refer to the plant (Mabou *et al*., 2018). *T. diversifolia* grows as invaders of agricultural and non-agricultural lands and can be easily studied for phytochemicals thanks to the large amount of material. That feature makes it interesting for the production of phytomedicines and its production in large scale. Another important feature about *T. diversifolia* is the allelopathy pattern which consists in the inhibition of surroundings plants growth suggesting the release of secondary metabolites.

T. diversifolia is a 2-3 m high shrub or tree with solitary yellow inflorescence heads (capitulum) and glandular trichome on the areal parts. The sub-ovate and petiolate leaves are around 20 cm long. They are 3 to 7 lobed, hairy and alternatively to oppositely arranged. The plant flowers and produces seeds throughout the year and, a mature *T. diversifolia* plant can produce around 100000 seeds/m^2 (Yang *et al*., 2012; Orsomando *et al*., 2016). Because of its stoutness and showy capitula, *T. diversifolia* is widely used as an ornamental plant. The stem is striated with a hairy green surface which turns woody with a hollow core as the plant maturates. As it grows very fast, it is frequently invasive of agricultural and non-agricultural lands (Ayeni *et al*., 1997), and potentially useful as a green biomass to improve soil fertility (Jama *et al*., 2000). Several attempts to use *T. diversifolia* as a daily supplement in poultry diet have been carried out in Nigeria (Ekeocha, 2012). A recent paper published by Isrun *et al*. pointed out the attention on the use of *T. diversifolia*

compost as one of the methods to reduce the mercury (Hg) poisoning in soil contaminated by heavy metals and to improve the nutrient availability and uptake in plants (Isrun *et al*, 2018).

T. *diversifolia* compost bonds mercury in the soil and reduces the absorption of Hg^{2+} into plant tissues of vegetables that grow near gold mines.

Fig. 1. *Tithonia diversifolia* (Hemsl.) A. Gray. 1. Flowering branch; 2. Straight and glandular trichomes; 3. Outer phyllary; 4. Inner phyllary; 5. Palea; 6. Marginal sterile floret; 7. Disk floret; 8. Anthers; 9. Stylar branches; 10. Cypsela.

In tropical and sub-tropical regions, thanks to its abundant availability, *T*. *diversifolia* has become commonly used in the traditional medicine by local ethnic groups (Heinrich, 2000). In the native American traditional medicine the juice obtained from stems and leaves is used for the treatment of hematomas, abscesses and muscular cramps (Játem-Lásser *et al*., 1998), whereas taken orally is employed against malaria (Heinrich *et al*., 1998). Antique civilization such as Maya used the powder obtained by crashing toasted leaves to treat various skin diseases (Heinrich, 2000). In Africa, *T*. *diversifolia* is used orally for the treatment of diverse ailments. In Uganda, it is administered orally or to make baths to treat sexual transmitted infections. In Kenya, the Kikuyus tribe uses the leaf infusion for malaria treatment, as an antidote to snake bites as well as a veterinary medicine for cattle (Owuor *et al*., 2006; Njoroge *et al*., 2006). In Asia, the leaf aqueous extract is taken for the treatment of diabetes (Miura *et al*., 2005; Takahashi, 1998). Other applications of *T*. *diversifolia* include the treatment of ailments like fever, pains, diarrhea and hepatitis (Chagas *et al*., 2012; Mabou *et al*., 2018) and the effectiveness of some traditional uses above reported was demonstrated by rigorous scientific studies (Passoni *et al*., 2013).

To date, *T*. *diversifolia* has been largely studied and more than one hundred compounds have been isolated. The most abundant secondary metabolites isolated from *T*. *diversifolia* are mainly terpenoids, including sesquiterpenoids and diterpenoids. Other compounds include alkaloids, tannins, flavonoids, saponins and phenols (Olayinka *et al*., 2015). The major sesquiterpenoids isolated are sesquiterpene lactones (STL) which are considered as chemomarkers for Asteraceae and include germacronalide, eudesmanolides and guaianolides. The bitter tasting compounds tagitinins are the most studied germacronalides and nine classes have been identified so far that differ from each other according to oxygenation and unsaturation patterns (Mabou *et al*., 2018).

2.2 Chapter objectives

The objective of this study was to perform a complete phytochemical analysis on both polar and volatile compounds of *T*. *diversifolia* collected from a geographically isolated population living in Dschang, Cameroon and to assess their biological activity, namely the antitrypanosomal and amtimicrobial activities. For this purpose, the main secondary metabolites occurring in the *T*. *diversifolia* methanolic extract were isolated by column chromatography and structurally elucidated by MS and NMR techniques.

The essential oil was hydrodistilled from the flowerheads (capitula) of *T*. *diversifolia* and analyzed by GC-FID and GC-MS. To complete the screening of biological effects of essential oil, the antioxidant capacity and antiproliferative effects on human tumor cells were also evaluated using the DPPH, ABTS, FRAP, and MTT methods.

Besides its extensive utilizations in the traditional medicine, mainly to treat malaria, the plant is believed to have a great potential in agriculture of developing countries as a green biomass to produce fertilizer, fodder and biopesticides. For this reason, we decided to evaluate the potential of *T*. *diversifolia* polar extracts against the two-spotted spider mite *Tetranychus urticae* (Tetranychidae), which is one of the most economically important arthropod pests worldwide.

2.3 Discovery of antitrypanosomal agents through bioassay-guided fractionations of *T. diversifolia* extracts

As pointed out before, among several medicinal plants traditionally used in Africa to treat different diseases and having potential as a source of trypanocidal compounds, our attention has been attracted by *T. diversifolia*. Given its abundance in tropical areas of South America and Africa where it can be considered as a weed of cultivated and non-cultivated lands, *T. diversifolia* enjoys a long use as a traditional remedy in tropical regions (Heinrich, 2000). In particular, the plant leaves are used in Africa to treat malaria (Heinrich *et al*., 1998; Oyewole *et al*., 2004; Njoroge *et al*., 2006), due to the presence of bioactive compounds identified as germacranolide-type sesquiterpene lactones (called tagitinins) and tagitinin C represents the lead compound (Goffin *et al*., 2002; Ferreira *et al*., 2005). These sesquiterpene lactones (STLs) were also proven to exhibit anti-inflammatory/ analgesic (Mabou *et al*., 2018), antiproliferative (Liao *et al*., 2011), antifeedant (Ambrósio *et al*., 2008) and insecticidal activities (Castaño-Quintana *et al*., 2013). Other secondary characteristic metabolites of *T. diversifolia* are chlorogenic acid derivatives, diterpenoids, flavonoids, and essential oils (Orsomando *et al*., 2016).

Taking into the account that the potential of *T. diversifolia* secondary metabolites to interact with protozoan parasites (Goffin *et al*., 2002), we decided to investigate the effect of a *T. diversifolia* methanolic leaf extract against *T. brucei* using a bioassay-guided fractionation approach. To our knowledge, nothing is known about either the anti-trypanosomal activity of *T. diversifolia* extract or the components responsible for this effect.

Different techniques were applied for the identification of various phytoconstituents. Pure methanolic extract was initially studied by ^{1}H NMR and 2D NMR to obtain information about the main compounds. The total extract was subsequently fractionated by flash chromatography in 19 fractions of increasing polarity which were tested against *T. brucei in vitro* and only few fractions showed good antitrypanosomal activity. Active fractions were then analyzed by HPLC MS-MS and by NMR to assess the phytoconstituents responsible for activity towards protozoan parasites.

2.3.1 Results and discussion

2.3.1.1 Characterization of *T. diversifolia* extracts by NMR and HPLC-MS^n

The phytochemical composition of the *T. diversifolia* methanolic extract (Tith-MeOH), has been determined by using a multi-technique approach. As a first step the Tith-MeOH extract was dissolved in deuterated chloroform (final concentration 20 mg/mL) and different spectra were acquired with ^{1}H-NMR, HSQC-DEPT, HMBC and COSY experiments. Diagnostic signals of sesquiterpene protons were detected, and assigned on the basis of the ^{1}H, HSQC, HMBC and COSY data as compared with those reported in literature (Baruah *et al*., 1979) and are shown in Table 1. The structure of tagitinin C was assigned based on ^{1}H NMR spectrum that showed signals ascribable to sesquiterpene sp2 protons namely the doublets at δ 6.93 (d, J = 13.5), 6.21 (d, J = 1.3), and the signals in overlapped zone at δ 5.82, 5.88, and 6.36 corresponding to positions 1, 2, 5 and 13, respectively. The directly linked carbons observed in the HSQC-DEPT were 124.0 (CH_2), 129.5 (CH), 137.6 (CH), and 159.6 (CH). For what concern the structure of tagitinin A the signals that have been assigned are the proton at the position 1 (δ 4.23), the isobutyryl moiety at the position 8 (δ 4.55), the protons at the range δ 5.53 – 6.25 (position 13), the methyne supporting the ester linkage at δ 5.59 (position 8), and the methyl groups 14 and 15 at δ 1.45 and 1.10, respectively.

Table 1. Diagnostic assignments of tagitinins A and C from NMR spectra of Tith-MeOH extract. Assignments were obtained by comparing HSQC-DEPT, HMBC and COSY data with the literature (Baruah *et al*., 1979).

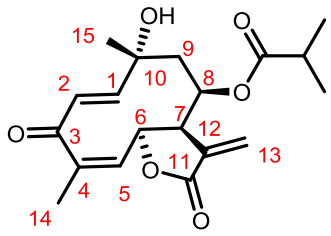

Tagitinin C

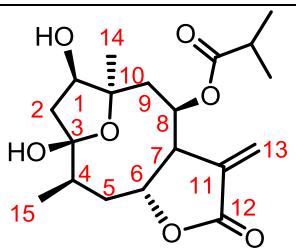

Tagitinin A

Position	δH	δC	Position	δH	δC
1	6.93 d J = 13.5	159.6	**1**	4.23	78.4
2	6.21 d J = 1.3	129.5	**6**	4.55	81.8
5	5.88	137.6	**8**	5.59	69.9
13	5.81 - 6.36	124.0	**13**	5.53-6.25	121.7

A representative portion of a HSQC-DEPT spectrum of tagitinins A and C is shown in Figure 2 indicating the assigned positions.

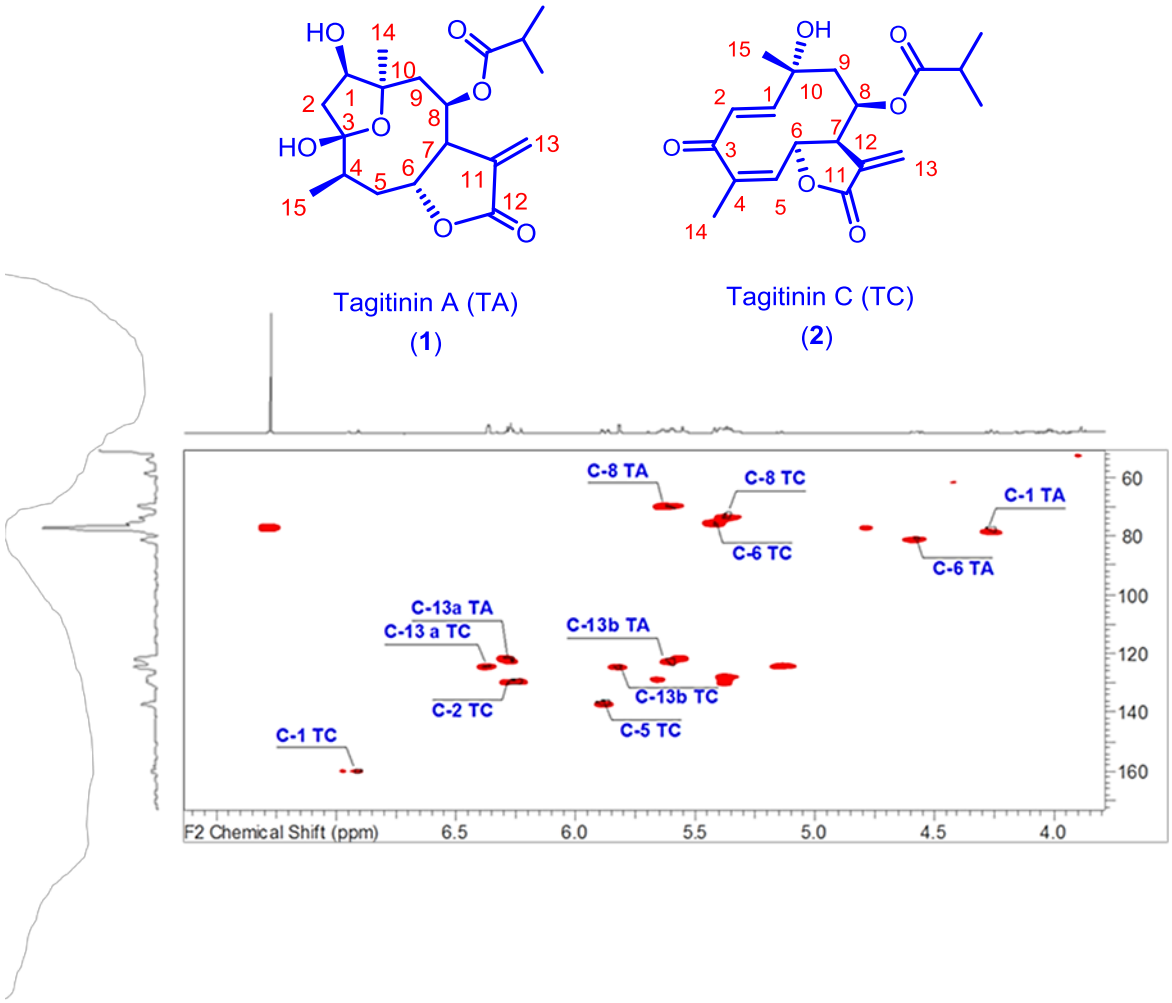

Fig. 2. HSQC-DEPT (MeOD) of a *T. diversifolia* extract. TA and TC indicate signals of tagitinin A and tagitinin C, respectively.

Many other signals were detected allowing the tentative identification of 14 constituents that may be linked to other phytoconstituents and are reported in Table 2. For this reason, HPLC-MS^n analysis were performed both in positive and negative ion mode using ESI source, in order to identify other secondary metabolites occurring in the crude extract.

Exemplificative chromatograms are shown in Figure 3 and the fragmentation pathways for the main sesquiterpenes of *T. diversifolia* are reported in Figure 4. Six different sesquiterpenes were detected and their presence was determined on the basis of HPLC-MS^n analysis. Unfortunately, regarding ESI/MS behaviour of these sesquiterpenes only limited information are available in literature.

Just recently, Abea *et al*. (Abea *et al*., 2015) published a paper where they proposed the fragmentation pathways of tagitinin F.

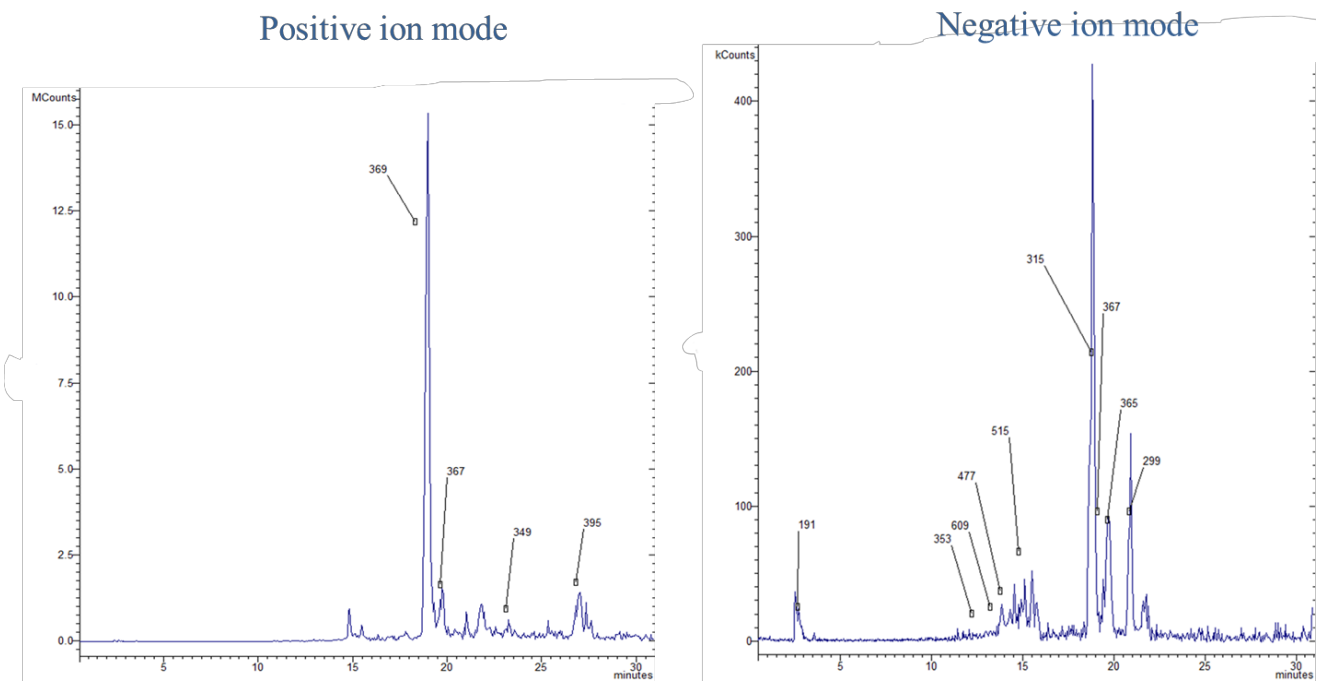

Fig. 3. HPLC-ESI-MS of *T. diversifolia* methanol extract, in positive and negative ion mode. Identified compounds are indicated with their m/z values (see Table 2 for additional details).

Table 2. Constituents identified in the *T. diversifolia* methanolic extract by HPLC-MS.

Retention time	Compound	Polarity	[M-H] or [M+H]	Fragments
2.53	Quinic acid[a]	Negative	191	85
12.0	Chlorogenic acid[a]	Negative	353	191-179
13.9	Rutin[a]	Negative	609	301-271-255-179-151
14.5	Quercetin-glucuronide	Negative	477	301-179-151
14.6	1,5-Dicaffeoylquinic acid[a]	Negative	515	353-191-173-127
14.8	3,4-Dicaffeoylquinic acid	Negative	515	353-191-179-173
15.7	3,5-Dicaffeoylquinic acid[a]	Negative	515	353-191-173-127-111-85
18.8	Isorhamnetin	Negative	315	300-272-228
19.5	Tagitinin A	Negative	367	279-261-235
		Positive	369	281-263-245
19.7	Tirotundin 3-*O*-methylether	Positive	367	279-261-243-233-215
		Negative	365	277-233-215-191-176
20.8	Hispidulin	Negative	299	284
24.6	Tagitinin C	Positive	349	261-243-215-173
27.4	3-O-Methyl titonin	Positive	395	293-275-261-199-181

[a] confirmed by injection of reference compound

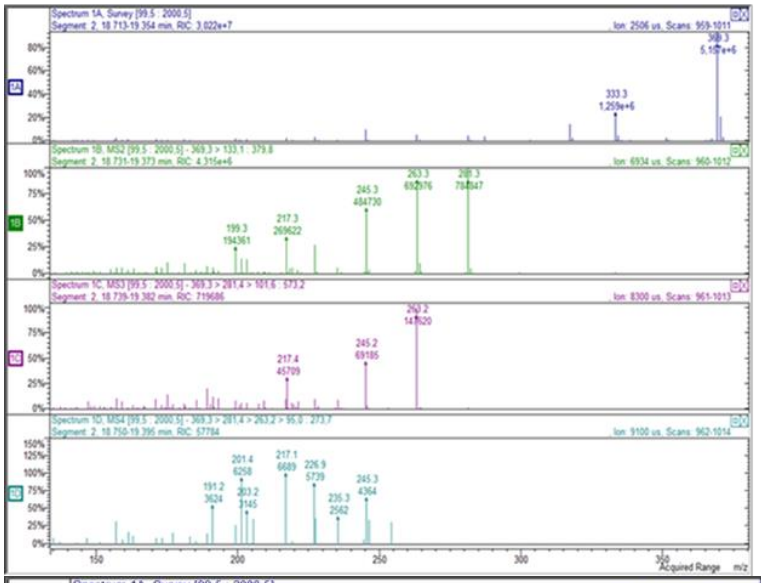

Tagitinin A

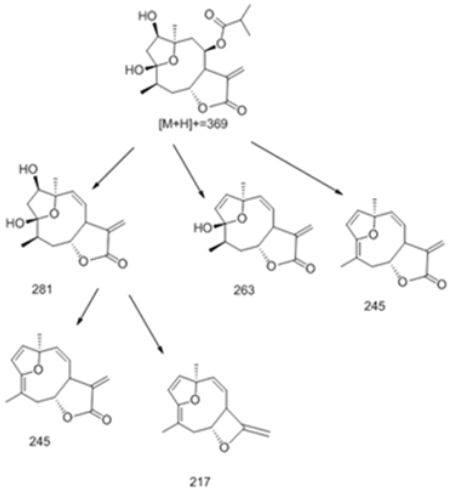

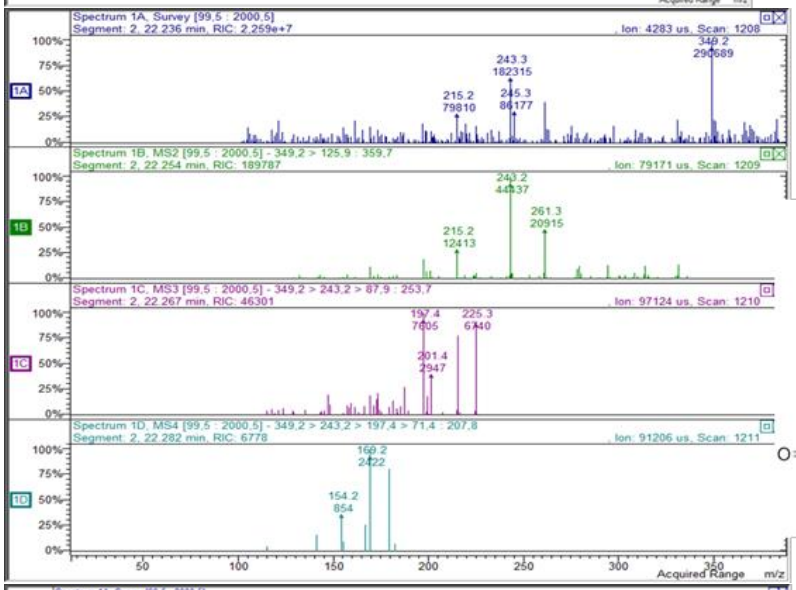

Tagitinin C

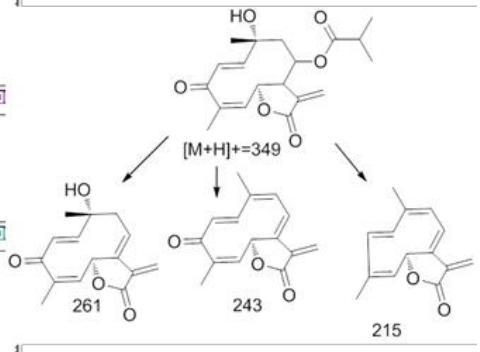

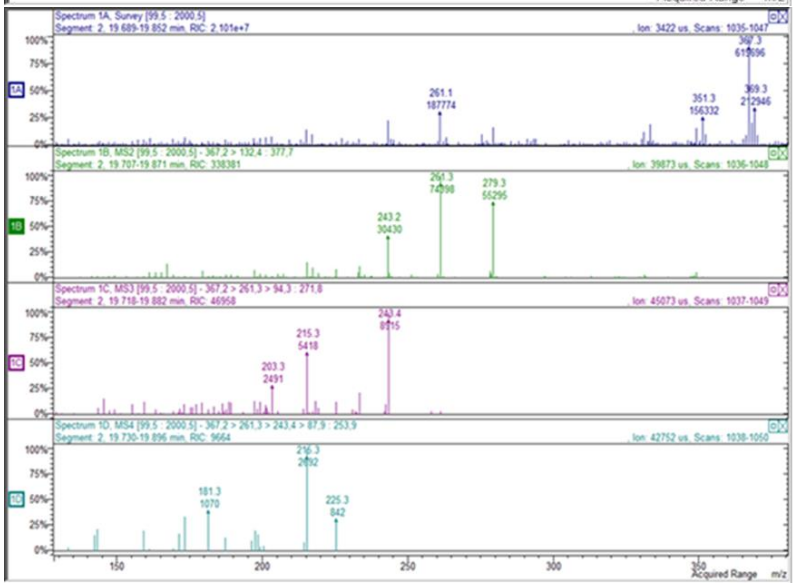

Tirotundin-3-*O*-methlyether

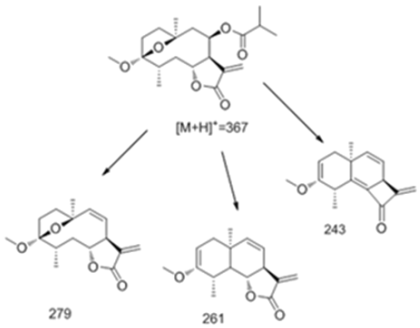

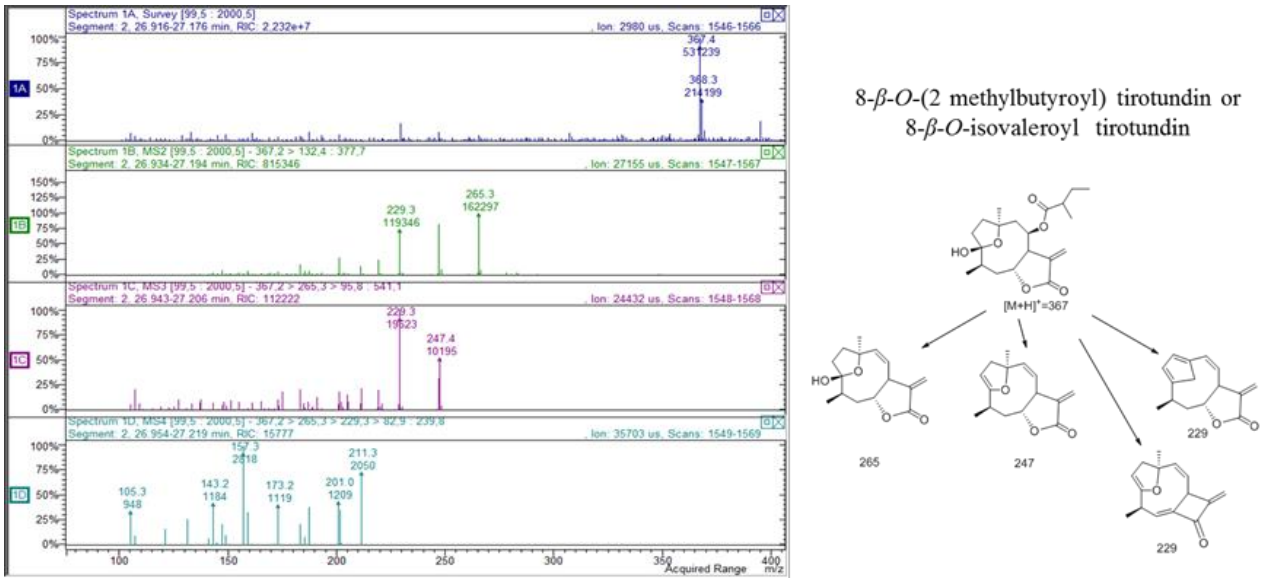

Fig. 4. Mass spectra of the main sesquiterpenoids of *T. diversifolia* and proposed fragmentation pathways.

In our analysis, we observed that the tirotundin derivatives **4** and **5** (Figure 5) are characterized in MS^2 by three main fragments ascribable to the loss of an ester side chain, a water molecule and an ether bridge or lactone ring with rearrangement at m/z 265, 247 and 229, respectively.

The same fragments are detectable in the MS^2 spectra of tirotundin-3-*O*-methylether (compound **6**) at m/z 279, 261 and 243 presenting additional 14 Da due to the presence of a methyl group. Polyphenol derivatives, mainly caffeic acid derivatives and flavonoids, were also identified.

From a quantitative point of view, due to the non-availability of tagitinins as reference compounds, the quantification of tagitinins A and C was performed by ^{1}H NMR using caffeine as internal standard using a previously published method (Comai *et al*., 2010). The amount of tagitinins A and C and phenolic compounds in the methanolic extract is reported in Table 3. The lipophilic flavonoids (hispidulin **7** and isorhamnetin **8**) were also isolated together with sesquiterpene lactones (Figure 6).

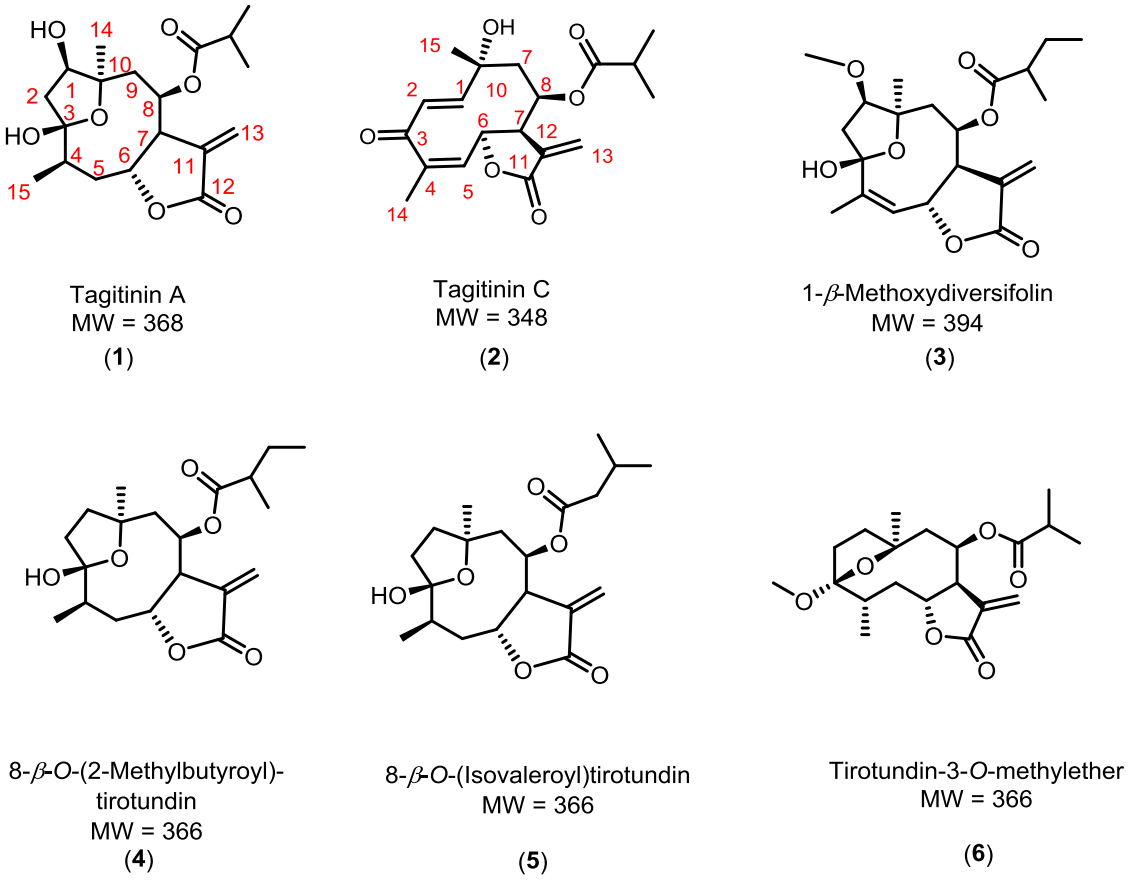

Fig. 5. Structures of the six sesquiterpenes identified in *T. diversifolia* extracts.

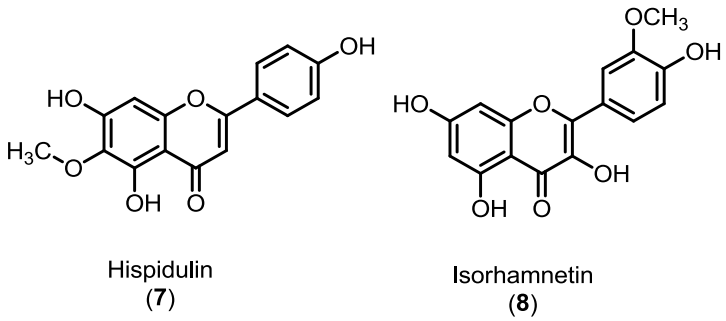

Fig. 6. Structures of lipophilic flavonoids hispidulin (**7**) and isorhamnetin (**8**).

Table 3. HPLC-DAD quantitative determination of the main constituents of the *T. diversifolia* extracts.

Compound	Methanolic extract metabolite contents $mg.g^{-1}$	Ethyl acetate extract metabolite contents $mg.g^{-1}$
Phenolic acids		
Chlorogenic acid	0.05 ± 0.01	n.d.[a]
1,5-Dicaffeoylquinic acid	0.33 ± 0.01	n.d.
3,4-Dicaffeoylquinic acid	0.40 ± 0.01	n.d.
3,5-Dicaffeoylquinic acid	1.42 ± 0.01	n.d.
Chlorogenic acids content	2.2	n.d.
Flavonoids		
Rutin	0.52 ± 0.01	n.d.
Quercetin glucuronide	0.08 ± 0.01	n.d.
Isorhamnetin	7.92 ± 0.01	3.96 ± 0.01
Hispidulin	3.08 ± 0.01	3.11 ± 0.01
Flavonoid total content	11.6	11.6
Sesquiterpene lactones		
Tagitinin A	0.83 ± 0.01	1.16 ± 0.01
Tagitinin C	1.10 ± 0.01	1.69 ± 0.01

[a] *n.d. = not detected*

The first conclusion to be drawn concerning the extensive phytochemical analysis of *T. diversifolia* extract is that the composition of the extract is extremely complex and contains sesquiterpene-, phenylpropanoid- and flavonoid derivatives as main constituents.

2.3.1.2 *In vitro* evaluation of antiprotozoal activity and composition of bioactive fractions

Two extracts of increasing polarity (Tith-MeOH and Tith-H_2O) have been prepared from the aerial parts of *T*. *diversifolia* to assess their *in vitro* antitrypanosomal activity (Table 4, Figure 7). The methanolic extract was two times more active against *T*. *brucei* than the aqueous extract (IC_{50} = 1.08 and 2.18 μg/mL, respectively) and was therefore chosen for further fractionation. The methanolic extract was then subjected to chromatographic separations. The fractions with increasing polarity collected after each purification step (F1-F19) were tested against the TC221 cells with the aim of monitoring and chasing the antitrypanosomal activity. The bio-guided purification of the Tith-MeOH extract gave two fractions (F8 and F9, Table 4) showing significantly higher antitrypanosomal effects in our cell-based assay (IC_{50} = 0.41 and 0.43 μg/mL, respectively). The bio-guided analysis of fractions F8 and F9 gave two major secondary metabolites, which turned out to be STLs, namely tagitinins A and C.

Bioassays performed on obtained medium polarity fractions from Silica-based chromatography of Tith-MeOH extracts showed the effect on *T*. *brucei vs*. mammalian cell proliferation (Table 4). ^{1}H-NMR of the 16 assayed fractions (Figure 8) clearly shows the presence of signals ascribable to sesquiterpene derivatives as well as other aromatic compounds in the most active mixtures, namely F7 to F11. In all the fractions, the signals ascribable to phenolic and phenylpropanoid derivatives were not detectable or poorly detectable. Given the progress achieved, we decided to consider the most active fractions, thus the ones showing IC_{50} <1.6 μg/mL, i.e. fractions 8-11, which were analysed for the content of tagitinins A and C. The amounts of these STLs in the active fractions were reported in Table 5.

Results showed that bioactivity of the obtained fractions can at least in part be ascribed to STLs constituents and for this reason isolated tagitinins A and C were also tested. As reported in Table 4, tagitinin C resulted by far the most active compound (IC_{50} = 0.0042 μg/mL) compared with active fractions and resulted 85 times more active than tagitinin A (IC_{50} = 0.356 μg/mL, Figure 9).

Table 4. Activity of *T. diversifolia* leaves extracts and fractions 1-19 against *T. brucei* TC221 and BALB/3T3.

Samples	**IC_{50} (μg/mL)**		**Selectivity Index (SI)**
	***T. brucei* (TC221)**	**BALB/3T3**	
Crude methanol extract (Tith-MeOH)	1.05 ± 0.18	5.15 ± 0.82	4.9
Crude aqueous extract (Tith-H_2O)	2.18 ± 0.06	6.71 ± 0.48	3
***Fractions from methanol extract* (Tith-MeOH)**			
Fraction 1	62.05 ± 20.4	-	-
Fraction 2	13.69 ± 1.8	52.16 ± 3.1	3.8
Fraction 3	8.29 ± 0.79	17.52 ± 2.9	2.1
Fraction 4	8.28 ± 0.56	12.85 ± 1.1	1.5
Fraction 5	4.37 ± 1.98	7.65 ± 0.85	1.7
Fraction 6	1.66 ± 0.66	4.37 ± 0.61	2.6
Fraction 7	1.67 ± 0.51	2.78 ± 0.03	1.6
Fraction 8	0.41 ± 0.22	1.44 ± 0.04	3.3
Fraction 9	0.43 ± 0.09	1.47 ± 0.04	3.4
Fraction 10	1.09 ± 0.37	2.36 ± 0.17	2.1
Fraction 11	1.20 ± 0.21	2.66 ± 0.18	2.2
Fraction 12	2.34 ± 0.55	4.24 ± 0.49	1.8
Fraction 13	3.16 ± 0.89	6.03 ± 1.86	1.9
Fraction 14	2.02 ± 0.88	5.10 ± 0.64	2.5
Fraction 15	1.63 ± 0.61	3.17 ± 0.14	1.9
Fraction 16	7.65 ± 1.61	19.34 ± 2.76	2.5
Fraction 17	>100	-	-
Fraction 18	>100	-	-
Fraction 19	>100	-	-
Pure compounds	**μg/mL (μM)**	**μg/mL (μM)**	
Tagitinin A	0.356 ± 0.17 (0.97)	0.467 ± 0.21 (1.27)	1.3
Tagitinin C	0.0042 ± 0.0005 (0.0121)	0.012 ± 0.001 (0.036)	3
Reference drug	**μg/mL (μM)**	**μg/mL (μM)**	
Suramin	0.0191 ± 0.002 (0.0147)	n.d.	-

n.d. = not determined

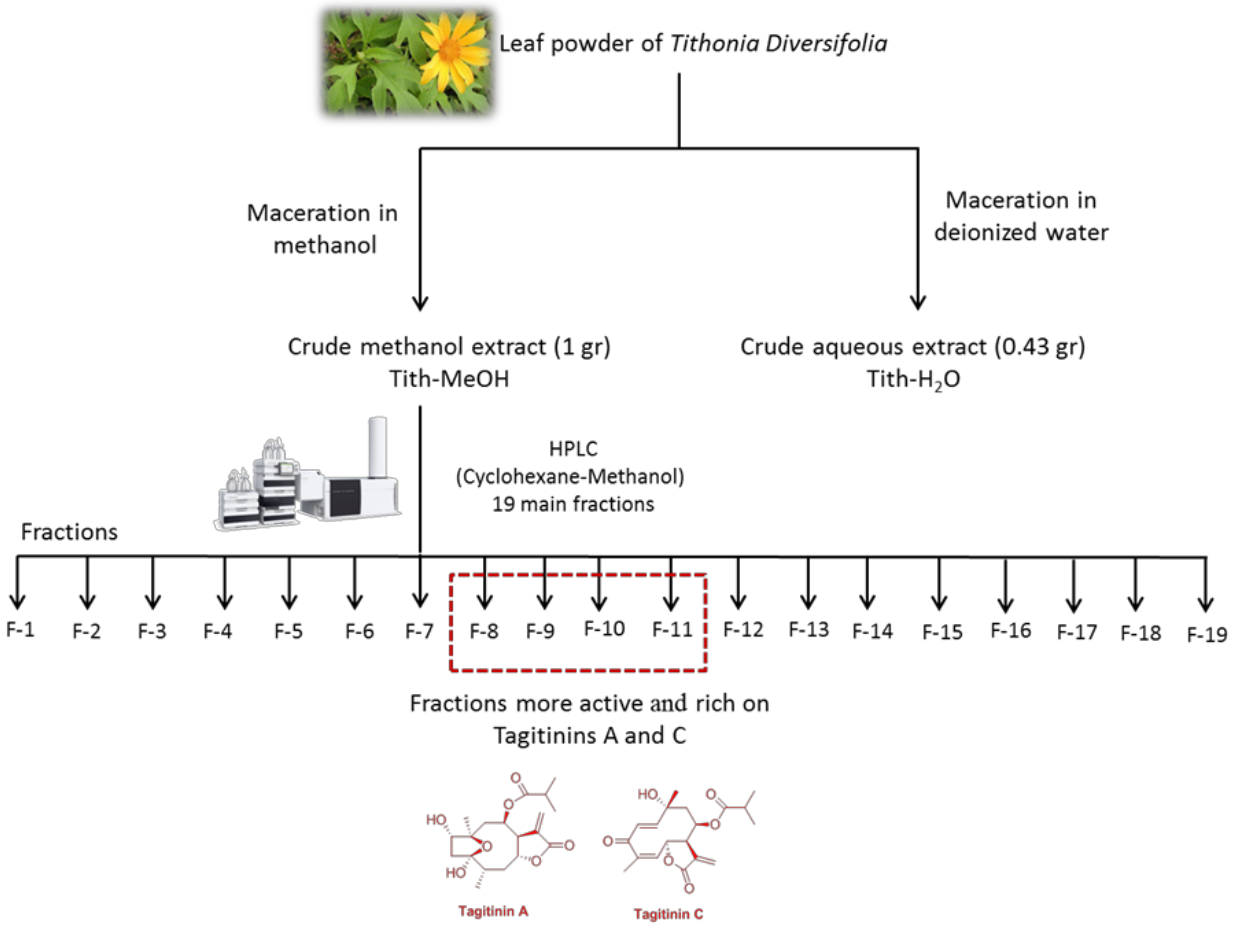

Fig. 7. Representation of continuous procedure of extraction and fractionation of *T. diversifolia*.

Furthermore, it was 4.5 times more active than the reference compound suramin. Selective index for tagitinin C against mouse fibroblasts (BALB/3T3) was 3 showing preferential effect on target cells compared with tagitinin A (1.3). The large difference in bioactivity observed for the tagitinins C and A indicates the need for the evaluation of other tagitinin derivatives in order to explore possible structure activity relationships and build-up a privileged scaffold library.

However, potent and selective antitrypanosomal activity of different sesquiterpene-rich plants has been previously reported (Otoguro *et al*., 2011), as well as the possible usefulness of sesquiterpenes as lead compounds for the development of new antitrypanosomal drugs (Saeidnia *et al*., 2013).

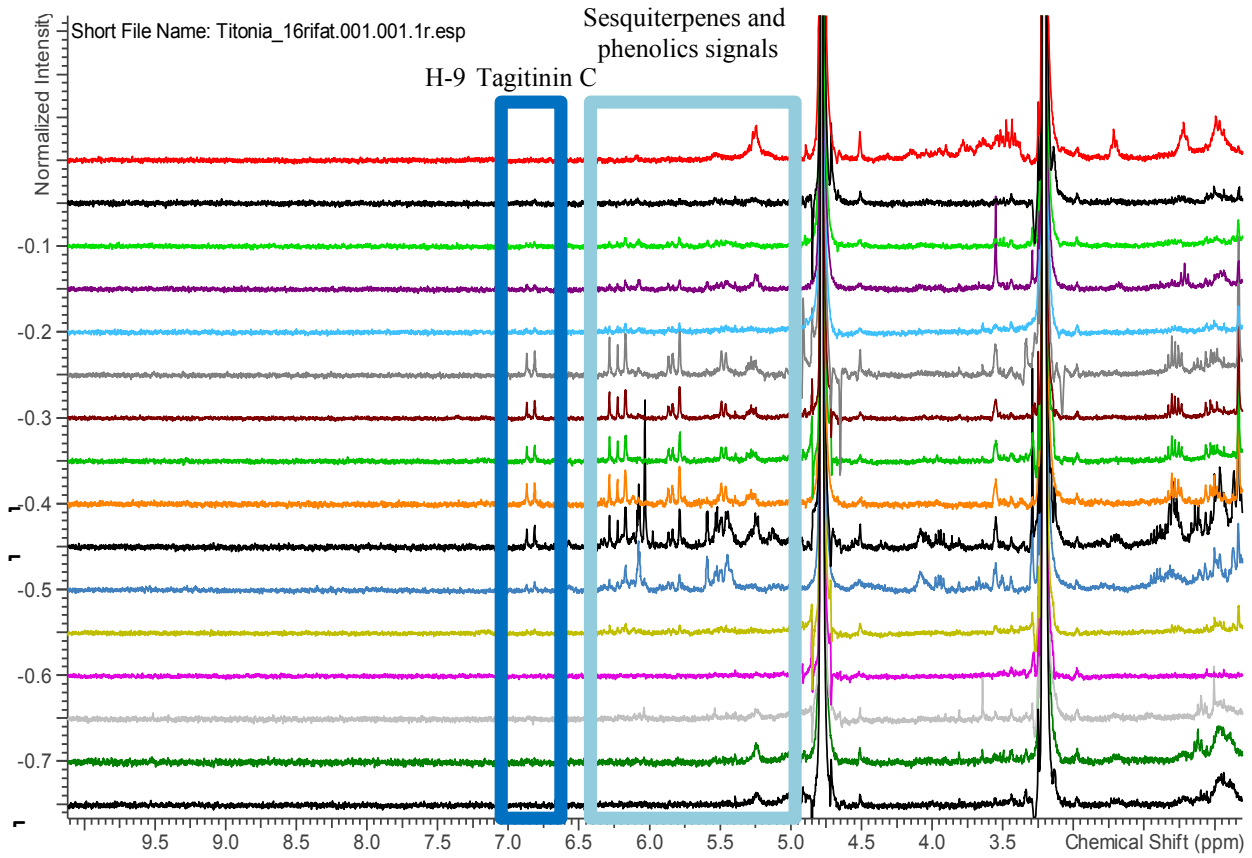

Fig. 8. ^{1}H NMR analysis of *T. diversifolia* fractions 1-16.

Table 5. Amount of tagitinins in the bioactivity-guided selected fractions. The amount is shown as the percentage of the total volume.

Samples	**Tagitinin A %**	**Tagitinin C %**	***T. brucei* (TC221) IC_{50} (µg/mL)**
Crude methanol extract (Tith-MeOH)	0.83 ± 0.01	1.10 ± 0.01	1.05 ± 0.18
***Active fractions from methanol extract* (Tith-MeOH)**			
Fraction 8	10.8 ± 0.01	9.39 ± 0.01	0.41 ± 0.22
Fraction 9	8.36 ± 0.01	8.18 ± 0.01	0.43 ± 0.09
Fraction 10	7.03 ± 0.01	7.09 ± 0.01	1.09 ± 0.37
Fraction 11	7.07 ± 0.01	6.51± 0.01	1.20 ± 0.21

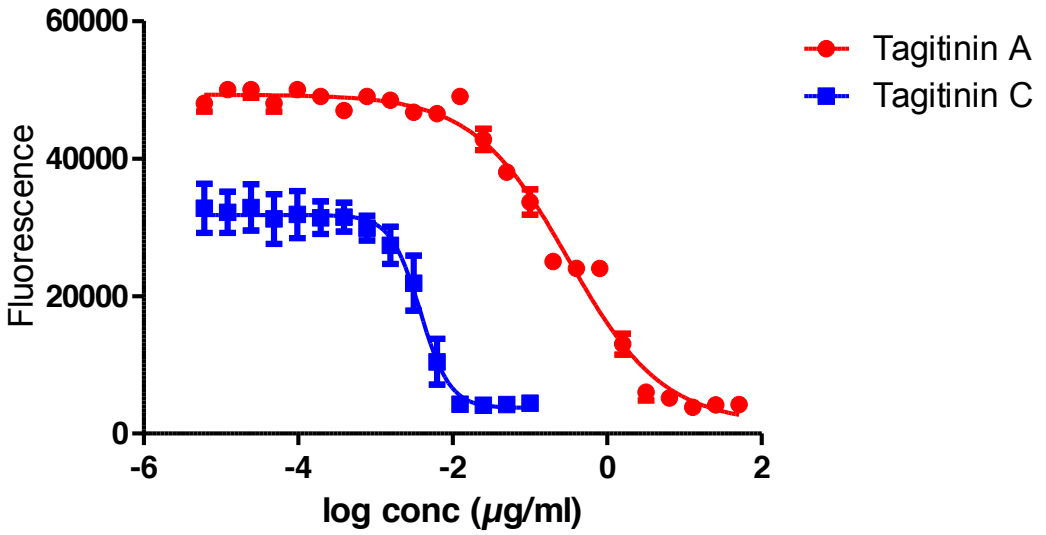

Fig. 9. Growth inhibition of *T. brucei* TC221 cells induced by tagitinins A (red) and C (blue). Each graph shows the average results from eight independent experiments with standard errors.

The high antitrypanosomal activity observed for the crude methanolic extract, despite a relatively low content of STLs, suggests that the inhibitory effects on *T. brucei* may also be related to other phytoconstituents such as flavonoids or phenylpropanoids. Further studies are needed in order to clarify or establish synergistic effects of different classes of phytoconstituents.

Regarding the mechanism of action of *T. diversifolia* STLs on trypanosome cell, some considerations can arise from the data already obtained.

Considering that STLs owned an α,β-unsaturated moiety in the form of α-methylene-γ-lactone, they can react with nucleophiles such as free thiol groups (R-SH) in proteins, acting as a Michael acceptor. This phenomenon leads to macromolecular dysfunction, oxidative stress, and genetic mutations as a result of the oxidative stress.

The presence of one potentially reactive α,β-unsaturated carbonyl group as a pharmacophore is often associated with significant antiprotozoal and cytotoxic activities.

The tagitinins A and C, two of the major components of fractions 8 and 9, display in their chemical structures one or three reactive sites, respectively (Figure 10), which are probably responsible of their antiprotozoal activity. Tagitinin A has only an α,β-unsaturated carbonyl group in the γ-lactone ring, whereas tagitinin C has a carbonyl group conjugated with two double bonds in the germacrene ring and an α,β-unsaturated carbonyl group in the γ-lactone ring.

The hypothesized mechanism of these compounds against trypanosomes may be related to the capability to form thiol adducts with components found in the cellular environment such as trypanothione, glutathione and SH-groups in proteins.

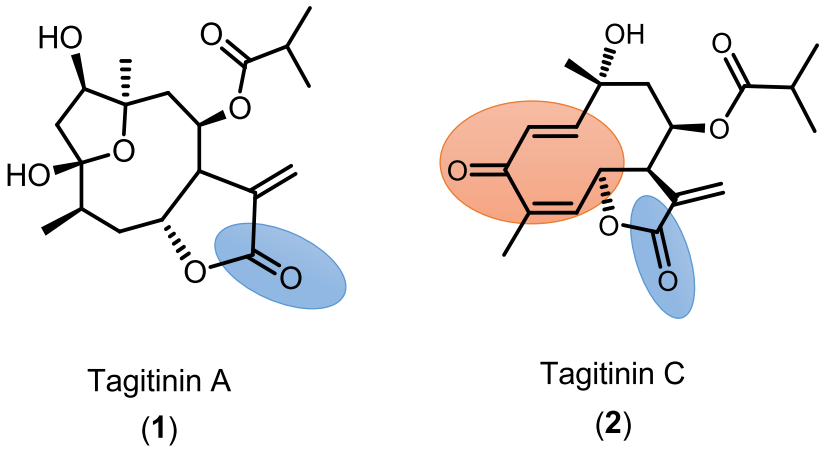

Fig. 10. Potentially reactive α,β-unsaturated carbonyl groups in tagitinins A and C.

The lack of reduced trypanothione and other SH-group containing substances may in turn lead to that the parasite cells become more vulnerable to oxidative stress (Wink, 2008). Unfortunately, the same mechanism of action may occur in the mammalian fibroblasts (BALB/ 3T3), where glutathione depletion renders the cells prone to oxidative stress.

2.3.2 Summary and conclusions

Overall our results, although preliminary, confirmed the usefulness of *T. diversifolia* as an effective herbal remedy in the African traditional medicine and highlighted good prospects of using isolated compounds from the leaf methanolic extracts as inspiring leads for designing future trypanocidal drugs.

However, further studies are needed to better understand the mechanism of action underlying the antitrypanosomal activity of tagitinins as well as to assess the real efficacy *vs*. toxicity through *in vivo* assays. The opportunity to study different derivatives as well as strictly related sesquiterpenes could be a good alternative to improve selectivity toward mammalian cells.

Another valuable alternative might be also the synthesis of sesquiterpene derivatives starting from commercially available building blocks, that could help us to build-up a new series of more active drug candidates.

2.4 Biological activities of the essential oil from *T. diversifolia*

2.4.1 What is an Essential oil?

Essential oils (EOs), also known as etheric oils, aetheroleum, volatile oils, or essences, are considered an intricate lipophilic combination of volatile compounds (Sangwan *et al*., 2001; Baser *et al*., 2007). According to the European Pharmacopoeia (Council of Europe 2004) and the International Standard Organization on Essential Oils an EO is referred to as "*the product obtained from plant raw material by hydrodistillation, steam distillation or dry distillation or by a suitable mechanical process (e.g. for Citrus fruits)*" The Pharmacopoeia definition of an EO does not take into account other aromatic/volatile products obtained by different extractive techniques like supercritical fluid extraction or by extraction with solvents (defined concretes or absolutes). Fixed oils or fatty oils differ from EOs in both physical and chemical properties.

EOs incorporate volatile compounds that fade away rapidly without leaving any halo, whereas fatty oils leave a permanent stain attributable to glycerides. In the wilderness, they play very important roles in term of plant defense and signaling processes (Bowsher *et al*., 2008; Taiz *et al*., 2010). They are deeply embroiled in plant defense against insects and microorganisms, and are important for water regulation, allelopathic interactions and attraction of pollinating insects (Pichersky *et al*., 2002; Bakkali *et al*., 2008). Furthermore, EOs are good sources of substances with commercial potential useful for chemical synthesis and they also represent valuable natural products utilized as raw materials in pharmaceutical, food, cosmetic, agronomic, and perfume industry fields (Buchbauer, 2000). Nowadays, more than 3000 different EOs are known and about 300 of them are currently in use in different fields.

EOs represent the "soul" of the plant and can be found in various plant organs (seeds, stems, leaves, roots, fruits, and flowers) being produced and stored in secretory structures that differ in distribution, structure, morphology, and function. These specialised structures are present on the surface of the plant organs or within the plant tissues and minimize the risk of auto-toxicity. They are classified in internal external or external secretory structures. The yields of EOs vary widely and are difficult to predict. These variations depending on agronomic factors (soil type, influence of drought and water stress, climate, stresses caused by microorganism and insects) and farming methods. For this reason, it is important to have the knowledge of harvesting time, harvesting methods, storage, and location of the oil cells within the plant.

The useful procedure to obtain essential oil is hydrodistillation, by Clevenger apparatus, that has been introduced in the European Pharmacopoeia (Figure 11). This apparatus consists of a

heated round-bottom flask, where water and chopped plant material are introcude, and is connected to a vertical condenser and a graduated tube for the volumetric determination of the oil. At the bottom of the tube a three-way valve allows to direct the water back to the flask, since it is a continuous closed-loop distillation apparatus, and to separate EO from the water phase at the end of the distillation process. The length of distillation it is usually fixed to 4-5 h or when no more EO is obtained. After that, the EO is collected and storaged before chemical analysis, commonly by gas-chromatography-mass spectrometry.

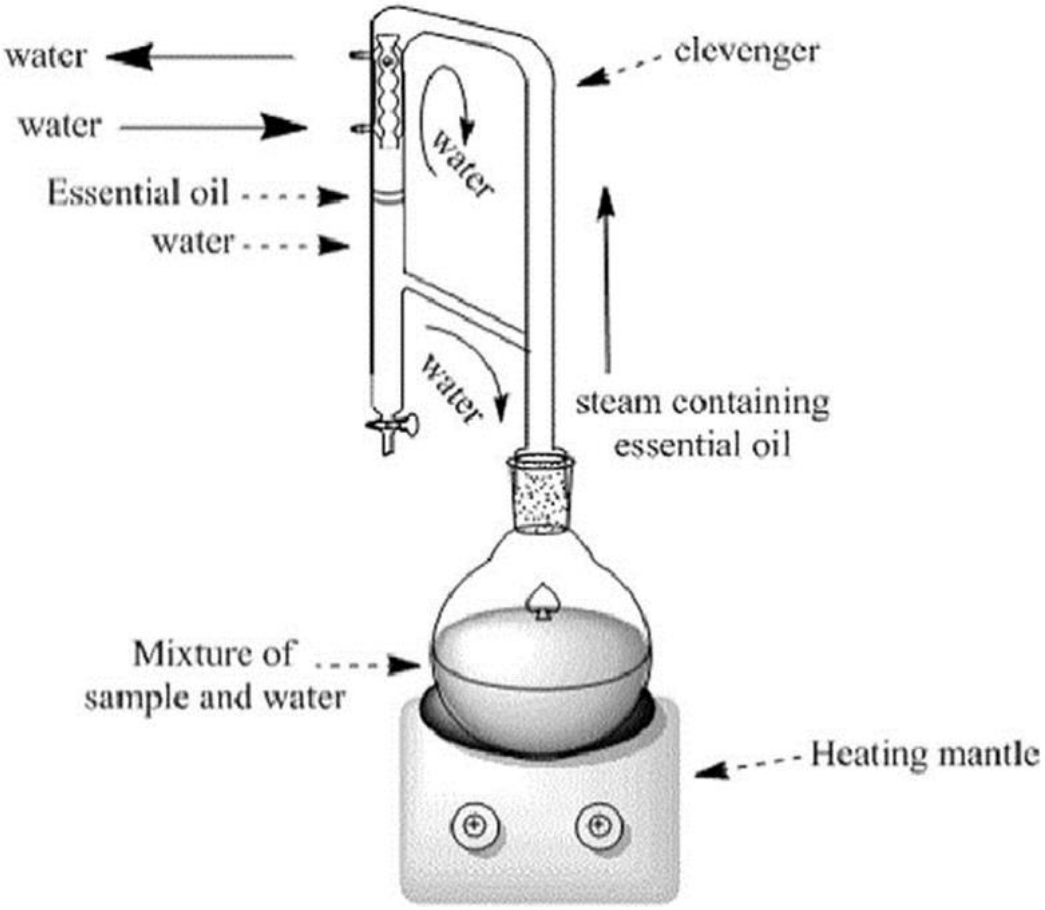

Fig. 11. Clevenger apparatus according to European Pharmacopoeia.

2.4.2 Aim of research

Focusing on the volatile fraction of *T*. *diversifolia* only a few studies are available so far, reporting the monoterpenes α-pinene, β-pinene, limonene, and (Z)-β-ocimene as the major EO components of *T*. *diversifolia* inflorescences (Menut *et al*., 1992; Gbolade *et al*., 2008; Lawal *et al*., 2013). Nevertheless, we couldn't find any reports on the biological activities of *T*. *diversifolia* essential oil. For this reason, in the present chapter, we decided to investigate the *in vitro* biological effects of *T*. *diversifolia* essential oil, namely its antibacterial and antioxidant activity, and its cytotoxicity on human tumor cells.

To achieve this, naturalized and spontaneous *T*. *diversifolia* plants from Western highlands of Cameroon have been used. The different biological activities were assessed by agar disc-diffusion, DPPH, ABTS, FRAP, and MTT methods. Furthermore, we evaluated the inhibitory effects of the whole EO mixture, and of some of its isolated components on nicotinate mononucleotide adenylyltransferase (NadD, EC 2.7.7.18), a key NAD biosynthetic enzyme shared by most bacterial pathogens (Sorci *et al*., 2009; Rodionova *et al*., 2015), as well as on the three orthologue isozymes in the mammalian host that are known as nicotinamide mononucleotide adenylyltransferase (NMNAT, EC 2.7.7.1) (Sorci *et al*., 2007; Orsomando *et al*., 2012; Mori et al., 2014). Is now considered a "well-recognized scenario" that microbes have developed resistance to various therapies and although chemical modifications of existing drugs and the development of novel inhibitors against well-established targets, these new approaches have proven to be successful only in the short term. It thus seems clear that new drug targets need to be explored to maintain and extend efficacious antibacterial therapy in the long run. Given all of that and since NadD is considered essential for cell/organism survival, it might represent a very promising druggable target for developing novel drug entities with either antiproliferative or antimicrobial activities (Zhai et al., 2009; Petrelli *et al*., 2011; Pankiewicz *et al*., 2015).

Taken together, all these findings point to new insights into the potential pharmaceutical applications of *T*. *diversifolia* as a renewable biomass.

2.4.3 Results and discussion

2.4.3.1 Essential oil analysis

The composition of the EO distilled from flowerheads of *T*. *diversifolia* is reported in Table 6. As we can see from the Table 6 the chemical profile (obtained by GC-M) is very complex, with 255 peaks detected. 161 out of 255 peaks were identified, accounting for 87.3% of the total area. 18 volatile components were present in relative percentages equal or above 1%, while 143 components were detected in low relative percentages (below 1%).

The oil was mainly composed of monoterpenes (47.6%) with hydrocarbons and oxygenated compounds in similar amounts (24.7 and 22.2%, respectively). Among them, cis-chrysanthenol (6.2), limonene (7.6%), and α-pinene (13.7%) were the most representatives.

Sesquiterpenes (23.4%) were the second group characterizing the EO, with oxygenated compounds more abundant than hydrocarbons (14.1 and 9.3%, respectively). Main representatives of these classes were α-copaene (3.7%) and spathulenol (3.5%). Aliphatics were a minor fraction of the oil (13.4%). Aldehydes, and saturated and unsaturated hydrocarbons accounted for 5.3% and 3.5%, respectively, and fatty acids represented the most abundant groups (3.1%). Fatty acids are mainly represented by 1-pentadecene (1.7%), n-hexadecanoic acid (2.8%), and n-pentadecanal (1.6%).

The composition reported herein showed some relevant differences than that previously published by Menut and co-authors (Menut *et al*., 1992).

In particular, the EO examined by us revealed a poor amount of (Z)-β-ocimene (0.3%), which instead has been reported as one of the major volatile components of flowers by the other authors (Menut *et al*., 1992). Additionally, the sample examined by us showed significantly lower levels of α-pinene if compared with other samples previously analyzed (from Cameroon and South Africa), where the relative percentage ranged from 61.5 to 76.7% (Lawal *et al*., 2012).

Substantial differences have been also found with regard to the sample collected in Nigeria (Moronkola *et al*., 2007), where the bicyclogermacrene (8.0%), the β-caryophyllene (20.1%), and the sequiterpenes germacrene D (20.3%), resulted as the most abundant components. Another substantial difference with published papers can be traced back on higher number of volatiles identified in our study (161 compounds) with respect to the previous ones, where a maximum of 57 constituents were identified (Moronkola *et al*., 2007). However, the differences in composition observed might be due to the different geographic origin, altitude, genetics and processing (e.g. fresh *vs* dry samples undergoing distillation) of the sample analyzed.

Table 6. Chemical composition of the EO from flowerheads of *T.diversifolia*.

N.	Component[a]	RI calc.[b]	RI lit[c]	%[d]	ID[e]
1	*n*-hexanal	801	801	0,2	Std
2	1,3-cyclopentadiene, 1,2,5,5-tetramethyl-	837	835	Tr[f]	RI,MS
3	(2*E*)-hexenal	850	846	Tr	RI,MS
4	*n*-hexanol	866	863	Tr	RI,MS
5	2-heptanone	892	892	0,1	RI,MS
6	4-heptenal	893	895	1,0	RI,MS
7	*n*-nonane	899	900	0,1	Std
8	*n*-heptanal	903	902	0,1	RI,MS
9	tricyclene	920	921	Tr	RI,MS
10	α-thujene	925	924	0,1	RI,MS
11	α-pinene	932	932	13,7	Std
12	camphene	945	946	0,1	Std
13	thuja-2,4(10)-diene	951	953	0,3	RI,MS
14	(2*E*)-heptenal	957	947	Tr	RI,MS
15	benzaldehyde	961	952	0,1	Std
16	sabinene	971	969	0,6	RI,MS
17	β-pinene	973	974	0,3	Std
18	1-octen-3-ol	980	974	0,1	Std
19	2,3-octanedione	986	985	Tr	RI,MS
20	6-methyl-5-hepten-2-one	989	981	0,2	RI,MS
21	2-pentyl furan	991	984	2,3	RI,MS
22	*m*-cymene	1004	1002	0,2	RI,MS
23	α-terpinene	1017	1014	0,1	RI,MS
24	1,2,4-trimethyl benzene	1023	1021	Tr	RI,MS
25	*p*-cymene	1026	1024	0,4	Std
26	limonene	1030	1024	7,6	Std
27	(*Z*)-β-ocimene	1043	1032	0,3	RI,MS
28	benzene acetaldehyde	1048	1036	0,1	RI,MS
29	(*E*)-β-ocimene	1052	1044	0,2	RI,MS
30	γ-terpinene	1061	1054	0,3	Std
31	(2*E*)-octen-1-al	1063	1054	0,1	RI,MS
32	*cis*-sabinene hydrate	1069	1065	0,3	RI,MS
33	*cis*-linalool oxide	1075	1067	0,1	RI,MS
34	terpinolene	1087	1086	0,2	Std
35	*p*-cymenene	1089	1089	0,2	RI,MS
36	6-camphenone	1092	1095	0,4	RI,MS

37	*trans*-sabinene hydrate	1096	1098	0,1	RI,MS
38	(*Z*)-6-nonenal	1098	1100	0,6	RI,MS
39	linalool	1100	1095	2,0	Std
40	*n*-nonanal	1105	1100	0,5	RI,MS
41	1,3,8-*p*-menthatriene	1108	1109	Tr	RI,MS
42	*trans*-thujone	1115	1112	Tr	Std
43	6-camphenol	1117	1111	0,1	RI,MS
44	*trans*-*p*-mentha-2,8-dien-1-ol	1120	1119	0,5	RI,MS
45	α-campholenal	1125	1122	1,9	RI,MS
46	*cis*-limonene oxide	1130	1132	0,1	RI,MS
47	*trans*-pinocarveol	1136	1135	0,7	Std
48	*cis*-verbenol	1141	1137	0,6	RI,MS
49	*trans*-verbenol	1144	1140	1,3	RI,MS
50	1,4-dimethyl-3-cyclohexenyl methyl ketone	1151	1145	0,1	RI,MS
51	sabina ketone	1152	1154	0,1	RI,MS
52	lilac aldehyde A	1154	1155	0,1	RI,MS
53	*trans*-pinocamphone	1158	1158	0,6	RI,MS
54	pinocarvone	1161	1160	0,4	RI,MS
55	*cis*-chrysanthenol	1165	1160	6,2	RI,MS
56	*p*-mentha-1,5-dien-8-ol	1168	1166	0,6	RI,MS
57	*cis*-pinocamphone	1171	1172	0,3	RI,MS
58	terpinen-4-ol	1175	1174	1,1	Std
59	*p*-cymen-8-ol	1185	1179	0,5	RI,MS
60	α-terpineol	1188	1186	0,3	Std
61	myrtenal	1191	1195	0,2	Std
62	myrtenol	1193	1194	0,6	RI,MS
63	safranal	1196	1197	0,1	RI,MS
64	verbenone	1205	1204	Tr	Std
65	*n*-decanal	1206	1201	0,5	Std
66	*trans*-carveol	1217	1215	0,9	RI,MS
67	nerol	1231	1227	0,2	RI,MS
68	cumin aldehyde	1238	1238	0,2	RI,MS
69	carvone	1243	1239	0,4	Std
70	β-cyclohomocitral	1255	1254	Tr	RI,MS
71	(4*E*)-decen-1-ol	1258	1259	0,3	RI,MS
72	geraniol	1259	1249	0,3	Std
73	*n*-decanol	1264	1266	0,1	RI,MS
74	phellandral	1271	1271	0,3	RI,MS
75	geranial	1273	1264	0,3	Std
76	α-terpinen-7-al	1281	1283	0,1	RI,MS

77	(2*E*,4*Z*)-decadienal	1294	1292	0,2	RI,MS
78	2-undecanone	1295	1293	0,1	RI,MS
79	*n*-tridecane	1300	1300	0,1	Std
80	2,3,4-trimethyl benzaldehyde	1311	1313	0,1	RI,MS
81	(2*E*,4*E*)-decadienal	1316	1315	0,3	RI,MS
82	*p*-mentha-1,4-dien-7-ol	1330	1325	0,1	RI,MS
83	presilphiperfol-7-ene	1334	1334	0,1	RI,MS
84	α-longipinene	1342	1350	0,1	RI,MS
85	2,3,6-trimethyl benzaldehyde	1350	1352	0,1	RI,MS
86	α-copaene	1370	1374	3,7	RI,MS
87	α-isocomene	1377	1387	0,2	RI,MS
88	7-decen-1-ol acetate	1379	1389	0,1	RI,MS
89	(*E*)-β-damascenone	1382	1383	0,1	RI,MS
90	β-isocomene	1393	1407	0,2	RI,MS
91	α-*cis*-bergamotene	1400	1411	0,1	RI,MS
92	*n*-tetradecane	1400	1400	0,1	Std
93	β-cedrene	1408	1419	0,2	RI,MS
94	(*E*)-caryophyllene	1408	1417	0,2	Std
95	α-*trans*-bergamotene	1432	1432	0,1	RI,MS
96	aromadendrene	1443	1439	0,1	RI,MS
97	α-humulene	1445	1454	0,1	Std
98	*allo*-aromadendrene	1452	1458	0,1	RI,MS
99	geranyl acetone	1454	1453	0,4	RI,MS
100	(*E*)-β-farnesene	1458	1454	0,1	RI,MS
101	selina-4,11-diene	1469	1474*	0,2	RI,MS
102	germacrene D	1473	1484	0,3	RI,MS
103	β-selinene	1477	1489	0,4	RI,MS
104	eremophilene	1480	1482	0,4	RI,MS
105	(*E*)-β-ionone	1482	1487	0,2	Std
106	δ-selinene	1484	1492	0,3	RI,MS
107	α-selinene	1486	1498	0,2	RI,MS
108	*epi*-cubebol	1488	1493	0,1	RI,MS
109	1-pentadecene	1493	1493	1,7	RI,MS
110	(*Z*,*E*)-α-farnesene	1495	1494	0,9	RI,MS
111	β-bisabolene	1505	1505	0,1	RI,MS
112	cubebol	1507	1514	0,1	RI,MS
113	*trans*-calamenene	1517	1521	0,3	RI,MS
114	δ-cadinene	1517	1523	0,3	RI,MS
115	α-calacorene	1535	1544	0,4	RI,MS
116	β-calacorene	1556	1564	0,2	RI,MS
117	(*E*)-nerolidol	1564	1561	1,0	Std

118	spathulenol	1569	1577	3,5	RI,MS
119	caryophyllene oxide	1572	1582	1,2	Std
120	β-copaen-4-α-ol	1578	1590	0,7	RI,MS
121	β-oplopenone	1594	1607	0,7	RI,MS
122	junenol	1605	1618	1,4	RI,MS
123	tetradecanal	1612	1611	0,2	RI,MS
124	humulane-1,6-dien-3-ol	1618	1619	0,3	RI,MS
125	muurola-4,10(14)-dien-1-β-ol	1621	1630	0,4	RI,MS
126	silphiperfol-6-en-5-one	1626	1624	0,2	RI,MS
127	*iso*-spathulenol	1630	1631*	0,2	RI,MS
128	*epi*-α-cadinol	1633	1638	0,5	RI,MS
129	cubenol	1636	1645	0,2	RI,MS
130	β-eudesmol	1640	1649	0,2	RI,MS
131	selin-11-en-4-α-ol	1645	1660	1,1	RI,MS
132	α-cadinol	1647	1652	0,3	RI,MS
133	*cis*-calamenen-10-ol	1653	1660	0,2	RI,MS
134	*trans*-calamenen-10-ol	1661	1668	0,3	RI,MS
135	cadalene	1673	1675	0,1	RI,MS
136	amorpha-4,9-dien-2-ol	1698	1700	0,3	RI,MS
137	2-pentadecanone	1699	1697	0,1	RI,MS
138	n-pentadecanal	1714	1714	1,6	RI,MS
139	γ-costol	1739	1745	0,5	RI,MS
140	eupatoriochromene	1753	1761	0,4	RI,MS
141	α-costol	1763	1773	0,2	RI,MS
142	tetradecanoic acid	1768	1767	0,1	RI,MS
143	*epi*-cyclocolorenone	1776	1774	0,1	RI,MS
144	1-tridecene-3,5,7,9,11-pentayne	1805	1809*	0,1	RI,MS
145	*n*-hexadecanal	1816	1816	Tr	RI,MS
146	2-pentadecanone, 6,10,14-trimethyl-	1846	1845	0,4	RI,MS
147	2-phenyltridecane	1903	1903	Tr	RI,MS
148	(5*E*,9*E*)-farnesyl acetone	1916	1913	0,1	RI,MS
149	methyl hexadecanoate	1928	1921	0,2	RI,MS
150	isophytol	1948	1946	0,1	RI,MS
151	*n*-hexadecanoic acid	1965	1959	3,0	Std
152	methyl linoleate	2097	2095	0,1	RI,MS
153	*n*-heneicosane	2100	2100	0,1	Std
154	(*E*)-phytol	2116	2116	Tr	Std
155	*n*-tricosane	2300	2300	0,6	Std
156	*n*-tetracosane	2400	2400	0,1	Std
157	*n*-pentacosane	2500	2500	0,6	Std
158	methyl docosanoate	2534	2531	Tr	RI,MS

159	*n*-heptacosane	2700	2700	0,1	Std
160	squalene	2837	2847	0,1	RI,MS
161	*n*-nonacosane	2903	2900	Tr	Std
	Total identified (%)			87,3	
	Grouped compounds (%)				
	Terpenoids				
	Monoterpene hydrocarbons			24,7	
	Oxygenated monoterpenes			22,2	
	Sesquiterpene hydrocarbons			9,3	
	Oxygenated sesquiterpenes			14,1	
	Diterpenes			0,1	
	Norisoprenoids			0,4	
	Aromatics			0,4	
	Aliphatics				
	Fatty acids			3,1	
	Alkanes, alkenes and alkynes			3,5	
	Esters			0,5	
	Alcohols			0,5	
	Aldehydes			5,3	
	Ketones			0,5	
	Others			2,8	

[a] Compounds are listed in order of their elution from a HP-5MS column. [b] Linear retention index on HP-5MS column, experimentally determined using homologous series of C_8-C_{30} alkanes. [c] Linear retention index taken from Adams (2007) and/or NIST 08 (2008). [d] Relative percentage values are means of three determinations with a RSD% in all cases below 10%. [e] Identification methods: std, based on comparison with authentic compounds; NMR, based on spectroscopic data; MS, based on comparison with WILEY, ADAMS, FFNSC2 and NIST 08 MS databases; RI, based on comparison of calculated RI with those reported in ADAMS, FFNSC 2 and NIST 08. [f] Tr, % below 0.1%.

2.4.3.2. Antimicrobial activity

As shown in Table 7 the *T. diversifolia* EO was mostly active against *Staphylococcus aureus* (inhibition zone of 14 mm) and exhibited a moderate to low activity against *E. faecalis* and *E. coli* (inhibition zones of 8 and 9, respectively, Table 7). Results from the microdilution test has highlighted a MIC value of 2 mg/mL on *S. aureus*. As noted above, the high heterogeneity of the oil composition made it hard to detect the major components responsible of the observed activity. Indeed, we tested the major component α-pinene and we found that almost 10 mg of the pure compound had not been able to exert any inhibitory effect. Since that 10 mg of EO has been spotted onto the paper disc during the diffusion test, the relative amount of α-pinene into the EO (13.7 %) might be considered to be 1.37 mg. Hence we want to conclude by claiming that α-

pinene was not a significantly active part of the EO. Also the relative important amount of limonene (7.6%) may have not played an active role in the observed activity. Other minor components, such as n-hexadecanoic acid, may have contributed to some extent. However, no other pure compounds other than α-pinene have been tested in the present work.

Table 7. Antimicrobial activity of *T*. *diversifolia* EO by the diffusion disk method. Each value represents the diameter of the inhibition zone (millimeter) and is the average of three determinations. When appropriate, standard deviation is also indicated (± SD).

	S. aureus **ATCC 29213**	***E. faecalis*** **ATCC 29212**	***E. coli*** **ATCC 25922**	***P. aeruginosa*** **ATCC 27853**
Essential oil	14.0 ± 1.0	8.0 ± 0.5	9.0 ± 0.5	6.0 [a]
α-pinene	6.0 [a]	6.0 [a]	6.0 [a]	6.0 [a]
Ciprofloxacin	21.7 ± 1.5	20.3 ± 0.6	30.3 ± 0.6	29.3 ± 1.2

[a] no activity (no inhibition zone diameter)

2.4.3.3 Enzyme inhibition tests

The good results obtained from the disc diffusion test reported above (Table 7) prompted us to focus mainly on *S*. *aureus* NadD as antibacterial target. Furthermore, to assess the oil -selectivity we tested in parallel the oil inhibitory effects on the mammalian counter-targets. To this extent, we chose the three known murine NMNAT isoforms, that were all available and highly studied in the Department of Clinical Sciences-Section of Biochemistry of Prof. Giuseppe Orsomando (Polytechnic University of Marche), as representative of the mammalian hosts, being highly conserved and related, both structurally and functionally, to the corresponding human isozymes (Orsomando *et al*., 2012).

Overall these NaMN/NMN adenylyltransferases catalyze the same reaction but are distinguished based on their mononucleotide substrate preference. Indeed, NadD strictly utilizes nicotinate mononucleotide (NaMN) and ATP to form deamido-NAD and pyrophosphate, while all three NMNAT isozymes can also use the amidated substrate NMN to form NAD directly.

The three NMNATs in mammals originate from three distinct genes and are endowed with distinct tissue distribution, oligomeric structure, and subcellular localization (Sorci *et al*., 2007). Their apparent redundancy plays important roles at the mammalian organism level and is functional to maintain relevant levels of NAD within different organelles. Both NadD and individual NMNATs are vital enzymes for the corresponding organisms because essential for cellular NAD synthesis, as demonstrated by knocking down experiments, targeted protein degradation, and gene deletion (Sorci *et al*., 2013; Gilley *et al*., 2015). Thus, selective drug targeting of enzymes belonging to this family, for which no naturally-occurring compounds have been reported yet, is of recognized therapeutic value and prompted us to investigate on the biological effects of the EO from *T*. *diversifolia*. The results of our *in vitro* assays are shown in Figure 12.

Enzyme mixtures containing 80 μg/mL of essential oil showed ~70% inhibition of *S*. *aureus* NadD and ~50% inhibition of murine NMNAT2 compared to their blank controls, with no substantial effect on the other two mammalian isoforms (top panel). This lack of inhibition of NMNAT1 and NMNAT3 in parallel assays and the addition of 0.1 mg/ml of bovine serum albumine in the assay mixture, suggests that the inhibitory effect observed on NadD (and NMNAT2) is specific, and not due to promiscuous activities triggering general structural unfolding. Moreover, both enzyme targets were inhibited in a dose-dependent manner with similar calculated IC_{50} values of 60-70 μg/mL (bottom panel). It must be noted that all data in Figure 12 refer to assays carried out at substrates concentration just above the corresponding *K*m, but very similar results were also achieved using saturating concentration of both substrates (data not shown), thus suggesting a likely non-competitive inhibition mechanism exerted by some oil component(s), yet to be identified. Among the compounds listed in Table 6, the most abundant are α-pinene and limonene.

For this reason, we decide to test them individually against all the target enzymes under similar assay conditions. As a result, no inhibition was observed with both compounds (data not shown), despite being tested at 20 μg/mL, i.e. a far higher concentration than predicted in the oil mixture.

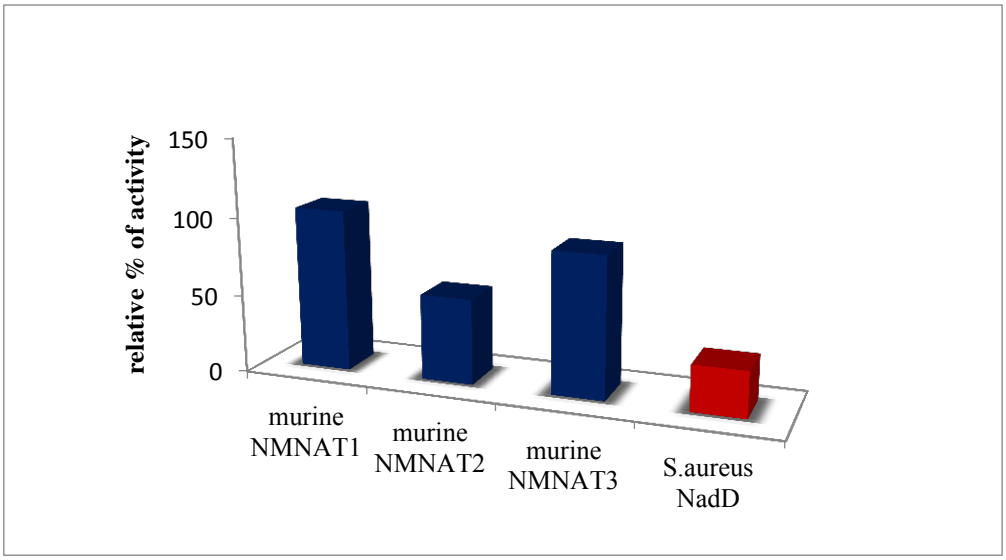

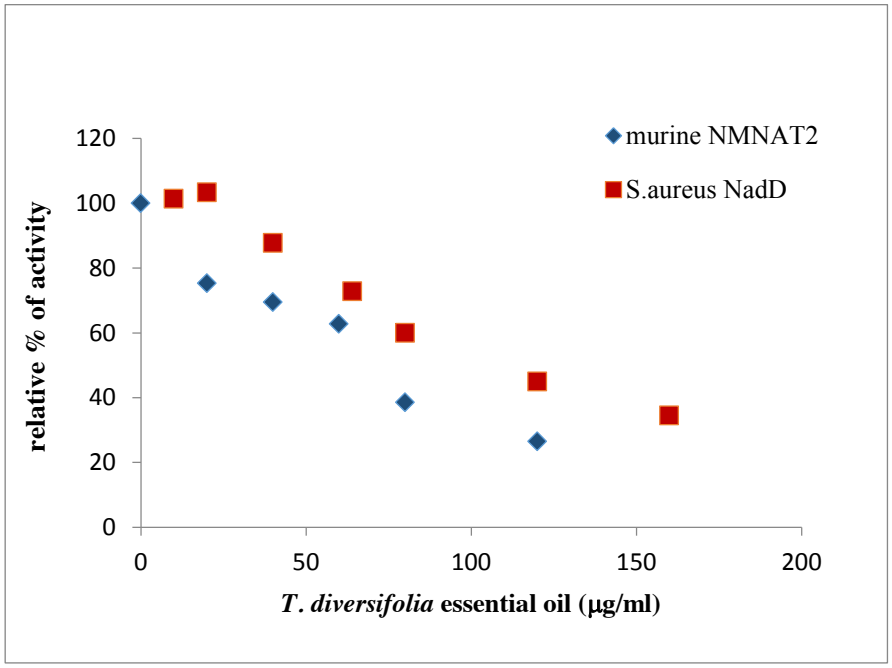

Fig. 12. *In vitro* effect of *T. diversifolia* EO on indispensable NaMN/NMN adenylyltransferases from various sources. Data reported were from either the continuous (blue bars and squares) or the discontinuous (red bar and squares) assay described in M&M, carried out at 80 µg/ml fixed oil concentration (top panel) or variable oil concentration (bottom panel). The continuous assay of the three individual murine NMNAT isoforms was carried out in 30 mM HEPES buffer, pH 7.5, 0.04 mM NMN, 0.08 mM ATP, 12.5 mM $MgCl_2$, 1% (v/v) DMSO, 75 mM ethanol, 30 mM semicarbazide, 12.5 U/ml yeast alcohol dehydrogenase, and 0.5 mg/ml BSA. The discontinuous assay of *S. aureus* NadD was carried out in 100 mM HEPES buffer, pH 7.5, 0.05 mM NaMN, 0.1 mM ATP, 10 mM $MgCl_2$, 1% (v/v) DMSO), 2 U/ml yeast inorganic pyrophosphatase, and 0.1 mg/ml BSA. Each enzymatic assay was at least in duplicate, and the activity values were reported as percentages relative to parallel blank controls.

Two main conclusions could be drawn from the data reported before. First, the *T. diversifolia* EO contains potential inhibitors of vital NAD biosynthetic enzymes that peculiarly show selectivity versus NadD, and thus potentially versus most bacterial pathogens. These molecules, once identified, will then represent valuable novel antibacterials from natural sources. Second, such bioactive compounds contained into the EO, should be highly potent. Indeed, based on the relative abundance of single components in the *T. diversifolia* oil mixture (see Table 6), and having ruled out that the inhibitory effect is attributable to the most abundant components of the mixture (α-pinene and limonene, respectively), we estimate that the observed inhibition is due to some EO components present in the mixture at sub-nanomolar concentrations.

From a pharmacological point of view, the observed parallel targeting of NMNAT2 in the mammalian host organism appears scarcely significant, being this isozyme almost exclusively located in neuronal tissues and less relevant with respect to the ubiquitous human isoform NMNAT1. However, the identification of potent and selective inhibitors of NMNAT2 might help the crystallization of this enzyme, being the only human isoform still missing a 3D definition.

2.4.3.4 Antioxidant activity

To accurately evaluate the antioxidant properties of *T. diversifolia* EO, three different antioxidant assays, DPPH free radical scavenging activity, ABTS radical cation scavenging activity and ferric reducing antioxidant power (FRAP) have been carried out. The results obtained are reported in Table 8 and have been expressed as IC_{50} and in absolute terms (i.e., μmol trolox equivalent (TE)/g).

T. diversifolia EO showed a relevant antioxidant activity, with IC_{50} values of only 30 times lower than that of trolox (a synthetic analogue of vitamin E) used as positive control for DPPH (108.8 μg/ml) and ABTS+ (41.7 μg/ml). Different studies associated the antioxidant activity observed with electron donation capacity of bioactive constituents and the results obtained with our FRAP assay (Table 8) confirmed the meaningful antioxidant reducing potential of *T. diversifolia* EO (Arabshahi-Delouee *et al*., 2007). Usually, in the plant EOs, the antioxidant potential is allocated to monoterpene hydrocarbons and oxygenated monoterpenes (Ruberto *et al*., 2000; Miguel, 2010). In line with what has been stated before and according to our phytochemical analysis, it was established that monoterpene hydrocarbons (24.7%) and oxygenated monoterpenes (22.2%) were the main components of the *T. diversifolia* EO and they probably played a significant role to the antioxidant activity observed.

Based on what has been described by Fogang *et al*. (Fogang *et al*., 2012), the presence in high percentage of some constituents such as α-pinene (13.7%) and limonene (7.6%), (Table 6) might contribute to the total antioxidant activity observed. Furthermore, the synergistic action of the complex mixture of minor components detected in the EO might also play a role on the free radical scavenging activity found.

Table 8. *In vitro* radical-scavenging activities of EO from *T*. *diversifolia*

	DPPH TEAC (μmolTE/g)	**IC_{50} (μg/mL)**	**ABTS TEAC (μmol TE/g)**	**IC_{50} (μg/mL)**	**FRAP TEAC (μmol TE/g)**
Essential oil	139.0 ± 10.5	108.8 ± 4.30	142.0 ± 8.20	41.7 ± 1.8	167.3 ± 11.5
Positive control					
Trolox		3.78 ± 0.13	30.3 ± 0.6	1.48 ± 0.2	

2.4.3.5 Cytotoxic activity

The EO of *T*. *diversifolia* was tested *in vitro* for its potential tumour cell growth inhibitory effect on A375 human malignant melanoma cell line, MDA-MB 231 human breast adenocarcinoma cell line, HCT116 human colon carcinoma and T98G human glioblastoma multiforme cell line, using the MTT assay. As summarized in Table 9, the EO hold promising results with cell inhibition observed at seventy-two-hours of incubation. The results suggested that *T*. *diversifolia* EO inhibits the proliferation of A375, MDA-MB 231, HCT116 and T98G cells in a dose-dependent manner. The data show that the highest activity was observed on A375, with IC_{50} values of 3.02, 3.79, and 3.46 μg/mL, respectively. If we take into the account MDA-MB 231 and HCT116 cells, the IC_{50} values obtained are very close to those reported for cisplatin, an anticancer drug used as the positive control (IC_{50} values of 2.29 and 2.34 μg/mL, respectively). On the other hand, EO resulted less active on T98G cells with IC_{50} value of 12.82 μg/mL. However, regardless of the intrinsic IC_{50} value obtained (12.82 μg/mL), this result should be taken into the consideration since glioblastoma is one of the most lethal and aggressive/invasive human brain tumors reported so far and is particularly resistant to the current chemotherapy regimen (Karmakar *et al*., 2006).

The observed cytotoxicity of *T*. *diversifolia* EO was not specific toward a cancer cell line and unfortunately an isolated compound responsible for the cytotoxic activity on human tumor cell lines do not do not emerge from the composition of EO. Fogang *et al*. already reported that α-pinene and limonene showed a significant antiproliferative activity on the same cell lines with IC_{50} values ranging from 27.3 to 63.1 μg/mL and 18.4 to 124.0 μg/mL, respectively (Fogang *et al*., 2012). As indeed reported by Bansal *et al*. α-pinene exerts antiproliferative activity on MDA-MB-231 (mammary adenocarcinoma), MDA-MB-468 (mammary adenocarcinoma), MCF-7 (mammary adenocarcinoma), and UACC-257 (malignant melanoma) in the same range of concentrations (Bansal *et al*., 2007). Limonene shows antitumor activity on lung adenocarcinoma A549 (IC_{50} = 0.098 μL/mL) and hepatocarcinoma HepG2 (IC_{50} = 0.150 μL/mL) (Manassero *et al*., 2013) as well as induces apoptosis in LS174T colon cancer cells and in lymphoma cell line (IC_{50} = 35 μg/mL) (Jia *et al*., 2013).

Spathulenol is weakly active on human epidermoid carcinoma (KB) and inactive on human breast cancer (BC) and human small cell lung cancer (NCIH187) cell lines (Prawat *et al*., 2013). On the other hand, data reporting on the cytotoxic activity of *cis*-chrysanthenol, epoxycyclooctane, and α-copaene are incomplete or missing. Drawing some conclusions from the data reported below, we can argue that the concentrations of α-pinene (13.1%), limonene (7.6%), and cis chrysanthenol (6.2%) cannot fully explain the observed cytotoxic activity of *T*. *diversifolia* EO.

This means that the other minor compounds or a synergism between them might contribute to the activity of the EO. Based on the guidelines of the plant screening program of the National Cancer Institute (NCI, USA) of the USA, a crude oil is generally considered promising as cytotoxic agent when it shows an IC_{50} value (after incubation of 72 h) less than 20 μg/mL (Boik 2001).

In conclusion, *T*. *diversifolia* EO shows an excellent inhibitory activity against the three human tumor cell lines with IC_{50} values comparable and in line with those reported in the NCI guidelines, and for this reason deserves further investigation.

Table 9. *In vitro* cytotoxic activity of *T*. *diversifolia* EO.

	Cell line (IC_{50} μg/mL)[a]			
	A375[b]	**MDA-MB 231[c]**	**HCT116[d]**	**T98G[e]**
Essential oil	3.02	3.79	3.46	12.82
95% C.I.[f]	2.64-3.47	3.28-4.38	3.25-3.68	11.56-14.22
Positive control				
Cisplatin	0.40	2.29	2.34	2.07
95% C.I.	0.33 - 0.46	2.04 - 2.78	2.14 - 2.59	1.86 - 2.23

[a] IC_{50} = The concentration of essential oil/compound that affords a 50% reduction in cell growth (after 72 h of incubation). [b] Human malignant melanoma cell line. [c] Human breast adenocarcinoma cell line. [d] Human colon carcinoma cell line. [e]Human glioblastoma multiforme cell line. [f]Confidence interval.

2.4.4 Summary and conclusions

T. *diversiflora* is a tropical shrub which is growing very fast in developing countries and for this reason is getting invasive of agricultural and non-agricultural lands. Given the enormous availability, this "green biomass" can be considered as renewable source of EO and could be exploited for therapeutic purposes or on an industrial level.

Results of this work showed that S. aureus cell growth, as well as its essential NAD biosynthetic enzyme NadD, are both inhibited by *T*. *diversiflora* EO, and that these effects are not attributable to its two major components, α-pinene and limonene. Further studies are required to verify if the *S*. *aureus* growth suppression is due to an on-target activity of the *T*. *diversifolia* EO mixture. Enzyme inhibition also appears to be selective against NadD from this bacterial pathogen, since none effects were observed with mammalian orthologue enzymes. The *T*. *diversifolia* EO revealed to be also a potent cytotoxic agent against a panel of tumor cells and the activity can be comparable to some extent at the anticancer drug cisplatin.

The major drawbacks of chemotherapy for treatment of human brain tumors are the incapability of many drugs to cross the blood-brain barrier. In this regard, *T*. *diversifolia* EO, being a mixture of many small lipophilic molecules, may constitute a new strategy for the treatment of glioblastoma.

2.5 Oviposition inhibitory activity of *T. diversifolia* extracts against the two-spotted mite *Tetranychus urticae* (Tetranychidae)

Given the potential of *T. diversifolia* to grow up very fast, the plant has been used in agriculture to improve soil fertility (Jama *et al*., 2000) and as feed for chickens for fattening (Ekeocha, 2012). Recently, based on the observation that some herbivores such as the caterpillar *Chlosyne lacinia* avoid the plant secretory structures (the place where the bitter sesquiterpene lactones are generated), the *T. diversifolia* extracts have attracted a lot of attention of scientists as useful tools in crop protection (Ambrósio *et al*., 2008).

These preliminary results are sufficiently documented by other studies where, for example, the leaf methanolic extract has been tested against the generalist phytophagous *Atta cephalotes*, showing a significant insecticidal effect (Castaño-Quintana *et al*., 2013). In another study carried out by Mikenda *et al*. (Mikenda *et al*. 2015), the authors found that *T. diversifolia* extract is active against key pest species like spiders, aphids, and beetles.

Adedire *et al*. (Adedire *et al*., 2004) reported that the leaf ethanolic extract of *T. diversifolia* has a highly oviposition inhibitory activity against the cowpea seed beetle, called *Callosobruchus maculatus*, that infests commonly stocked legumes. Finally Radhakrishnan *et al*. (Radhakrishnan *et al*., 2014), showed that the aqueous extract of the mexican sunflower exhibits a significiative effect against one the major pests infesting tea plantations, the red spider mite *Oligonychus coffeae*.

Nowadays, there is an urgent need to develop newer and safer control tools against arthropods of agricultural and medical importance (Pavela *et al*., 2016) and in this scenario fully lies our continuing investigations on the potential application of *T. diversifolia* on the industrial level (Orsomando *et al*., 2016). Hence, here we evaluated the acaricidal and oviposition inhibitory activity of the *T. diversifolia* polar extracts against the two-spotted spider mite *T. urticae* Koch (Tetranychidae), building on acute and chronic toxicity tests, as well as on experiments evaluating the oviposition inhibition potential. The chemical composition of the extracts determined by NMR and HPLC-MS measurements and previously described on subparagraph 3.1.1, have been correlated with the biological activity detected.

The two-spotted spider mite, *Tetranychus urticae* Koch (*Tetranychidae*), one of the most economically important arthropod pests, has been reported infesting over 1200 species of plants, including cereals, legumes (especially soybean), fruit trees and ornamental plants (Errard *et al*., 2016) (Figure 13). The high number of population outbreaks registered for this species lie principally to the short developmental time, to the long adult survival, and mainly to the rapid population growth (Zhang, 2003). This features, coupled with haplo-diploid sex determination,

flow into a speed-up rate of development of pesticide resistance. It has been recently reported that the mites have developed resistance to more than 90 acaricides (Pavela, 2015a). Therefore, is becoming increasingly important the reduction of synthetic acaricides in Integrated Pest Management programs and it is getting particularly crucial to alternate them with products showing different mechanisms of action (Naqqash *et al*., 2016).

In this framework, naturally-occurring compounds emerged as potential new control tools to be used against arthropod pests, including mites (Cheng *et al*., 2015).

Fig. 13. *Tetranychus urticae* - a plant pest.

2.5.1 Results and discussion

2.5.1.1 Toxicity and inhibition of oviposition on *Tetranychus urticae*

In this study, we evaluated the potential acaricidal and oviposition inhibition activities of the *T*. *diversifolia* leaf methanolic extract and its ethyl acetate fraction of *T*. *diversifolia*. Although both tested extracts caused mortality in *T*. *urticae* adults, significant differences were found between them. As we can see from Table 10 the methanolic and ethyl acetate extracts showed only low acute toxicity, and observed mortality did not exceed 39%. For this reason the lethal doses cannot be objectively estimated.

However, mortality of *T*. *urticae* adults increased in time (after 5 days the observed mortality was 100%) and this can be considered as a clear manifestation of chronic toxicity. The methanolic extract was the most toxic against mites, with a LD_{50} value of 41.3 $\mu g.cm^{-3}$ and a LD_{90} of 98.7 $\mu g.cm^{-3}$ (Table 10). In addition, both *T*. *diversifolia* extracts were able to inhibit oviposition

in *T*. *urticae*, with the ethyl acetate extract as the most active oviposition inhibitor with an ED_{50} value of 44.3 $\mu g.cm^{-3}$ and an ED_{90} of 121.5 $\mu g.cm^{-3}$ (Table 10). Mortality usually starts to be seen after few days from application and is frequently linked with substances contained in the extracts that also showed repellent effects or inhibition of oviposition of the insects on the treated plants. These kind of substances play an important role in natural defensive capacity of plants against pests and pathogens and some of them were contained in our tested *T*. *diversifolia* extracts.

If we compared the obtained lethal doses of *T*. *diversifolia* extracts to other plant extracts already published, we can easily see that our samples showed comparable efficacy. For example, Chen *et al*. (Chen *et al*., 2015) tested the *Cinnamomum camphora* extract against *Tetranychus cinnabarinus* and after 7 days of treatment, the LC_{50} values of two isolated compounds, 2,4-di-*tert*-butylphenol and ethyl oleate, were found to be 1850 and 2481 $mg.kg^{-1}$, respectively.

The acaricidal and ovicidal efficacy of the methanolic extract obtained from *Ammi visnaga* was also tested and two major substances (khellin and visnagin), belonging to the group of furanochromenes, were isolated from the extract. Adult mortality was calculated both for the extract and for the two isolated compounds and the LD_{50} values resulted to be 17, 10 and 98 $\mu g.cm^{-2}$, respectively.

However, is important to note that, besides the low toxicity of the tested extracts, their oviposition inhibition was very good, with special reference to the ethyl acetate extract (ED_{50} = 44.3 $\mu g.cm^{-3}$).

Chemical analysis of ethyl acetate extract highlighted a different qualitative profile compared with the methanolic one, with absence of caffeoylquinic acid derivatives and glycosylated flavonoids, and enrichment in tagitinins A and C. This is a clear evidence that the two tagitinins might play the major role as repellent and antifeedant agents against the two-spotted spider mite. Therefore, the relatively good yield rate of the extract (about 7%) and the high crop yield (5 t of dry matter ha^{-1}) (Jama *et al*., 2000) highlighted good prospects of using the *T*. *diversifolia* polar extracts for the development of oviposition inhibitors effective in pest control programs.

To our mind, the acaricidal and oviposition inhibitory effects of *T*. *diversifolia* extracts on *T*. *urticae* mainly lie on the sesquiterpene lactones tagitinins, which are reported as biologically active molecules of the Asteraceae family (Chagas-Paula *et al*., 2012). Notably, the bitter taste of this group of secondary metabolites plays an important role and makes the plant less palatable to herbivores. This might explain the antixenosis observed on *T*. *urticae*.

As reported by Susurluk *et al*. is now well-established that sesquiterpene lactones showed antifeedant activities on several arthropod pests (Susurluk *et al*., 2007). Indeed, tagitinin C,

exhibited pronounced antifeedant activity on the caterpillar *Chlosyne lacinia* (Lepidoptera) and when tagitinin C levels decreases in the plant, the infestation by caterpillar rises again.

We hypothesized that the mechanism of action by which the sesquiterpene lactones exerted their biological activities may be mediated by alkylation of biological macromolecules (e.g. Michael type additions) or by receptor-meditated interactions. In order to better clarify their mechanism of action on the two-spotted spider mite *T. urticae* as well as on non-target organisms, further studies are scheduled on tagitinins.

Regarding the possible role played by the other constituents detected in the extracts, little is known on their specific effect against *T. urticae*. In general, phenolic acids and flavonoids are believed to be responsible for reduction in the arthropod's growth and caffeoylquinic acids are capable of reducing the growth of the cabbage looper, *Trichoplusia ni*, (Beninger *et al*., 2004). One of the most common representative of this group, chlorogenic acid, was reported to be converted, in damaged plant tissue, into orthoquinones that are able to alkylate $–NH_2$ and –SH groups of amino acids and proteins leading to alteration of solubility and digestibility by arthropods.

On the other hand, hispidulin derivatives were found to be abundant components in some plant extracts (e.g. *Cnidoscolus aconitifolius*) and resulted to be highly toxic against the two-spotted spider mite (Numa *et al*., 2015). Finally, the synthesis of flavonoids isorhamnetin and quercetin, that are involved in the machinery of defense mechanisms, is considered to be a specific defense response of conifers against insect herbivory (Mohanta *et al*., 2012).

2.5.2 Summary and conclusions

Overall, the results of this study highlighted the promising potential of *T. diversifolia* as an effective and cheap biomass for the development of oviposition inhibitors against mites. On the other hand, in-depth studies focusing on the mechanisms of action of tagitinins A and C, against the *T. urticae*, are urgently needed, as well as the validation of the efficacy of *T. diversifolia* extracts.

Table 10. Acute toxicity, chronic toxicity and inhibition of oviposition evoked by the *T.diversifolia* methanolic and ethyl acetate extracts on the two-spotted spider mite Tetranychus urticae Koch.

Solvent	Dose ($\mu g.cm^{-2}$)	Acute toxicity		Chronic toxicity				Inhibition oviposition			
		Mortality[a] (±SE)	LD_{50}[b]	Mortality[a] (±SE)	LD_{50}[b] (CI_{95})	LD_{90}[b] (CI_{95})	Chi	Inhibition[a] (±SE)	ED_{50}[c] (CI_{95})	ED_{90}[c] (CI_{95})	Chi
Methanol	150	38.6 ± 3.8	>150	100.0 ± 0.0	41.3 (39.8-45.6)	98.7 (93.3-101.5)	0.895	62.8 ± 3.3	108.3 (98.6-121.7)	>150	2.325
	100	18.9 ± 2.5		95.7 ± 5.2				48.2 ± 3.2			
	80	5.8 ± 1.6		75.6 ± 3.9				38.7 ± 5.2			
	50	2.7 ± 0.9		58.3 ± 2.8				21.5 ± 5.3			
	25	2.5 ± 0.6		39.8 ± 5.6				9.8 ± 2.2			
Ethyl acetate	150	27.6 ± 2.8	>150	80.7 ± 6.8	85.3 (81.4-89.8)	153.5 (141.1-178.3)	0.965	100.0 ± 0.0	44.3 (41.8-51.9)	121.5 (111.6-138.9)	3.253
	100	21.5 ± 3.5		68.3 ± 8.2				87.3 ± 5.2			
	80	10.3 ± 5.2		46.6 ± 6.3				66.3 ± 4.7			
	50	0.0 ± 0.0		32.5 ± 6.2				46.2 ± 5.5			
	25	0.0 ± 0.0		16.5 ± 2.9				26.9 ± 3.3			

[a]Average mortality or inhibition oviposition (all in % ± the Standard Error).
[b]Lethal doses LD_{50} (LD_{90}) in $\mu g.cm^{-2}$ causing 50% (90%) mortality of T. urticae adults 24 h (for acute toxicity) and 5 days (for chronic toxicity) after application.
[c]Effective doses ED_{50} (ED_{90}) in $\mu g.cm^{-2}$ causing 50% (90%) inhibition oviposition of T. urticae in compared by control. CI95 = 95% confidence intervals, extract activity is considered significantly different when the 95% CI fail to overlap. Chi = square value, not significant (P>0.05).

2.6 Material and methods

2.6.1 Chemical and reagents

LC–MS grade acetonitrile (ACN) and methanol (MeOH) were obtained from J. T. Baker (Phillipsburg, USA). HPLC-grade formic acid was purchased from Dikma Tech. Inc. (Beijing, China). Cycloexane, deuterated chloroform, ethyl acetate and methanol were purchased from Sigma-Aldrich (Milan, Italy). Water (H_2O) was purified by a Milli-Q system (Millipore, Billerica, MA, USA) in our laboratory. The analytical standards of n-hexanal, n-nonane, α-pinene, camphene, benzaldehyde, β-pinene, 1-octen-3-ol, p-cymene, limonene, γ-terpinene, terpinolene, linalool, trans-thujone, trans-pinocarveol, terpinen-4-ol, α-terpineol, myrtenol, verbenone, n-decanal, geraniol, geranial, (*E*)-caryophyllene, α-humulene, (*E*)-β-ionone, (*E*)-nerolidol, caryophyllene oxide, n-hexadecanoic acid were purchased from Sigma-Aldrich (Milan, Italy) and used for identification of some peaks; (*E*)-phytol was previously isolated from *Onosma echioides* (Maggi *et al*., 2009). A mixture of n-alkanes (C8-C30) was purchased from Supelco (Bellefonte, PA) and used to calculate the temperature-programmed retention indices of chromatographic peaks. n-Hexane was purchased from Carlo Erba (Milan, Italy).

2.6.2 Plant material

Leaves and flowerheads (capitula) of *T*. *diversifolia* were harvested in Dschang, western region of Cameroon (N 05°26'18", E 10°04'07", 1450 m a.s.l), by Stephane Landry Ngahang Kamte and Saague T. Maximiliene in January 2016 during the dry season. Botanical authentication was performed by taxonomist Dr. Prosper C. Biapa Nya and a voucher specimen has been stored at the National Herbarium of Yaoundé, Cameroon, under the code 10196/HNC. Before extraction, leaves were air-dried in the dark at room temperature (≈25°C) for 3 days and stored in wrapping papers. Flowerheads were dried at ≈25°C in the shade for seven days before undergoing hydrodistillation.

2.6.3 Preparation of plant extracts

Fifty grams of *T*. *diversifolia* leaves were air-dried in the shade at room temperature (≈25 °C) conserved in wrapping papers, reduced into powder using a blender MFC DCFH 48 IKA-WERK (D-Staufen) and macerated in 500 ml of methanol for 24 h. After filtration, the extract was

concentrated under reduced pressure at 30°C with a rotary evaporator and freeze-dried to obtain a crude MeOH extract (2.64 g, 5.5% yield, Tith-MeOH). A portion of the methanolic extract (1.05 g) was then macerated in 200 ml of ethyl acetate for 24 h, yielding, after filtration and evaporation, 0.55 g (52.6%) of a dense ethyl acetate phase. Using the same protocol, an aqueous extract was obtained by maceration of 4 g of leaves in 50 mL of deionized water to get 0. 43 g (11.2%, Tith-H_2O) of extract. The extracts were kept in glass vials protected from light at −20 °C before chemical analysis and anti-trypanosomal and acaricidal experiments.

2.6.4 Analysis of *T. diversifolia* secondary metabolites by chromatography

Analysis of *T. diversifolia* secondary metabolites was performed on a LC–MS system. LC–MS equipment (Varian) comprised a binary chromatographic system (Varian LC-212) coupled with a mass spectrometer Varian 500-MS (ion trap). An ion source electrospray (ESI) (Varian) was used. MS^n spectra were recorded during the chromatography run by using of the turbo-dds (tdds) utility giving the MS fragmentation pathways of ionic species whose intensity was higher than a threshold level. HPLC-DAD analysis was carried out by an Agilent 1100 series liquid chromatograph equipped with autosampler (Agilent 1100 series) and Diode Array Detector (DAD) (Agilent 1100 series). An Eclipse XDB-C8 5µm 4.6 x150 mm (Agilent) column was used as stationary phase. The mobile phases were formed by aqueous formic acid (0.1%) (A) and acetonitrile (B). The gradient elution was as follows: 0–30 min, linear gradient from 10% to 100% of B; 30–35 min, isocratic conditions at 100% of B; 35–36 min, linear gradient from 100% to 10% of B; 36-40 min, isocratic conditions at 10% of B. Flow rate: 1 ml/min. Calibration curves were obtained by standard solutions of rutin for flavonoid derivatives (UV detection at 350 nm), chlorogenic acid for caffeoylquinic acid derivatives (UV detection at 330 nm), and gallic acid for small phenols (UV detection at 280 nm). The concentration ranges were 11.7–117 µg/ml and 13.2–132 µg/ml for chlorogenic acid and rutin, respectively. The limits of detection (LOD) and quantification (LOQ) were 1.5 and 4.0 µg/ml, and 0.5 and 1.5 µg/ml for chlorogenic acid and rutin, respectively.

2.6.5 Fractioning of the extracts and isolation of tagitinins A and C

The crude methanolic extract of *T. diversifolia* leaves (1 g) was dissolved in methanol and adsorbed on silica gel (40 mesh, 2 g). Subsequently, the solvent was removed under vacuum to obtain a dried powder. This powder was packed in a pre-column, which was fixed on a Silica column (Buchi Sepacore® silica 12 g). Separation was performed on a Varian Intelliflash Flash chromatograph.

The eluent was initially cyclohexane followed by an increasing percentage of methanol up to 30% in 120 min. The flow rate was 1 mL/min and the chromatogram was monitored at 220 and 340 nm. Eluted fractions were checked by TLC and collected in 19 groups. The solvent was removed under vacuum and the weight of each fraction obtained was as follows: 1 (21.2 mg), 2 (17.3 mg), 3 (19.1 mg), 4 (16.4 mg), 5 (21.5 mg), 6 (24.2 mg), 7 (16.1 mg), 8 (15.5 mg), 9 (13.3 mg), 10 (19.1 mg), 11 (10.1 mg), 12 (6.7 mg), 13 (7.8 mg), 14 (3.2 mg), 15 (102.2 mg), 16 (122.1 mg) 17 (81.3 mg), 18 (55.1 mg), 19 (35.1 mg). For tagitinins isolation 300 g of dried plant material was extracted using dichloromethane (600 mL× 3 times) using ultrasound bath. Liquids were collected, filtered and pooled and solvent was evaporated under vacuum. The crude extract (11.2 g) was used for chromatographic separation. A silica gel column (10 × 100 cm) was packed using hexane as solvent. Extract was charged in the column and hexane was used for elution, then hexane/ethyl acetate with an increasing ratio, starting from 6/1 to 1/1, was used as eluent system. 58 fractions were pooled on the basis of their chromatographic behaviour. Further separations were achieved on Sephadex LH20 column (5 ×40 cm) eluting with dichloromethane. Tagitinins A and C were isolated as pale oil (530 and 220 mg, respectively). Their spectral data were compared with those reported in literature (Baruah *et al*., 1979).

2.6.6 Qualitative and quantitative NMR analysis

NMR analysis was obtained on a Bruker AVANCE III spectrometer operating at 400.13 MHz for ^{1}H-NMR and 100 MHz for ^{13}C. 2D spectra, HSQC-DEPT, HMBC, COSY and TOCSY were used for compound identification in mixture. Samples were dissolved in deuterated methanol and used for analysis. For quantitative purposes, the extract was dissolved in deuterated chloroform at a final concentration of 30 mg/ml in a 5-mm NMR tube, and the solvent signal ^{1}H at 7.26 ppm was used for pulse calibration (Comai *et al*., 2010). Signals ascribable to tagitinin derivatives were deduced based onwhat has been reported in literature. The quantitative ^{1}H-NMR measurements were performed using caffeine as internal standard, because its ^{1}H-NMR signals (methoxy groups and aromatic proton) are clearly separated from those of extract components. A stock solution of caffeine in deuterated chloroform was prepared and 500 µl of this solution (3.1×10^{-5} mol) were added to an NMR tube with 30 mg of the extract. Each measurement was performed in triplicate.

2.6.7 Hydrodistillation of essential oil

Dry flowerheads (capitula) (500 g) were chopped up into small pieces, then subjected to hydrodistillation in a Clevenger-type apparatus for 5 h using 7 L of deionized water. The essential oil yield (0.11%) was determined on a dry-weight basis (w/w). Once obtained, the oil was dried using Na_2SO_4, filtered off and stored into an amber glass flask, and kept at −20◦C before chemical analysis and biological experiments.

2.6.8 Chemical analysis of essential oil

Gas chromatographic separation of *T*. *diversifolia* of volatiles was achieved on an Agilent 6890N gas chromatograph coupled to a 5973 N mass spectrometer. For the purpose a HP-5 MS (5%phenylmethylpolysiloxane, 30 m, 0.25 mm i.d., 0.1 μm film thick-ness; J & W Scientific, Folsom) capillary column was used with the following temperature program: 5 min at 60 °C, subsequently 4 °C/min up to 220 °C, then 11°C/min up to 280 °C, held for 15 min, for a total run of 65 min. Injector and detector temperatures were 280 °C. The carrier gas was He, with a flow rate of 1 mL/min. The split ratio employed was 1:50. Acquisition of mass spectra (m/z 29–400) was in electron-impact (EI) mode with an ionization volt-age of 70 eV. Before injection, the essential oil was diluted 1:100 in n-hexane, then 2 μL of the solution were injected into GC–MS system. For identification of essential oil components co-injection with the above standards was used, together with correspondence of retention indices and mass spectra with respect to literature data (Adams, 2007; NIST 08, 2008; FFNSC2, 2012). Semi-quantification of essential oil components was made by peak area normalization without calculating GC response factors.

2.6.9 *T. brucei* and mammalian cell culture

The cell culture conditions and the growth inhibition assay on *T*. *brucei* and BALB/3T3 cells were performed as described before (Petrelli *et al*., 2016). *T*. *brucei* bloodstream forms (TC221) were cultured at 37 °C with 5% CO_2 in HMI-9 medium supplemented with 10% (v/v) heat-inactivated fetal bovine serum (Gibco). Mouse BALB/3T3 fibroblast (ATCC no CCL-163) were cultivated at 37 °C and 5% CO2 in Dulbecco's modified Eagle's medium (Sigma), supplemented with 10% (v/v) heat-inactivated fetal bovine serum, glutamine (0.584 g/L) and 10 mL/L of 100 x penicillin-streptomycin(Gibco BRL) (Hirumi *et al*., 1989).

2.6.10 Growth inhibition assay and *T.brucei* and BALB/3T3 cells

The methanolic extract and its fractions were dissolved in dimethyl sulfoxide (DMSO). They were serially diluted with growth medium to concentrations ranging from 2×10^{-5} to 200 µg/mL in 96-wells microtiter plates (100 µL/well). Subsequently, 100 µL of *T. brucei* or mammalian cell culture was added to each well (20,000 cells/well). After 48 h incubation, the plates were treated for 24 h with 20 µL of 0.5 mM resazurine (Sigma-Aldrich). They were subsequently quantified by fluorescence (540 nm excitation and 590 nm emission) using an Infinite M200 microplate reader (Tecan Group, Ltd.). The IC_{50} values were calculated by fitting the data to a log inhibitor *vs*. response curve (variable slope, four parameters) using the GraphPad Prism 5.04 software.

2.6.11 Antibacterial activity

T. diversifolia EO was assayed by agar disc diffusion method against a panel of bacterial species including *Staphylococcus aureus* ATCC 25923 (American Type Culture Collection, Rockville, MD, USA), *Escherichia coli* ATCC 25922, *Pseudomonas aeruginosa* ATCC 27853, *Enterococcus faecalis* ATCC 29212 following the Clinical and Laboratory Standards Institute (CLSI) guidelines (CLSI, 2009). Strains were maintained overnight at 37◦Cin blood agar plates (Oxoid, Basingstoke, UK). Tested microorganisms (1–2 x 10^8 cells per mL in saline) were spread on the media plates using a sterile cotton swab. Paper discs of 6 mm in diameter were placed on the surface of inoculated plates and spotted with 10 µL of the EO. The plates were incubated 24 hat 35 ± 1 °C. The inhibition zones were measured with a calliper. A reading of more than 6 mm meant growth inhibition. The fluoroquinolone ciprofloxacin (5 µg disc) was used as a reference antibiotic. α-Pinene, the most prevalent compound into the EO, was also added to the series to test its activity in the pure form (10 µL per disc). The inhibition on *S. aureus* was also investigated by the microdilution method following the international guidelines (CLSI, 2009). Briefly, two-fold serial dilutions of mixture in Cation Adjusted Mueller Hinton Broth was set in 96-well plates starting from 8 mg/L. An equal volume of the microbial inoculum(106 cfu/mL), obtained by direct colony suspension of an overnight culture, was added to each well of the microtiter plate containing 0.1 mL of the serially diluted test oil. After incubation for 18–24 hat 35 °C, in normal atmosphere, the Minimum Inhibitory Concentration (MIC) was calculated as the lowest concentration of the EO inhibiting the growth of the bacterium. All microbial tests were done in triplicate.

2.6.12 Enzyme inhibition assay

Selected NaMN/NMN adenylyltransferase enzymes were chosen to represent either pathogenic bacteria or their mammalian hosts. Pure recombinant NadD from *S*. *aureus* subsp. aureus N315 was a generous gift from Dr. Andrei Osterman (Sanford Burnham Prebys Medical Discovery Institute, La Jolla, Ca, USA). The three *Mus musculus* isozymes NMNAT1, NMNAT2, and NMNAT3 were obtained after bacterial overexpression and purification as previously described (Orsomando *et al*., 2012). Enzyme rates were measured by using two equivalent spectrophotometric coupled methods, namely a continuous assay based on detection at 340 nm of the NADH formed, and a discontinuous assay based on detection at 620 nm of the phosphate formed (Vitali *et al*., 2015). The reaction mixtures, in addition to the buffer, substrates, and ancillary system reactants, contained 1.5–4 mU/mL of either *S*. *aureus* NadD or one of the three mammalian NMNAT isoforms. The EO from *T*. *diversifolia* was previously diluted in DMSO and then added to the reaction mixtures at 20–160 μg/mL final concentration. Blank mixtures without the oil but with equal amounts of DMSO were set in parallel and their rates fixed as 100% activity. Each enzyme was pre-incubated with the oil for 5 min at 37 °C, and then reactions were started by adding NMN for mammalian NMNATs or NaMN for bacterial NadD. Measured rates were linear under these conditions for at least 20 min.

2.6.13 Antioxidant activity

The antioxidant activity of *T*. *diversifolia* EO was measured by determining the hydrogen donating or radical scavenging ability, using the stable radical DPPH. The assay was assessed on a microplate analytical assay following a previously-described protocol (Srinivasan *et al*., 2007). Total radical scavenging capacity of the EO was measured by the ABTS assay modified as by Re *et al*. (Re *et al*., 1999), for application to a 96-well microplate assay. The ferric reducing antioxidant power (FRAP assay) was carried by monitoring the reduction of Fe3+-tripyridyl triazine (TPTZ) to blue-coloured Fe^{2+}-TPTZ. The ability of *T*. *diversifolia* EO to scavenge the different radicals in all assays was compared to Trolox used as positive control and expressed as tocopherol-equivalent antioxidant capacity μmol TE/g of product. Each experiment was repeated at least three times.

2.6.14 MTT assay

A375 (human malignant melanoma cells) and MDA-MB 231cells (human breast adenocarcinoma cells) were cultured in Dulbecco's Modified Eagle's Medium (DMEM) with 2 mM l-glutamine, 100 IU/mL penicillin, 100 μg/mL streptomycin, and supplemented with 10% heat-inactivated fetal

bovine serum (HI-FBS). HCT116 cells (human colon carcinoma cells), were cultured in RPMI1640 medium with 2 mM l-glutamine, 100 IU/mL penicillin,100 μg/mL streptomycin, and supplemented with 10% HI-FBS.T98 G cells (human glioblastoma multiforme cells) were cultured in Eagle's minimum essential medium (EMEM) with 2 mM L-glutamine, 0.1 mM non-essential amino acids, 1 mM sodium pyruvate, 100 IU/mL penicillin, 100 μg/mL streptomycin, and supplemented with 10% HI-FBS. Cells were cultured in a humidified atmosphere at 37◦C in presence of 5% CO_2. The MTT assay was used as a relative measure of cell viability. Cell-viability assays were carried out as described (Quassinti *et al*., 2013). Briefly, cells were seeded at the density of 2 x 104 cells/mL. After 24 h,samples were exposed to different concentrations of EO (0.78–200 μg/mL). Cells were incubated for 72 h in a humidified atmosphere of 5% CO_2 at 37 °C. Cisplatin was used as the positive control (0.05–20 μg/mL). At the end of incubation, each well received 10 μL of 3-(4,5-dimethyl-2-thiazolyl)-2,5-diphenyl-2H-tetrazoliumbromide (MTT) (5 mg/mL in phosphate-buffered saline,PBS) and the plates were incubated for 4 h at 37◦C. The extent of MTT reduction was measured spectrophotometrically at 540 nm using a Titertek Multiscan microElisa (Labsystems, FI-Helsinki).Experiments were conducted in triplicate. Cytotoxicity is expressed as the concentration of compound inhibiting cell growth by 50% (IC_{50}). The IC_{50} values were determined with GraphPad Prism 4computer program (GraphPad Software, S. Diego, CA, USA).

2.6.15 Mites

Two-spotted spider mites, *T*. *urticae*, were obtained from the cultures maintained at the Crop Research Institute (Czech Republic). The two-spotted spider mite used in the experiments was reared on bean plants (Phaseolus vulgaris L. var. Carmen) in a growth chamber (22–25 °C; 16 h photoperiod) (Pavela, 2015).

2.6.16 Acute and chronic toxicity

The toxicity, measured as mortality after 24 h (acute toxicity) or 120 h (chronic toxicity) of exposure, was determined by tarsal application to adults of *T*. *urticae*. The experiment was done in blackberry leaf disks (*Rubus fruticosus* L., Rosaceae) sized 1 cm^{-2}. The *T*. *diversifolia* methanolic and ethyl acetate extracts were dissolved in acetone. The compounds isofuranodiene, germacrone and isofuranodiene/$AgCF_3SO_3$ were dissolved in acetone. Subsequently, an automatic pipette was used to uniformly apply to the cut pieces always 10 μl of acetone containing a defined dissolved amount of the extracts in order to obtain a concentration series equivalent to the doses of 150, 100,

80, 50, 25, and 12.5 μg cm^{-2}. After application, the disks were placed in Petri dishes (5 cm in diameter) with an agar layer 0.3 cm thick on the bottom (to maintain the freshness of the disks and standard ambient humidity). Only acetone was applied to the control disks. After evaporation of the solvent (approximately 10 min from application), a fine brush was used to transfer 10 females of *T. urticae* (2–3 days old) on each of the treated sides of the leaf disks. The Petri disks were placed in a growth chamber (L16:D8, 25 °C). The cut leaf disks were checked after 24 h from application, determining the number of dead adults. Death was recorded when the larvae did not respond to prodding with forceps. The experiments were repeated five times.

2.6.17 Oviposition inhibitory potential

In order to determine the potential oviposition inhibitory potential capacity of the *T. diversifolia* extracts, an experiment was carried out using a methodological procedure identical to that described above for acute and chronic toxicity, with some modifications (Pavela, 2015). Five females (3–4 days old) were transferred using a fine brush onto each of the cut bean leaf disks sized 1 cm^{-2}. The leaf disks were obtained from those bean leaves that had been treated identically as described for acute and chronic toxicity, and after drying of the spray, using a cork borer. The cut disks with the mite females were placed in Petri dishes with an agar bottom. The females were removed after 48 h, and the laid eggs were counted. Subsequently, the number of eggs was determined for individual concentrations, and the lethal concentration causing oviposition inhibition by 50 or 90% compared to the control was estimated using probit analysis. The Petri dishes were placed in a growth chamber (L16:D8, 25 °C). The experiments were repeated five times.

2.6.18 Data analysis

Experimental tests demonstrated that more than 20% of the controlled mortality was discharged and repeated. When the controlled mortality reached 1–20%, the observed mortality was corrected by Abbott's formula (Abbott, 1925). Probit analysis of dose–mortality data was conducted to estimate the LD_{50} and LD_{90} values and associated 95% confidence limits for each treatment (Benelli, 2017).

References

Abea, A.E., de Oliveira, C.E., Dalboni, T.M., Chagas-Paula, D.A. *et al*. (2015). Anti-inflammatory sesquiterpene lactones from Tithonia diversifolia trigger different effects on human neutrophils. *Braz*. *J*. *Pharmacog*. *25*, 111–116.

Abbott, W.S. (1925). A method of computing the effectiveness of an insecticide. *J*. *Econ*. *Entomol*. *18*, 265–267.

Adams, R. (2007). Identification of Essential Oil Components by Gas Chromatography/Mass Spectrometry, fourth ed. Allured Publishing Corp., CarolStream, IL, USA.

Adedire, C.O., Akinneye, J.O. (2004). Biological activity of tree marigold, Tithonia diversifolia, on cowpea seed bruchid, Callosobruchus maculatus (Coleoptera: Bruchidae). *Ann*. *Appl*. *Biol*. *144*, 185-189.

Ambrósio, S.R., Oki, Y., Heleno, V.C.G., Chaves, J.S. *et al*. (2008). Constituents of glandular trichomes of Tithonia diversifolia: Relationships to herbivory and antifeedant activity. *Phytochemistry 69*, 2052-2060.

Arabshahi-Delouee, S., Urooj A. (2007). Antioxidant properties of various solvent extracts of mulberry (Morus indica L.) leaves. *Food Chem*. *102* , 1233–1240.

Ayeni, A.O., Lordbanjou, D.T., Majek, B.A. (1997). Tithonia diversifolia (Mexican sunflower) in south-western Nigeria: occurrence and growth habit. *Weed Res*. *37*, 443-449.

Bakkali, F., Averbeck, S., Averbeck, D., Steer, M. *et al*. (2008). Biological effects of essential oils-a review. *Food Chem*. *Toxicol*. *46*, 446–475.

Bansal, A., Moriarity, D.M., Takaku, S., Setzer, W.N. (2007). Chemical composition and cytotoxic activity of the leaf essential oil of Ocotea tonduzii from Monteverde, Costa Rica. *Nat*. *Prod*. *Comm*. *2*, 781–784.

Baruah, N.C., Sharma, R.P., Madhusudanan, K., Thyagarajan, G. *et al*. (1979). Sesquiterpene Lactones of Tithonia diversifolia. Stereochemistry of the tagitinins and related compounds, J. Org. Chem. *44*, 1831–1835.

Baser, K.H.C., Demirci, F. (2007). Chemistry of essential oils. In: Berger RG (ed) Flavours and fragrances-chemistry, bioprocessing and sustainability. Springer, Berlin, 43–86.

Bauer, K., Garbe, D. (2001). Common fragrance and flavour materials. Preparation, properties and uses. VCH Verlagsgesellschaft, Weinheim.

Benelli, G. (2017). Commentary: Data analysis in bionanoscience–issues to watch for. *J Clust Sci*. *6*, 1143-1148.

Beninger, C.W., Abou-Zaid, M.M., Kistner, A.L.E., Hallett, R.H. *et al*. (1998). *J*. *Chem*. *Ecolo*. *30*, 589-606.

Boik, J. (2001). Natural compounds in cancer therapy. MN, USA: Oregon Medicinal Press.

Bowsher, C., Steer, M., Tobin, A. (2008). Plant biochemistry. Garland Science, New York.

Buchbauer, G. (2000). The detailed analysis of essential oil leads to the understanding of their properties. *Perfumer Flavorist 25*, 64–67.

Castaño-Quintana, K., Montoya-Lerma, J., Giraldo-Echeverri, C. (2013). Toxicity of foliage extracts of Tithonia diversifolia (Asteraceae) on Atta cephalotes (Hymenoptera, Myrmicinae) workers. *Ind. Crops Prod. 44*, 391-395.

Chagas-Paula, D.A., Oliveira, R.B., Rocha, B.A., Da Costa, F.B. (2012). Ethnobotany, chemistry, and biological activities of the genus Tithonia (Asteraceae). *Chem. Biodivers. 9*, 210-235.

Cheng, Y., Dai, G. (2015). Acaricidal, repellent, and oviposition-deterrent activities of 2,4-di-tert-butylphenol and ethyl oleate against the carmine spider mite Tetranychus cinnabarinus. *J. Pest Sci. 88*, 645–655.

Chen, Y., Dai, G. (2015). Acaricidal activity of compounds from Cinnamomum camphora (L.) Presl against the carmine spider mite, Tetranychus cinnabarinus. *Pest Manag. Sci. 71*, 1561–1571.

CLSI (Clinical and Laboratory Standards Institute), (2009). Performance Standards for Antimicrobial, Disk Susceptibility Tests. Approved Standard M02-A10, 10th ed. CLSI, Wayne.
Comai, S., Dall'Acqua, S., Grillo, A., Castagliuolo, I. *et al*. (2010). Essential oil of Lindera neesiana fruit: Chemical analysis and its potential use in topical applications. *Fitoterapia 81*, 11-16.

Duke, L.A. (1982). Flavonoid chemistry and systematics of Tithonia (Compositae). *Am. J. Bot. 69*, 784-792.

Ekeocha, A.H. (2012). Utilization of Mexican Sunflower (Tithonia diversifolia, Hemsley a Gray) Leaf Meal on the Average Production Cost and Returns of Broiler Chicks. *J. Rec. Adv. Agri. 1*, 34-42.

Errard, A., Ulrichs, C., Kuhne, S., Mewis, I. *et al*. (2016). Metabolite Profiling Reveals a Specific Response in Tomato to Predaceous *Chrysoperla carnea* Larvae and Herbivore(s)-Predator Interactions with the Generalist Pests *Tetranychus urticae* and *Myzus persicae*. *Front. Plant Sci. 7*, 1256.

Ferreira, M.J., Brant, A.J., Alvarenga, S.A.V., Emerenciano, V.P. (2005). Neural networks in chemosystematic studies of Asteraceae: a classification based on a dichotomic approach. *Chem. Biodivers. 2*, 633-644.

FFNSC2 (2012). Flavors and fragrances of natural and synthetic compounds. In: Mass Spectral Database. Shimadzu Corps, Kyoto.

Gbolade, A.A., Biondi, D.M., Ruberto, G. (2008). Comparative analysis of the essential oils from two Asteraceous plants found in Nigeria, Acanthospermum hispidum and Tithonia diversifolia. *Nat. Prod. Comm. 3*, 1735-1738.

Goffin, E., Ziémons, E., De Mol, P., Madureira, M.C. *et al*., (2002). In vitro antiplasmodial activity of Tithonia diversifolia and identification of its main active constituent tagitinin C. *Planta Med. 68,* 543-545.

Heinrich, M. (2000). Ethnobotany and its role in drug development. *Phytother. Res.14*, 479–488.
Heinrich, M., Robles, M., West, J.E., de Montellano, B.R.O. *et al*. (1998). Ethnopharmacology of mexican asteraceae. *Annu. Rev. Pharmacol. Toxicol. 38*, 539–565.

Hirumi, H., Hirumi, K. (1989). Continuous cultivation of Trypanosoma brucei blood stream forms in a medium containing a low concentration of serum protein without feeder cell layers, *J. Parasitol. 75*, 985–989.

Karmakar, S., Banik, N.L., Patel, S.J., Ray, S.K. (2006). Curcumin activated both receptor-mediated and mitochondria-mediated proteolytic pathways for apoptosis in human glioblastoma T98G cells. *Neurosci. Lett. 407*, 53-58.

Isrun, B., Basir-Cyio, M., Wahyudi, I., Hasanah, U. *et al*. (2018). Tithonia diversifolia compost for decreasing the activity of mercury in soil. *J. Environm. Sci. Technol. 11*, 79-85.

Jama, B., Palm, C.A., Buresh, R.J., Niang, A. *et al*. (2000). Tithonia diversifolia as a green manure for soil fertility improvement in western Kenya: A review. *Agroforestry Syst. 49*, 201–221.

Játem-Lásser, A., Ricardi, M.S., Adamo, G. (1998). Herbal traditional medicine of Venezuelan Andes: an ethnopharmacological study. *Phytother. Res. 12*, S53–S59.

Jia, S.S., Xi, G.P., Zhang, M., Chen, Y.B. *et al*. (2013). Induction of apoptosis by D-limonene is mediated by inactivation of Akt in LS174T human colon cancer cells. *Oncol. Rep. 29*, 349-354.

Lawal, O.A., Kasali, A.A., Opoku, A.R., Oyedeji, A.O. (2012). Volatile constituents of the flowers, leaves, stems and roots of Tithonia diversifolia (Hemsely) A. Gray. *J. Essent. Oil-Bear. Plants 15*, 816-821.

Mabou Tagne, A., Marino, F., Cosentino, M. (2018). Tithonia diversifolia (Hemsl.) A. Gray as a medicinal plant: A comprehensive review of its ethnopharmacology, phytochemistry, pharmacotoxicology and clinical relevance. *J. Ethopharmacol. 220*, 94-116.

Maggi, F., Tirillini, B., Vittori, S., Sagratini, G. *et al*. (2009). Analysis of the volatilecomponents of Onosma echioides (L:) L. var. columnae lacaita growing in centralItaly. *J. Ess. Oil Res. 21*, 441-447.
Mohanta, T.K., Occhipinti, A., Zebelo, S.A., Foti, M. *et al*. (2012). Ginkgo biloba Responds to Herbivory by Activating Early Signaling and Direct Defenses. *PLoS one 7*, e32822.

Manassero, C.A., Girotti, J.R., Mijailovsky, S., García de Bravo, M. *et al*. (2013). In vitro comparative analysis of antiproliferative activity of essential oil from mandarin peel and its principal component limonene. *Nat. Prod. Res. 2*, 1475–1478.

Menut, C., Lamaty, G., Amvam Zollo, P.-H., Kuiate, J.R. *et al*. (1992). Aromatic Plants of Tropical Central Africa. IX. Chemical Composition of Flower Essential Oils of Tithonia diversifolia (Hemsl.) A. Gray from Cameroon. *J. Ess. Oil Res. 4*, 651-653.

Miguel, M.G. (2010). Antioxidant and anti-inflammatory activities of essential oils: a short review. *Molecules 15*, 9252-9287.

Mikenda P., Mwanauta R., Stevenson P.C., Ndakidemi P. *et al*. (2015). Extracts from field margin weeds provide economically viable and environmentally benign pest control compared to synthetic pesticides. *PLoS one 10*, e0143530.

Miura, T., Nosaka, K., Ishii, H., Ishida, T. (2005). Antidiabetic effect of nitobegiku, theherb Tithonia diversifolia, in KK-Ay diabetic mice. *Biol*. *Pharm*. *Bull*. *28*, 2152–2154.

Moronkola, D.O., Ogunwande, I.A., Walker, T.M., Setzer, W.N. *et al*. (2007). Identification of the main volatile compounds in the leaf and flower of Tithonia diversifolia (Hemsl) Gray. *J*. *Nat*. *Med*. *61*, 63–66.

Mori, V., Amici, A., Mazzola, F., Di Stefano, M. *et al*. (2014). Metabolic Profiling of Alternative NAD Biosynthetic Routes in Mouse Tissues. PlosOne 9, e113939.

Naqqash, M.N., Gökçe, A., Bakhsh, A., Salim, M. (2016). Insecticide resistance and its molecular basis in urban insect pests. *Parasitol*. *Res*. *115*, 1363-1373.

NIST 08 (2008). Mass Spectral Library (NIST/EPA/NIH). National Institute ofStandards and Technology, Gaithersburg, USA.

Njoroge, G.N., Bussman, R.W. (2006). Herbal usage and informant consensus inethnoveterinary management of cattle diseases among the Kikuyus (CentralKenya). *J*. *Ethnopharmacol*. *108*, 332–339.

Numa, S., Rodriguez, L., Rodriguez, D., Coy-Barrera, E. (2015). Susceptibility of *Tetranychus urticae* Koch to an ethanol extract of *Cnidoscolus aconitifolius* leaves under laboratory conditions. *Springer Plus 4*, 338-347.

Olayinka, B.U., Raiyemo, D.A., Obukohwo, E. (2015). Phytochemical and proximate composition of T. diversifolia (HEMSL.) A. Gray. *Ann*. *Food Sci*. *Technol*. *16*, 195-200.

Orsomando, G., Agostinelli, S., Bramucci, M., Cappellacci, L. *et al*. (2016). Mexican sunflower (Tithonia diversifolia, Asteraceae) volatile oil as a selective inhibitor of Staphylococcus aureus nicotinatemononucleotide adenylyltransferase (NadD). *Ind*. *Crops Prod*. *85*, 181-189.

Orsomando, G., Cialabrini, L., Amici, A., Mazzola, M. *et al*. (2012). Simultaneous single-sample determination of NMNAT isozyme activities in mouse tissues. *PLoS one 7*, e53271.

Otoguro, K., Iwatsuki, M., Ishiyama, A., Namatame, M. *et al*. (2011). In vitro antitrypanosomal activity of plant terpenes against Trypanosoma brucei. *Phytochemistry 72*, 2024–2030.

Owuor, B.O., Kisangau, D.P. (2006). Kenyan medicinal plants used as antivenin: acomparison of plant usage. *J*. *Ethnobiol*. *Ethnomed*. *2*, 7.

Oyewole, I.O., Ibidapo, C.A., Moronkola, D.O., Oduola, A.O. *et al*. (2008). Anti-malarial and repellent activities of Tithonia diversifolia (Hemsl.) leaf extracts. *J*. *Med*. *Plants Res*. *2*, 171-175.

Pankiewicz, K.W., Petrelli, R., Singh, R., Felczak, K. (2015). Nicotinamide Adenine Dinucleotide Based Therapeutics, Update. *Curr*. *Med*. *Chem*. *22*, 3991-4028.

Passoni, F.D., Oliveira, R.B., Chagas-Paula, D.A., Gobbo-Neto, L. *et al*. (2013). Repeated-dose toxicological studies of Tithonia diversifolia (Hemsl:) A. gray and identification of the toxic compounds. *J*. *Ethnopharmacol*. *147*, 389–394.

Pavela, R. (2015). Acaricidal properties of extracts and major furanochromenes from the seeds of Ammi visnaga Linn. against Tetranychus urticae Koch. *Ind*. *Crops Prod*. *67*, 108–113.

Pavela, R. (2016). Acaricidal properties of extracts of some medicinal and culinary plants against Tetranychus urticae Koch. *Plant Prot*. *Sci*. *52*, 54-63.

Petrelli, R., Felczak, K., Cappellacci, L. (2011). NMN/NaMN adenylyltransferase (NMNAT) and NAD kinase (NADK) inhibitors: chemistry and potential therapeutic applications. *Curr*. *Med*. *Chem*. *18*, 1973-1992.

Petrelli, R., Orsomando, G., Sorci, L., Maggi, F. *et al*. (2016). Biological activities of the essential oil from Erigeron floribundus, *Molecules 21*, 1065.

Pichersky, E., Gershenzon, J. (2002). The formation and function of plant volatiles: perfumes for pollinator attraction and defense. *Curr*. *Opin*. *Plant Biol*. *5*, 237–243.

Prawat, U., Chairerk, O., Lenthas, R., Salae, A.W. (2013). Tuntiwachwuttikul P. Two new cycloartane-type triterpenoids and one new flavanone from the leaves of Dasymaschalon dasymaschalum and their biological activity. *Phytochemistry Lett*. *6*, 286-290.

Quassinti, L., Lupidi, G., Maggi, F., Papa, F. *et al*. (2013). Antioxidant and antiproliferative activity of Hypericum hircinum L: subsp.majus (Aiton) N. Robson essential oil. *Nat*. *Prod*. *Res*. *27*, 862–868.

Radhakrishnan, B., Prabhakaran, P. (2014). Biocidal activity of certain indigenous plant extracts against red spider mite, Oligonychus coffeae (Nietner) infesting tea. *J*. *Biopestic*. *7*, 29-34.

Re, R., Pellegrini, N., Proteggente, A., Pannala, A. *et al*. (1999). Antioxidant activity applying an improved ABTS radical cation decolorizationassay. *Free Rad*. *Biol*. *Med*. *26*, 1231–1237.

Rodionova, I.A., Zuccola, H.J., Sorci, L., Aleshin, A.E. *et al*. (2015). Mycobacterial nicotinate mononucleotide adenylyltransferase: structure, mechanism, and implications for drug discovery. *J*. *Biol*. *Chem*. *290*, 7693-7706.

Ruberto, G., Baratta, M.T. (2000). Antioxidant activity of selected essential oil components in two 545 lipid model systems. *Food Chem*. *69*, 167-174.

Saeidnia, S., Gohari, A.R., Haddadi, A. (2013). Biogenic trypanocidal sesquiterpenes: Lead compounds to design future trypanocidal drugs - A mini review. *DARU, J*. *Pharm*. *Sci*.*15*, 21-35.

Sangwan, N.S., Farooqi, A.H.A., Shabih, F. *et al*. (2001). Regulation of essential oil production in plants. *Plant Growth Regul*. *34*, 3–21.

Srinivasan, R., Chandrasekar, M.J.N., Nanjan, M.J., Suresh, B. (2007). Antioxidantactivity of Caesalpinia digyna root. *J*. *Ethnopharmacol*. *113*, 284–291.

Sorci, L., Cimadamore, F., Scotti, S., Petrelli, R.. *et al*. (2007). Initial-rate kinetics of human NMN-adenylyltransferases: substrate and metal ion specificity, inhibition by products and multisubstrate analogues, and isozyme contributions to NAD+ biosynthesis. *Biochemistry 46*, 4912-4922.

Sorci, L., Pan, Y., Eyobo, Y., Rodionova, I. *et al*. (2009). Targeting NAD biosynthesis in bacterial pathogens: Structure-based development of inhibitors of nicotinate mononucleotide adenylyltransferase NadD. *Chem*. *Biol*. *16*, 849-861.

Susurluk, H., Caliskan, Z., Kirmizigul, S., Goren, N. (2007). Antifeedant activity of some Tanacetum species and bioassay guided isolation of the secondary metabolites of Tanacetum cadmeum ssp. cadmeum (Compositae). *Ind*. *Crops Prod*. *26*, 220-228.

Taiz, L., Zeiger, E. (2010). Plant physiology, 5th edn. Sinauer Associates Inc. Publishers, Sunderland.

Takahashi, M. (1998). Compositions for curing diabetes mellitus, processes for the preparation of same, and usage of same US Pat. 5 773 004 (Fukuoka 1998,814-01).

Wink, M. (2008). Evolutionary advantage and molecular modes of action of multi-component mixtures used in phytomedicine. *Curr*. *Drug Metab*. *10*, 996–1009.

Yang, J., Tang, L., Guan, Y.-L., Sun, W.-B. (2012). Genetic Diversity of an Alien Invasive Plant Mexican Sunflower (Tithonia diversifolia) in China. *Weed Sci*. *60*, 552–557.

Vitali, L.A., Beghelli, D., Biapa Nya, P.C., Bistoni, O. *et al*. (2016). Diverse biological effects of theessential oil from Iranian Trachyspermum ammi. *Arabian J*. *Chem*. *9*, 775-786.

Zhai, R.G., Rizzi, M., Garavaglia, S. (2009). Nicotinamide/nicotinic acid mononucleotide adenylyltransferase, new insights into an ancient enzyme. *Cell*. *Mol*. *Life Sci*. *66*, 2805-2818.

Zhang, Z. (2003). Mites of Greenhouses: Identification Biology and Control. CABI Publishing, Wallingford, UK.

CHAPTER 3.

Identification of Skinonin derivatives from *Onosma visianii* roots extract as potential antitrypanosomal drugs or botanical insecticides.

"A bad wound deserves

a strong medicine."

Cameroon proverb

Chapter 3 Outline

Abbreviation

AchE = Acetylcholinesterase

ATCI = Acetylthiocholine iodide

BBBP = Blood brain barrier penetration

BSA = Bovine serum albuin

COSY = Correlation Spectroscopy

DEPT= Distortionless Enhancement by Polarisation Transfer

DQF-COSY = Double-Quantum Filtered Correlation Spectroscopy

DTNB = 5,5'-Dithiobis[2-nitrobenzoic acid]

gpAchE = *Glossina palpalis* acetylcholinesterase

hAchE = *Human* acetylcholinesterase

HMBC = Heteronuclear Multiple-Bond Correlation

HMQC = Heteronuclear Multiple-Quantum Correlation

HSQC = Heteronuclear Single Quantum Correlation

HSQC-TOCSY = Heteronuclear Single Quantum Correlation with additional TOCSY transfer

NOE = Nuclear Overhauser Effect

NOESY = Nuclear Overhauser Effect Spectroscopy

OPs = Organophosphates

TOCSY = Total Correlation Spectroscopy

Abstract

There is an increasing need for the discovery of reliable, cost-effective and safe antitrypanosomal drugs and naturally-occurring products may play a crucial role as source of active drug candidates. With this vision in mind, we investigated a lipophilic extract of *Onosma visianii* roots containing 12% of shikonin derivatives. The phytochemical investigation of the lipophilic extract resulted in the isolation of 12 naphtoquinone derivatives that were identified by spectral techniques and were then tested against *Trypanosoma brucei*. The activity was also studied against mammalian cells (BALB/3T3 mouse fibroblast), used as counter-screen for toxicity. The majority of the 12 naphtoquinone derivatives showed a significant antitrypanosomal activity and isobutylshikonin (**2**) and isovalerylshikonin (**3**) emerged as the most active, with an IC_{50} of 3.3 and 2.7 μg/mL, respectively.

Furthermore, isovalerylshikonin (**3**) provides a stronger inhibition of *Glossina palpalis* acetylcholinesterase (*gp*AChE) (IC_{50} = 7.1 μg/mL) than isobutyrylshikonin (IC_{50} = 91.3 μg/mL), with a significant tse-tse fly *versus* human selectivity (SI = 7.2). These findings provided new insights into the potential of shikonin-based derivatives as new valuable lead compounds for the development of innovative trypanocidal drugs or botanical insecticides.

3.1 Introduction

Parasitic protozoal diseases, including trypanosomiasis, remain to be tackled and represent the cause of considerable morbidity and mortality globally, leading to over one million deaths annually (Lee *et al*., 2013; Mansueto *et al*., 2014). They threaten almost one-third of the world's population and pose a serious health risk for hundreds of millions worldwide that results in financial difficulties.

The absence of vaccines, and in some cases, the emergence of resistant parasite strains, underlines the importance of the successful track record of natural-based antiprotozoal drug discovery drawing attention to the value of the "natural heritage" as an important source for the development of new drugs. Natural products are considered to have significant advantages as lead compounds over synthetic molecules. The criteria for choosing a natural product for in-depth studies rely either on the pre-existing traditional use (ethnobotanical knowledge) or on structurally related molecules with known pharmacologically pharmacophores.

The oxygen-derivatives of naphthalene, the naphthoquinones, are a class of plant secondary metabolites based on a C6-C4 skeleton (molecular formula $C_{10}H_6O_2$) originated from the shikimate pathway and widespread in several plant families, including Droseraceae, Juglandaceae, Nepenthaceae, Plumbaginaceae and Boraginaceae, where they act as defence against predators and/or allelochemicals (Akhtar *et al*., 2012).

This wide group of secondary metabolites have attracted research attention due to their remarkable pharmacological activities. Indeed, the naphtoquinones are considered privileged scaffolds in medicinal chemistry because of their biological activities which include antimicrobial, anticancer, wound healing, anti-inflammatory, antithrombotic, and antiprotozoal uses (Babula *et al*., 2009; Soeiro *et al*., 2009). They have also been employed as cosmetics, dyes, pigments, and food additives (Lubbe *et al*., 2011). Main examples are given by plumbagin, juglone, lawsone, alkannin, shikonin and its derivatives, with skikonin as the most important pigments used in the market (Malik *et al*., 2016).

Naphthoquinones are present in various families of plants, serving as vital connectors in the electron transport chains in multiple biological oxidative processes (O'Brien, 1991). The main feature of quinone scaffold is its ability to act as an oxidising or dehydrogenating agent (redox property) which is driven by the formation of a fully aromatic system (Hillard *et al*., 2008). The redox cycling of quinones may be initiated by either a one- or two-electron reduction, generating highly reactive species that may react directly with DNA or other cellular macromolecules (e.g. lipids and proteins) leading to cell damage.

The reported activity of naphthoquinones in increasing oxygen consumption and stimulating hydrogen peroxide formation, as has been demonstrated by menadione on *T.b*. *brucei*, provided the rationale for a study of antitrypanosomal activity on a plant known to be rich on naphtoquinones. For this reason, *Onosma visianii* Clem. has been selected as a source of bioactive napthoquinones to be studied against *T*. *brucei*.

O. *visianii*, belonging to Boraginaceae family, sect. *Haplotricha* Boiss., is a biennial herb occurring in steppic and rocky calcareous sites of Central and Southeastern Europe (Strid *et al*., 1991) (Figure 1). The plant is characterized by simple indumentum on green organs, composed of multicellular tubercles, with single setae on the top of tubercle and without asterosetules and short rays radially attached to the base of tubercle.

The species is characterized by a sterile rosette of linear-lanceolate densely setose leaves in first vegetation season; then usually a single reddish, erect and branched stem with terminal cymes arises from the rosette in the second vegetation season. Flowers are sympetalous, heterochlamydeous with short pedicels and pale yellow tubular corolla. Fruits are minutely tuberculate beaked nutlets (Tutin, 1964). Roots are characterized by a showy red bark and are traditionally used to heal wounds and burns (Tosun *et al*., 2008) .They are also used in folk veterinary medicine as a feed additive for cattle in Montenegro.

Compared with other members of the Boraginaceae family, such as *Lithospermum erythrorhizon* Siebold & Zucc., *Alkanna tinctoria* (L.) Tausch, *Arnebia euchroma* (Royle) I.M.Johnst., *Echium plantagineum* L. and *O*. *heterophylla* Griseb. (Papageorgiou et al., 1999), *O*. *visianii* has been hitherto poorly investigated for secondary metabolites as well as for its biological activity.

To the best of our knowledge the antitrypanosomal activity of this plant has not been investigated yet. Therefore, in the present research we evaluated the efficacy of the hexane extract obtained from the roots of *O*. *visianii* against *T*. *brucei*. This extract was analyzed by proton Nuclear Magnetic Resonance (^{1}H NMR) highlighting the presence of shikonin derivatives. Twelve constituents (**1**–**12**) were isolated by column chromatography and semi-preparative High Performance Liquid Chromatography (HPLC) and characterized by spectral techniques (Figure 2).

Fig. 1. *Onosma visianii* Clem.

Then, the antitrypanosomal activity of compounds **1-12** was also determined. Furthermore, we evaluated the acetylcholinesterase (AChE) inhibitory effects and the antioxidant activity of the *O. visianii* root hexane extract and its most active naphthoquinone derivatives (**2**, isobutyrylshikonin and **3**, isovalerylshikonin).

The findings of this work provide new insights into the potential of *O. visianii* as a source of highly effective naphthoquinone derivatives as potential antitrypanosomal drugs.

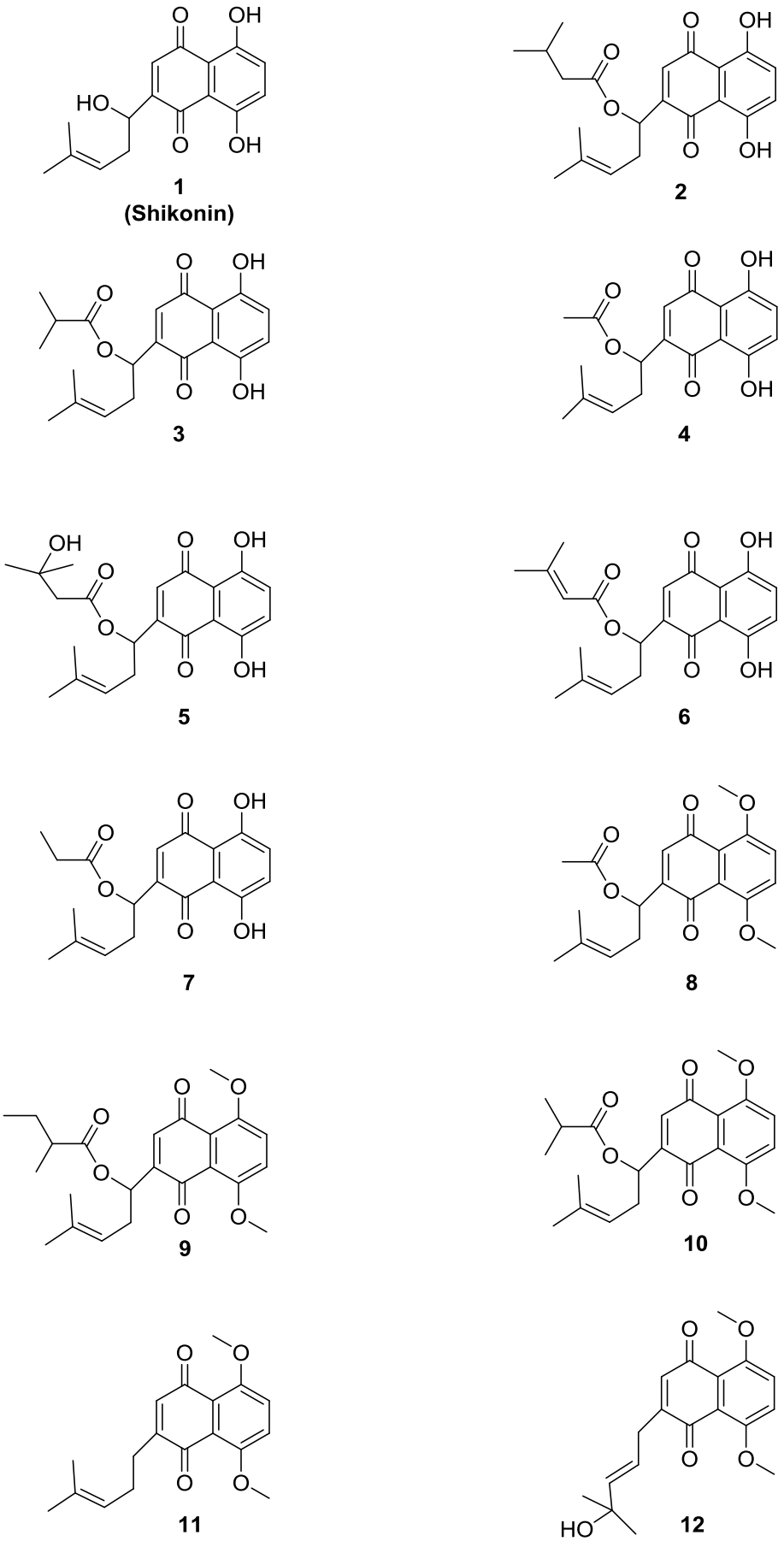

Fig. 2. Structures of the **1-12** naphthoquinones isolated from *O. visianii* roots.

3.2 Results and Discussion

3.2.1 *In vitro* evaluation of antitrypanosomal activity of *O. visianii* root extracts

Two extracts with different polarity (named Onos-Hex and Onos-MeOH) were prepared from the roots of *O.visianii* to assess their *in vitro* antitrypanosomal activity. The hexane extract was almost three times more active against *T. brucei* than the methanolic extract (IC_{50} = 12.59 and 37.44 μg/mL, respectively) and it was expected that may contain antitrypanosomal drug candidates (Figure 3 and Table 1).

Additionally, mouse BALB/3T3 fibroblast viability was quite significant with a selectivity index (SI) of 7.2. Based on the results of this preliminary screening, Onos-Hex was therefore chosen for extensive chromatographic purification.

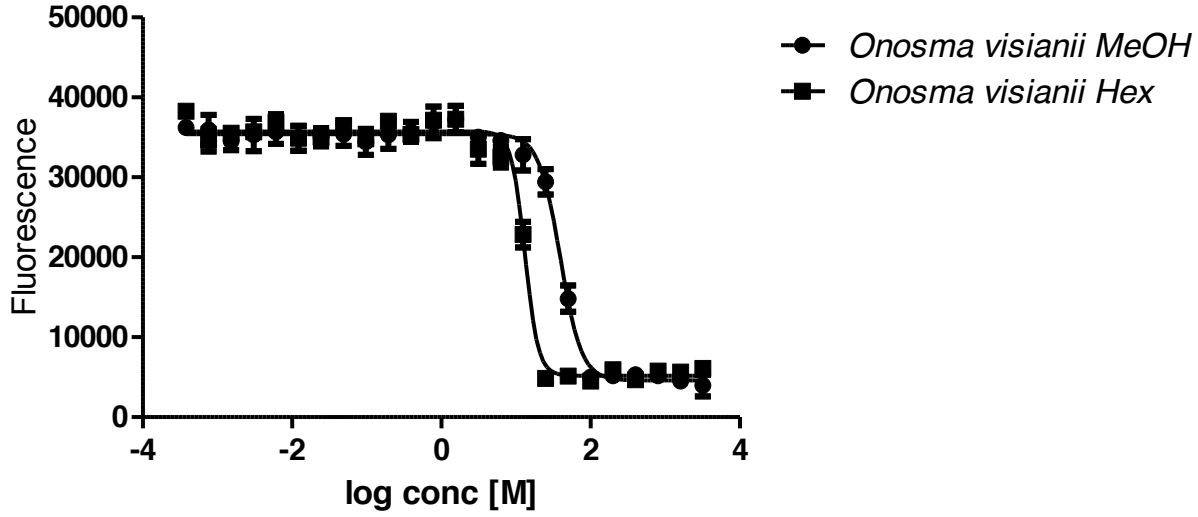

Fig. 3. Growth inhibition of *T. brucei* TC221 cells induced by *O. visianii* MeOH (●) and *O. visianii* Hex (■) extracts. The graph shows the average results from eight independent experiments with standard errors.

Table 1. Activity of *O. visianii* extracts and pure compounds against TC221 and Balb3T3.

Samples	IC_{50} (μg/mL)		Selectivity Index (SI)
	***T. b. brucei* (TC221)**	**Balb3T3**	
O. visianii methanolic extract (Onos-MeOH)	37.44 ± 0.62	22.86 ± 4.5	-
O. visianii hexane extract (Onos-Hex)	12.99 ± 1.05	93.52 ± 2.1	7.21
Pure compounds	**μM (μg/mL)**	**μM (μg/mL)**	
Compound 1 (Shikonin)	38.65 ± 6.27 (11.33)	56.37 ± 4.33 (18.33)	1.45
Compound 2	2.27 ± 0.33 (0.61)	12.73 ± 2.96 (3.46)	5.62
Compound 3	3.31 ± 1.02 (1.28)	7.32 ± 0.19 (2.84)	2.21
Compound 4	27.86 ± 0.15 (9.58)	22.71 ± 3.73 (7.81)	-
Compound 5	51.22 ± 9.06 (14.33)	58.42 ± 7.03 (15.03)	1.14
Compound 6	43.55 ± 2.95 (12.51)	76.41 ± 0.91 (22.01)	1.75
Compound 7	53.61 ± 10.26 (17.69)	38.95 ± 1.65 (12.85)	-
Compounds 8	>100	n.d.	-
Compound 9	>100	n.d.	-
Compound 10	>100	n.d.	-
Compound 11	>100	n.d.	-
Compound 12	>100	n.d.	-
Reference drug	**μM (μg/mL)**	**μM (μg/mL)**	
Suramin	0.05 ± 0.004 (0.071)	>5	>100

3.2.2 Quantification of shikonin derivatives and isolation of pure naphthoquinones from the *O. visianii* root extracts

Since the lipophilic Onos-Hex extract is rich in red pigments belonging to the group of napthoquinones, as a first step we performed a direct ^{1}H-NMR analysis.

As shown in Figure 4 signals ascribable to the 5 and 8 hydroxyl protons of shikonin derivatives are clearly visible at δ 12.2 and 12.4 while signals ascribable to H-6, H-7 and H-3 are visible at δ 7.11 and 6.92 respectively. ^{1}H-NMR quantitative measurement of the overall shikonin derivatives was performed using caffeine as internal standard and the amount of compounds was determined as 12% (w/w). The hexane extract was then subjected to extensive separation by column chromatography and further purification by semi-preparative HPLC yielding shikonin (**1**) and 11 shikonin derivatives named isovalerylshikonin (**2**), isobutyrylshikonin (**3**), acetylshikonin (**4**), hydroxyisovalerylshikonin (**5**), shikonin-β,β-dimethylacrylate (**6**), propionylshikonin (**7**), 5,8 dimethoxy acetylshikonin (**8**), 1-(5,8-dimethoxy-1,4-dioxo-1,4-dihydronaphthalen-2-yl)-4-methylpent-3-en-1-yl 2-methylbutanoate (**9**), 5,8 dimethoxy isobutyrylshikonin (**10**), 5,8-O-dimethyldeoxyshikonin (**11**), and (*E*)-2-(4-hydroxy-4-methylpent-2-en-1-yl)-5,8-dimethoxynaphthalene-1,4-dione (**12**), whose structures are reported in Figure 2.

Among them, two structures (**9** and **12**, respectively) have been identified as new natural entities (Figure 2).

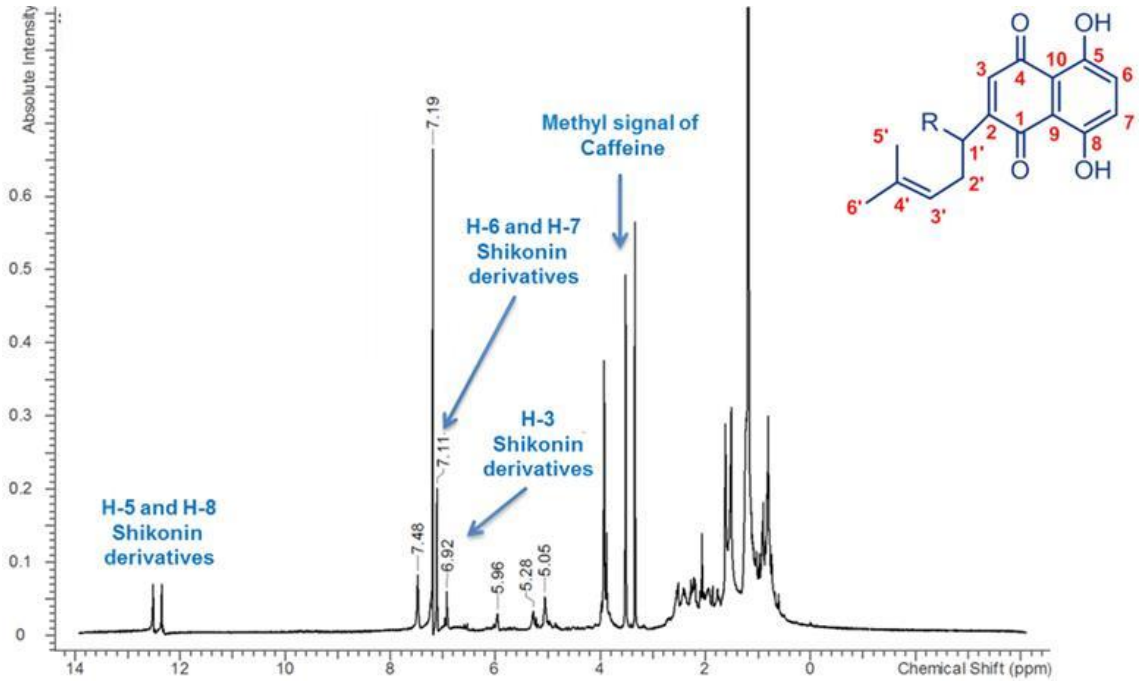

Fig. 4. ^{1}H-NMR of the *O. visianii* hexane extract. Diagnostic resonances assigned to specific H of shikonin are highlighted in blue. For quantitative purposes caffeine was added as internal standard, and signal of methyl group (highlighted in the figure with a blue arrow) was used for quantification.

The extract contained ester of naphtoquinones with side chain linked to the 1′ OH, that can be seen into the compounds **2** (isovalerylshikonin) and **3** (isobutyrylshikonin). Minor amounts of 5,8-dimethoxy derivatives have been also identified (compounds **8**-**12**).

The compound **9** was isolated as a yellow solid. The HR-MS spectrum of **9** showed the presence of a pseudomolecular ion at *m/z* 401.1940 corresponding to molecular formula of $C_{23}H_{28}O_6$ (calculated 401.1964 Da). **9** presented a single HPLC peak and the ^{1}H-NMR spectrum showed signals suggesting the presence of 2-(1-hydroxy-4-methylpent-3-en-1-yl)-5,8-dimethoxynaphthalene-1,4-dione moiety with ester substituent at OH in position 1′ (Figure 5). The aromatic part was characterized by the presence of two singlets at δ 7.32 (H-6/7) and 6.60 (H-3) and two identical methoxy groups in positions 5 and 8 (δ 3.96). The ester chain presents a triplet at δ 0.92 (3H, *J* = 7.42), and from a correlation spectroscopy (COSY) spectrum the spin system was deduced (Figure 6). The spin system was assumed to be from H-4′′ (CH_3 at δ 0.92) to H-3′′ (δ 2.25, CH_2), from this latter to H-2′′ (δ 2.42, CH) and from H-2′′ to the methyl group H-5′′ (δ 1.15, d, *J* = 7.02, 3H). The HMBC and HSQC correlations from CH_3-5′′ with carbon resonances at δ 44.8 (C-3′′), 42.4 (C-2′′) and 175.0 (C-1′′) support the presence of a residue of 2-methylbutanoate (Figures 7 and 8). Thus, compound **9** was identified as 1-(5,8-dimethoxy-1,4-dioxo-1,4-dihydro-naphthalen-2-yl)-4-methylpent-3-en-1-yl-2-methyl-butanoate.

The compound **12** was isolated as a pale yellow solid. The HR-MS spectrum of compound **12** showed the presence of a pseudomolecular ion at *m/z* 317.3520 corresponding to molecular formula of $C_{18}H_{20}O_5$ (calculated 317.3563 Da). The ^{1}H-NMR spectrum was characterized by the presence of a series of signals ascribable to naphthoquinone moiety, namely the singlets at δ 7.31 (2H, s), 7.21 (1H s), partially overlapped to chloroform signal, a doublet at δ 5.80 (1H, d, *J* = 15.85, Hz) and a doublet of triplets at δ 5.73 (1H, dt, *J* = 5.68, 15.85, Hz) that support the presence of a *trans* olefin linked to a CH_2, a singlet at δ 3.95 (6H, s) justifying the presence of two identical methoxy groups, a broad doublet at δ 3.25 (2H, d, *J* = 5.68, Hz) and two aliphatic singlets at δ 1.35 and 1.27 (3H each, s) suggesting the presence of two quaternary methyl groups (Figure 9).

The HSQC-DEPT (heteronuclear single quantum correlation-distortionless enhancement by polarization transfer) experiment allowed the assignments of the chemical shift of the non-quaternary carbon positions, and revealed the presence in the molecule of four different sp^2 CH, one sp^3 CH_2 and three CH_3. From the comparison of H, HSQC-DEPT and HMBC the correlations between H and C were deduced and the structure of compound was assigned (Figures 10 and 11). Namely the aromatic portion was assigned to a 1 substituted 5,8-dimethoxynaphthalene-1,4-dione.

Diagnostic HMBC correlations were observed from H-6/7 (δ 7.31) with carbon resonances at δ 153.05 (C-5/8) and 121.05 (C-6/7) and 100.25 (C-9/10).

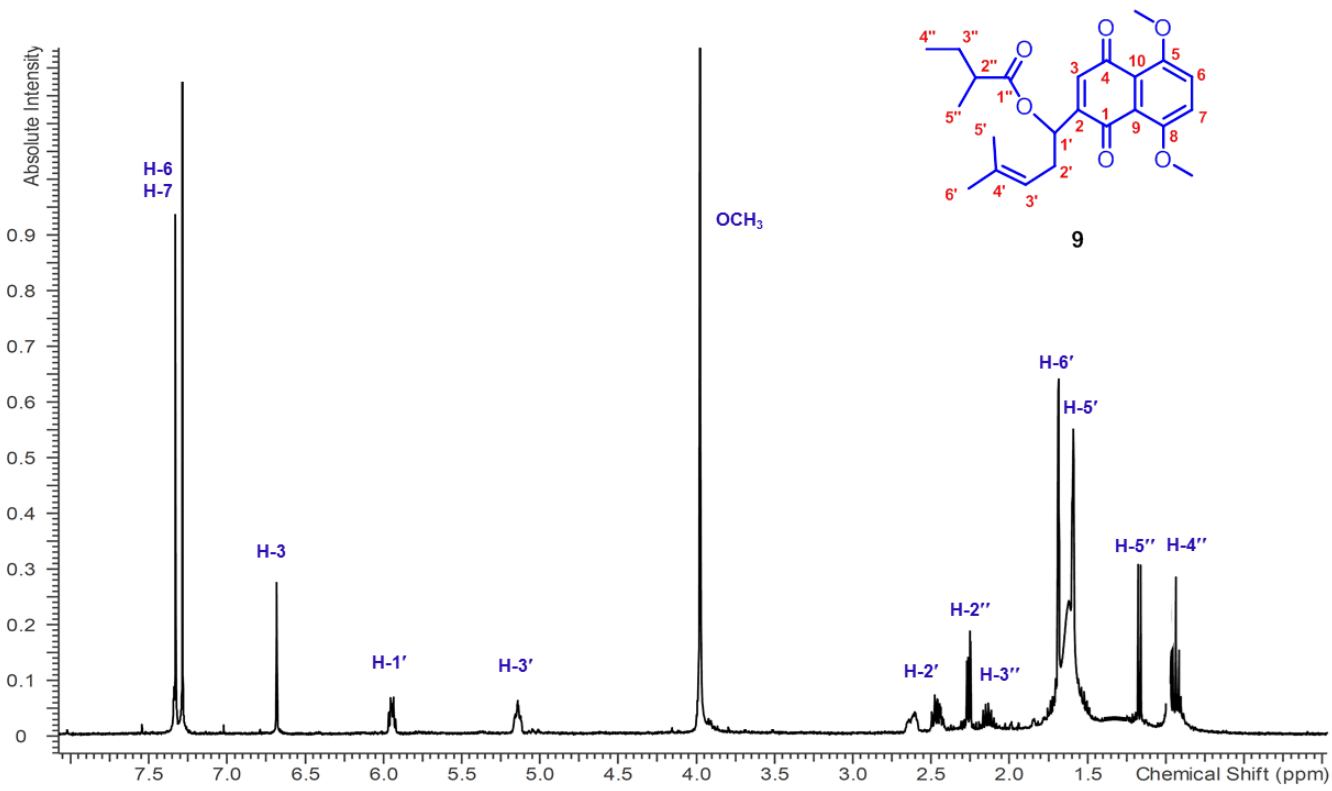

Fig. 5. ^{1}H-NMR spectrum of compound **9**.

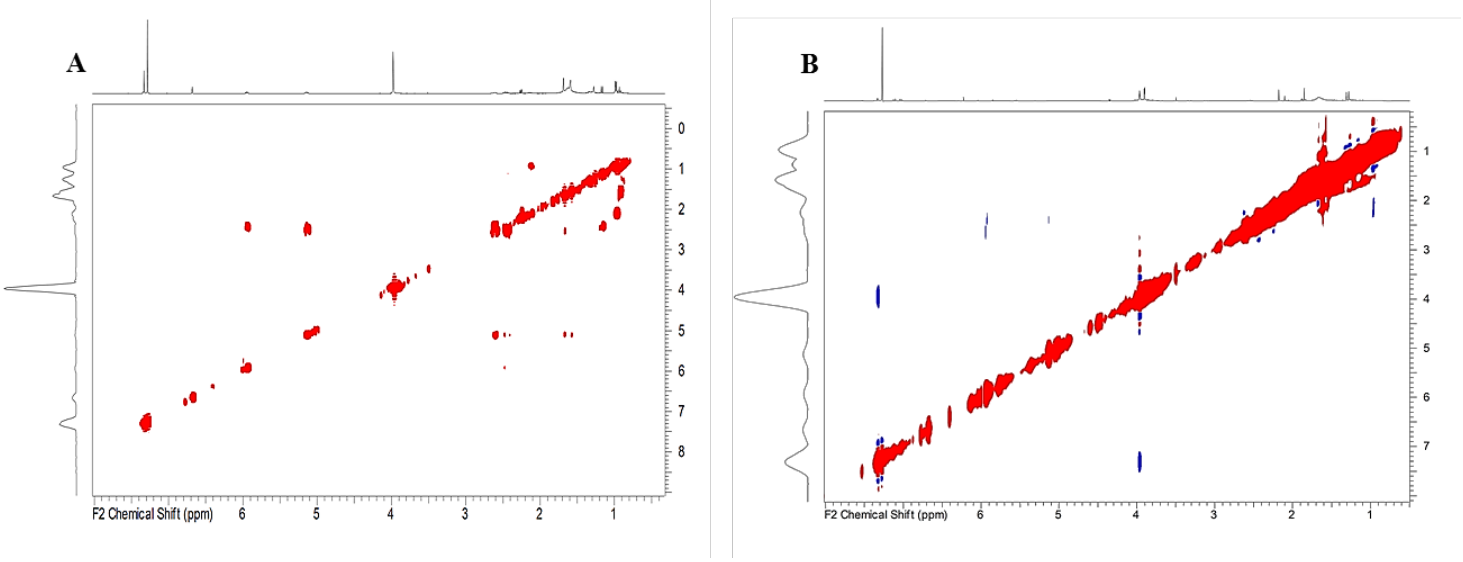

Fig. 6. COSY (A) and NOESY (B) spectra of compound **9**.

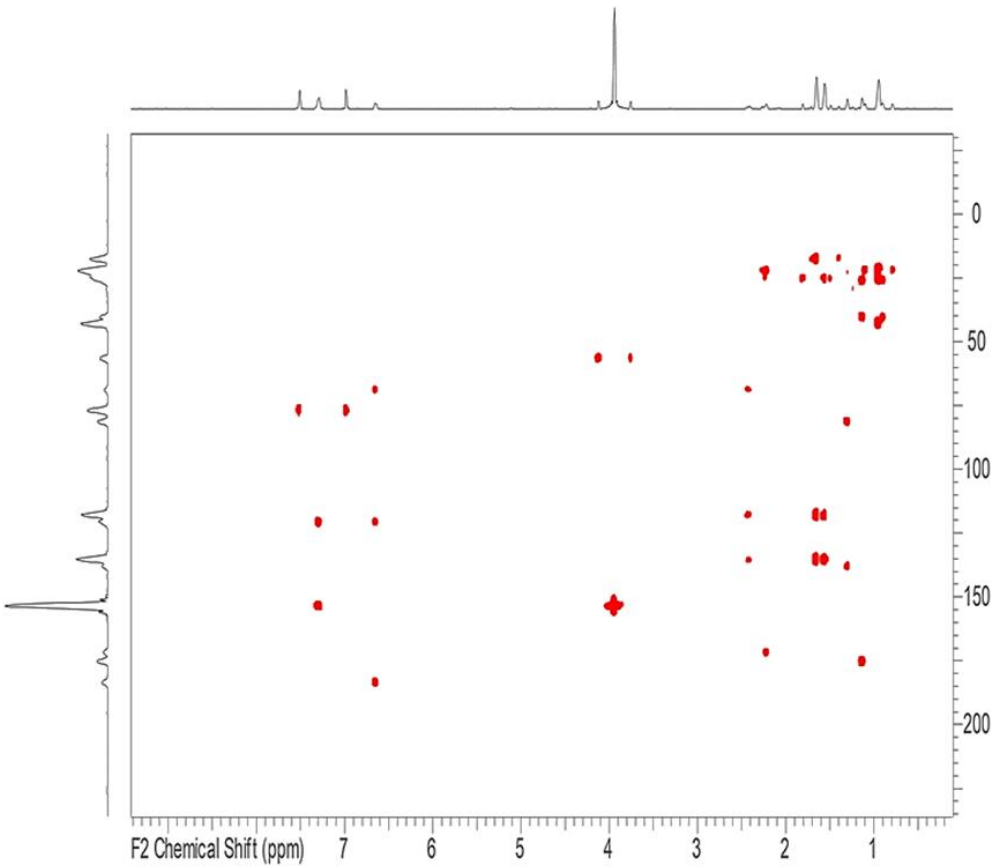

Fig. 7. HMBC spectrum of compound **9**.

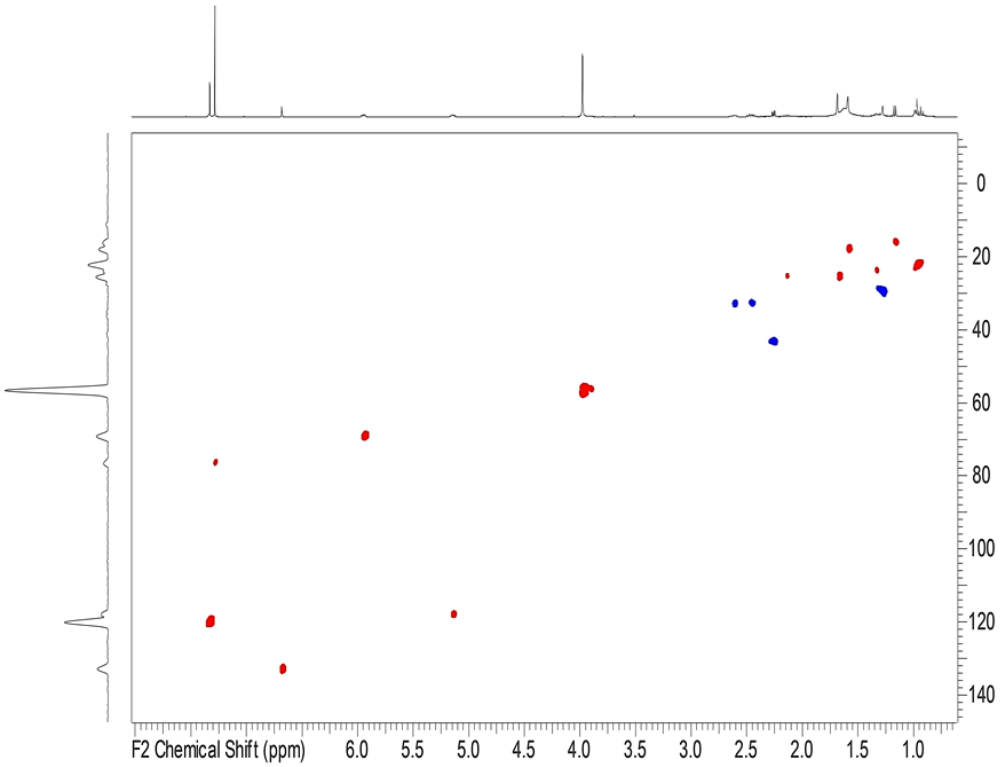

Fig. 8. HSQC spectrum of compound **9**.

Further HMBC correlations were observed from H-3 (δ 7.21) with carbon resonances at δ 184.7 (C-1) supporting the presence of keto group, and with quaternary carbon at δ 148.3 (C-2) suggesting the presence of substituent in position 2. Considering the signals ascribable to a side chain HMBC correlations were observed from H-1′ with C-2 and C-1 (δ 184.7) supporting the linkage with naphthalene moiety at position 2. Further diagnostic HMBC were also observed from H-1′ with C-2′ (δ 121.8) and C-3′ (δ 142.1) supporting the presence of double bond in the side chain. COSY correlation revealed the scalar coupling between H-1′ and H-2′ and from this latter to H-3′.

The coupling constant of H-3′ (J = 15.85, Hz) supports a *trans* geometry for the double bond. A linkage at position 3′ of a hydroxyl-isopropyl moiety was deduced from the HMBC correlations observed from H-3′ with C-4′ (δ 69.9) and with C-5′ (δ 30.43) and C-4′, also NOESY correlation from H-6′ (δ 1.27) and H-2′ confirms the structure of the side chain as a (*E*)-2-(4-hydroxy-4-methylpent-2-en-1-yl) moiety (Figure 12). Thus, the structure of the compound **12** was assigned to (*E*)-2-(4-hydroxy-4-methylpent-2-en-1-yl)-5,8-dimethoxynaphthalene-1,4-dione.

The NMR assignments of the new isolated compounds are reported in Table 2.

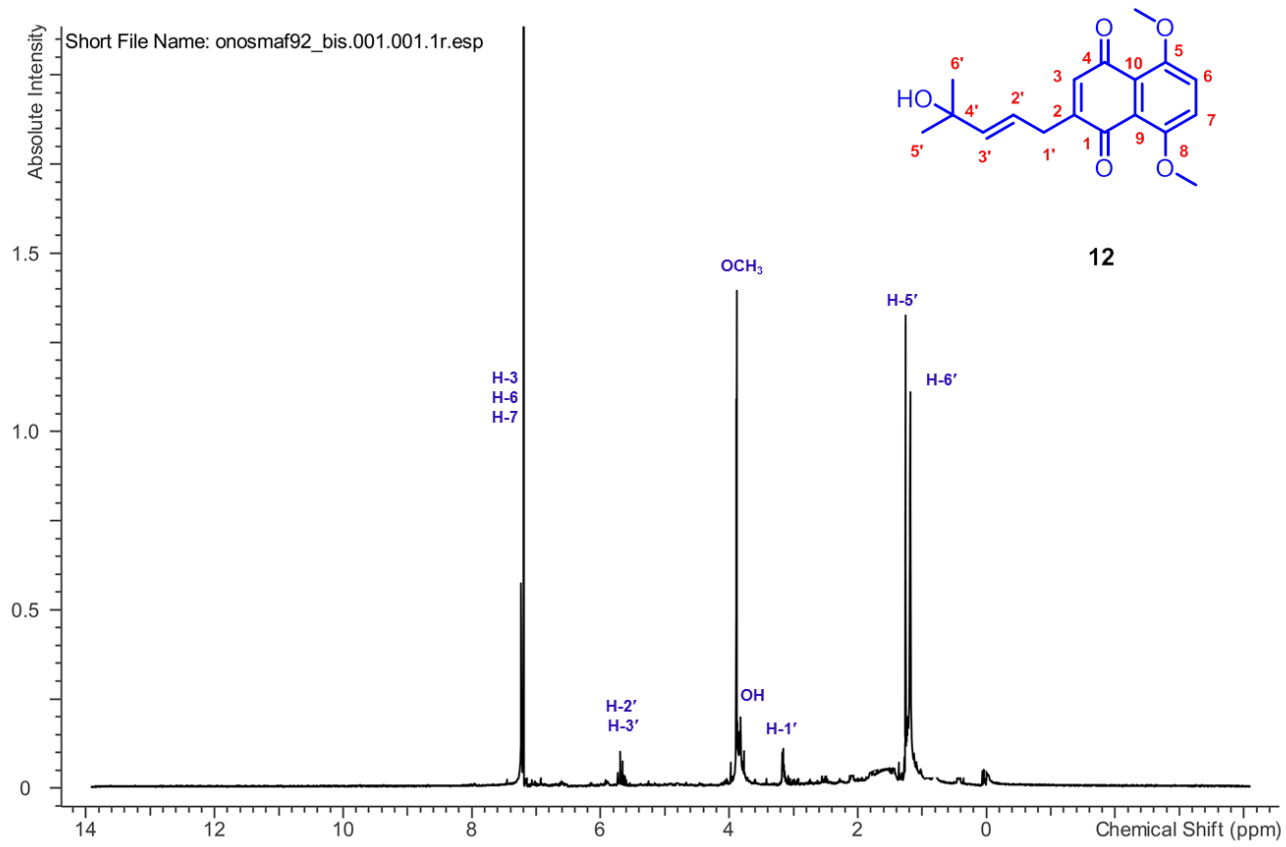

Fig. 9. ^{1}H-NMR spectrum of compound **12**.

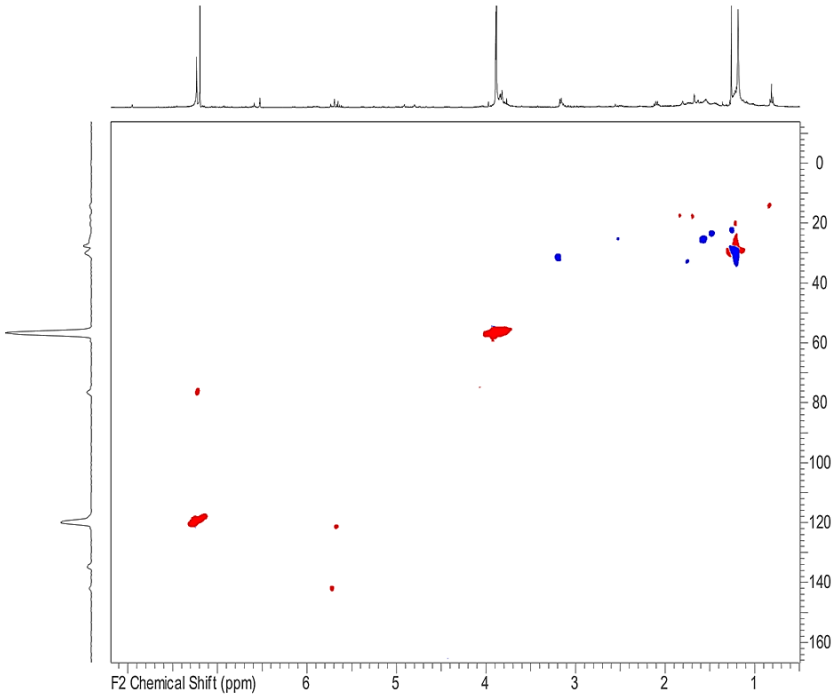

Fig. 10. HSQC spectrum of compound **12**.

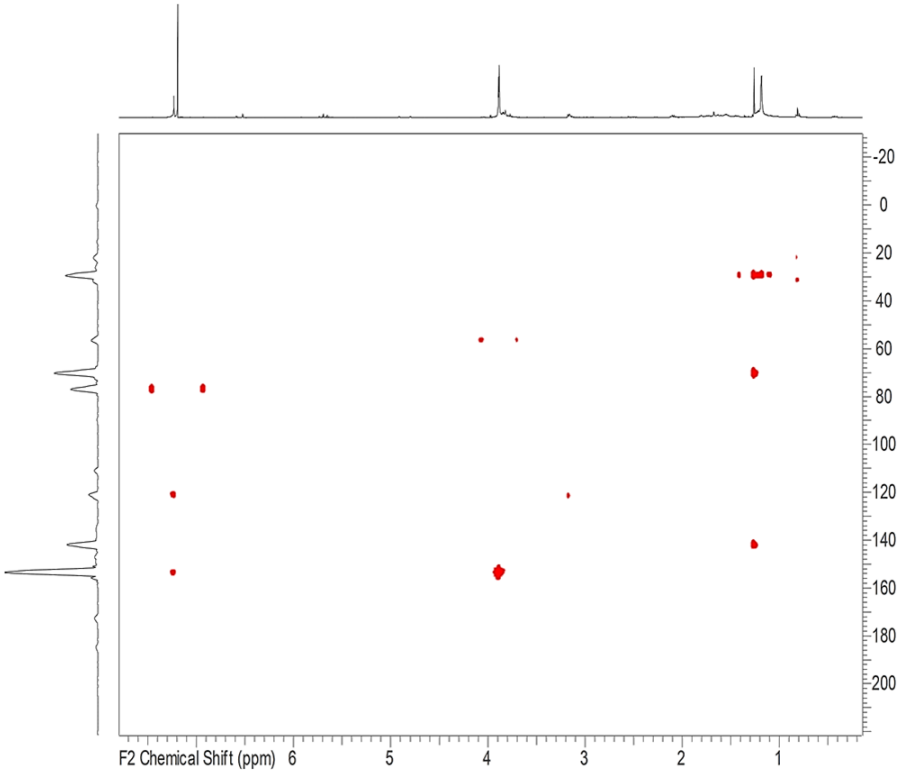

Fig. 11. HMBC spectrum of compound **12**.

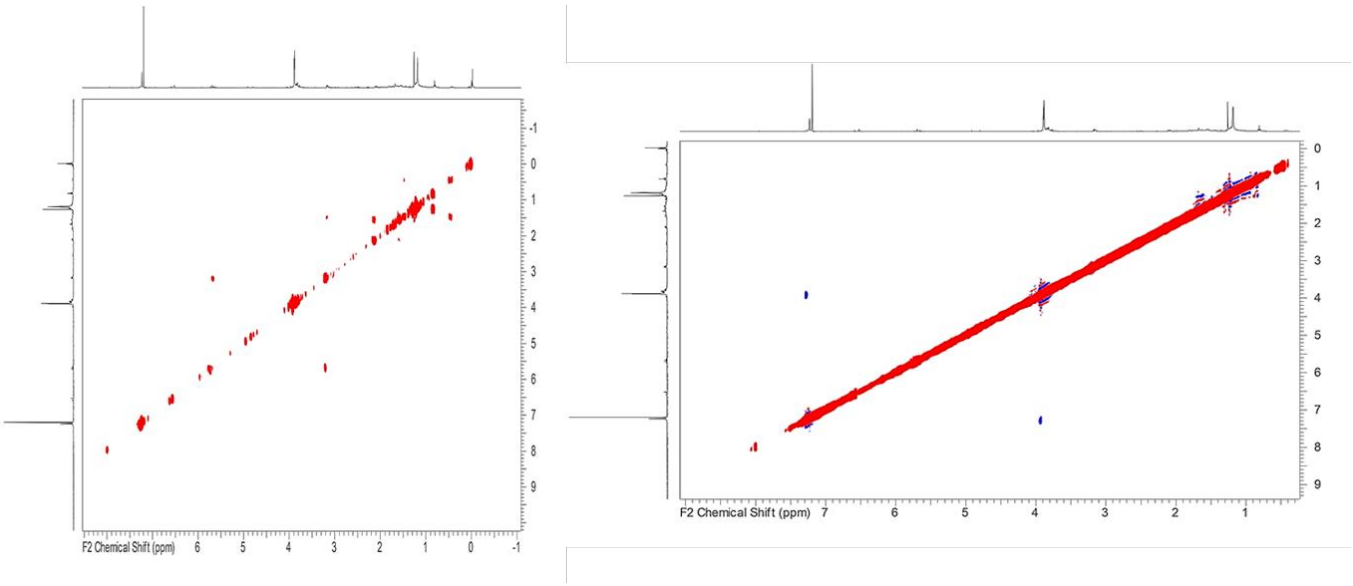

Fig. 12. COSY (A) and NOESY (B) spectra of compound **12**.

Table 2. NMR assignments for the new isolated compounds **9** and **12**.

Position	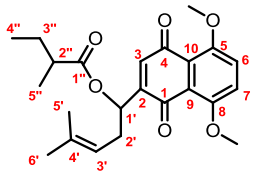 9		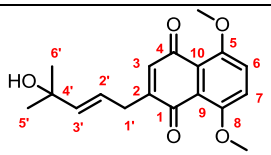 12	
	δH	**δC**	**δH**	**δC**
1	-	182.8	-	184.7
2	-	147.5	-	148.3
3	6.60 t, *J* = 1.22	133.6	7.21 s	118.9
4	-	182.8	-	184.7
5	-	153.4	-	153.1
6	7.32 s	120.8	7.31 s	121.1
7	7.32 s	120.8	7.31 s	121.1
8	-	153.4	-	153.1
9	-	120.9	-	121.2
10	-	120.9	-	121.2
OCH_3	3.96 s	57.8	3.95 s	57.3
1′	5.94 m	70.0	3.25 d, *J* = 5.68	32.0
2′	2.45-2.60 m	31.1	5.73 dt, *J* = 15.85, 5.68	121.8
3′	5.11 m	117.1	5.80 d, *J* = 15.85	142.1
4′	-	134.9	-	69.9
5′	1.57 brs	14.9	1.35 s	30.4
6′	1.64 brs	27.1	1.27 s	26.9
1″	-	175.0	-	-
2″	2.42 m	42.4	-	-
3″	2.25 m	44.8	-	-
4″	0.92 t, *J* = 7.32	12.7	-	-
5″	1.15 d, *J* = 7.02	17.6	-	-

Note: Spectra were acquired at 500 MHz for ^{1}H and 125 MHz for ^{13}C in $CDCl_3$ using TMS as internal reference.

3.2.3 Antitrypanosomal activity of isolated compounds (1-12)

All isolated compounds (**1-12**) were evaluated *in vitro* against *T. brucei* (using the corresponding Alamar-Blue assay), as well as against mammalian cells (BALB/3T3 mouse fibroblasts) as a counter-screen for toxicity and suramin was used as a reference. The bioevaluation data of all isolated compounds is reported in Table 2. The isolated naphthoquinone derivatives **1-7** were quite active with IC_{50} values between 2.3 and 56.6 μM, whereas compounds **8-12** were not active at all. Notably, isobutyrylshikonin (**2**) and isovalerylshikonin (**3**) resulted by far the most active compounds among the isolated naphthoquinone derivatives (IC_{50s} = 2.27 and 3.31 μM, respectively). Unfortunately, **2** and **3** were found to be 4.5 and 6.6 times less active than the reference compound suramin.

However, the selectivity index for **2** was 5.6 showing a preferential effect on target cells compared with **3** (SI = 2.21). Despite the relatively low number of isolated compounds, a preliminary structure activity relationship (SAR) consideration may be drawn. Inspecting structures of the active naphthoquinone derivatives revealed that methoxylation of position 5 and 8 (see compounds **8-12**) caused loss of activity suggesting an important role of the two *p*-hydroxy groups (C-5 and 8) for the antitrypanosomal activity.

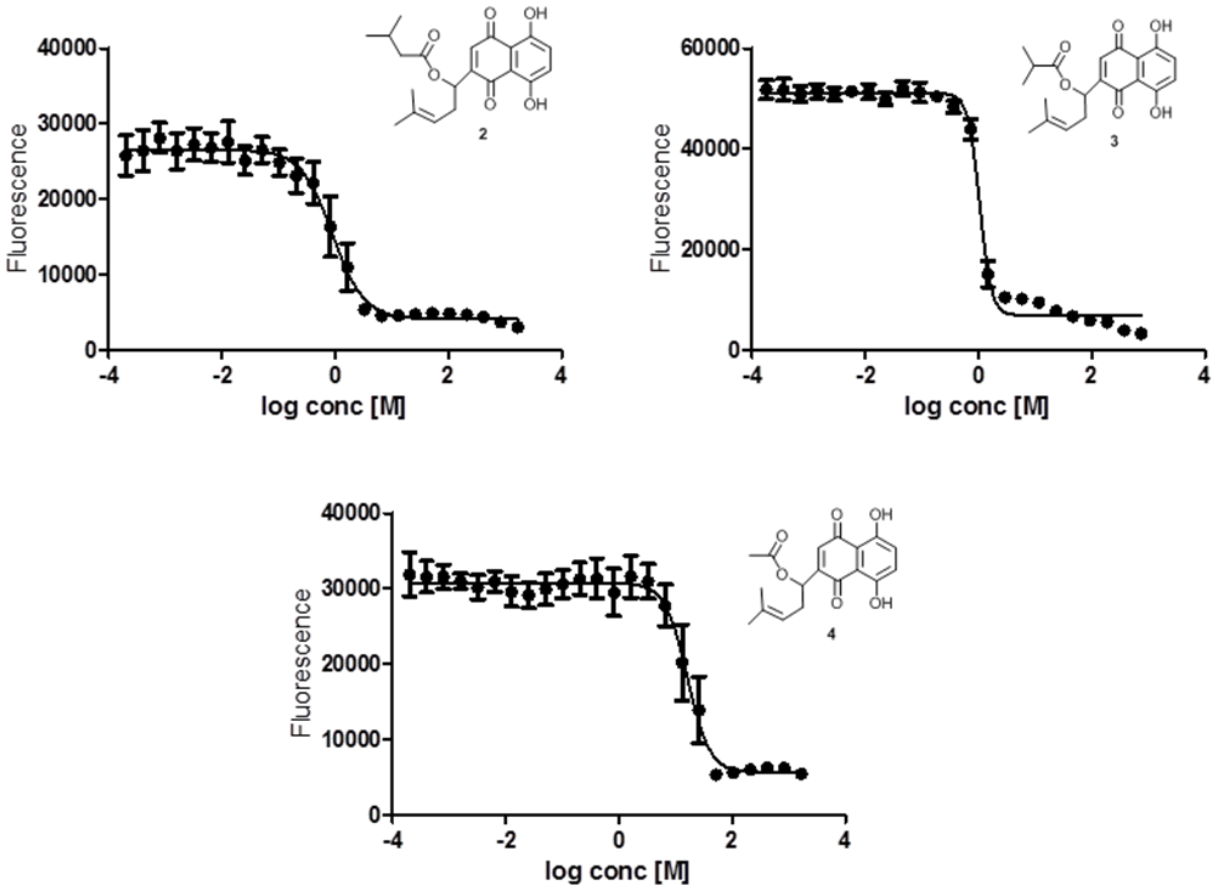

Fig. 13. Growth inhibition of *T. brucei* TC221 cells induced by **2**, **3** and **4**. Each graph shows the average results from eight independent experiments with standard errors.

Besides their widespread presence in nature, the great interest in the study and mechanisms of action of compounds with a quinoidal structure is due to their multiple roles in organisms. As reported before naphthoquinone derivatives have been reported as one of the major natural product classes with significant activity against Trypanosoma (Pinto *et al*., 2009). For example, lapachol, a natural phenolic compound isolated from the bark of the lapacho tree, has shown a marked anti-trypanosomal profile, simultaneously displaying no serious side effects in humans (Krohn *et al*., 2007). The trypanocidal effect of naphthoquinones are due to their capacity to act as uncouplers of oxidative phosphorylation (Ferraz *et al*., 2001), as DNA intercalating and alkylating agents, as potent inhibitors of electron transport (Vennerstrom *et al*., 1998), as well as producers of reactive oxygen radicals (Monks *et al*., 1992).

With regard to the latter, the ability of naphthoquinones to generate reactive oxygen species enhances the feeding deterring effects (Tokunaga *et al*., 2004), thus playing a pivotal role in the protection of plants against pathogens (Babula *et al*., 2009). This observation has been confirmed in our experiments on naphthoquinone derivatives, where the presence of free hydroxyl groups played an important role for the observed bioactivity. On the other hand, the derivatives with

methoxylation in position 5 and 8 were not active at all compared to the parent non-substituted compounds.

In view of the well-known biological properties of naphthoquinones, it is highly possible that this class of compounds exerts their anti-trypanosomatid profile by means of a multitarget mechanism.

3.2.4 Haemolytic and *in silico* ADMET properties of active naphthoquinone derivatives (1-7)

Hemocompatibility is an important aspect to be considered in drug discovery process since one of the mainly routes of antitrypanosomal drugs is intravenous administration. Considering that the mechanism of action involving naphthoquinones is related to oxidative stress, erythrocytes are vulnerable and may suffer lysis after exposure to these compounds (Munday *et al*., 2007). For this reason we tested our active naphthoquinone derivatives (**1-7**) for this profile. Side effects on human blood can be analyzed through hemolysis and our results showed no haemolytic effect for the active compounds **1-7**. As the lysis rate was less than 10%, **1-7** can be can be regarded as hemocompatible.

Several theoretical methods to predict ADMET parameters are important tools to select good chemotypes in drug development process. In this context the naphthoquinones **1-7** were submitted to *in silico* pharmacokinetics and toxicological analysis.

Similar to suramin, none of compounds showed tendency to cross blood-brain barrier (BBB) (Table 3), a region of brain that ruled out about 98% of drugs, due to problems in adsorptive endocytosis, transmembrane diffusion, extracellular pathways, or saturable transports. The software used by us (admetSAR@ LMMD software) also analyzed interaction between compounds **1-7** and Caco-2 cells, predicting a good profile for intestinal drug absorption. CYP3A4 is part of isoenzyme group of the cytochrome P450 family playing important role in drug metabolism (Rowan *et al*., 2012).

Interestingly, based on our theoretical analysis, most of our compounds, except **7**, did not inhibit CYP3A4. Thus, they could be administrated in association with other drugs that depends on CYP3A4 to be metabolized. Theoretical toxicity analysis of naphthoquinone derivatives (**1-7**) showed that they have mutagenic effects, similar to the two antiprotozoal agents already in the market, eflornithine and nifurtimox (Table 3).

Apparently, this mutagenic profile associated to our compounds could be related to one of their multiple mechanisms of action. In addition to mutagenic effects and oxidative stress, another mechanism of action associated with naphthoquinones is the ability to bind to topoisomerase complex and cause damage to the DNA replication process (Coelho-Cerqueira *et al*., 2014).

Since the ADMET profile of naphthoquinone derivatives (**1-7**) is similar to that of eflornithine and nifurtimox (except for the BBB penetration), they may represent new potential antiprotozoal prototypes.

Table 3. Comparison of ADMET (Absorption, Distribution, Metabolism, Excretion and Toxicity) parameters of naphthoquinone derivatives (**1**-**7**) with four clinical antitrypanosomal drugs (Suramin, Melarsoprol, Eflornithine, and Nifurtimox) calculated by using admetSAR software.

Compounds	ADMET parameters					
	BBB	Caco2	CYP3A4	Carcinogenic	Mutagenic	LogP
1	-	-	NI	-	+	2.12
2	-	+	NI	-	-	3.72
3	-	+	NI	-	+	3.33
4	-	+	NI	-	+	2.69
5	-	+	NI	-	+	2.83
6	-	+	NI	-	+	2.64
7	-	+	I	-	+	3.08
Suramin	-	-	I	+	-	6.74
Melarsoprol	-	-	NI	-	-	0.32
Eflornithine	+	+	NI	-	+	-0.23
Nifurtimox	+	+	NI	-	+	0.64

+ = positive effect; - = negative effect, I = inhibitor; NI = non inhibitor.

3.2.5 Targeting the tse-tse fly vector by inhibition of the enzyme acetylcholinesterase (AChE)

Vector-borne infectious diseases are based on infections that are transmitted via a disease-vector and are considered a significant global threat to public health with more than one billion people infected each year. The widespread usage of insecticides for control of disease-transmitting vectors has made it possible to obtain good results in seeking to prevent malaria, trypanosomiasis, dengue, and Zika virus infections and the positive impact of these public-health interventions emerged from the hundreds of millions of averted malaria cases in sub-Saharan Africa on the last decade (Bhatt *et al*., 2015). Unfortunately, the massive and indiscriminate use of insecticides has led to the development and widespread of resistant vectors to all the major classes of insecticides recommended for vector control by the WHO. The appearance of resistant strains has significantly undermined the important benefits obtained by using insecticide in vector control. Furthermore, many of the currently used insecticides lack specificity for the vector over other non-target species. It is obvious that all of this may have devastating effects on both humans and beneficial insects such as the pollinators. For this reason, there is an urgent need of new chemical entities with insecticidal activity.

Nowadays, there are four chemical classes of insecticides that are recognized by WHO for controlling vectors: chlorinated hydrocarbons, organophosphates (OPs), carbamates, and pyrethroids. In addition, some re-purposed agricultural insecticides have recently been prequalified by the WHO for vector control use (WHO, 2018). The mechanism of action of many synthetic or natural insecticides is the inhibition of the essential enzyme acetylcholinesterase (AChE), which results in disruption of the insect's nervous system. The insecticides bind and inhibit the AChE, causing overstimulation of the neuron which leads to rapid spasms of the muscles, convulsions, and ends up with the death of the vectors (Yu, 2014).

The reason why AChE enzyme has gained so much attention is due to its important physiological role to terminate nerve signaling by rapidly hydrolyzing the acetylcholine (Toutant, 1989). Most insects, including mosquitoes and flies, have two genes encoding AChE enzymes named *ace-1* and *ace-2*, while humans carry only one *ace* gene. In insects, it has been experimentally established that AChE1 (from the *ace-1* gene) is the main catalytic enzyme and represents a validated insecticide target to control vectors (Weill *et al*., 2013; Zhao *et al*., 2013).

Therefore, we investigated the inhibition power of *O. visianii* root hexane extracts and their two more active shikonin derivatives (**2** and **3**) on two representative AChE enzymes: the recombinant human acetylcholinesterase (*h*AChE) enzyme and the arthropod counterpart tse-tse fly *Glossina palpalis* (*gp*AChE). Results are reported in Table 4 where the alkaloid galantamine was

used as the positive control. All tested products exhibited a dose-dependent inhibitory effect on the enzyme. The root hexane extract showed IC_{50} values of 142.3 µg/mL and 58.6 µg/mL against *h*AChE and gsAChE which were 15 and 25 times higher than that of reference drug galantamine (9.5 µg/mL and 2.3 µg/mL, respectively). Of the two shikonin derivatives tested, **3** exhibited a notable *gp*AChE inhibition (IC_{50} of 7.1 µg/mL) which was only three times lower than that of galantamine. On the other hand, **2** showed an IC_{50} value (91.3 µg/mL) against the arthropod enzyme quite similar to that of the root extract.

As pointed out before, the total amount of shikonin derivatives in the hexane extract is 12% thus the equivalent amount of shikonin at IC_{50} value is 6.6 µg/mL. This result indicates that the total extract is slightly more effective than the pure compounds in the *gp*AChE inhibitory effect. An important outcome of this study shows that compound **3** combines a relevant vector (*gp*AChE) *versus* human AChE selectivity (SI = 7.2) with a high potency, two properties that have proven useful to combine in an single insecticide candidate.

Table 4. Acetylcholinesterase inhibitory properties of *O. visianii* root hexane extract and its bioactive constituents isobutyrylshikonin (**2**) and isovalerylshikonin (**3**).

Product	IC_{50} (µg/mL)		SI
	***h*AChE**	***gp*AChE**	
Root hexane extract	142.3 ± 8.0	58.6 ± 4.2	2.43
Isobutyrylshikonin (**2**)	162.0 ± 1.2	91.3 ± 0.9	1.77
Isovalerylshikonin (**3**)	51.4 ± 1.5	7.1 ± 0.06	7.23
Galantamine	9.5 ± 0.08	2.3 ± 0.04	4.13

*h*AChE = recombinant human acetylcholinesterase, *gp*AChE = *Glossina palpalis* acetylcholinesterase. SI = Selectivity Index computed by taking the compound's IC_{50} value for *h*AChE and dividing by its IC_{50} value for *gp*AChE.

In a formulation of a botanical insecticide, the addition of an antioxidant is recommended to preserve and extend the shelf-life and efficacy of the potential candidate. On this regard, we investigated the radical scavenging activity of *O. visianii* extract and the two bioactive shikonin derivatives (compounds **2** and **3**). For the purpose, DPPH, ABTS and FRAP assays were carried out and Trolox was utilized as the positive control.

As shown in Table 5, root extract and **2** and **3** showed a noteworthy capacity to capture free radicals although they displayed different activity in the three assays performed. In the DPPH assay

the three products showed a similar level of radical inhibition, with IC_{50} values of 122.7, 139.9 and 143.2 μg/mL for **3**, root extract and **2**, respectively.

On the other hand, in the ABTS assay the root extract showed the strongest radical scavenging effect with an IC_{50} value of 46 μg/mL, which was twelve times higher than that of Trolox. In this case **2** (IC_{50} of 75.5 μg/mL) was slightly more active than **3** (IC_{50} of 103.7 μg/mL). In the FRAP assay, the two shikonin derivatives exhibited a more pronounced reducing/oxidant power of the ferric chloride (TEAC values of 331.1 and 583.5 μmol TE/g for **2** and **3**, respectively) than the root extract (TEAC of 120 μmol TE/g).

Table 5. *In vitro* radical scavenging activities of *O. visianii* root hexane extract and its bioactive constituents isobutyrylshikonin (**2**) and isovalerylshikonin (**3**).

Product	**DPPH**		**ABTS**		**FRAP**
	TEAC[a] **μmol TE/g**	**IC_{50}**[b] **μg/mL**	**TEAC μmol TE/g**	**IC_{50} μg/mL**	**TEAC μmol TE/g**
Root Hexane Extract	278.8 ± 27	139.2 ± 12	317.3 ± 29	46.2 ± 4.9	120.2 ± 3.8
Isobutyrylshikonin (**2**)	272.6 ± 19	143.2 ± 9.6	193.7 ± 19	75.5±8.1	331.1 ± 4.8
Isovalerylshikonin (**3**)	316.0 ± 15	122.7 ± 4.5	140.4 ± 14	103.7 ± 11	583.5 ± 9.8
Trolox		9.7 ± 0.3		3.6 ± 0.1	

[a] TEAC = Trolox equivalent (TE) antioxidant concentration. [b] IC_{50} = The concentration of extract/compound that affords a 50% reduction in the assay.

3.3. Conclusion

In conclusion, the overall results of this work, although preliminary, shed light into the phytochemical and biological properties of *O*. *visianii* as a relevant source of bioactive compounds and highlighted the opportunity to use the naturally-occurring naphthoquinone derivatives as inspiring tools for future antiprotozoal drugs development. The exhibited trypanocidal activity of root extract and isolated shikonin derivates, on the one side, confirmed partially the traditional use of naphthoquinone-rich plants in the treatment of protozoal diseases, and on the other side, renders *O*. *visianii* as a potential plant-candidate for standardized herbal medicines against trypanosomiasis that are particularly required in developing countries who have difficulty to access to conventional health care and have poor medical equipment and infrastructure. However, further studies are needed to increase the knowledge about shikonin derivates mechanisms of action and the potential molecular targets linked to their antitrypanosomal activity. Hemocompatibility and theoretical pharmacokinetics and toxicological parameters revealed that the two most active shikonin derivatives (**2** and **3**) hold in their promising profiles the enormous potential to be developed as future trypanocidal drugs.

Beside the antitrypanosomal activity, the evaluated root extract and the isolated shikonin derivatives **2** and **3** showed a significant inhibition of the *gp*AChE enzyme (an enzyme that represents a validated insecticide target), but at higher doses compared with the positive control galantamine. In addition, our preliminary results confirmed the radical scavenging activities of both root extract and its isolated shikonin derivatives, that may be related to the napthoquinone moiety presenting free OH groups in the aromatic ring. One of the most important requirements for the scalability of a botanical insecticide is its availability in nature. In this respect, the shikonin derivative **3**, exhibiting a relevant *gp*AChE inhibition (IC_{50} of 7.1 µg/mL), can also be taken out from other Boraginaceae sources, as reported by Pietrosiuk *et al*. (Pietrosiuk et al., 2008). As for its limited stability (e.g., photosensitivity), microencapsulation might be an ideal method to protect it from degradation and to prolong its shelf life. On the other hand, as reported by Andújar *et al*., the heat resistance and non-volatility of many shikonin derivatives make them ideal candidates for persistent and effective botanical insecticides (Andújar *et al*., 2013). Although naphtoquinones are generally considered relatively safe on non-target organisms, further in-depth studies are required in order to evaluate their efficacy on beneficial species.

3.4 Materials and Methods

3.4.1 Plant material

Roots of *O. visianii* were collected in Strážovské vrchy hills, Dolné Vestenice, Rokošské predhorie foothill, Stredná dolina valley, Trenčín Region, Slovakia (N: 48°44'01.0", E: 18°23'50.8", ca. 500 m a.s.l.) in November 2014. The plant identification was performed by V. Kolarčik, after checking against The Plant List database (www.theplantlist.org) and available literature (Ball, 1972) . A voucher specimen was deposited in the KO herbarium (Herbarium of the Botanical Garden, P. J. Šafárik University, Košice, Slovakia) with the codex DV13.

3.4.2 Preparation of extracts

O. visianii roots were air-dried in the shade at room temperature (≈25°C) for one week and conserved in wrapping papers before extraction. Dry roots were then powdered using a blender MFC DCFH 48 IKA-WERK (D-Staufen) equipped with sieves of 2-mm size in diameter. One hundred g of powder were extracted in a Soxhlet apparatus using 700 mL of *n*-hexane for 6 h. These extraction conditions assured the highest efficiency to extract naphtoquinones as reported in literature (Babula *et al*., 2009). The obtained extracts were concentrated under reduced pressure at 30 °C with a rotary evaporator up to constant weight (yield 2.9 % w/w dry weight). The extract was kept in a glass vial sealed with silicon septa and stored under darkness at -4 °C before chemical analysis and biological experiments.

3.4.3 Isolation and chemical analyses

Silica gel plates (cod 5171 Merck) and silica gel (60 mesh) were from Sigma (Milan, Italy). Solvents from Carlo Erba (Milan, Italy). HPLC Varian 920 chromatograph was used for preparative chromatography. NMR (1D and 2D) spectra were obtained on a Bruker Avance 400 spectrometer. The soxhlet hexane extract of *O. visianii* root (3 g) was eluted in a silica gel column (5 x 30 cm, 300 g Silica Gel 80 mesh) using cyclohexane (A) and ethyl acetate (B) as eluting system, starting from 100% A and gradually increasing the B amount up to 50%. Fractions of 13 mL were collected and pooled on the basis of their chromatographic behavior by TLC in 15 different fractions: fr-1 (0.22

g), fr-2 (0.12 g), fr-3 (0.32 g), fr-4 (0.68 g), fr-5 (0.43 g), fr-6 (0.31 g), fr-7 (0.09 g), fr-8 (0.08 g), fr-9 (0.08 g), fr-10 (0.11 g), fr-11 (0.06 g), fr-12 (0.06 g), fr-13 (0.04 g), fr-14 (0.11 g) and fr-15 (0.01 g). All the fractions were used for compound isolation. Further purifications were obtained with semipreparative HPLC on a Zorbax SB C-18 (21.2 x 150 mm, 5 μm) column using as mobile phase methanol and water (0.1% formic acid) in isocratic elution (90:10) for 25 min. The flow rate was of 5 mL/min. UV detection was used at 545 and 254 nm. Purity of isolated compounds was checked by HPLC analysis and was >97% by software integration. Quantification of shikonin derivatives in the crude extract was performed using ^{1}H-NMR as previously described. Briefly 50 mg of crude extracts were exactly weighted and dissolved in a deuterated chloroform solution of caffeine (1 mg/mL). Peaks assigned to methyl group of caffeine (δ 3.43) and clearly resolved peaks assigned to the H-3 of shikonin derivative (δ 7.00) were then used for quantitative analysis using a previously published approach (Comai *et al*., 2010). Isolated compounds were: shikonin **1** (12.1 mg), isovalerylshikonin **2** (31.5 mg), isobutyrylshikonin **3** (56.1 mg), acetylshikonin **4** (12.1 mg), hydroxyisovalerylshikonin **5** (2.1 mg), shikonin-β,β-dimethylacrylate **6** (47.6 mg), propionylshikonin **7** (1.4 mg), 5,8 dimethoxy acetylshikonin **8** (8.8 mg), 1-(5,8-dimethoxy-1,4-dioxo-1,4-dihydronaphthalen-2-yl)-4-methylpent-3-en-1-yl 2-methylbutanoate **9** (0.7 mg), 5,8 dimethoxy isobutyrylshikonin **10** (0.9 mg), 5,8-O-dimethyldeoxyshikonin **11** (4.4 mg), (*E*)-2-(4-hydroxy-4-methylpent-2-en-1-yl)-5,8-dimethoxynaphthalene-1,4-dione **12** (0.7 mg). Structure of compounds were elucidated on the basis of 1D and 2D NMR measurements, comparing obtained data with previously published literature (Spyros *et al*., 2005; Ito *et al*., 2011; Kim *et al*., 2012; Ito *et al*., 2012).

3.2.5. *T. brucei* and mammalian cell culture and growth inhibition assay

The cell culture conditions and the growth inhibition assay on *T. brucei* and Balb/3T3 cells were performed as described before (Petrelli *et al*., 2016). *T. brucei* TC221 bloodstream forms (BSFs) and mouse embryonic fibroblast Balb/3T3 cells (ATCC no CCL-163) were cultivated in vented plastic flasks at 37 °C with 5% CO_2. For *T. brucei*, the growth medium was HMI-9 (Hirumi *et al*., 1989) supplemented with 10% (v/v) fetal bovine serum (Gibco,Waltham, MA, USA), whereas the Balb/3T3 cells were grown in Dulbecco's Modified Eagle's Medium (Sigma-Aldrich) supplemented with 10% (v/v) heat-inactivated fetal bovine serum, glutamine (0.584 g/L), and 10 mL/L 100 x penicillin-streptomycin (Thermo Fisher Scientific, Gibco).

The *O. visianii* root extract or pure compounds identified from the Onos-Hex extracts were dissolved in dimethyl sulfoxide (DMSO) and serially diluted with growth medium in white 96-well

microtiter plates. 20,000 bloodstream forms of *T. brucei* or Balb/3T3 cells were added to each well in a final volume of 200 µL. In the case of mammalian cells, we also tested 2000 cells/well with similar results. To avoid any damage to the cells, the concentration of DMSO in the solution was never higher than 1% (no cell growth inhibition was observed with this concentration of DMSO). Cell viability was verified by a drug-free control for each compound. After 48 h incubation, the plates were treated for 24 h with 20 µL of resazurine (Sigma-Aldrich). They were subsequently quantified by fluorescence (540 nm excitation and 590 nm emission) using an Infinite M200 microplate reader (Tecan Group Ltd., Männedorf, Switzerland). The IC_{50} values were calculated by fitting the data to a log inhibitor vs. response curve (variable slope, four parameters) using the GraphPad Prism version 5.04 software.

3.2.6. Haemolytic assay

The derivatives were evaluated for their haemolytic activity according to Sathler and coworkers (Sathler *et al*., 2014). First, human blood was collected in a tube and the erythrocytes separated by centrifugation at 2500 rpm for 15 min. The supernatant was removed and the pellet washed three times with PBS (pH 7.4). Each derivative (300 µg/mL)was then placed in a microtube and incubated with the erythrocyte suspension for 5 h at 37 °C. Triton X-100 (1%) lysis was used as positive control. After incubation, the possible hemoglobin released from the erythrocytes was detected by optical density of the supernatant at 540 nm. Hemolysis less than 10% was considered within acceptable standards. Blood samples were obtained from healthy human subjects according to the ethics committee in human research number 621196.

3.2.7 Analysis of the in silico ADMET properties

The *in silico* analysis involved calculation of pharmacokinetics and toxicology parameters of the naphthoquinone derivatives using the admetSAR@ LMMD software (http://lmmd.ecust.edu.cn/admetsar2/). The results were compared with the profiles of four antitrypanosomal drugs (Suramin, Melarsoprol, Eflornithine, and Nifurtimox). The ADMET (Absorption, Distribution, Metabolism, Excretion and Toxicity) properties of the molecules were calculated based on a databank containing over 210,000 pieces of ADMET information for more than 96,000 compounds with 45 ADMET-associated properties in the scientific literature. In this work, the carcinogenic/mutagenic parameters and the ADME properties, such as human intestinal

absorption (Caco-2 permeability), blood brain barrier penetration (BBBP) and CYP450 substrate and inhibition (CYP3A4) (Cheng *et al*., 2012) of the derivatives were analyzed.

3.2.8. AChE inhibitory activity

Acetylthiocholine iodide (ATCI), recombinant human acetylcholinesterase (*h*AChE), 5,5′-dithiobis[2-nitrobenzoic acid] (DTNB), and bovine serum albumin (BSA) were purchased from Sigma-Aldrich (St. Louis., MO, USA). *Glossina palpalis* acetylcholinesterase (*gp*AChE) enzyme homogenate was prepared as follow: approximately 150 adults, mixed-sex tse-tse flies (from a colony maintained at Centre International de Recherche-Développement sur l'Elevage en zone Subhumide, CIRDES, Bobo-Dioulasso, Burkina Faso), were decapitated on dry ice and the tse-tse fly heads were homogenized in Tris buffer (pH 7.4). The enzyme homogenate was clarified by centrifugation, and stored at -20 °C before being used in the assay.

Inhibition of both acetylcholinesterases (*h*AChE and *gp*AChE) activity was determined by a spectrophotometric method previously developed (named Ellmann assay) (Pereira *et al*., 2009). Briefly, 50 µL of 50 mM phosphate buffer pH 8, 125 µL dithionitrobenzoic acid (DTNB, 3 mM in 50 mM phosphate buffer pH 8) and 25 µL of recombinant *h*AChE or 30 µL of *gp*AChE, 3 U/mL in 50 mM phosphate buffer pH 8) were added to each well of the microplate containing methanolic aliquots of hexane extract or shikonin derivatives and incubated for 15 min at 25°C. Afterward, 25 µL of acetylthiocholine iodide (ACTI, 15 mM in 50 mM phosphate buffer pH 7.0) were added as a substrate, and *h*AChE and *gp*AChE activities were measured from the absorbance changes at 412 nm at 25°C for 3.0 min using a Fluostar Omega (BMG-Labtech) plate reader. The concentration of the root hexane extract or shikonin derivatives which caused 50% inhibition of both acetylcholinesterases activity (IC_{50}) was calculated via nonlinear regression analysis. Galantamine (Sigma, Milan, Italy) was used as reference substance. Experiments were performed in triplicate measurements.

3.2.9. Antioxidant assays

The antioxidant activity of root hexane extract and isolated shikonin derivatives was measured with multiple radical generating systems as DPPH, ABTS and FRAP assay that can provide a better insight into the antioxidant potential of *O*. *visianii*. For all three assays, the experiments were conducted on 96-well microplate following previously-described protocols (Orsomando *et al*., 2016) for the measurement of the total radical scavenging capacity and ferric

reducing antioxidant power. The ability of root hexane extract and shikonin derivatives to scavenge the different radicals in all assays was compared with Trolox used as positive control. All results were expressed as tocopherol-equivalent antioxidant capacity mmol TE/g of product. Each experiment was repeated at least three times.

References

Akhtar, Y., Isman, M.B., Niehaus, L.A., Lee, C. (2012). Antifeedant and Toxic Effects of Naturally Occurring and Synthetic Quinones to the Cabbage Looper, Trichoplusia Ni. *Crop Prot*. *31*, 8-14.

Babula, P., Adam, V., Havel, L., Kizek, R.(2009). Noteworthy Secondary Metabolites Naphthoquinones - their Occurrence, Pharmacological Properties and Analysis. *Curr*. *Pharm*. *Anal*. *5*, 47-68.

Babula, P., Adam, V., Kizek, R., Sladký, Z. *et al*. (2009). Naphthoquinones as Allelochemical Triggers of Programmed Cell Death. *Environ*. *Exp*. *Bot*. *65*, 330-337.

Ball, P.W. (1972). Onosma L., In: Tutin T.G. et al., (eds), Flora Europea, Vol. 3, Univ. Press, Cambridge. 89–94.

Bhatt, S., Weiss, D. J., Cameron, E., Bisanzio, D. *et*. *al*. (2015). The effect of malaria control on Plasmodium falciparum in Africa between 2000 and 2015. *Nature 526*, 207-211.

Chaouche, T., Haddouchi, F., Bekkara, F.A. (2012). Identification of Shikonin from the Roots of Echium Pycnanthum Pomel. *Asian J*. *Pharm*. *Clin*. *Res*. *5*, 30-32.

Cheng, F., Li, W., Zhou, Y., Shen, J., *et al*. (2012). admetSAR: a comprehensive source and free tool for assessment of chemical ADMET properties. *J*. *Chem*. *Inf*. *Model*. *52*, 3099–3105.

Coelho-Cerqueira, E., Netz, P.A., do Canto, V.P., Pinto, A.C. *et al*. (2014). Beyond topoisomerase inhibition: antitumor 1,4-naphthoquinones as potential inhibitors of human monoamine oxidase *Chem*. *Biol*. *Drug Des*. *83*, 401-410.

Comai, S., Dall'Acqua, S., Grillo, A., Castagliuolo, I. *et al*. (2010). Essential Oil of Lindera Neesiana Fruit: Chemical Analysis and its Potential use in Topical Applications. *Fitoterapia, 81*, 11-16.

Ferraz, P.A.L., De Abreu, F.C., Pinto, A.V., Glezer, V. *et al*. (2001). Electrochemical Aspects of the Reduction of Biologically Active 2-Hydroxy-3-Alkyl-1, 4-Naphthoquinones. *J*. *Electroanal*. *Chem*. *507*, 275-286.

Hillard, E.A., Abreu, F.C., Ferreira, D.C., Jaouen, G., *et al*. (2008). Electrochemical parameters and techniques in drug development, with an emphasis on quinones and related compounds. *Chem*. *Commun*. *23*, 2612–2628.

Hirumi, H., Hirumi, K.C. (1989). Continuous cultivation of Trypanosoma brucei blood stream forms in a medium containing a low concentration of serum protein without feeder cell layers. *J*. *Parasitol*. *75*, 985–989.

Ito, Y., Onobori, K.; Yamazaki, T., Kawamura, Y. (2011). Tigloylshikonin, a New Minor Shikonin Derivative, from the Roots and the Commercial Root Extract of Lithospermum Erythrorhizon. *Chem*. *Pharm*. *Bull*. *59*, 117-119.

Kim, J.Y., Jeong, H.J., Park, J., Kim, Y.M. *et al*. (2012). Selective and Slow-Binding Inhibition of Shikonin Derivatives Isolated from Lithospermum Erythrorhizon on Glycosyl Hydrolase 33 and 34 Sialidases. *Bioorg*. *Med*. *Chem*. *20*, 1740-1748.

Krohn, K., Hussain, H., Viqar, U.A., Ghulam, A.M. *et al*. (2007). Lapachol: An Overview. *Arkivoc* Special Issue Reviews and Accounts: 145–171.

Lee, B.Y., Bacon, K.M., Bottazzi, M.E., Hotez, P.J. (2013). Global economic burden of Chagas disease: a computational simulation model. *Lancet Infec Dis*. *13*, 342–348.

Lubbe, A., Verpoorte, R. (2011). Cultivation of Medicinal and Aromatic Plants for Specialty Industrial Materials. *Ind*. *Crops Prod*. *34*, 785-801.

Malik, S., Bhushan, S., Sharma, M., Ahuja, P.S. (2016). Biotechnological Approaches to the Production of Shikonins: A Critical Review with Recent Updates. *Crit*. *Rev*. *Biotechnol 36*, 327-340.

Mansueto, P., Seidita, A., Vitale, G., Cascio, A. (2014). Leishmaniasis in travelers: A literature review. *Travel Med*. *Infect*. *Dis*. *12*, 563–581.

Monks, T.J., Hanzlik, R.P., Cohen, G.M., Ross, D. *et al*. (1992). Quinone Chemistry and Toxicity. *Toxicol*. *Appl*. *Pharmacol*. *112*, 2-16.

Munday, R., Smith, B.L., Munday, C.M (2007). Structure-activity relationships in the haemolytic activity and nephrotoxicity of derivatives of 1,2- and 1,4-naphthoquinone. *J*. *Appl*. *Toxicol*. *27*, 262–269.

O'Brien, P.J. (1991). Molecular mechanisms of quinone cytotoxicity. *Chem*. *Biol*. *Interact*.*80*, 1–41.

Orsomando, G., Agostinelli, S., Bramucci, M., Cappellacci, L. *et al*. (2016). Mexican sunflower (Tithonia diversifolia, Asteraceae) volatile oil as aselective inhibitor of Staphylococcus aureus nicotinatemononucleotide adenylyltransferase (NadD). *Ind*. *Crops Prod*. *85*, 181-189.

Papageorgiou, V.P., Assimopoulou, A.N., Couladouros, E.A., Hepworth, D., *et al*. (1999).The Chemistry and Biology of Alkannin, Shikonin, and Related Naphthazarin Natural Products. *Angew*. *Chem*. *Int*. *Ed*. *38*, 270-300.

Pereira, D.M., Ferreres, F., Oliveira, J., Valentão, P. *et al*. (2009). Targeted metabolite analysis of Catharanthus roseus and its biological potential. *Food Chem*. *Toxicol*. *47*, 1349–1354.

Petrelli, R., Orsomando, G., Sorci, L., Maggi, F. *et al*. (2016). Biological Activities of the Essential Oil from Erigeron floribundus. *Molecules 21*, 1065.

Pinto, A.V., de Castro, S.L. (2009). The trypanocidal activity of naphthoquinones: a review. *Molecules 14*, 4570–4590.

Rowan, C.G., Brunelli, S.M., Munson, J., Flory, J. *et al*. (2012). Clinical importance of the drug interaction between statins and CYP3A4 inhibitors: a retrospective cohort study in the health improvement network. *Pharmacoepidemiol*. *Drug Saf*. *21*, 494-506.

Sathler, P.C., Lourenço, A.L., Rodrigues, C.R., da Silva, L.C. *et al*. (2014). In vitro and in vivo analysis of the antithrombotic and toxicological profile of new antiplatelets N-acylhydrazone derivatives and development of nanosystems: determination of novel NAH derivatives antiplatelet and nanotechnological approach. *Thromb*. *Res*. *134*, 376–383.

Soeiro, M.N.C., De Castro, S.L. (2009). Trypanosoma cruzi targets for new chemotherapeutic approaches. *Exp*. *Opin*. *Ther*. *Targets 13*, 105–121.

Spyros, A., Assimopoulou, A.N., Papageorgiou, V.P. (2005). Structure Determination of Oligomeric Alkannin and Shikonin Derivatives. *Biomed*. *Chromatogr*. *19*, 498-505.

Strid, A., Tan, K. (1991). Mountain Flora of Greece; Edinburgh Unive-sity Press: Edinburgh.

Tokunaga, T., Dohmura, A., Takada, N., Ueda, M. (2004). Cytotoxic Antifeedant from Dionaea Muscipula Ellis: A Defensive Mechanism of Carnivorous Plants Against Predators. *Bull*. *Chem*. *Soc*. *Jpn*. *77*, 537-541.

Tosun, A., Akkol, E.K., Bahadir, O., Yesilada, E. (2008). Evaluation of Anti-Inflammatory and Antinociceptive Activities of some Onosma L. Species Growing in Turkey. *J*. *Ethnopharmacol*. *120*, 378-381.

Toutant, J. P. (1989). Insect acetylcholinesterase: catalytic properties, tissue distribution and molecular forms. *Prog*. *Neurobiol*. *32*, 423-446.

Tutin, T.G. (1964). *Flora Europea*. Cambridge Univ. Press: Cambridge.

Vennerstrom, J.L., Eaton, J.W. (1998). Oxidants, Oxidant Drugs, and Malaria. *J*. *Med*. *Chem*. *31*, 1269-1277.

Weill, M., Lutfalla, G.; Mogensen, K., Chandre, F. *et al*. (2003). Comparative genomics: insecticide resistance in mosquito vectors. *Nature 423*, 136-137.

WHO (2018). Prequalification Vector Control - Prequalified Lists. http://www.who.int/pq-vectorcontrol/prequalified-lists/en/ (accessed 26 October 2018).

Yu, S.J. (2014). The Toxicology and Biochemistry of Insecticides. *CRC Press* 1-380.

Zhao, P., Wang, Y., Jiang, H. (2013). Biochemical properties, expression profiles, and tissue localization of orthologous acetylcholinesterase in the mosquito, Anopheles gambiae. *Insect Biochem*. *Mol*. *Biol*. *43*, 260-271.

CHAPTER 4.

Searching for highly effective trypanocidal compounds in the essential oils from the Apiaceae family

"Money is not the

medicine against death."

Ghana proverb

Chapter 4 Outline

Abbreviation

BALB/3T3 = Mouse fibroblasts

DMSO = Dimethylsulfoxide

EOs = Essential oils

HAT = Human African Trypanosomiasis

NTDs: Neglected tropical diseases

SAR: Structure-activity relationship

SI = Selectivity index

T. brucei = *Trypanosoma brucei*

TC221 = *T. brucei* bloodstream-form parasites

TLC = Thin layer chromatography

Abstract

The Apiaceae family includes aromatic plants of economic importance employed in perfumery, food-processing industry, cosmetics and pharmaceuticals. Apiaceae are rich sources of essential oils (EOs) because of the riches of secretory structures (referred to as ducts and vittae) they are endowed with. The Apiaceae essential oils are available on an industrial level because of the wide disposability of the bulky starting material as well as their relatively cheap price. Since in the fight against protozoal infections EOs may represent new therapeutic options. In the present work, we focused on a panel of nine Apiaceae species (*Crithmum maritimum*, *Echinophora spinosa*, *Helosciadium nodiflorum*, *Heracleum sphondylium Kundmannia sicula*, *Pimpinella anisum*, *Siler montanum*, *Sison amomum*, and *Trachyspermum ammi*) and their essential oils. The EOs might represent a source of inspiration for the identification of new trypanocidal compounds to be used as alternative/integrative therapies in the treatment of HAT and/or as starting material for drug design. Biological evaluation of the inhibitory effects of the Apiaceae EOs against *T. brucei* showed that some of them (*C. maritimum, E. spinosa, H. nodiflorum*, and *S. amomum*) were active showing EC_{50} in the range 2.7-10.7 μg/mL. Most of these oils were selective against *T. brucei*, except the one from *C. maritimum* that was highly selective against the BALB/3T3 mammalian cells. Testing nine major isolated components (α-pinene, sabinene, α-phellandrene, p-cymene, limonene, β-ocimene, γ-terpinene, terpinolene, myristicin) in these oils showed that some of them had much higher selectivity than the oils themselves. Terpinolene was particularly active with an EC_{50} value of 0.035 μg/mL (0.26 μM) and a selectivity index (SI) of 180. Four other compounds with EC_{50} in the range 1.0-6.0 μg/mL (7.4-44 μM) had also good SI: sabinene (>17), β-ocimene (>91), α-pinene (>100) and limonene (>18). In conclusion, these results bring out the message that the EOs from the Apiaceae family might be considered as a reservoir of substances that can be used as lead compounds for the development of naturally-occurring trypanocidal drugs.

4.1 Introduction

The family of Apiaceae is one of the most important botanical families including essential oil-producing aromatic plants and has a relevant economic importance. In these plants, EOs are stored inside ducts and vittae, which are the plant secretory structures occurring in all organs, from roots to schizocarps (seeds) (Maggi *et al*., 2015). The Apiaceae EOs are employed in different fields such as pharmaceutics, cosmetics, food and beverages (Leung *et al*., 1996). In addition, they benefit of excellent reputation as promising candidates for eco-friendly biocides for arthropod pest and vector control (Evergetis *et al*., 2013; Benelli *et al*., 2017). Given that they are available at industrial level because of their wide cultivation, they might be used as a source of new and effective naturally-occurring trypanocidal agents.

As regards the chemical composition, the Apiaceae EOs display a high rate of variability, being characterized by different classes of components such as monoterpene hydrocarbons, oxygen-containing and aromatic monoterpenes, phenylpropanoids, sesquiterpene hydrocarbons and aliphatic compounds. Based on what has been said before, we decided to investigate the potential of nine Apiaceae species as a source of trypanocidal scaffolds with high effectiveness against *T. brucei*. For the purpose, we selected a panel of species differing each other for the volatile chemical profile, i.e. *Crithmum maritimum* L., *Echinophora spinosa* L., *Helosciadium nodiflorum* (L.) Koch, *Heracleum sphondylium* subsp. *ternatum* (Velen.) Brummit, *Kundmannia sicula* (L.) DC., *Pimpinella anisum* L., *Siler montanum* Crantz subsp. *siculum* (Spreng.) Iamonico, Bartolucci & F. Conti, *Sison amomum* L., and *Trachyspermum ammi* (L.) Sprague.

These species include seasonal (*P. anisum* and *T. ammi*), biennial (*S. amomum, H. sphondylium*) or perennial (the remaining ones) herbs growing in different environments of the Mediterranean area, such as mountainous rocky hills (*S. montanum*) and meadows (*H. sphondylium*), moist woody places (*S. amomum*), rivers, marshes, ditches and lakes (*H. nodiflorum*), sea shores (*E. spinosa*, *K. sicula* and *C. maritimum*), or often cultivated as spices (*P. anisum* and *T. ammi*). Some of them have been used in Italian folk medicine to treat several animal diseases or as antiparasitic agents (Viegi *et al*., 2001; Viegi *et al*., 2003).

This study therefore aimed at screening selected Apiaceae EOs and providing new insights into the therapeutic potential of those EOs as sources of lead compounds for the development of new drug entities against HAT. After determining the EO compositions by GC-MS, we have evaluated their inhibitory effects on blood-stream trypomastigotes of *T. brucei*. Furthermore, for the most active EOs, we assessed their toxicity on mouse BALB/3T3 fibroblasts in order to determine their selectivity.

4.2 Results and discussion

4.2.1 Essential oil compositions

The EO compositions for the nine Apiaceae species were obtained by GC-MS analysis and the results are reported in Table 1. As expected, their chemical profiles were significantly different. The highest value (3.7%) was obtained with *T*. *ammi* followed by *P*. *anisum* (2.0%), whereas the remaining samples were all below 1%.

The composition of *S*. *montanum subsp*. *siculum* EO was characterized by similar amounts of sequiterpene and monoterpene hydrocabons (33.8 and 31.5%, respectively) with a lower content of oxygenated monoterpenes (21.4%) and oxygenated sesquiterpenes (5.5%). The major component was chamazulene (32.2%) (reflecting the characteristic blue color of the oil), followed by limonene (17.8%), sabinene (6.0%) and cis-chrysanthenyl acetate (5.9%). Other noteworthy components (≥2%) resulted to be terpinen-4-ol (4.0%) and γ-terpinene (2.8%). The above chemical profile slightly defers from those reported from Kapetanos *et al*. (Kapetanos *et al*., 2008), where the authors found limonene and perilla aldehyde as the major components of *S*. *montanum* collected in Serbia.

The EO of *S*. *amomum* was almost entirely composed of monoterpene hydrocarbons (79.4%), with minor amounts of sesquiterpene hydrocarbons (9.2%) and oxygenated monoterpenes (5.8%). Sabinene (54.4%) was the major component, followed by β-phellandrene (16.6%) and germacrene D (6.7%). Other noteworthy components were terpinen-4-ol (3.8%), γ-terpinene (2.4%) and myrcene (2.0%) (Figure 1). The chemical profile was quite consistent with that has been previously published by Pavela *et al*. (Pavela *et al*., 2018).

The EO from *E*. *spinosa* roots was dominated by phenylpropanoids (41.6%), with minor amounts of monoterpene hydrocarbons (25.3%) and aliphatic compounds. Main representatives of these groups were myristicin (41.3%), terpinolene (22.2%) and (Z)-falcarinol (23.3%), respectively (Figure 1). A different chemical profile was displayed by the essential oil obtained from aerial parts, which was almost entirely composed of monoterpene hydrocarbons (96.3%), with α-phellandrene (47.2%), p-cymene (25.6%), β-phellandrene (8.3%), 2,6-dimethyl-1,3,5,7-octatetraene, E,E- (6.3%) and α-pinene (5.5%) as the main compounds. Here, the phenylpropanoid myristicin and the polyacetylene falcarinol, the major components of the root essential oil, were present at scarce level (1.5%) or non-detectable, respectively.

The *K*. *sicula* EO was largely dominated by sesquiterpene hydrocarbons (92.3%) with germacrene D (81.2%) as the predominant compound. Minor compounds were (E)-caryophyllene (2.0%), bicyclogermacrene (1.5%) and β-elemene (1.0%).

The *C*. *maritimum* EO was mainly composed of monoterpene hydrocarbons (83.3%), with limonene (38.4%), γ-terpinene (19.9%) and sabinene (12.4%) as the major compounds. Minor contributions were given by (Z)-β-ocimene (4.8%), *p*-cymene (2.6%) and α-pinene (1.8%). Phenylpropanoids accounted for 8.2% of the oil and were mainly represented by dill apiole (8.1%). Oxygenated monoterpenes (7.9%) completed the sea fennel oil chemical profile, with carvacrol methyl ether (4.2%) and terpinen-4-ol (3.1%) as the most abundant components (Figure 1).

The *H*. *nodiflorum* EO oil was dominated by phenylpropanoids (49.1%) and monoterpene hydrocarbons (42.0%), with myristicin (49.1%) and (Z)-β-ocimene (19.0%) as the most representative compounds. Other constituents occurring in noteworthy levels were limonene (7.8%), terpinolene (7.1%) and germacrene D (6.0%) (Figure 1).

The EO from *P*. *anisum* was almost entirely composed of phenylpropanoids (98.8%), with (E)-anethole (94.8%) as the predominant compound. Among the minor components, we detected other phenylpropanoids such as methyl chavicol (2.6%), and (E)-pseudoisoeugenyl 2-methyl butyrate (1.3%).

The EO from *H*. *sphondylium subsp*. *ternatum* was almost completely constituted by aliphatic compounds, representing 94.5% of the total oil. Among them, esters were the most abundant components (89.9%) with a minor contribution by aldehydes (4.9%). The major constituent was octyl acetate (61.0%), followed by minor amounts of octyl butyrate (9.4%) and octyl hexanoate (8.3%). Other noteworthy components (≥2%) were (3Z)-3-octenyl acetate (3.0%) and n-octanal (2.4%).

Finaly, the EO from *T*. *ammi* was characterized by oxygenated monoterpenes (59.6%) and monoterpene hydrocarbons (40.2%), with thymol (58.8%), p-cymene (21.9%) and γ-terpinene (16.3%) as the main components.

Table 1. Chemical composition of the nine Apiaceae EOs tested for antitrypanosomal activity.

No.	Component[a]	RI calc[b]	RI lit[c]	%[d]									ID[e]
				Siler montanum	*Sison amomum*	*Echinophora spinosa* rt	*Echinophora spinosa* ap	*Kundmannia sicula*	*Crithmum maritimum*	*Heloscidium nodiflorum*	*Pimpinella anisum*	*Heracleum sphondylium*	*Trachyspermum ammi*	
1	*n*-hexanol	863	863									tr[f]		RI,MS
2	isopropyl-2-methyl butyrate	884	880									1.4		RI,MS
3	isopropyl-isovalerate	893	894									0.8		RI,MS
4	*n*-heptanal	903	901		tr				0.1			tr		RI,MS
5	isobutyl isobutyrate	911	908									0.1		RI,MS
6	α-thujene	921	924	0.2	0.4	tr	0.4		0.4				0.2	RI,MS
7	α-pinene	926	932	1.4	0.3	0.3	5.5	tr	1.8	0.2		0.2	0.1	RI,MS,Std
8	camphene	939	946	0.1		tr			tr			tr		RI,MS,Std
9	thuja-2,4(10)-diene	945	953	tr										RI,MS
10	butyl-isobutyrate	946	944									tr		RI,MS
11	benzaldehyde	958	952					tr						RI,MS,Std
12	sabinene	965	969	6.0	54.4		0.2	tr	12.4				tr	RI,MS
13	β-pinene	968	974	0.1	tr		0.2	tr	0.1	2.3			0.7	RI,MS,Std
14	isobutyl, 2-methyl-butyrate	982	985									tr		RI,MS
15	myrcene	989	988	0.5	2.0	0.2	1.2	tr	1.1	0.8		tr	0.3	RI,MS,Std
16	2-pentyl furan	989	984									tr		RI,MS
17	α-phellandrene	1002	1002		0.5	0.5	47.2		tr	0.1			tr	RI,MS,Std
18	*n*-octanal	1004	998	tr	tr			tr	0.1	0.2		2.4		RI,MS,Std
19	isobutyl isovalerate	1007	1006									0.3		RI,MS
20	δ-3-carene	1007	1008		tr				tr					RI,MS,Std
21	isoamyl isobutyrate	1012	1007									0.1		RI,MS
22	hexyl acetate	1013	1007									0.1		RI,MS
23	α-terpinene	1014	1014	1.0	1.1	tr			1.2				0.2	RI,MS
24	2-methylbutyl isobutyrate	1017	1015									tr		RI,MS
25	*p*-cymene	1022	1020	1.2	0.6	0.5	25.6	tr	2.6	0.7		0.1	21.9	RI,MS,Std
26	β-phellandrene	1024	1025		16.6		8.3						0.3	RI,MS
27	limonene	1026	1024	17.8		1.5		tr	38.4	7.8		0.2		RI,MS,Std
28	1,8-cineole	1028	1026									tr	tr	RI,MS,Std
29	(*Z*)-β-ocimene	1037	1032	tr	0.3	tr	0.1	tr	4.8	19.0		0.2		RI,MS

30	butyl 2-methylbutyrate	1042	1043									0.3		RI,MS
31	benzene acetaldehyde	1043	1036						tr					RI,MS,Std
32	(*E*)-β-ocimene	1047	1044	tr	0.1	tr	0.3	0.1	0.2	1.4				RI,MS
33	butyl isovalerate	1047	1048									0.3		RI,MS
34	γ-terpinene	1055	1054	2.8	2.4	tr		tr	19.9	1.5		0.1	16.3	RI,MS,Std
35	pentyl isobutyrate	1059	1057									0.1		RI,MS,Std
36	*cis*-sabinene hydrate	1063	1065	0.5	0.7				0.1				tr	RI,MS
37	*n*-octanol	1071	1071									1.3		RI,MS
38	1-nonen-3-ol	1080	1078	tr										RI,MS
39	terpinolene	1084	1086	0.4	0.5	22.2	0.2	tr	0.4	7.1			tr	RI,MS,Std
40	*p*-cymenene	1086	1089	0.1			tr			tr			tr	RI,MS
41	*trans*-sabinene hydrate	1094	1098	0.3	0.4				0.1				0.1	RI,MS
42	linalool	1100	1095	0.4				tr	tr			0.2		RI,MS,Std
43	isopentyl 2-methylbutanoate	1102	1100									0.3		RI,MS
44	*cis*-thujone	1104	1101	0.1										RI,MS,Std
45	2-methyl butyl-2-methyl butyrate	1105	1100									0.7		RI,MS
46	*n*-nonanal	1105	1100	0.1				tr	tr					RI,MS
47	isopentyl isovalerate	1107	1102									0.2		RI,MS
48	1,3,8-*p*-menthatriene	1108	1108	tr						tr				RI,MS
49	2-methyl butyl isovalerate	1110	1110									0.3		RI,MS
50	*trans*-thujone	1113	1112	tr										RI,MS,Std
50	heptyl acetate	1116	1115									0.1		RI,MS
51	*cis*-*p*-menth-2-en-1-ol	1116	1118		0.2				0.1					RI,MS
52	*trans*-*p*-mentha-2,8-dien-1-ol	1117	1119	0.8										RI,MS
53	1,3,8-*p*-menthatriene	1120	1115				0.8							RI,MS
54	α-campholenal	1123	1122	0.1										RI,MS
55	*allo*-ocimene	1123	1128						0.1	1.1				RI,MS,Std
56	*E*,*E*-2,6-dimethyl-1,3,5,7-octatetraene	1128	1134				6.3							RI,MS
57	*cis*-*p*-mentha-2,8-dien-1-ol	1131	1133	0.5										RI,MS
58	geijerene	1131	1138								tr			RI,MS
59	*trans*-limonene oxide	1135	1137	0.1										RI,MS
60	*trans*-*p*-menth-2-en-1-ol	1135	1136		0.1				tr					RI,MS
61	*trans*-sabinol	1136	1137	0.3										RI,MS
62	*cis*-verbenol	1140	1137	0.2										RI,MS
63	epoxyterpinolene	1143	1148			1.0								RI,MS
64	hexyl isobutyrate	1151	1150									0.2		RI,MS

65	menthofuran	1152	1159	0.1										RI,MS
66	sabina ketone	1154	1154	0.1										RI,MS
67	eucarvone	1157	1146	0.1										RI,MS
68	pinocarvone	1157	1160	0.1										RI,MS
69	(2*E*)-nonen-1-al	1159	1157			tr		tr						RI,MS
70	*p*-mentha-1,5-dien-8-ol	1159	1166							tr				RI,MS
71	*cis*-chrysanthenol	1160	1160	1.2										RI,MS
72	*p*-mentha-1,5-dien-8-ol	1164	1166	tr										RI,MS
73	*cis*-sabinol	1165	1170	0.1										RI,MS
74	2-methoxy-3-(1-methylpropyl)pyrazine	1169	1168			tr								RI,MS
75	terpinen-4-ol	1172	1174	4.0	3.8			tr	3.1				0.1	RI,MS,Std
76	dill ether	1172	1184			tr								RI,MS
77	1,8-menthadien-4-ol	1177	1182							0.7				RI,MS
78	*p*-cymen-8-ol	1178	1179			0.9			tr	0.3				RI,MS
79	*p*-methyl-acetophenone	1181	1179			0.1								RI,MS
80	cryptone	1182	1183		0.1									RI,MS
81	*trans*-*p*-mentha-1(7),8-dien-2-ol	1184	1187	1.0										RI,MS
82	α-terpineol	1187	1186	0.2	0.2			tr	0.1					RI,MS,Std
83	*cis*-piperitol	1190	1195		tr				0.1					RI,MS
84	methy chavicol	1190	1195								2.6			RI,MS,Std
85	myrtenol	1191	1194	0.3										RI,MS,Std
86	*cis*-dihydro carvone	1192	1191	0.7										RI,MS
87	hexyl butyrate	1195	1195									0.1		RI,MS
88	(4*Z*)-decenal	1197	1193									0.2		RI,MS
89	(3*Z*)-3-octenyl acetate	1200	1200									3.0		RI,MS
90	*trans*-dihydro carvone	1200	1200	0.2										RI,MS
91	*trans*-piperitol	1204	1207	0.2	tr				tr					RI,MS
92	*n*-decanal	1206	1206									0.5		RI,MS
93	*trans*-carveol	1216	1215	0.7					tr					RI,MS
94	4-methylene-isophorone	1217	1216					tr						RI,MS,Std
95	octyl acetate	1218	1219									61.0		RI,MS,Std
96	isobornyl formate	1222	1235			0.2								RI,MS
97	*cis*-*p*-mentha-1(7),8-dien-2-ol	1224	1227	0.8										RI,MS
98	*cis*-carveol	1227	1226	0.2										RI,MS
99	thymol, methyl ether	1229	1232		tr			tr	0.1					RI,MS
100	trans-chrysanthenyl acetate	1230	1238							tr				RI,MS

101	carvacrol methyl ether	1233	1241		tr	tr		4.2					RI,MS
102	*cis*-3-hexenyl-pentanoate	1235	1235								0.1		RI,MS
103	cumin aldehyde	1236	1238	tr									RI,MS
104	*n*-hexyl 2-methyl butanoate	1239	1240								0.6		RI,MS
105	carvone	1240	1239	0.4									RI,MS,Std
106	hexyl isovalerate	1244	1244								0.4		RI,MS
107	(2*Z*)-decenal	1247	1249				tr						RI,MS
108	(*Z*)-anethole	1247	1249							0.1			RI,MS
109	*p*-anisaldehyde	1252	1247				tr						RI,MS,Std
110	geraniol	1253	1249				tr						RI,MS,Std
111	*cis*-chrysanthenyl acetate	1259	1261	5.9									RI,MS
112	(2*E*)-decenal	1260	1260				0.1				tr		RI,MS
113	*n*-decanol	1262	1266					tr					RI,MS
114	perilla aldehyde	1268	1269	0.7									RI,MS
115	dihydro-edulan I	1278	1280	tr									RI,MS
116	(*E*)-anethole	1282	1282	0.2						94.8			RI,MS,Std
117	isobornyl acetate	1280	1283	0.1	0.2						0.1		RI,MS,Std
118	bornyl acetate	1282	1287			0.1		tr					RI,MS,Std
119	thymol	1289	1289	0.1				tr				58.8	RI,MS,Std
120	*trans*-sabinyl acetate	1291	1289	tr									RI,MS
121	perilla alcohol	1294	1294	0.4									RI,MS
122	benzyl isobutyrate	1297	1297								tr		RI,MS
123	carvacrol	1302	1298	0.1			0.2	tr				0.5	RI,MS,Std
124	octyl propanoate	1306	1302								0.1		RI,MS
125	*p*-vinyl-guaiacol	1311	1309	tr									RI,MS,Std
126	nonyl acetate	1314	1315								tr		RI,MS
127	(2*E*,4*E*)-decadienal	1315	1315	tr									RI,MS
128	*p*-mentha-1,4-dien-7-ol	1326	1325	0.2									RI,MS
129	δ-elemene	1337	1335				0.7			tr			RI,MS
130	octyl isobutyrate	1348	1348								0.3		RI,MS
131	α-cubebene	1349	1345				tr						RI,MS
132	eugenol	1355	1356	tr									RI,MS,Std
133	cyclosativene	1367	1369				tr						RI,MS
134	α-ylangene	1371	1373				tr						RI,MS
135	α-copaene	1368	1374	0.1	0.1		0.3		0.2		tr		RI,MS,Std
136	β-bourbonene	1376	1387	tr	tr		0.2				tr		RI,MS

137	(E)-β-damascenone	1381	1383					tr				RI,MS
138	β-cubebene	1383	1387	tr	tr		0.2		tr			RI,MS
139	isobutyl phenylacetate	1384	1386								0.1	RI,MS
140	β-elemene	1386	1389	0.1	tr	tr	1.0		tr		tr	RI,MS
141	octyl butyrate	1392	1394								9.4	RI,MS,Std
142	methyl eugenol	1405	1403			0.2						RI,MS
143	(*E*)-caryophyllene	1409	1417	0.4	0.3		2.0	tr	0.4		0.2	RI,MS,Std
144	decyl acetate	1411	1407								0.4	RI,MS
145	β-ylangene	1414	1419				tr					RI,MS
146	β-copaene	1415	1430		0.1		0.9		0.1			RI,MS
147	α-*trans*-bergamotene	1431	1432					tr				RI,MS
148	γ-elemene	1434	1434				0.4					RI,MS
149	octyl 2-methylbutanoate	1435	1434								0.3	RI,MS
150	aromadendrene	1440	1439				0.4					RI,MS,Std
151	octyl isovalerate	1440	1440								0.1	RI,MS
152	α-himachalene	1442	1449							tr		RI,MS
153	α-humulene	1443	1454	0.5	tr							RI,MS,Std
154	isogermacrene D	1445	1452				0.4					RI,MS
155	4,5-*di*-*epi*-aristolochene	1460	1471			tr						RI,MS
156	dehydro-sesquicineole	1461	1469		tr							RI,MS
157	*cis*-cadina-1(6),4-diene	1465	1461				0.2					RI,MS
158	γ-decalactone	1465	1465								0.1	RI,MS
159	γ-himachalene	1470	1481							0.8		RI,MS
160	germacrene D	1472	1484	0.4	6.7		81.2		6.0	0.2	0.2	RI,MS
161	β-selinene	1476	1489			tr						RI,MS
162	*ar*-curcumene	1479	1479					tr				RI,MS
163	(*E*)-β-ionone	1481	1487	tr								RI,MS,Std
164	phenyl ethyl 3-methyl butanoate	1484	1488								0.1	RI,MS
165	α-selinene	1486	1498			0.6						RI,MS
166	bicyclogermacrene	1487	1500	tr	0.1		1.5	0.1	0.1			RI,MS
167	phenethyl isovalerate	1488	1489								tr	RI,MS
168	α-muurolene	1488	1500		0.1		0.2					RI,MS
169	β-himachalene	1490	1500							tr		RI,MS
170	α-zingiberene	1492	1493	tr				tr		tr	tr	RI,MS
171	γ-amorphene	1497	1495				0.3					RI,MS
172	(*E*,*E*)-α-farnesene	1502	1505		1.6						0.1	RI,MS

173	β-bisabolene	1504	1505	tr		tr			tr			tr	RI,MS
174	(*Z*)-α-bisabolene	1504	1506		tr								RI,MS
175	germacrene A	1507	1508					0.1					RI,MS
176	δ-amorphene	1509	1511					0.2					RI,MS
177	γ-cadinene	1515	1513					0.3					RI,MS
178	myristicin	1516	1517			41.3	1.5		0.1	49.1		0.6	RI,MS
179	δ-cadinene	1517	1522	tr	0.2			0.8					RI,MS
180	β-sesquiphellandrene	1519	1521						tr			0.2	RI,MS
181	*trans*-cadina-1,4-diene	1533	1533					0.1					RI,MS
182	α-cadinene	1539	1537					0.1					RI,MS
183	germacrene B	1558	1559					0.7	0.1				RI,MS
184	elemecin	1559	1559			0.1			tr			tr	RI,MS
185	germacrene D-4-ol	1576	1574					0.2					RI,MS
186	spathulenol	1576	1577	1.1				0.1	tr	tr			RI,MS
187	*ar*-turmerol	1576	1582	0.1									RI,MS
188	caryophyllene oxide	1578	1583	1.8				0.1					RI,MS,Std
189	octyl hexanoate	1580	1575									8.3	RI,MS
190	salvial-4(14)-en-1-one	1583	1594	0.1	tr			0.2		tr			RI,MS
191	decyl butyrate	1590	1590									0.1	RI,MS
192	guaiol	1591	1600			0.1							RI,MS
193	humulene epoxide II	1597	1608	1.1									RI,MS,Std
194	β-atlantol	1610	1608					0.1					RI,MS
195	isomyristicin	1610	1616			tr							RI,MS
196	β-oplopenone	1612	1607					0.1					RI,MS
197	1,10-di-epi-cubenol	1616	1618					tr					RI,MS
198	benzophenone	1617	1626						tr				RI,MS
199	junenol	1621	1618					0.4					RI,MS
200	dill apiole	1622	1620						8.1				RI,MS
201	caryophylla-4(12),8(13)-dien-5α-ol	1632	1639	0.3									RI,MS
202	caryophylla-4(12),8(13)-dien-5β-ol	1634	1639	0.4									RI,MS
203	*epi*-α-cadinol	1640	1638					0.3		0.1			RI,MS
204	*epi*-α-muurolol	1642	1640					0.3					RI,MS
205	α-cadinol	1648	1652	tr	tr		0.1	0.7		0.1			RI,MS,Std
206	bulnesol	1662	1670			0.3							RI,MS
207	14-hydroxy-9-*epi*-(*E*)-caryophyllene	1663	1668	0.2									RI,MS
208	eudesma-4(15),7-dien-1β-ol	1676	1687	0.4	0.3			0.6		0.1			RI,MS

209	chamazulene	1720	1730	32.2									RI,MS,Std
210	mint sulfide	1739	1740				1.1		0.2				RI,MS
211	*n*-tetradecanoic acid	1765	1765	tr									RI,MS
212	14-hydroxy-α-muurolene	1778	1779				tr						RI,MS
213	octyl octanoate	1779	1779								0.1		RI,MS
214	2-ethylhexyl-salycilate	1799	1807					tr					RI,MS
215	14-hydroxy-δ-cadinene	1803	1803				0.1						RI,MS
216	(*E*)-pseudoisoeugenyl 2-methylbutyrate	1833	1841							1.3			RI,MS
217	neophytadiene	1834	1842						0.2				RI,MS
218	2-pentadecanone, 6,10,14-trimethyl-	1844	1845	0.1									RI,MS
219	*n*-hexadecanol	1879	1879								tr		RI,MS
220	*n*-hexadecanoic acid	1968	1959	0.8									RI,MS,Std
221	*n*-heptadecanol	1978	1979		0.3								RI,MS
222	*iso*-bergaptene	2034	2033								0.1		RI,MS
223	(*Z*)-falcarinol	2035	2035			23.3		0.1					RI,MS
224	*n*-octadecanol	2078	2077								0.4		RI,MS
225	*n*-tricosane	2300	2300					tr					RI,MS,Std
226	*n*-pentacosane	2500	2500	tr				tr					RI,MS,Std
227	*n*-heptacosane	2700	2700	tr	tr			0.1					RI,MS,Std
228	*n*-nonacosane	2900	2900		0.3	tr		0.1					RI,MS,Std
	Total identified (%)			93.5	95.5	93.7	98.0	97.3	99.9	99.8	99.9	97.4	99.8
	Oil yield (% dw)			0.2	0.6	0.1	0.2	0.3	0.6	0.4	2.0	0.4	3.7
	Grouped compounds (%)												
	Monoterpene hydrocarbons			31.5	79.4	25.3	96.3	0.3	83.3	42.0	tr	0.7	40.2
	Oxygenated monoterpenes			21.4	5.8	2.3		0.2	7.9	1.0		0.3	59.6
	Sesquiterpene hydrocarbons			33.8	9.2	0.7		92.3	0.2	6.8	1.2	0.9	
	Oxygenated sesquiterpenes			5.5	0.4	0.4	0.1	2.9	tr	0.4			
	Phenylpropanoids			0.2		41.6	1.5	tr	8.2	49.1	98.8	0.6	
	Aliphatics			1.0	0.7	23.4		0.3	0.2	0.2		94.8	
	Others			0.1		0.1		1.2	0.1	0.3		0.1	

[a] Compounds are listed in order of their elution from a HP-5MS column. [b] Linear retention index on HP-5MS column, experimentally determined using homologous series of C_8-C_{30} alkanes. [c] Linear retention index taken from Adams (2007), NIST 08 (2008) and FFNSC 2 (2012). [d] Relative percentage values are means of three determinations with a RSD% for the main components below 18%. [e] Identification methods: STD, based on comparison of RI, MS and RT with those of analytical standard; MS, based on comparison with WILEY, ADAMS, FFNSC 2 and NIST 08 MS databases; RI, based on comparison of calculated RI with those reported in ADAMS, FFNSC 2 and NIST 08. [f] tr, % below 0.1%.

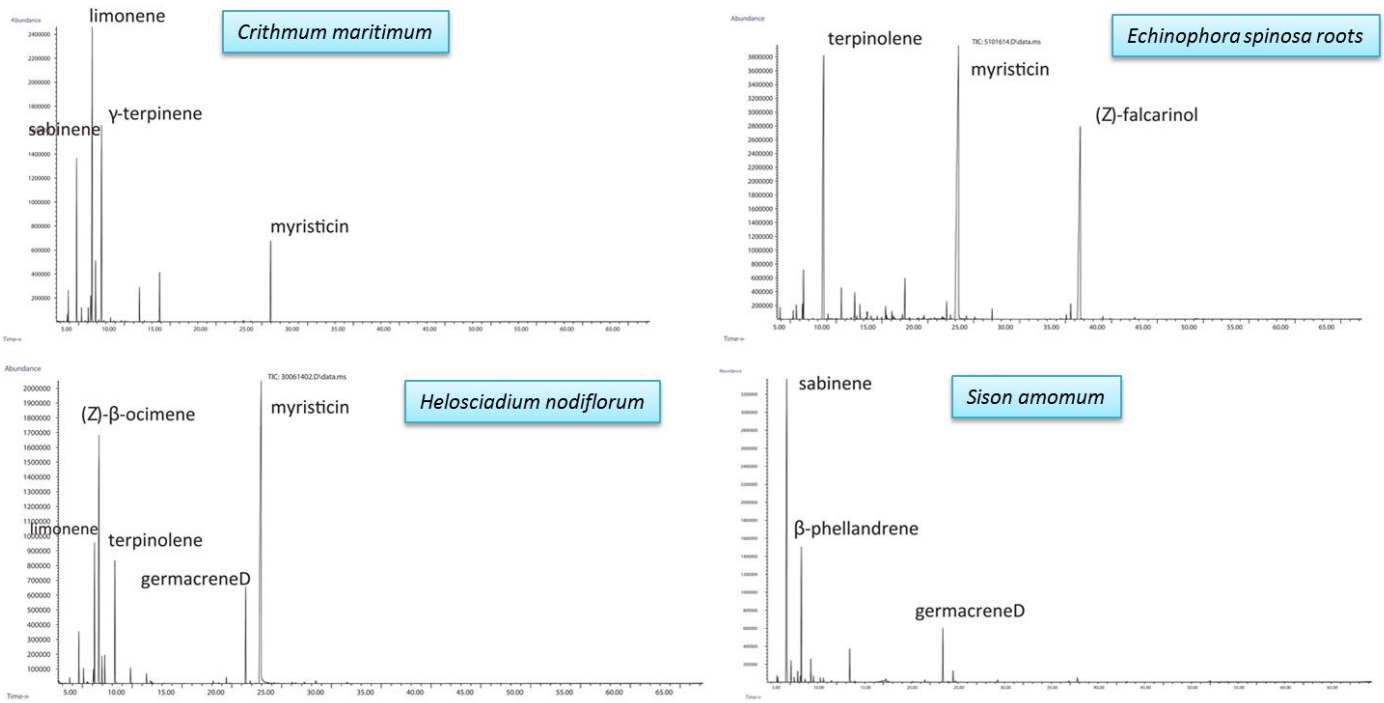

Fig. 1. GC-MS chromatograms of the bioactive EOs from: *Crithmum maritimum*, *Echinophora spinosa* roots, *Helosciadium nodiflorum* and *Sison amomum*.

4.2.2. Trypanocidal activity

The evaluation of trypanocidal activity of the Apiaceae EOs showed that five out of nine were active against *T. brucei* (Table 2). Most of these oils were selective against *T. brucei*, except the one from *C. maritimum* that was highly selective against the mammalian cells. Testing the major individual components in these oils showed that some of them had much higher selectivity than the oils themselves. Terpinolene was particularly active with an EC_{50} value of 0.035 µg/mL (0.26 µM) and a selectivity index (SI) of 180. Four other compounds had also good selective indexes: sabinene (>17), β-ocimene (>91), α-pinene (>100) and limonene (>18) (Figure 2).

Our experiments highlighted the good inhibitory activity on *T. brucei* observed for four out of nine species, namely *S. amomum* (EC_{50} = 4.3 µg/mL), *E. spinosa* (EC_{50} root = 2.7 µg/mL; EC_{50} aerial parts = 4.0 µg/mL), *H. nodiflorum* (EC_{50} = 10.7 µg/mL) and *C. maritimum* (EC_{50} = 5.0 µg/mL), which are attributable to the main essential oil components although a synergism with minor constituents should not be underestimated.

The major components found in the bioactive essential oils belong to three chemical groups, namely phenylpropanoids, polyacetylenes and monoterpene hydrocarbons. Therefore, these

secondary metabolites represent promising starting point chemotypes for the development of drugs for the treatment of HAT. It is worth noting that although only two of the active essential oils had a good selectivity against *T*. *brucei*, i.e. *S*. *amomum* (SI = 13) and *H*. *nodiflorum* (SI > 9), all four are still interesting because they contain different components that are selective against *T*. *brucei* but not against mammalian cells.

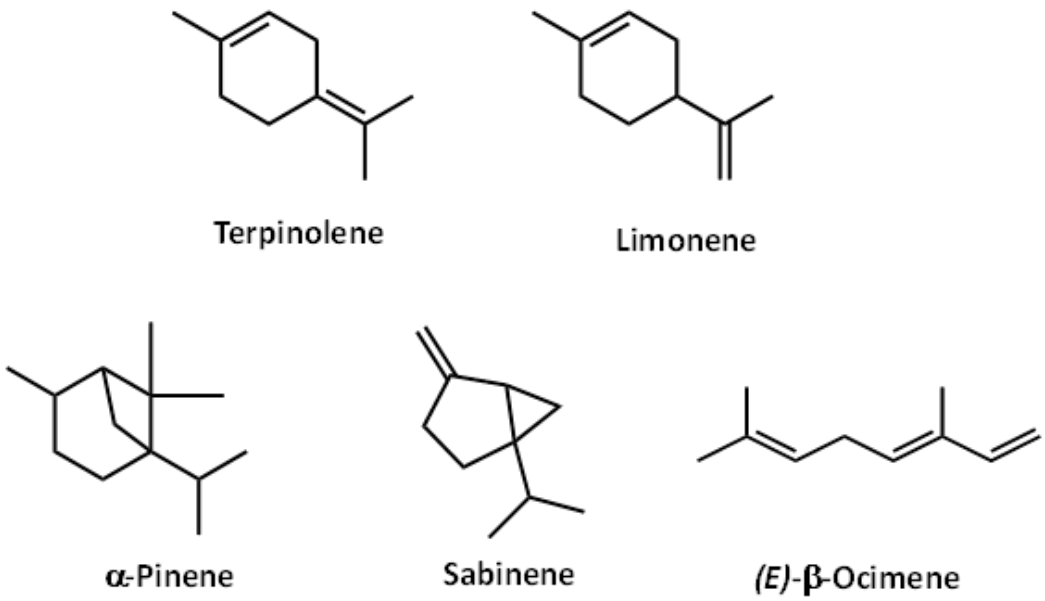

Fig. 2. Chemical structures of antitrypanosomal monoterpenes (EC_{50} < 10 μg/mL) with the best selective index occurring in the Apiaceae EOs tested.

Table 2. Antitrypanosomal activity and selectivity of the nine Apiaceae EOs.

Essential oil Treatment	IC_{50} (μg/mL)		Selectivity Index (SI)
	***T. b. brucei* (TC221)**	**Balb3T3**	
S. montanum	>100	n.d.	
S. amomum	4.31 ± 0.7	56.3 ± 12.3	13.1
E. spinosa roots	2.67 ± 0.6	5.71 ± 0.39	2.1
E. spinosa aerial parts	4.03 ± 1.6	14.9 ± 2.2	3.7
K. sicula	>100	n.d.	-
C. maritimum	5.01 ± 0.8	0.38 ± 0.03	0.07
H. nodiflorum	10.7 ± 4.1	>100	>9.3
P. anisum	>100	n.d.	-
H. Sphondylium	>100	n.d.	-
T. ammi	>100	n.d.	-
Pure compounds	**μg/mL (μM)**	**μg/mL (μM)**	
Sabinene	5.96 ± 1.51 (43.8)	>100	>16.77
β-Ocimene	1.08 ± 0.47 (8.02)	>100	>92.66
α-Pinene	1.01 ± 0.34 (7.44)	>100	>99
γ-Terpinene	>100	n.d.	-
Terpinolene	0.035 ± 0.005 (0.258)	6.34 ± 0.53	181
Myristicin	74.42 ± 3.71 (390)	>100	>1.34
p-Cymene	4.51 ± 1.04 (33.3)	28.47 ± 7.22	6.31
α-Phellandrene	24.11 ± 8.06 (177)	115 ± 21.43	4.77
Limonene	5.61 ± 1.62 (41.2)	>100	>17.85
Reference drug	**μg/mL (μM)**	**μg/mL (μM)**	
Suramin	0.0191 ± 0.002 (0.0147)	>5	>262

n.d., not determined

The trypanocidal activity of the major compounds assayed was in the order: terpinolene > α-pinene > β-ocimene > *p*-cymene > limonene > sabinene > α-phellandrene > myristicin > γ-terpinene (Table 2). The chemical structures of the bioactive compounds (Figure 2) varied from linear (β-ocimene) to monocyclic (terpinolene, *p*-cymene and limonene) and bicyclic derivatives (α-pinene and sabinene), and are endowed with one to three unsaturations.

Terpinolene was the most potent trypanocidal among those tested pure compounds. It was particularly abundant (22.2%) in the most active essential oil from the roots of *E*. *spinosa*. Noteworthy, when tested alone, terpinolene exerted a very strong inhibition (77 and 115 times more active than *E*. *spinosa* root and aerial part EOs, respectively) on *T*. *brucei* showing an EC_{50} value of 0.035 μg/mL (0.26 μM) with a significant SI (180). This makes it an interesting chemotype for the development of novel trypanocidal drugs.

α-Pinene, one of the most ubiquitous volatile components produced by higher plants, is found abundant in several Apiaceae EOs (Evergetis *et al*., 2013). However, in the EO samples examined herein, α-pinene was not particularly abundant (maximum 5.5% in *E*. *spinosa*). It exerted strong inhibition on *T*. *brucei* (EC_{50} of 1.1 μg/mL) with a very good selectivity index (SI > 100).

(*Z*)-β-Ocimene, one of the major components of the *H*. *nodiflorum* EO (19.0%), is an acyclic monoterpene hydrocarbon involved in the plant defense against predators (Cascone *et al*., 2015). This compound showed a similar effect to that exhibited by α-pinene on *T*. *brucei* (EC_{50} of 1.1 μg/mL and SI > 91).

p-Cymene, an aromatic monoterpene particularly abundant in the EOs from the aerial parts of *E*. *spinosa* (25.6%) and *T*. *ammi* (21.9%), is reported to be able of swelling the cytoplasmic membrane. Being highly hydrophobic, *p*-cymene is easily incorporated in the lipid bilayer facilitating the penetration of other bioactive components (Ultee *et al*., 2002). Monzote *et al*. has already reported the antiprotozoal properties of *p*-cymene (Monzote *et al*., 2012).

Limonene, one of the most ubiquitous and major volatile monoterpenes in plants, resulted to be particularly active against *T*. *brucei* showing an EC_{50} value of 5.6 μg/mL together with average selectivity (SI > 17) (Petrelli *et al*., 2016). In our study, it was found as one of the major constituents of the essential oils from *C*. *maritimum* (38.4%) and *H*. *nodiflorum* (7.8%). This compound is characterized by a cycle bearing one double bond and is endowed with an exocyclic methylene group which can react with functional groups of proteins producing cell oxidative damage (Wink, 2008). A similar chemical motif occurs in terpinolene, one of the major components of *E*. *spinosa* and *H*. *nodiflorum* EOs.

Sabinene, a bicyclic monoterpene occurring in many EOs of the Apiaceae family (Nehlin *et al*., 1996), has been detected as particular abundant in the EOs of *S*. *amomum* (54.4%) and *C*. *maritimum* (12.4%). Together with α-pinene has been previously reported as effective against *Leishmania major* and *T*. *brucei* (Mikus *et al*., 2000).

It is important to emphasise that EOs rich in thymol (*T*. *ammi*) and germacrene D (*K*. *sicula*), which are reported in the literature as antitrypanosomal compounds (Halldor, 2011; Monzote *et al*., 2012), were here not active on *T*. *brucei*. This means that other components occurring in these oils that antagonize the biocidal effects of these constituents or that their amount in the oil is not sufficient to exert the effect. Similar considerations can be also made for the *P*. *anisum* EO, which is strongly characterized by the presence of the insecticidal (*E*)-anethole (94.8%) (Benelli *et al*., 2017), but resulted ineffective against *T*. *brucei* proliferation.

In the most active EO (*E*. *spinosa* roots, EC_{50} = 2.7 μg/mL) we found detectable amounts of (*Z*)-falcarinol, a polyacetylene also known as panaxynol. This volatile component is typical in ginseng (*Panax ginseng* C.A.Mey) and in several Apiaceae plants such as carrot (Crosbya *et al*., 1967). (*Z*)-Falcarinol acts as a natural pesticide, protecting roots from fungal diseases (Yates *et al*., 1982) and its presence might be linked with the trypanocidal effects seen for *E*. *spinosa* root EO. In fact, falcarinol is one of the main components of hexane extracts from roots of *P*. *ginseng* and showed a very low EC_{50} value (0.01 μg/mL) on *T*. *b*. *brucei*, with a selectivity index of 858 which was higher than that of the reference compound suramin (Herrmann *et al*., 2013). Being highly lipophilic, (Z)-falcarinol can easily cross the cell membrane. Here it is converted into a stable carbocation which reacts with SH and amino groups of proteins and other biomolecules (Wink, 2008). Its selectivity toward *T*. *brucei* may be linked to the inhibition on trypanothione reductase, an enzyme specific for trypanosomastids which protects the cell against reactive oxygen species (Krauth-Siegel *et al*., 2005). Other plausible mechanisms of action might be the inhibition of the mitochondrial respiration that causes the cell cycle arrest (Hao *et al*., 2005) or the inhibition of trypanosome sterols biosynthesis (Urbina, 2002).

A structure-activity relationship (SAR) analysis of terpinolene in relation with other related compounds such as limonene, *p*-cymene, α-phellandrene and γ- terpinene has been reported in Figure 3. As shown in Figure 3, the chemical structure of limonene differs from terpinolene only in the position of the exocyclic methylene group, whereas the α-phellandrene and γ-terpinene have no double bonds in their side-chains. Among these related compounds, only *p*–cymene has an aromatic ring. The influence of the position of the double bond in the side-chain upon the trypanocidal activity of terpinolene was evaluated in comparison with limonene. Terpinolene showed the highest trypanocidal activity compared with limonene (a 160-fold increase of activity, Table 2),

demonstrating that the position of exocyclic methylene group can significantly influence the trypanocidal activity.

Furthermore, the significant trypanocidal activity observed with *p*–cymene suggested that the presence of multiple π bonds in the six-membered ring may also play an important role against the parasite. On the other hand, the weak and lack of trypanocidal activity observed with α-phellandrene and γ-terpinene, respectively (Table 2), may be due to the absence of an exocyclic methylene group and an aromatic system.

Overall, the monoterpene compounds, are known to cause chromatin alterations, disruption of the protozoal plasma membrane, mitochondrial swelling and cell lysis (Saeidnia *et al*., 2012; Raut *et al*., 2014). Furthermore, the presence of methylene groups may increase the oxidative damage in the parasite by enhancing the bonding with SH groups of proteins such as trypanothione synthase (Wink, 2008). In addition, some monoterpenoids are capable of interfering with the isoprenoid pathway present in the protozoa (Rodrigues Goulart *et al*., 2004). An interesting perspective of using EOs as therapeutic agents in the treatment of HAT may be to investigate their unexplored immunomodulatory action (Venditti *et al*., 2015; Vitali *et al*., 2016) which can induce a cascade of events leading to the parasite death (Antony *et al*., 2005).

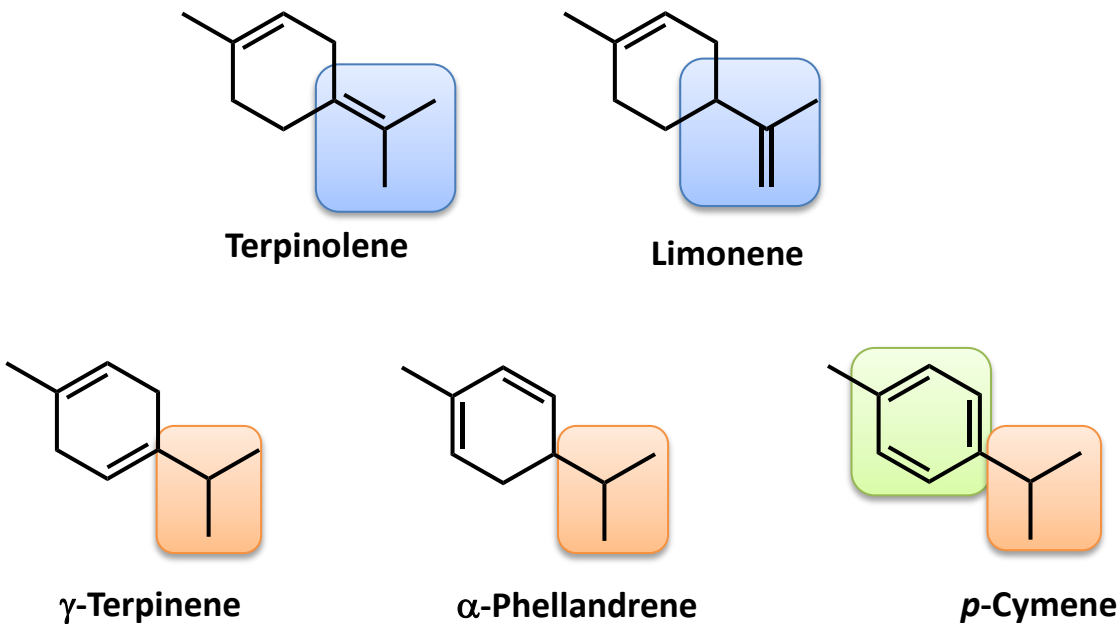

Fig. 3. Chemical structures of some monoterpenes hydrocarbons tested for antitrypanosomal activity.

4.3 Conclusions

Overall, this research highlights the use of EOs from the Apiaceae family as a reservoir of compounds to be further investigated as possible chemotypes for the development of natural drugs for the treatment of HAT. Structures related to monoterpene hydrocarbons, aromatic monoterpenes and polyines showed a good inhibition profile against HAT and the presence and the position of an exocyclic methylene group and/or π bonds in the six-membered ring are factors that increase the activity of monoterpenes.

These features might be explored and could be employed for further delineation of biologically active terpinolene-based drugs. As sources of such compounds the EOs of the Apiaceae family present several advantages, e.g. they are widely available on an industrial level at reasonable costs and they represent a sustainable raw material.

In order to better define the mechanism of action behind this novel class of trypanocidal compounds extended studies are needed and some of them are ongoing in our laboratory.

4.4 Materials and methods

4.4.1 Plant material

Flowering aerial parts of *S*. *montanum* subsp. *siculum* were collected in Santa Colomba c/o Gran Sasso (Teramo, N 47°01'8", E 38°07'3", 1620 m a.s.l.), in July 2016. Flowering aerial parts of *S*. *amomum* were collected at Sorgenti del Pescara, Popoli, central Italy (N 42°10'03", E 13°49'10", 285 m a.s.l.), in June 2017. Roots and flowering aerial parts of *E*. *spinosa* were collected at Salinelle Beach, Lascari, Palermo, Sicily, Italy (N 38°01'48", E 13°18'40", 6 m a.s.l.), in October 2016. Inflorescences of *K*. *sicula* were collected at San Martino delle Scale, Palermo, Sicily, Italy (N 38°05'27", E 13°14'58", 616 m a.s.l.), in July 2016. Flowering aerial parts of *C*. *maritimum* were collected in the beach of Senigallia, central Italy (N 43°44'29", E 13°11'05", 0 m a.s.l.), in August 2017. *H*. *nodiflorum* whole plants were collected in Badia Morronese-Fonte d'Amore, Sulmona, central Italy (N 42°05'3", E 13°55'19", 354 m a.s.l.), in August 2016. Seeds of *P*. *anisum* were collected in a field of Castignano, Ascoli Piceno, central Italy (N 42°56'10", E 13°35'00", 496 m a.s.l.), in September 2017. Seeds of *H*. *sphondylium* subsp. *ternatum* were collected in Montelago (Appennino Umbro-Marchigiano, Camerino, N 43°06'30"; E 12°58'25", 900 m a.s.l.), in July 2016. Seeds of *T*. *ammi* were purchased from a local market of Tabriz (East Azarbaijan Province, Iran) in July 2017. Except for *P*. *anisum* and *T*. *ammi* seeds, the plant identification was performed using available literature (Pignatti, 1982) and the voucher specimens have been deposited in the *Herbarium Universitatis Camerinensis* (CAME) c/o School of Bioscience and Veterinary Medicine, University of Camerino, Camerino, Italy (for *S*. *amomum*, *C*. *maritimum*, *H*. *nodiflorum* and *H*. *sphondylium* subsp. *ternatum*), *Herbarium* of the Centro Ricerche Floristiche dell'Appennino (APP), Barisciano, L'Aquila, Italy (for *Siler montanum* subsp. *siculum*), and Department STEBICEF, University of Palermo, Palermo, Italy (for *E*. *spinosa* and *K*. *sicula*). After collection, the plant material was dried at room temperature under darkness for one week.

4.4.2 Hydrodistillation

Plant material (*Siler montanum* subsp. *siculum*: 180 g; *S*. *amomum*: 550 g; *E*. *spinosa*: 700 g of roots, 380 g of aerial parts; *K*. *sicula*: 320 g; *C*. *maritimum*: 870 g; *H*. *nodiflorum*: 750 g; *P*. *anisum*: 40 g; *H*. *sphondylium* subsp. *ternatum*: 1290 g; *T*. *ammi*: 150 g) has been hydrodistilled in a Clevenger-type apparatus using different volumes of deionized water (0.8-5 L) for 3 h. Once

obtained, the EOs were treated with anhydrous sodium sulphate to remove water drops, then filtered and stored in amber vials sealed with silicon septa caps at -20 °C before use. The oil yields were calculated on a dry weight basis (w/w), ranging from 1.2 % to 2.7%.

4.4.3 GC-MS analysis

The analytical conditions and instruments used for the separation of Apiaceae EO components were the same of those reported in Chapter 2 paragraph 2.6.8. The identification, whenever possible, was made by comparison with authentic standards available in the authors' laboratory. In addition, the correspondence of retention indices (RIs) and mass spectra (MS) with respect to those reported in commercial databases (Adams, 2007; NIST 08, 2008; FFNSC2, 2012) and home-made libraries was used to confirm the peak assignment. Semi-quantification of EO components was made by peak area normalization considering the same GC response of the mass spectrometer detector towards all volatile constituents.

4.4.4. Cell culture and growth inhibition assay

The cultures of *T. brucei* TC221 BSFs and mouse Balb/3T3 fibroblasts (ATCC No CCL-163) as well as the EC_{50} determinations, were performed in a similar way as reported previously in Chapeter 2 paragraph 2.6.9, with an adjustment of the seeding density for the mammalian cells. Briefly, to assess the EC_{50} values for growth inhibition the essential oils and pure compounds were dissolved in dimethylsulfoxide (DMSO) and serially diluted with growth medium in 96- well microtiter plates (100 µL/well). To each well, 20 000 bloodstream forms of *T. brucei* or 5 000 Balb/3T3 cells (100 µL/well) were added with a final volume of 200 µL. After 48 h of incubation, 20 µL of 0.5 mM resazurine (Sigma Aldrich) was added to each well for a 24 h treatment. The fluorescence (540 and 590 nm excitation and emission filters) was measured using an infinite M200 microplate reader (Tecan Group, Ltd). The software GraphPad Prism 7.03 was used to calculate EC_{50} values on a log inhibitor versus response curves by non-linear regression.

References

Adams, R., 2007. Identification of Essential Oil Components by Gas Chromatography/Mass Spectrometry, fourth ed. Allured Publishing Corp., Carol Stream, IL, USA.

Anthony, J.P., Fyfe, L., Smith, H. (2005). Plant active components: are source for antiparasitic agents? *Trends Parasitol*. *21*, 462–468.

Benelli, G., Pavela, R., Iannarelli, R., Petrelli, R. *et al*. (2017). Synergized mixtures of Apiaceae essential oils and related plant-borne compounds: larvicidal effectiveness on the filariasis vector *Culex quinquefasciatus* Say. *Ind*. *Crop*. *Prod*. *96*, 186–195.

Cascone, P., Iodice, L., Maffei, M.E., Bossi, S. *et al*. (2015). Tobacco overexpressing β-ocimene induces direct and indirect responses against aphids in receiver tomato plants. *J*. *Plant Physiol*. *173*, 28-32.

Crosbya, D.G., Aharonson, N. (1967). The structure of carotatoxin, a natural toxicant from carrot. *Tetrahedron 23*, 465–472.

Evergetis, E., Michaelakis, A., Haroutounian, S.A. (2013) Exploitation of Apiaceae family essential oils as potent biopesticides and rich source of phellandrenes. *Ind*. *Crops Prod*. *41*, 365-370.

FFNSC 2, 2012. Flavors and fragrances of natural and synthetic compounds. Mass spectral database. Shimadzu Corps, Kyoto.

Halldor, T. (2011). Lipids and Essential Oils as Antimicrobial Agents. John Wiley & Sons Ltd, The Atrium, Southern Gate, Chichester, UK.

Hao, W., Xing-Jun, W., Yong-Yao, C., Liang, Z. *et al*. (2005). Up-regulation of M1 muscarinic receptors expressed in $CHOm_1$ cells by panaxynol via cAMP pathway. *Neurosci*. *Lett*. *383*, 121–126.

Herrmann, F., Sporer, F., Tahrani, A., Wink, M. (2013). Antitrypanosomal Properties of *Panax ginseng* C. A. Meyer: New Possibilities for a Remarkable Traditional Drug. *Phytother*. *Res*. *27*, 86–98.

Kapetanos, C., Karioti, A., Bojovic, S., Marin, P. *et al*. (2008). Chemical and principal-component analyses of the essential oils of apioideae taxa (Apiaceae) from central Balkan. *Chem*. *Biodivers*. *5*, 101–119.

Krauth-Siegel, R.L., Bauer, H., Schirmer, R.H. (2005). Dithiol proteins as guardians of the intracellular redox milieu in parasites: old and new targets in trypanosomes and malaria-causing plasmodia. *Angew*. *Chem*. *Int*. *Ed*. *Engl*. *44*, 690–715.

Leung, A.Y., Foster S. (1996). Encyclopedia of Common Natural Ingredients Used in Food, Drugs, and Cosmetics, 2nd edn. Wiley: New York.

Maggi, F., Papa, F., Giuliani, C., Maleci Bini, L. *et al*. (2015). Essential oil chemotypification and secretory structures of the neglected vegetable *Smyrnium olusatrum* L. (Apiaceae) growing in central Italy. *Flavour Fragr*. *J*. *30*, 139-159.

Maggi, F., Quassinti, L., Bramucci, M., Lupidi, G. *et al*. (2014). Composition and biological activities of hogweed [*Heracleum sphondylium* L. subsp. *ternatum* (Velen.) Brummitt] essential oil and its main components octyl acetate and octyl butyrate. *Nat*. *Prod*. *Res*. *28*, 1354-1363.

Mikus, J., Harkenthal, M., Steverding, D., Reichling, J. (2000). *In vitro* effect of essential oils and isolated mono- and sesquiterpenes on *Leishmania major* and *Trypanosoma brucei*. *Planta Med*. *66*, 366-368.

Monzote, L., Alarcon, O., Setzer, W.N. (2012). Antiprotozoal activity of essential oils. *Agric*. *Conspec*. *Sci*. *77*, 167–175.

Nehlin, G., Valterová, I., Borg-Karlson, A.K. (1996). Monoterpenes released from Apiaceae and the egg-laying preferences of the carrot psyllid, *Trioza apicalis*. *Entomol*. *Exp*. *Appl*. *80*, 83-86.

NIST 08, 2008. Mass spectral library (NIST/EPA/NIH). National Institute of Standards and Technology, Gaithersburg, USA.

Pavela, R., Maggi, F., Cianfaglione, K., Dauvergne, X. et al. (2018). Larvicidal activity of essential oils of five Apiaceae taxa and some of their main constituents against Culex quinquefasciatus. *Chem*. *Biodiv*. *15*, e1700382.

Petrelli, R., Orsomando, G., Sorci, L., Maggi, F. *et al*. (2016). Biological Activities of the Essential Oil from *Erigeron floribundus*. *Molecules 21*, 1065-1079.

Pignatti, S. (1982). Flora d'Italia. Edagricole Ed., Bologna, Italy, vol. 2.

Raut, J.S., Karuppayil, S.M. (2014). A status review on the medicinal properties of essential oils. *Ind*. *Crop*. *Prod*. *62*, 250-264.

Rodrigues Goulart, H., Kimura, E.A., Peres, V.J., Couto, A.S. *et al*. (2004). Terpenes arrest parasite development and inhibit biosynthesis of isoprenoids in *Plasmodium falciparum*. *Antimicrob*. *Agents Chemother*. *48*, 2502–2509.

Saeidnia, S., Gohari, A.R. (2012). Trypanocidal monoterpenes: lead compounds to design future trypanocidal drugs. *Stud*. *Nat*. *Prod*. *Chem*. *37*, 173–189.

Ultee, A., Bennink, M.H.J., Moezelaar, R. (2002). The phenolic hydroxyl group of carvacrol is essential for action against the food-borne pathogen Bacillus cereus. *Appl*. *Environ*. *Microbiol*. *68*, 1561–1568.

Urbina, J.A. (2002). Chemotherapy of Chagas disease. *Curr*. *Pharm*. *Des*. *8*, 287–295.

Venditti, A., Bianco, A., Frezza, C., Conti, F. *et al*. (2015). Essential oil composition, polar compounds, glandular trichomes and biological activity of *Hyssopus officinalis* subsp. *aristatus* (Godr.) Nyman from central Italy. *Ind*. *Crop*. *Prod*. *77*, 353-363.

Viegi, L., Maccioni, S., Pieroni, A., Guarrera, P.M. (2001). Piante usate in Italia in medicina veterinaria popolare. Ann. Facoltà Med. Vet. Pisa 54, 405–442.

Viegi, L., Pieroni, A., Guarrera, P.M., Vangelisti, R. (2003). A review of plants used in folk veterinary medicine in Italy as basis for a databank. *J*. *Ethnopharmacol*. *89*, 221-244.

Vitali, L.A., Beghelli, D., Biapa Nya, P.C., Bistoni, O. *et al*. (2016). Diverse biological effects of the essential oil from Iranian *Trachyspermum ammi*. *Arab*. *J*. *Chem*. *9*, 775–786.

Wink, M. (2008). Evolutionary advantage and molecular modes of action of multi-component mixtures used in phytomedicine. *Curr*. *Drug Metab*. *10*, 996–1009.

Yates, S.G., England, R.E. (1982). Isolation and analysis of carrot constituents: myristicin, falcarinol, and falcarindiol. *J*. *Agric*. *Food Chem*. *30*, 317–320.

CHAPTER 5.

A neglected vegetable, *Smyrnium olusatrum*, as potential weapon against a neglected tropical disease, African trypanosomiasis

"*A bad wound deserves*

a strong medicine."

Cameroon proverb

Chapter 5 Outline

Abbreviation

1D and 2D NMR = One and two-dimensional nuclear magnetic resonance

BALB//3T3 = Mouse fibroblasts

COSY = Correlation Spectroscopy

DEPT= Distortionless Enhancement by Polarisation Transfer

DHFR = Dihydrofolate reductase

DMSO = Dimethylsulfoxide

EOs = Essential oils

HAT = Human African Trypanosomiasis

HMBC = Heteronuclear Multiple-Bond Correlation

HMQC = Heteronuclear Multiple-Quantum Correlation

HSQC = Heteronuclear Single Quantum Correlation

MS = Mass spectra

NOE = Nuclear Overhauser Effect

NOESY = Nuclear Overhauser Effect Spectroscopy

RIs = retention indices

SAR: Structure-activity relationship

SI = Selectivity index

T. brucei = *Trypanosoma brucei*

TC221 = *T. brucei* bloodstream-form parasites

TLC = Thin layer chromatography

TOCSY = Total Correlation Spectroscopy

WHO = World Health Organization

Abstract

As part of the extended family of naturally-occurring products, sesquiterpenes hold promising inhibitory effects against the bloodstream forms of *Trypanosoma brucei* (*T. brucei*). *Smyrnium olusatrum*, also known as Alexanders or wild celery, is a neglected horticultural crop exploited as a vegetable and traditional remedy during the Roman age, then abandoned after the domestication of common celery (*Apium graveolens*). The plant is characterized by the presence of oxygenated sesquiterpenes containing a furan ring. For this reason, we decided to explore the potential of its essential oils (EOs) obtained from different organs and its main oxygenated sesquiterpenes, namely germacrone, isofuranodiene, and β-acetoxyfuranoeudesm-4(15)-ene, as potential inhibitors of *T. brucei*. The EOs obtained efficiently inhibited the growth of parasite with IC_{50} ranging from 1.9 to 4.0 μg/mL. Among the isolated main EOs constituents, isofuranodiene exhibited a significant and selective inhibitory activity against *T. brucei* (IC_{50} = 0.6 μg/mL, SI = 30), with β-acetoxyfuranoeudesm-4(15)-ene giving a moderate potentiating effect. These results, albeit preliminary, emphasise once again the role of a naturally-occurring compound, within this framework isofuranodiene, as a potential anti-protozoal agent to be included in combination treatments aimed not only at curing patients but also at preventing the diffusion of Human African Trypanosomiasis (HAT).

5.1 Introduction

From the discovery of artemisinin as the most promising therapeutic agent against malaria, research on natural products as useful weapons against various types of parasites has constantly grown (Benelli *et al*., 2016). Concerning protozoan infections, new therapeutic options come from EOs, which contain a plethora of components of different biogenetic origins (e.g. aliphatics, monoterpenes, phenylpropanoids, sesquiterpenes). In the last years, many studies on the antiprotozoal activity of EOs have been published (Monzote *et al*., 2012; Raut *et al*., 2014) and different components were proven to be effective against *Trypanosoma* species (Bero *et al*., 2013; Do Carmo *et al*., 2015). Among them, sesquiterpenes have proved promising inhibitory effects against bloodstream forms of *T*. *brucei* (Mikus *et al*., 2000; Wube *et al*., 2010).

Based on these results, we decided to explore the potential of sesquiterpene-rich essential oils as a source of trypanocidal agents and we directed our attention to *Smyrnium olusatrum* L. (Apiaceae), also known as Alexanders or wild celery, a biennial herb with historical uses as a culinary and medicinal plant during the Roman age. The plant has then been abandoned after the introduction of common celery (*Apium graveolens* L.) in the Middle Ages (Maggi *et al*., 2012).

Its generic name comes from the Greek word 'σμυρνα' that means myrrh, and is due to the particular aroma of the fruits that exude a pungent myrrh-like oil. The epithet of the species derives from the latin '*olus atrum'* that means black vegetable, alluding to the colour of the ripe fruits.

The plant is known under several names: in Italian as "Macerone", or "wild celery", in English as "Alexanders"; this name comes from the old city of Alexandria in Egypt, the site of origin of the plant, from which it has been brought to Europe. *S*. *olusatrum* is widespread in countries bordering the Mediterranean basin up to its northern limit in Great Britain where it is fully naturalized after its introduction during Roman age. In Italy it is present in almost all regions even if more frequent in those bordering the sea. From anecological point of view, the plant grows in shady, uncultivated places, on deep substrate rich in nitrogenous components, sea and lake cliffs and quarries, from the sea level to 800 m of altitude. In inland sites it is usually associated with old dwellings or ruins, churches or castles, where it is probably a relic of kitchen gardens.

S. *olusatrum* is a stout, glabrous, celery-scented biennial herb, up to 150 cm tall, flowering once before dying. The plant possesses an aromatic tuberous tap-root, 50-60 cm in length, with finer lateral roots developing in the first year. The stem is stout, solid, becoming hollow when old. The dark green and shiny leaves present fleshy petioles; lamina is ternate, with rhombic-ovate segments and crenate-dentate margins. Flowers are carried in yellowish-green umbrellas with 7 to 15 rays opening between March and April (Figure 1, left panel). The fruits are schizocarps of 7-8 mm

appearing in May, green at first, black at ripening, with evident costae on epicarp (Figure 1, right panel). The plant possesses an aromatic thickened tap-root, 50-60 cm in length, with finer lateral roots (Figure 2). During reproduction time roots begin to rot and cauline leaves die.

The plant was extensively cultivated in antiquity (the plant has been also mentioned by Pliny the Elder), and was also used as a medicinal remedy. Roots were used as antiscorbutic, the juice from the root for its aromatic, appetite stimulant, diuretic and laxative properties, the fruit as stomachic and antiasthmatic, the stems as depurative.

Fig. 1. Left panel: *S. olusatrum* at flowering. Right panel : Black schizocarps of S. *olusatrum*.

Fig. 2. Taproot slides from collected plants of *S. olusatrum*.

The phytochemistry of *S*. *olusatrum* EOs has been extensively investigated (Quassinti *et al*. 2013; Maggi *et al*. 2015) and revealed furan ring-containing sesquiterpenes as the main constituents. Among them, isofuranodiene was the most abundant in the various plant parts and its abundance might be related to the function as a precursor of sesquiterpene lactones (Figure 3) (Kawabata *et al*., 1985). Isofuranodiene occurs in both terrestrial plants and marine benthic invertebrates, and seems to act via smell (distance sense) on land and via taste (contact sense) in the sea (Mollo *et al*., 2014). Different publications showed that isofuranodiene is a hepatoprotective (Li *et al*., 2016), apoptotic (Quassinti *et al*. 2013) and neuritogenic agent (Mustafa *et al*. 2016). However, no information is available about its effects on protozoal organisms.

For this reason, we investigated the *in vitro* antitrypanosomal activities of EOs obtained from different parts of *S*. *olusatrum* and their main components, namely isofuranodiene, germacrone, glechomafuran and β-acetoxyfuranoeudesm-4(15)-ene (Figure 3), against *T*. *brucei*.

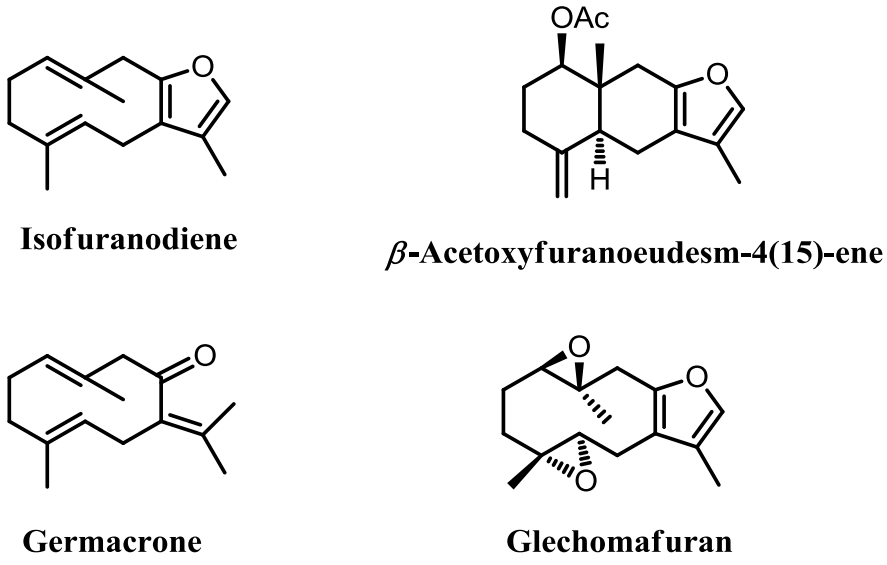

Isofuranodiene

β-Acetoxyfuranoeudesm-4(15)-ene

Germacrone

Glechomafuran

Fig. 3. Compounds isolated from *S*. *olusatrum* EOs and assayed for trypanocidal activity.

5.2 Results and discussion

5.2.1 Essential oil compositions

The roots, leaves, flowers and fruits of *S*. *olusatrum* contained different amounts of EO calculated on a dry weight basis. The richest part was given by flowers (2.0%), followed by roots (0.6%), leaves (0.3%) and fruits (0.1%). In the case of flowers, the high oil yield value might support its use on an industrial level.

GC-MS analysis was performed to identify the components of the four essential oils distilled (Table 1). The highest number of volatile components was identified in the EO extracted from fruits (66 components), followed by flowers (47 components), roots (45 components) and leaves (43 components).

From a phytochemical standpoint all EO compositions were dominated by oxygenated sesquiterpenes (68.2-74.5%), with minor contributions of monoterpene hydrocarbons (13.2-22.2%) and sesquiterpene hydrocarbons (3.1-14.1%). Among the former, the furan ring-containing sesquiterpenes constituted the major fraction in all EOs. The EOs obtained from different organs were characterized by different chemical profiles as determined by GC-MS. Curzerene (39.7%), furanoeremophil-1-one (24.4%), β-phellandrene (14.4%) and isofuranodiene (5.8%) were the main volatile components in roots; furanoeremophil-1-one (30.0%), curzerene (24.1%), germacrone (9.7%), β-pinene (9.5%) and isofuranodiene (4.8%) in leaves; curzerene (30.5%), myrcene (18.2%), furanoeremophil-1-one (12.1%), germacrone (10.4%) and isofuranodiene (9.8%) in flowers; β-acetoxyfuranoeudesm-4(15)-ene (31.2%), curzerene (23.8%), isofuranodiene (6.6%), β-phellandrene (6.2%) and α-pinene (5.4%) in fruits. These results are consistent with those of our previous investigation (Maggi *et al*., 2015).

It is important to point out that isofuranodiene and germacrone, that are particularly abundant in flowers, are thermosensitive compounds undergoing chemical rearrangement (Cope rearrangement) during the conventional gas chromatographic run giving rise to curzerene and *trans*-β-elemenone, respectively (Maggi *et al*., 2015). On this basis, isofuranodiene can be considered the main volatile component of the plant, and curzerene and *trans*-β-elemenone are believed to be artifacts derived from the thermal degradation of isofuranodiene and germacrone into the GC system, respectively (Maggi *et al*., 2012).

Therefore, its GC quantification is problematic and only the sum of curzerene + isofuranodiene can be considered as reliable for comparative purposes. For this reason, the total amount of isofuranodiene (*i.e*. isofuranodiene + curzerene) can then be approximately considered to

be ~45 % in the root, ~29% in the leaves, ~40 % in the flowers and ~30% in the fruits. The ^{1}H-NMR spectrum of pure crystals of isofuranodiene is showed in Figure 4 and its purification procedure and chemical characterization is widely reported in materials and methods section.

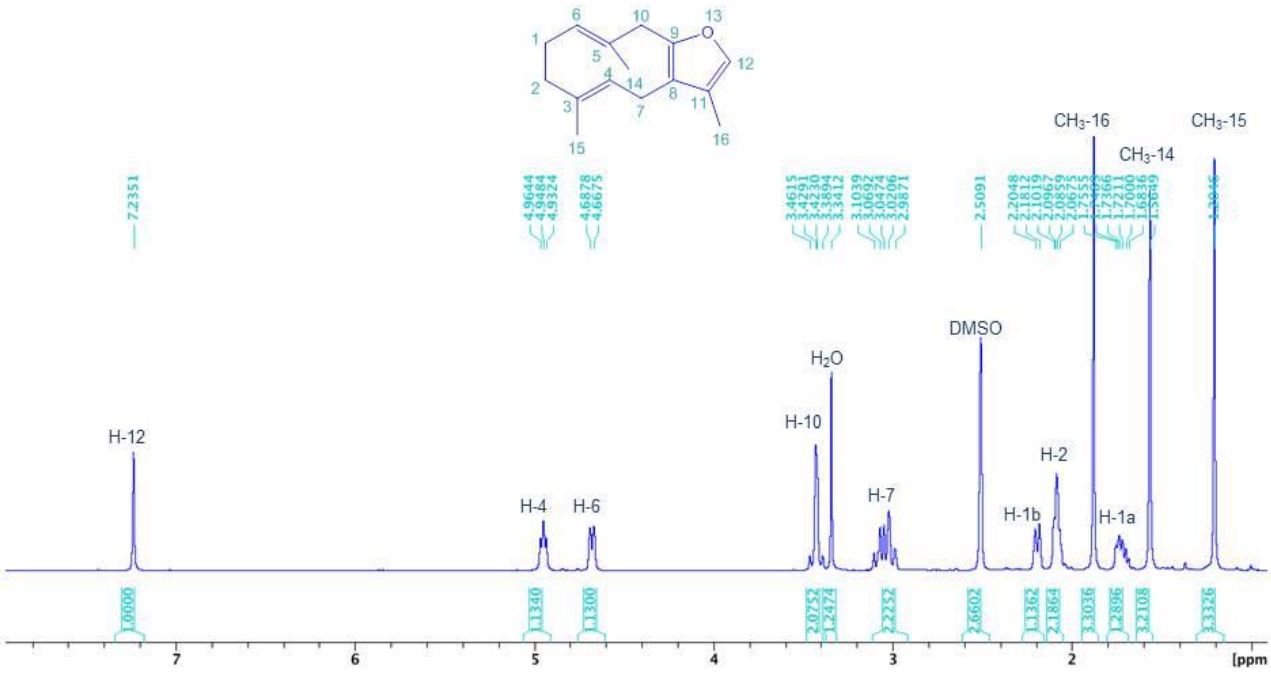

Fig. 4. ^{1}H NMR spectrum of pure crystals of isofuranodiene.

Table 2. Chemical composition of the EOs distilled from different parts of S. olusatrum.

N.	Component[a]	RI exp.[b]	RI lit.[c]	sample (%)[d]				ID
				Roots	*Leaves*	*Flowers*	*Fruits*	
1	α-thujene	921	924	0.1	0.4	tr	0.1	RI,MS
2	α-pinene	921	932	0.6	0.1	1.2	5.4	Std
3	camphene	939	946				tr	Std
4	thuja-2,4(10)-diene	945	953				tr	RI,MS
5	sabinene	965	969	0.1	0.2	tr	0.1	RI,MS
6	β-pinene	967	974	0.2	9.5	0.7	2.6	Std
7	myrcene	981	988	0.6	0.1	18.2	3.6	Std
8	α-phellandrene	996	1002	0.7	0.9	0.1	0.1	Std
9	δ-3-carene	1008	1008	3.2	0.3		0.4	Std
10	α-terpinene	1014	1014	0.1	tr			RI,MS
11	*p*-cymene	1018	1020	0.3	0.6	0.1	0.3	Std
12	sylvestrene	1019	1025		0.7			RI,MS
13	limonene	1020	1024			1.4	tr	Std
14	β-phellandrene	1025	1025	14.4			6.2	RI,MS
15	(*Z*)-β-ocimene	1032	1032		tr			RI,MS
16	(*E*)-β-ocimene	1041	1044	0.1	0.3	0.4		RI,MS
17	ɣ-terpinene	1049	1054		0.1	0.2	tr	Std
18	*n*-octanol	1070	1063			tr		RI,MS
19	terpinolene	1078	1086	0.6	0.0		tr	Std
20	*p*-cymenene	1081	1089				tr	RI,MS
21	*p*-mentha-2,4(8)-diene	1086	1085	tr				RI,MS
22	linalool	1099	1095		tr		0.2	Std
23	*n*-nonanal	1105	1100				0.1	RI,MS
24	1-octen-3-yl acetate	1115	1110				tr	RI,MS
25	*cis*-*p*-menth-2-en-1-ol	1121	1121	tr			tr	RI,MS
26	α-campholenal	1123	1122				tr	RI,MS
27	*trans*-pinocarveol	1133	1135				tr	Std
28	*trans*-verbenol	1141	1140				tr	RI,MS
29	pinocarvone	1158	1160				tr	RI,MS

30	terpinen-4-ol	1173	1174				0.1	Std
31	*p*-cymen-8-ol	1178	1179				0.1	RI,MS
32	cryptone	1186	1185	tr			0.1	RI,MS
33	α-terpineol	1188	1186				0.2	Std
34	methyl salicylate	1191	1190				tr	RI,MS
35	myrtenal	1191	1195				tr	Std
36	verbenone	1205	1204				tr	Std
37	octanol acetate	1212	1211			tr		RI,MS
38	coahuilensol,methyl ether	1224	1219				tr	RI,MS
39	citronellol	1224	1223	tr			tr	Std
40	cumin aldehyde	1236	1238				tr	RI,MS
41	2-phenyl ethyl acetate	1256	1254				0.1	RI,MS
42	*cis*-chrysanthenyl acetate	1262	1265	0.4				RI,MS
43	α-terpinen-7-al	1278	1283				tr	RI,MS
44	isobornyl acetate	1284	1285	tr			tr	Std
45	δ-elemene	1329	1335	tr	0.1	tr	tr	RI,MS
46	citronellyl acetate	1355	1350	tr	0.1	tr	0.1	Std
47	neryl acetate	1366	1359				tr	Std
48	β-elemene	1379	1389	0.9	2.1	1.2	1.3	RI,MS
49	β-bourbonene	1369	1387		0.1		tr	RI,MS
50	β-ionol	1408	1412			tr		RI,MS
51	(*E*)-caryophyllene	1411	1417	0.1	0.8	tr	tr	Std
52	β-copaene	1423	1430		0.1			RI,MS
53	ɣ-elemene	1428	1434	0.6	1.3	0.8	0.3	RI,MS
54	dihydro-β-ionone	1430	1434			tr	0.1	RI,MS
55	α-humulene	1449	1452	tr	0.2	0.1	tr	Std
56	γ-muurolene	1470	1478				tr	RI,MS
57	germacrene D	1475	1484	0.4	3.6	1.8	1.0	RI,MS
58	(*E*)-β-ionone	1477	1487			0.1		Std
59	β-selinene	1480	1489		0.0	tr		RI,MS
60	α-selinene	1489	1498		0.0	tr		RI,MS
61	bicyclogermacrene	1490	1500		0.1	tr		RI,MS

62	curzerene	1495	1499	39.7	24.1	30.5	23.8	Std
63	α-amorphene	1495	1500				0.2	RI,MS
64	β-bisabolene	1500	1505	tr	0.9	0.2		RI,MS
65	γ-cadinene	1506	1513				0.1	RI,MS
66	myristicin	1516	1517	tr				RI,MS
67	*trans*-calamenene	1516	1521				tr	RI,MS
68	δ-cadinene	1518	1522	0.1	0.2	0.1	0.2	RI,MS
69	hedycariol	1543	1546				0.1	RI,MS
70	germacrene B	1550	1559	0.9	2.7	1.9	0.9	RI,MS
71	elemicin	1556	1555	tr			tr	RI,MS
72	germacrene D-4-ol	1568	1574		0.2	tr	0.1	RI,MS
73	caryophylleneoxide	1577	1582		tr			Std
74	*cis*-β-elemenone	1587	1589	tr	0.1	0.2		RI,MS
75	*trans*-β-elemenone	1598	1601	0.7	2.0	2.5	0.1	RI,MS
76	*epi*-α-muurolol	1630	1640			0.1	0.3	RI,MS
77	α-cadinol	1638	1652	0.4	0.4	0.3	1.0	RI,MS
78	atractylone	1650	1657	0.2	0.1	0.1	0.3	Std
79	isofuranodiene	1681	1688	5.8	4.8	9.8	6.6	Std
80	germacrone	1683	1693	2.2	9.7	10.4	0.4	Std
81	furano-4(15)-eudesmen-1-one	1827	1833			1.3	1.8	RI,MS
82	2-pentadecanone,6,10,14-trimethyl-	1845	1845				0.1	RI,MS
83	furanoeremophil-1-one	1872	1879	24.4	30.0	12.1	1.0	Std
84	glechomafuran	1916	1925	0.3	0.2	tr	2.2	Std
85	1β-acetoxyfurano-4(15)-eudesmene	1984	1988	0.2		0.7	31.2	Std
86	1β-acetoxyfurano-3-eudesmene	1990	1998	0.7	tr	0.1	1.0	RI,MS
87	*n*-heneicosane	2100	2100			0.6		Std
88	*n*-docosane	2200	2200			0.1		Std
89	*n*-tricosane	2300	2300			1.1		Std
90	*n*-tetracosane	2400	2400			tr		Std
91	*n*-pentacosane	2500	2500			tr		Std
	Total identified (%)			99.3	97.0	98.5	94.6	
	Oil yield (%)			0.6	0.3	2.0	0.1	

Grouped compounds (%)				
Monoterpenehydrocarbons	21.3	13.2	22.2	18.8
Oxygenated monoterpenes	0.4	tr	0.1	1.1
Sesquiterpene hydrocarbons	3.1	14.1	6.1	4.3
Oxygenated sesquitepenes	74.5	71.6	68.2	70.2
Others	tr		1.9	0.3

[a] Compounds are listed in order of their elution from a HP-5MS column. [b] Linear retention index on HP-5MS column, experimentally determined using homologous series of C_8-C_{30} alkanes. [c] Linear retention index taken from Adams (2007) and/or NIST 08 (2008). [d] Relative percentage values are means of three determinations with a RSD% in all cases below 10%. [e] Identification methods: std, based on comparison with authentic compounds; NMR, based on spectroscopic data; MS, based on comparison with WILEY, ADAMS, FFNSC2 and NIST 08 MS databases; RI, based on comparison of calculated RI with those reported in ADAMS, FFNSC 2 and NIST 08. [f] Tr, % below 0.1%.

5.2.2. Antitrypanosomal activity

All the EOs obtained from different parts of *S*. *olusatrum* plant effectively inhibited *T*. *brucei* proliferation, especially the fruit EO with an IC_{50} value of 1.97 µg/mL (Table 2). The EOs resulted selective against *T*. *brucei* and much less active against the mammalian cells tested indicating that it is specifically targeting the parasites. We also tested some of the major compounds isolated from the *S*. *olusatrum* EOs and their chemical structures are reported in Figure 2. Isofuranodiene emerged as the most potent one with an IC_{50} value of 3.0 µM (0.65 µg/mL), whereas β-acetoxyfuranoeudesm-4(15)-ene was much less active and germacrone and glechomafuran had no effects (Table 2, Figure 5).

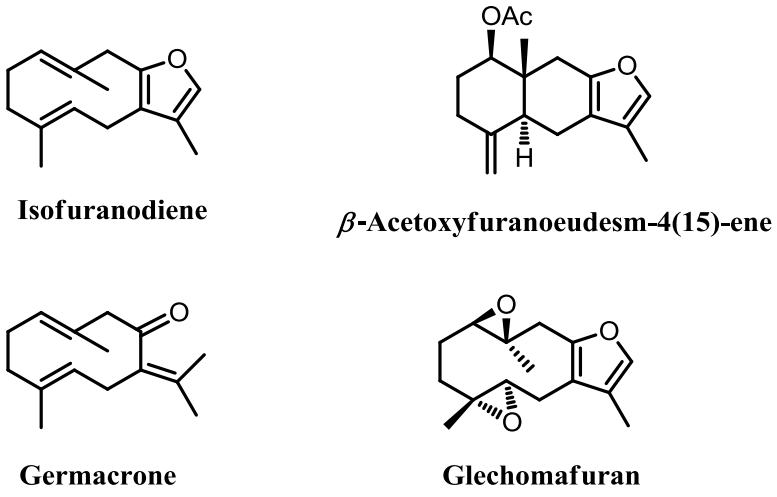

Fig. 5. Chemical structures of compounds isolated from *S*. *olusatrum* EOs and assayed for trypanocidal activity.

The IC_{50} value in µg/mL with pure isofuranodiene was within the range of the values obtained if the IC_{50} values of the different EOs were multiplied by their original fraction of isofuranodiene, including its thermal degradation product curzerene. These values varied between 0.6-1.8 µg/mL in the different EOs. The good correlation between these values and the IC_{50} value of isofuranodiene indicates that the inhibition activity of the EOs mainly comes from isofuranodiene. To better explain the higher antitrypanosomal activity of the fruits as compared to the other EOs, we tested if β-acetoxyfuranoeudesm-4(15)-ene could affect the potency of isofuranodiene. This compound is present in large amounts in the fruits (31.2%) but was poor in the other plant tissues (0.7%).

In accordance with our hypothesis, the sensitivity to isofuranodiene increased slightly in the presence of β-acetoxyfuranoeudesm-4(15)-ene and this increase was stronger than expected from just the additive effect of the two single compounds (Table 3). When used at a ratio of 1:1 (similar to the ratio in fruits), the IC_{50} of isofuranodiene had decreased to two-thirds of the value when it is used alone (2.09 *vs* 3.0 μM), which corresponds very well to the difference between the fruits and the other tissues. The concentration of β-acetoxyfuranoeudesm-4(15)-ene at this point (2.07 μM) is very far from its own IC_{50} value (26 μM), indicating a modest synergism between the two compounds rather than just an additive effect.

This work represents the first report on the antiprotozoal activity of *S*. *olusatrum*, a neglected horticultural crop and our results highlighted that isofuranodiene possesses a significant and selective inhibitory activity (SI = 30) against *T*. *brucei*. The IC_{50} value obtained for isofuranodiene against *T*. *brucei* allowed to classify its antiprotozoal activity as very good, according to the WHO guidelines

Being highly hydrophobic, this compound may be easily absorbed by cell membrane, thus causing destabilization of the phospholipid bilayer (Raut *et al*., 2014). Also its capability to alter the permeability of outer and inner mitochondrial membranes of eukaryotic cells leading to apoptotic effects may be taken into consideration (Quassinti *et al*., 2014). Its significantly higher activity with respect to germacrone can be ascribable to the furan ring that further increases the hydrophobicity of the molecule. This was also confirmed by the inhibitory activity showed by β-acetoxyfuranoeudesm-4(15)-ene. In addition, the electron delocalization of the furan moiety makes it reactive towards functional groups of biological molecules. Also its capability to inhibit enzymes involved in the protozoal metabolism can be taken into account. For instance, isofuranodiene was found as an important inhibitor of DHFR (DiHydroFolate Reductase), and a precursor of cofactors required for the biosynthesis of purines, pyrimidines, and several amino acids. Its inhibition results in a depletion of the reduced folate pools, DNA synthesis, and arrest of cell proliferation that ended up with cell death (Maggi *et al*., 2017).

Table 2. Inhibition constants of *T.b*. *brucei* TC221 and mouse Balb/3T3 cell proliferation post-treatment with *S*. *olusatrum* EOs and its main components.

Treatment	IC_{50}[a]		Selectivity Index (SI)
	***T. b. brucei* (TC221)**	**Balb3T3**	
***Smyrnium olusatrum* EOs**	**μg/mL**	**μg/mL**	
Flowers	3.0 ± 0.4	68 ± 8	23
Fruits	1.97 ± 0.06	58 ± 12	29
Leaves	3.7 ± 0.5	>100	>27
Roots	4.0 ± 0.5	>100	>25
Pure compounds	**μg/mL (μM)**	**μg/mL (μM)**	
Isofuranodiene	0.64 ± 0.01 (3)	19.45 ± 1.2 (91)	30
Germacrone	>100	-	-
Glechomafuran	>100	-	-
β-Acetoxyfuranoeudesm-4(15)-ene	7.12 ± 1.1 (26)	>100	>14

Table 3. IC_{50} values showing the Inhibition of *T.b*. *brucei* TC221 proliferation induced by isofuranodiene in the presence of different ratio of β-acetoxyfuranoeudesm-4(15)-ene. The IC_{50} of β-acetoxyfuranoeudesm-4(15)-ene in this set of experiments was 30 ± 4 μM.

Treatment	IC_{50}[a]
	***T. b. brucei* (TC221)**
Ratio isofuranodiene : β-acetoxyfuranoeudesm-4(15)-ene	**μM**
1: 0	3.0 ± 0.7
1 : 0.5	2.31 ± 0.07
1 : 1	2.09 ± 0.04
1 : 2	1.85 ± 0.14

[a]Each IC_{50} value represents the average of three independent experiments with standard errors.

5.3 Conclusions

In conclusion, our results showed that neglected local plants are a treasure to preserve either for biodiversity conservation or as source of lead compounds to fulfill the drug development pipeline, and in this context isofuranodiene represents an intriguing trypanocidal drug candidate. Hopefully, once its activity will be confirmed, pure isofuranodiene or simplified synthetic analogues, could fulfill the need for antitrypanosomal agents to be included in combination treatments aimed not only at curing patients but also at preventing the diffusion of this disease. Unfortunately, as many furans, isofuranodiene is quite prone to oxidation giving rise to five-membered lactones and it can also undergo photooxygenation after exposure to UV-light. In addition, when exposed to high temperatures, it undergoes the so-called 'Cope rearrangement' consisting in a [3,3] sigmatropic rearrangement giving rise to the artifact product curzerene, which is endowed with lower biological power. Last but not least, its very low water solubility (about 0.1 ppm) (US EPA 2012) limits significantly its potential application in aqueous solution. On this basis, it is of fundamental importance to develop proper formulations able to retain the trypanocidal power of the compound and, at the same time, to improve its stability and water solubility. In this respect, future researches are heading to develop isofuranodiene-containing microemulsions that represent an interesting approach for the development of effective, eco-friendly and botanical trypanocidal drugs.

5.4 Materials and methods

5.4.1 Plant material

Roots (3000 g), leaves (2900 g), flowers (700 g) and fruits (750 g) of *S*. *olusatrum* were collected in different localities of central Italy as follows: roots were collected in Serra San Quirico (N43°26'41"; E13°01'07", 280 m a.s.l.) in October 2017; leaves in Pierosara (Genga, N43°24'34"; E12°58'14", 360 m a.s.l.) in October 2017; flowers in Isola Maggiore (Lake Trasimeno, Perugia, Italy, N 43°10'41"; E 12°05'25", 250 m a.s.l.) in April 2017; fruits in Assisi (N43°04'33"; E12°36'06", 260 m s.l.m.) in July 2017. The herbarium specimens were authenticated by Prof. Filippo Maggi and deposited in the Herbarium Universitatis Camerinensis (CAME, included in the online edition of Index Herbariorum c/o School of Bioscience and Veterinary Medicine, University of Camerino, Camerino, Italy) under the voucher codes CAME 25871, CAME 25872, CAME 25875 and CAME 25876; they are also available in the "an Archive" system for botanical data (http://www.anArchive.it).

5.4.2 Hydrodistillation

Plant materials were hydrodistilled just after their collection in a Clevenger-type apparatus until no more EO was obtained. The oil yields (%, w/w) were expressed on a dry weight basis, by calculating the water content of material examined before each distillation. The yield values obtained were 0.6 (roots), 0.3 (leaves), 2.0 (flowers) and 0.1% (fruits).

5.4.3 Chemicals

For identification of volatiles the following analytical standards purchased from Sigma-Aldrich (Milan, Italy) were used: α-pinene, camphene, β-pinene, myrcene, α-phellandrene, δ-3-carene, *p*-cymene, limonene, γ-terpinene, terpinolene, linalool, *trans*-pinocarveol, terpinen-4-ol, α-terpineol, myrtenal, verbenone, citronellol, isobornyl acetate, citronellyl acetate, neryl acetate, (*E*)-caryophyllene, α-humulene, (*E*)-β-ionone, caryophyllene oxide, *n*-heneicosane, *n*-docosane, *n*-tricosane, *n*-tetracosane, *n*-pentacosane. Atractylone was obtained from isofuranodiene by rearrangement in acidic conditions (Gavagnin *et al*., 2003). Curzerene was prepared from isofuranodiene by reflux with ethylene glycole (Baldovini *et al*., 2001). Its structure was confirmed

by comparison of ^{1}H and ^{13}C-NMR data with those reported in the literature (Weyerstahl *et al*., 1988).

5.4.4 Isolation and identification of the main furanosesquiterpenoids

Roots EO from San Giusto (4 g) was kept for 1 month in the refrigerator at -20°C. During this period, colourless crystals precipitated from the oil. Then, the oil was filtered and the crude compound was recrystallized four times with methanol at -20°C. Finally, the crystals were separated from the solvent to give 853 mg of the pure compound 79 (Table 1) (98.9% as determined by HPLC, yield 21.0%), which was identified as isofuranodiene by comparison of NMR data with those reported in the literature (Dekebo *et al*., 2002). NMR spectra were performed on a Varian Mercury plus 400 Spectrometer, using $CDCl_3$ as solvent and the solvent signals as internal references. No traces of curzerene were detected in this sample by ^{1}H and ^{13}C-NMR. The HPLC-MS analysis of the isolated molecule gave a peak with retention time of 24 min showing a signal at m/z 217.2 that corresponds to the [M + H]+ ion of isofuranodiene. Because of thermal rearrangement, when injected to GC–MS using the above experimental conditions, the pure compound gave 82.2% of curzerene and 17.0% of isofuranodiene. According to previously published procedures (Quassinti *et al*., 2014; Maggi *et al*., 2015; Maggi *et al*. 2017), suitable single crystals of isofuranodiene (IFD, $C_{15}H_{20}O$, crystals, purity 99% by HPLC) have been obtained from the EO of inflorescences due to their highest yield in this furanosesquiterpene. Briefly, 20 mL of essential oil were diluted in 200 mL of hexane and stored at low temperature (− 20°C) for a prolonged period (1 week). Then, the crystals obtained were recrystallized two times with methanol and the structure was identified as isofuranodiene by comparison of NMR data with those reported in the literature and the standard compound available in our laboratory (Maggi *et al*. 2017). ^{1}H NMR and ^{13}C NMR spectra were recorded on 500 MHz NMR spectrometer (Bruker Avance III 500 MHz) (Figure 1). The chemical shift values are expressed in δ values (ppm), and coupling constants (J) are in hertz; tetramethylsilane (TMS) was used as an internal standard. Proton chemical data are reported as follows: chemical shift, multiplicity (s = singlet, d = doublet, dd = doublet of doublets, t = triplet, dt = doublet of triplets, q = quartet, m = multiplet, brs = broad singlet) coupling constant (s), integration. No traces of curzerene were detected in this sample by ^{1}H and ^{13}C-NMR. ^{1}H NMR (DMSO-d_6): δ 1.23 (s, 3H, CH_3), 1.65 (s, 3H, CH_3), 1.72-1.85 (m, 1H, H-1a), 1.89 (s, 3H, CH_3), 2.08 (dt, J = 2.6, 8.1 Hz, 2H, H-2), 2.25 (d, J = 11.8 Hz, 1H, H-1b), 2.97-3.11 (m, 2H, H-7), 3.42 (q, J = 16.8 Hz, 2H, H-10), 4.67(d, J = 10.1 Hz, 1H, H-6), 4.95(t, J = 8.1 Hz, 1H, H-4), 7.23 (s, 1H, H-

12). ^{13}C NMR (DMSO-d_6): 8.9 (C-16), 16.2 (C-14), 16.5 (C-15), 24.3 (C-7), 27.3 (C-10), 39.5 (C-1), 40.9 (C-2), 119.1 (C-8), 121.7 (C-3), 121.9 (C-11), 127.8 (C-4), 128.9 (C-6), 134.5 (C-5), 136.1 (C-12), 149.9 (C-9). MS (API-ESI): *m/z* 217.15 $[M+H]^+$. Anal. calcd. for ($C_{18}H_{20}O$) C, 83.28; H, 9.32; Found: C, 83.26; H, 9.33.

Other main volatile components of the inflorescences oil (1 g) were isolated by flash chromatography on a Silica gel 60F Baker column (40 mm diameter) with gradient elution: cyclohexane 100% (400 ml), cyclohexane–ethyl acetate 95:5 (200 ml), 90:10 (200 ml) and 85:15 (400 ml). Forty fractions (30 ml each) were collected and pooled on the basis of their chromatographic behaviour (monitored by TLC and GC–FID) in five different groups. Group 1 (fractions 6–8, 41 mg) contained monoterpenes and sesquiterpenes previously identified. Group 2 (fractions 9–17, 396 mg) yielded a mixture of curzerene and isofuranodiene. Group 3 (fractions 19–23, 248 mg) yielded 1β-acetoxyfuranoeudesm-4(15)-ene (80% purity). Group 4 (fractions 26–32, 13 mg) contained small amounts of several unknown furanosesquiterpenes. Group 5 (fractions 33–39, pale yellow liquid, 109 mg) yielded glechomafuran (60% purity). Thereafter, from group 3, a further purification was achieved by flash chromatography using cyclohexane 100% (200 ml), cyclohexane–ethyl acetate 97.5:2.5 (200 ml), 95:5 (200 ml), 90:10 (400 ml) as eluents. Fractions 19–20 were collected and pooled, yielding 1β-acetoxyfuranoeudesm-4(15)-ene (52 mg, colourless liquid, 97% purity). Group 5 (fractions 33–39) was dissolved in petroleum ether (boiling point 40–60 C) and kept for 48 h in the refrigerator at -20 °C, giving glechomafuran (17 mg, white crystals, 98% purity). The structures of the compounds glechomafuran and 1β-acetoxyfuranoeudesm-4(15)-ene were confirmed by ^{1}H-NMR and ^{13}C-NMR spectra, which were in agreement with those reported in literature (Mölleken *et al*., 1998).

5.4.5 GC-MS analysis

The analytical conditions and instruments used for the separation of *S*. *olusatrum* EO components were the same of those reported in Chapter 2 paragraph 2.6.8. The identification was made by comparison with authentic standards available in the authors' laboratory and the correspondence of retention indices (RIs) and mass spectra (MS) with respect to those reported in commercial databases (Adams, 2007; NIST 08, 2008; FFNSC2, 2012) and home-made libraries was used to confirm the peak assignment. Semi-quantification of EO components was made by peak area normalization considering the same detector response for all volatile components. Percentage values were the average of three independent experiments.

5.4.6 Cell culture

T. *brucei* TC221 bloodstream forms and mouse Balb/3T3 fibroblasts (ATCC no CCL-163) were grown at 37°C with 5% CO_2. For *T*. *brucei*, the growth medium was HMI-9 (Hirumi *et al*., 1989) supplemented with 10% (v/v) fetal bovine serum (Gibco)- The Balb/3T3 cells were cultured in Dulbecco´s Modified Eagle´s Medium supplemented with 10% (v/v) heat-inactivated fetal bovine serum, glutamine (0.584 g/l) and 10 ml/L 100× penicillin-streptomycin (Gibco).

5.4.7 Growth inhibition assay

The cultures of *T*. *brucei* TC221 BSFs and mouse Balb/3T3 fibroblasts (ATCC No CCL-163) as well as the EC_{50} determinations, were performed in a similar way as reported previously in Chapeter 2 paragraph 2.6.9, with an adjustment of the seeding density for the mammalian cells.
EOs or purified compounds were dissolved in dimethyl sulfoxide (DMSO) and serially diluted with growth medium in 96-well microtiter plates. An equal volume of *T*. *brucei* or mammalian cell culture was added to each well (20,000 cells and totally 200 µl in each well) and the plates were incubated for 48 h in the CO_2 incubator. IC_{50} values were calculated on log inhibitor *vs*. response curves by non-linear regression using the GraphPad prism 7.03 software.

References

Adams, R., 2007. Identification of Essential Oil Components by Gas Chromatography/Mass Spectrometry, fourth ed. Allured Publishing Corp., Carol Stream, IL, USA.

Baldovini, N., Tomi, F., Casanova, J. (2001). Identification and quantitative determination of furanodiene, a heat-sensitive compound, in essential oil by ^{13}C-NMR. *Phytochem. Anal. 12,* 58-63.

Benelli, G., Mehlhorn, H. (2016). Declining malaria, rising dengue and Zika virus: insights for mosquito vector control. *Parasitol. Res. 115,* 1747–1754.

Bero, J., Beaufay, C., Hannaert, V., Hérent, M.-F.*et al*. (2013). Antitrypanosomal compounds from the essential oil and extracts of *Keetia leucantha* leaves with inhibitor activity on *Trypanosoma brucei* glyceraldehyde-3-phosphate dehydrogenase. *Phytomedicine 20,* 270-274.

Dekebo, A., Dagne, E., Sterner, O. (2002). Furanosesquiterpenes from *Commiphora sphaerocarpa* and related adulterants of true myrrh. *Fitoterapia 73,* 48-55.

Do Carmo, G.M., Baldissera, M.D., Vaucher, R.A., Rech, V.C. *et al*. (2015). Effect of the treatment with *Achyrocline satureioides* (free and nanocapsules essential oil) and diminazene aceturate on hematological and biochemical parameters in rats infected by *Trypanosoma evansi*. *Exp. Parasitol. 149,* 39-46.

FFNSC 2, 2012. Flavors and fragrances of natural and synthetic compounds. Mass spectral database. Shimadzu Corps, Kyoto.

Gavagnin, M., Mollo, E., Castelluccio, F., Crispino, A. *et al*. (2003). Sesquiterpene Metabolites of the Antarctic Gorgonian *Dasystenella acanthine*. *J. Nat. Prod. 66,* 1517-1519.

Hirumi, H., Hirumi, K (1989). Continuous cultivation of *Trypanosoma brucei* blood stream forms in a medium containing a low concentration of serum protein without feeder cell layers. *J. Parasitol. 75,* 985-989.

Kawabata, J., Fukushi, Y., Tahara, S., Mizutani, J. *et al*. (1985). Isolation and structural elucidation of four sesquiterpenes from *Chloranthus japonicus* (Chloranthaceae). *Agric. Biol. Chem. 49,* 1479-1486.

Li, W., Shi, J., Papa, F., Maggi, F. *et al*. (2016). Isofuranodiene, the main volatile constituent of wild celery (*Smyrnium olusatrum* L.), protects d-galactosamin/lipopolysacchride-induced liver injury in rats. *Nat. Prod. Res. 30,* 1162-1165.

Maggi, F., Barboni, L., Papa, F., Caprioli, G. *et al*. (2012). A forgotten vegetable (*Smyrnium olusatrum* L., Apiaceae) as a rich source of isofuranodiene. *Food Chem. 135,* 2852-2862.

Maggi, F., Papa, F., Giuliani, C., Maleci Bini, L. *et al*. (2015). Essential oil chemotypification and secretory structures of the neglected vegetable *Smyrnium olusatrum* L. (Apiaceae) growing in central Italy. *Flavour Fragr. J. 30,* 139-159.

Maggi, F., Papa, F., Pucciarelli, S., Bramucci, M. *et al*. (2017). Stabilization of the cyclodecadiene derivative isofuranodiene by silver (I) coordination. Mechanistic and biological aspects. *Fitoterapia 117*, 52-60.
Mikus, J., Harkenthal, M., Steverding, D., Reichling, J. *et al*. (2000). *In vitro* effect of essential oils and isolated mono- and sesquiterpenes on *Leishmania* major and *Trypanosoma brucei*. *Planta Med*. *66*, 366-368.

Mölleken, U., Sinnwell, V., Kubeczka, K.-H. (1998). Essential oil composition of *Smyrnium olusatrum*. *Phytochemistry 49*, 1709-1714.

Mollo, E., Fontana, A., Roussis, V., Polese, G. *et al*. (2014). Sensing marine biomolecules: smell, taste, and the evolutionary transition from aquatic to terrestrial life. *Front Chem*. *2*, 1-6.

Monzote, L., Alarcón, O., Setzer, W.N. (2012). Antiprotozoal Activity of Essential Oils. *Agriculturae Conspectus Scientificus 77*, 167-175.

Mustafa, A.M., Maggi, F., Papa, F., Kaya, E. *et al*. (2016). Isofuranodiene: A Neuritogenic compound isolated from wild celery (*Smyrnium olusatrum* L., Apiaceae). *Food Chem*. *192*, 782-787.

NIST 08, 2008. Mass spectral library (NIST/EPA/NIH). National Institute of Standards and Technology, Gaithersburg, USA.

Quassinti, L., Bramucci, M., Lupidi, G., Barboni, L., Ricciutelli, M. *et al*. (2013). *In vitro* biological activity of essential oils and isolated furanosesquiterpenes from the neglected vegetable *Smyrnium olusatrum* L. (Apiaceae). *Food Chem*. *138*, 808-813.

Quassinti, L., Maggi, F., Barboni, L., Ricciutelli, M. *et al*. (2014). Wild celery (*Smyrnium olusatrum* L.) oil and isofuranodiene induce apoptosis in human colon carcinoma cells. *Fitoterapia 97*, 133-141.

Raut, J.S., Karuppayil, S.M. (2014). A status review on the medicinal properties of essential oils. *Ind*. *Crops Prod*. *62*, 250-264.

Ulubelen, A., Öksüz, S. (1983). Relative configuration of glechomafuran isolated from the fruits of *Smyrnium olusatrum*. *J*. *Nat*. *Prod*. *46*, 490-492.

Weyerstahl, P., Marschall-Weyerstahl, H., Christiansen, C., Oguntimein, B.O. *et al*. (1988). Volatile constituents of *Eugenia uniflora* leaf oil. *Planta Med*. *54*, 546-549.

Wube, A.A., Bucar, F., Gibbons, S., Asres, K. *et al*. (2010). Antiprotozoal activity of drimane and coloratane sesquiterpenes towards *Trypanosoma brucei rhodesiense* and *Plasmodium falciparum in vitro*. *Phytother*. *Res*. *24*, 1468-1472.

Yan, Y., Chen, G., Tong, S., Feng, Y. *et al*. (2005). Preparative isolation and purification of germacrone and curdione from the essential oil of the rhizomes of *Curcuma wenyujin* by high-speed counter-current chromatography. *J*. *Chromatogr*. *A 1070*, 207-210.

CHAPTER 6.

Trypanosoma brucei inhibition by essential oils from medicinal and aromatic plants traditionally used in Cameroon

"*However long the night,*

the dawn will break."

Cameroon proverb

Chapter 6 Outline

Abbreviation

1D and 2D NMR = One and two-dimensional nuclear magnetic resonance

BALB//3T3 = Mouse fibroblasts

COSY = Correlation Spectroscopy

DHFR = Dihydrofolate reductase

DMSO = Dimethylsulfoxide

EOs = Essential oils

HAT = Human African Trypanosomiasis

HMBC = Heteronuclear Multiple-Bond Correlation

HMQC = Heteronuclear Multiple-Quantum Correlation

MS = Mass spectra

NOE = Nuclear Overhauser Effect

NOESY = Nuclear Overhauser Effect Spectroscopy

RIs = Retention indices

SAR: Structure-activity relationship

SI = Selectivity index

STLs = Sesquiterpene lactones

T. brucei = *Trypanosoma brucei*

TC221 = *T. brucei* bloodstream-form parasites

TLC = Thin layer chromatography

TOCSY = Total Correlation Spectroscopy

WHO = World Health Organization

Abstract

As part of our ongoing campaign aimed to fight Trypanosoma infections, in the present work, we have selected six medicinal and aromatic plants (*Azadirachta indica*, *Aframomum melegueta*, *Aframomum daniellii*, *Clausena anisata*, *Dichrostachys cinerea* and *Echinops giganteus*) traditionally used in Cameroon to treat several disorders, including infections and parasitic diseases. Then we evaluated the activity of their essential oils (EOs) against *T. brucei* TC221 and their selectivity was also determined against Balb/3T3 cells, used as counter-screen for cytotoxicity.

The most relevant outcomes showed that the EOs from *A. indica, A. daniellii* and *E. giganteus* were the most active ones, with IC_{50} values of 15.21, 7.65 and 10.50 μg/mL, respectively. These EOs were characterized by different chemical components such as monoterpene hydrocarbons, sesquiterpene hydrocarbons, and oxygenated sesquiterpenes. Some of their isolated components were assayed as well on *T. brucei* TC221 and their effects linked to those of EOs.

6.1 Introduction

It has been estimated that 80% that a large part of the African population relies on herbal medicines as first-line treatment for different ailments. In this regard, the African flora environment represents a priceless reservoir of valuable source of potential trypanocidal drug candidates to be exploited (Ibrahim *et al*., 2014; Newman *et al*., 2003). In the fight against Trypanosoma infections, new therapeutic options can be represented by plant extracts, essential oils and plant-borne compounds (Nour *et al*., 2009; Bockman *et al*., 2015; Oyebode *et al*., 2016; Sun *et al*., 2016).

For this reason in the present study, we selected a panel of Cameroonian medicinal and aromatic plants as potential source of trypanocidal drug candidates. We focused on *Azadirachta indica* A. Juss (Meliaceae), *Aframomum melegueta* K. Schum. (Zingiberaceae), *Aframomum daniellii* (Hook. F.) K. Schum. (Zingiberaceae), *Clausena anisata* (Willd.) Hook.f. ex Benth. (Rutaceae), *Dichrostachys cinerea* (L.) Wight & Arn. (Mimosaceae) and *Echinops giganteus* A. Rich. (Asteraceae) (Figure 1).

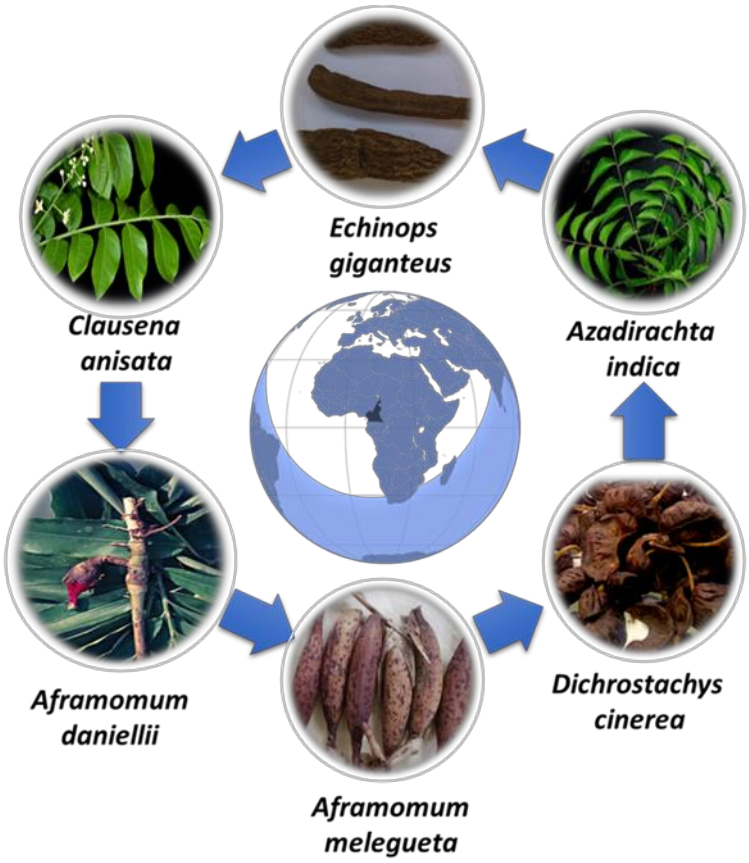

Fig. 1. Panel of Cameroonian medicinal and aromatic plants selected as sources of potential trypanocidal drug candidates.

A. indica also named "neem tree" is native to India and belongs to the Meliaceae family. The 12-24 m tall evergreen tree is fast growing and the plant is widespread in tropical and subtropical regions, especially in Africa, where it is used for a wide range of ailments. In fact, the plant is used as anthelminthic, antimalarial, anti-inflammatory and for the treatment of skin disease. Those properties were confirmed by scientific reports (Igbal *et al*., 2010; Tapanelli *et al*., 2016; Noorul *et al*., 2016). The main biologically active compounds from the neem seeds are azadirachtin, nimbin, nimbidin and nimbolides. Most of them showed insecticidal properties, particularly azadirachtin which is used as an insecticide because it is more eco-friendly (Dua *et al*., 2009). The neem seed bark ethanolic extract displayed an activity against *T.b. brucei* (Mbaya *et al*., 2010), but the leaf essential oil had never been investigated for antitrypanosomal activity.

A. melegueta, also known as "alligator pepper" or "grain of paradise" is a member of the Zingiberaceae family. The plant grows up to 1.5 m and flowers contain reddish-brown aromatic and pungent seeds. *A. melegueta* is a perennial herb native to West Africa where the seeds are used as a spice in food due to aromatic flavor and pungent taste. The local population use *A. melegueta* as an ingredient for the treatment of snakebites, stomachache and diarrhea (Ilic *et al*., 2010). Concerning seed volatile components, antimicrobial, anti-inflammatory and antioxidant properties have been recently reported (Adefegha *et al*., 2016).

A. daniellii, also known as "*African cardamom*" is an herbaceous plant present in West and Central Africa. As for other members of the *Afromomum* genus, its seeds are highly pungent and aromatic. This feature is important as the seeds are used for flavouring traditional dishes. Other uses of the plant by local population include laxative, anti-helmintic, and anti-fungal properties (Adegoke *et al*., 1994; Pavela *et al*., 2016).

C. Anisata also known as horsewood or "maggot killer" is an evergreen tropical tree from the Rutaceae family. The 10 m tall shrub grows in the savannah and the forest regions of West Africa. The leaves contain secretory glands emitting a strong smell (Moshi *et al*., 2005). They are used for the treatment of malaria, skin infections, ringworm and eczema (Agyepong *et al*., 2014). The stem bark of *C. anisata* showed antimicrobial properties (Chakraborty *et al*., 1995). Phytochemical investigation of *C. Anisata* reveals the presence of coumarins and alkaloids.

D. cinerea (Mimosaceae) is a tree present in tropical regions that grows up to eight feet tall with branches ending in spines. The species from the genus *Dichrostachys* are usually widespread from the Sudanese Sahel region to the Guinean areas. The plant has different vernacular names, in Gabon (Mbara y'orové and Punu), and in Ivory coast (N'gbagbémoto and Gboro). Traditional healers use the different parts of the plant to treat ailments such as rheumatism, venereal diseases,

stomach ache and malaria (Aworet *et al*., 2015). Phytochemical investigations revealed the presence of triterpenes, tannins, flavonoids, fatty acids and flavons.

E. *giganteus* belonging to the Asteraceae family is a 60-150 cm tall branched herb. The roots are used in Cameroonian and Nigerian traditional medicine to treat various ailments including gastric and hearth troubles, asthma, and to calm stomach ache (Pavela *et al*., 2016). Previous studies revealed the significant antibacterial, antifungal and antioxidant activities of the root methanolic extract (Fankam *et al*., 2011; Sawadogo *et al*., 2012; Dzoyem *et al*., 2014).

Overall, these Cameroonian plants are also traditionally used to control populations of arthropod pests (Karunamoorthi *et al*., 2014). With this vision in mind, we shed light on the growth inhibitory potential of the EOs obtained from the leaves of *A*. *indica*, *A*. *daniellii* and *C*. *anisate*, the seeds of *A*. *melegueta* and *D*. *cinerea*, and the roots of *E*. *giganteus* against *T*. *brucei* TC221. Selected pure constituents from the above mentioned EOs were also evaluated.

6.2 Results and discussion

6.2.1 Chemical composition of EOs from Cameroonian plants

The chemical compositions of EOs hydrodistilled from the six Cameroonian medicinal and aromatic plants are reported in Table 1. In the EO obtained from neem leaves, a total of 13 components were identified, accounting for 98.3% of the total composition. The oil was almost entirely composed by sesquiterpene hydrocarbons (97.4%), with germacrene B (74.0%) and γ-elemene (18.3%) as the predominant components. Minor constituents were (*E*)-caryophyllene (2.4%) and β-elemene (0.9%). To our knowledge, this work represents one of the few studies on the chemical composition of neem leaf EOs. Neem trees oil have been amply investigated and recently El-Hawary *et al*. (El-Hawary *et al*., 2013) reported the composition of Egyptian neem leaves, indicating β-elemene (33.39%), γ-elemene (9.89%), germacrene D (9.72%), caryophyllene (6.8%) and bicyclogermacrene (5.23%) as the major compounds. On the other hand, Dastan *et al*. (Dastan *et al*., 2010) found γ-elemene (20.8%), germacrene B (20.3%), *trans*-caryophyllene (13.5%), hexadecanal (12.8%) and methyl linoleate (10.5%) as major compounds in neem leaf oil from Iran.

A total of 59 components were identified in the EO of alligator pepper, accounting for 99.4% of the total composition. The oil was dominated by oxygenated monoterpenes (83.3%), with 1,8-cineole (58.5%) and α-terpineol (19.4%) as the major compounds. Monoterpene hydrocarbons gave a minor contribution (14.9%), with β-pinene (7.1%) and α-pinene (2.0%) as the most representative components. Interestingly, sesquiterpenoids, which are reported as volatile marker compounds of alligator pepper, were detected in only low levels here (0.6%). The chemical composition of the *A. melegueta* seed EO showed a significant variability depending on the geographic origin and genetic characteristics of the samples. Samples from Nigeria exhibited humulene (26.23%), (*E*)-ocimene (23.22%), (*E*)-caryophyllene (19.17%) and (S)-2-heptyl acetate (16.22%) as the major volatile constituents (Ukeh *et al*., 2009), whereas the seeds from Central African Republic contained high levels of β-pinene (>30%) and about 50% of sesquiterpene hydrocarbons (Lamaty *et al*., 1993). Finally, an oil sample from Cameroon was made up of β-caryophyllene (8.5%), α-humulene (31.3%) and their epoxides (17.9 and 27.7%, respectively) (Menut *et al*., 1997).

57 compounds were identified in the EO from African cardamom leaves, accounting for 99.3% of the total composition. This oil was mainly made up of monoterpene hydrocarbons (59.8% in leaves), accompanied by lower amounts of sesquiterpene hydrocarbons (20.0%), oxygenated

monoterpenes (11.0%) and oxygenated sesquiterpenes (8.4%). The major compounds were sabinene (43.9%) and (*E*)-caryophyllene (16.6%), whereas other components occurring at noteworthy levels were β-pinene (5.8%), terpinen-4-ol (3.7%) and α-pinene (2.4%). This is the first study that has been reported on the leaf EO from *A*. *daniellii*.

The EO extracted from leaves from *C*. *anisata* was characterized by high levels of phenylpropanoids (84.0%), which were mainly represented by (*E*)-anethole (64.6%), with minor contributions by (*E*)-methyl isoeugenol (16.1%) and methyl chavicol (2.0%). Terpenoids constituted a minor part of this oil, being represented mostly by *p*-cymene (2.9%), γ-terpinene (2.4%), myrcene (2.0%) and germacrene D (2.2%)

In the EO of *D*. *cinerea* seeds, a total of 49 volatile components were identified, accounting for 76.0% of the oil composition. Oxygenated monoterpenes were the most abundant constituents (50.6%), with geraniol (18.2%), terpinen-4-ol (7.5%), linalool (4.0%) and umbellulone (3.8%) as the most representative compounds. Oxygenated sesquiterpenes gave a lower contribution (12.1%), with none of the identified components exceeding 1.8%. Among other components occurring in the oil, it is worthy to note the presence of ligustrazin (5.1%), elemicin (3.0%) and decanoic acid (2.8%). To the best of our knowledge, no previous research has been published on the chemical composition of *D*. *cinerea* seed EO.

35 volatile compounds, all belonging to the sesquiterpene class (94.3%), were identified in the root EO from *E*. *giganteus* (54.7% of sesquitepene hydrocarbons and 39.6% oxygenated sesquiterpenes). The major compounds were tricyclic sesquiterpenoids, which are characterized by multiple rearrangements of the caryophyllene cation (Bohlmann *et al*., 1980; Bohlmann *et al*., 1981), namely silphiperfol-6-ene (23.0%) and presilphiperfolan-8-ol (22.7%), presilphiperfol-7-ene (7.8%) and cameroonan-7-α-ol (7.8%). Another noteworthy component occurring in the oil was (*E*)-caryophyllene (6.3%). The cameroonan-7-α-ol, is responsible for the patchouli-like smell of the root oil (Taber *et al*., 2011). The reported composition was quite consistent with that previously published by Menut *et al*. (Menut *et al*., 1997) for a root samples collected in Cameroon.

Table 3. Chemical composition of the EOs from *Azadirachta indica*, *Aframomum melegueta*, *Aframomum daniellii*, *Clausena anisata*, *Dichrostachys cinerea* and *Echinops giganteus*.

N.	Component[a]	RI calc.[b]	RI lit.[c]	(%)[d]						ID[f]
				Azadirachta indica	*Aframomum melegueta*	*Aframomum daniellii*[e]	*Clausena anisata*	*Dichrostachys cinerea*[e]	*Echinops giganteus*[e]	
1	isopentyl acetate	873	869		tr[g]					RI,MS
2	2-methyl butyl acetate	876	875		tr					RI,MS
3	2-heptanone	891	892		tr					RI,MS
4	2-heptanol	901	894		0.2					RI,MS
5	α-thujene	916	924		tr	1.0	0.1			RI,MS
6	α-pinene	921	932		2.0	2.4	0.2		tr	Std
7	α-fenchene	938	945		0.1					RI,MS
8	Camphene	939	946		0.3	tr				RI,MS
9	Sabinene	959	969		tr	43.9	0.6			RI,MS
10	β-pinene	963	974		7.1	5.8	0.3	0.1		Std
11	dehydro-1,8-cineole	979	988		0.1					RI,MS
12	Myrcene	982	988		0.2	1.5	2.0	0.3	tr	Std
13	α-phellandrene	996	1004		0.3	tr				Std
14	δ-3-carene	1003	1008						tr	Std
15	α-terpinene	1009	1014		0.3	0.9	tr			RI,MS
16	*p*-cymene	1016	1020		1.1	1.0	2.9	0.1		Std

17	Limonene	1020	1024	1.5	0.7	0.4	tr	tr	Std
18	1,8-cineole	1021	1026	58.5	0.5	0.2	2.3		Std
19	ethylhexanol	1031	1030				0.2		RI,MS
20	(*Z*)-β-ocimene	1037	1032			0.4			Std
21	(*E*)-β-ocimene	1041	1044	0.1	0.3	0.3			RI,MS
22	γ-terpinene	1050	1054	0.9	1.9	2.4			Std
23	*cis*-sabinene hydrate	1057	1065		1.1				RI,MS
24	*cis*-linalool oxide	1071	1067			tr	0.1		RI,MS
25	terpinolene	1079	1086	0.8	0.4	0.1		tr	Std
26	*p*-cymenene	1086	1089	0.2					RI,MS
27	Ligustrazin	1081	1083				5.1		RI,MS
28	*trans*-sabinene hydrate	1089	1098		0.9				RI,MS
29	2-nonanone	1094	1094	tr					RI,MS
30	linalool	1096	1095	tr	1.8	tr	4.0		Std
31	*n*-nonanal	1105	1100	tr					RI,MS
32	*endo*-fenchol	1108	1114	0.3					RI,MS
33	*cis*-*p*-menth-2-en-1-ol	1113	1118		0.2		0.3		RI,MS
34	α-campholenal	1123	1122	tr			0.1		RI,MS
35	*trans*-pinocarveol	1128	1135	0.2			0.7		Std
36	*trans*-*p*-menth-2-en-1-ol	1131	1136		0.1		0.3		RI,MS

37	*cis*-β-terpineol	1142	1140	tr				RI,MS
38	*cis*-verbenol	1142	1137				0.2	RI,MS
39	*trans*-pinocamphone	1151	1158				0.4	RI,MS
40	pinocarvone	1152	1160	tr			0.1	RI,MS
41	borneol	1156	1165	0.2			0.7	Std
42	*p*-mentha-1,5-dien-8-ol	1158	1166	1.1				RI,MS
43	*cis*-pinocamphone	1162	1172				0.8	RI,MS
44	umbelullone	1166	1167				3.8	RI,MS
45	terpinen-4-ol	1167	1174	1.4	3.7	tr	7.5	Std
46	*cis*-pinocarveol	1175	1182	tr				RI,MS
47	cryptone	1183	1183	tr				RI,MS
48	*p*-cymen-8-ol	1178	1179	tr		tr	0.3	RI,MS
49	α-terpineol	1181	1186	19.4	0.2	tr	3.3	Std
50	myrtenal	1184	1195	0.2	0.1		0.2	Std
51	myrtenol	1186	1194	0.2	0.4		1.1	Std
52	*cis*-piperitol	1199	1195		tr			RI,MS
53	γ-terpineol	1195	1199	tr				RI,MS
54	methyl chavicol	1196	1195			2.0		RI,MS
55	*trans*-piperitol	1205	1207				0.1	RI,MS
56	*trans*-carveol	1217	1215	tr			0.2	RI,MS

57	*cis*-carveol	1228	1226	tr				RI,MS
58	thymol, methyl ether	1224	1232	tr				RI,MS
59	nerol	1229	1227				0.2	Std
60	citronellol	1231	1223				0.3	Std
61	carvone	1240	1239	tr				Std
62	carvacrol, methyl ether	1237	1241	tr				RI,MS
63	neral	1241	1235				0.2	Std
64	piperitone	1250	1249				0.3	RI,MS
65	(*Z*)-anethole	1250	1249			0.3		RI,MS
66	*p*-anisaldehyde	1251	1247			0.7		RI,MS
67	geraniol	1251	1249				18.2	Std
68	*trans*-ascaridol glycol	1262	1266		tr			RI,MS
69	(*E*)-cinnamaldehyde	1267	1267	tr				RI,MS
70	phellandral	1269	1273	0.1				RI,MS
71	isobornyl acetate	1276	1283		tr			Std
72	(*E*)-anethole	1287	1282			64.6		Std
73	thymol	1291	1289	0.1			0.9	Std
74	*trans*-sabinyl acetate	1291	1289		tr			RI,MS
75	methyl myrtenate	1292	1293				2.0	RI,MS
76	carvacrol	1301	1298	0.5		tr	0.7	Std

77	*cis*-pinocarvyl acetate	1303	1311			0.1					RI,MS
78	myrtenyl acetate	1316	1324			1.9					RI,MS
79	silphiperfol-5-ene	1318	1326							2.1	RI,MS
80	δ-elemene	1326	1335	0.1			0.1				RI,MS
81	presilphiperfol-7-ene	1328	1334							7.8	RI,MS
82	silphinene	1333	1340							1.7	RI,MS
83	7-*epi*-silphiperfol-5-ene	1336	1349							3.5	RI,MS
84	α-terpinyl acetate	1341	1346		tr			0.3			RI,MS
85	α-copaene	1362	1374	0.2		0.2	tr				Std
86	β-bourbonene	1369	1387	0.3		tr					RI,MS
87	modheph-2-ene	1362	1382							3.0	RI,MS
88	silphiperfol-6-ene	1373	1377							23.0	RI,MS
89	β-bourbonene	1377	1387				0.1				RI,MS
90	β-cubebene	1377	1387			tr					RI,MS
91	α-isocomene	1379	1387							2.4	RI,MS
92	β-elemene	1380	1389	0.9		tr	0.1				Std
93	decanoic acid	1380	1386					2.8			RI,MS
94	anisyl methyl ketone	1382	1380				0.1				RI,MS
95	*iso*-longifolene	1383	1389							tr	RI,MS
96	β-isocomene	1400	1407							2.1	RI,MS

97	α-gurjunene	1400	1409							tr	Std
98	(*E*)-caryophyllene	1402	1417	2.4	tr	16.6	0.8			6.3	Std
99	methyl eugenol	1406	1403				0.3				RI,MS
100	α-*trans*-bergamotene	1425	1432			0.1					RI,MS
101	isoamyl benzoate	1433	1433		tr						RI,MS
102	γ-elemene	1427	1434	18.3			0.1				RI,MS
103	α-humulene	1436	1452	0.4	tr	1.5	0.8			2.0	Std
104	geranyl acetone	1449	1453					1.2			RI,MS
105	(*E*)-β-farnesene	1450	1454			tr				tr	RI,MS
106	germacrene D	1465	1484	0.5		0.3	2.2			0.3	RI,MS
107	selina-4,11-diene	1467	1474			0.1					RI,MS
108	β-selinene	1469	1489		tr						RI,MS
109	*ar*-curcumene	1472	1479				tr			0.1	RI,MS
110	bicyclogermacrene	1480	1500			0.1	0.1				RI,MS
111	benzaldehyde, 3,4-dimethoxy-	1482	1489				0.2				RI,MS
112	(*E*)-β-ionone	1481	1487	0.5							Std
113	*epi*-cubebol	1489	1493							0.1	RI,MS
114	α-zingiberene	1492	1493				0.1				RI,MS
115	(*Z*)-α-bisabolene	1493	1506			0.1					RI,MS
116	silphiperfolan-6-α-ol	1496	1507							1.0	RI,MS

117	β-bisabolene	1498	1505			0.9				RI,MS
118	(*E*)-methyl isoeugenol	1499	1491				16.1			RI,MS
119	cameroonan-7-α-ol	1500	1510						7.1	RI,MS
120	β-bisabolene	1506	1505				0.3			RI,MS
121	7-*epi*-α-selinene	1507	1520		tr					RI,MS
122	(*E*,*E*)-α-farnesene	1508	1505				0.3			Std
123	*trans*-calamenene	1508	1521			tr				RI,MS
124	*δ*-cadinene	1510	1522	0.2		tr	0.1		0.3	RI,MS
125	silphiperfolan-7-β-ol	1510	1519						2.5	RI,MS
126	β-sesquiphellandrene	1520	1521				tr			RI,MS
127	selina-3,7(11)-diene	1531	1545	0.2						RI,MS
128	silphiperfolan-6-β-ol	1535	1546						1.7	RI,MS
129	hedycaryol	1536	1546			1.5				RI,MS
130	germacrene B	1546	1559	74.0			0.3			RI,MS
131	elemicin	1556	1555					3.0		RI,MS
132	(*E*)-nerolidol	1556	1561			0.7				Std
133	isoaromadendrene epoxide	1560	1572					1.8		RI,MS
134	prenopsan-8-ol	1564	1575						3.2	RI,MS
135	caryophyllene oxide	1564	1582			2.2		1.1		Std
136	(3*Z*)-hexenyl benzoate	1566	1565	0.3						RI,MS

137	spathulenol	1568	1576			0.1			RI,MS
138	presilphiperfolan-8-ol	1578	1585					22.7	MS
139	guaiol	1583	1600		0.5				RI,MS
140	humulene epoxide II	1590	1608		0.1	tr			RI,MS
141	10-*epi*-γ-eudesmol	1600	1622	tr	0.3				RI,MS
142	eremoligenol	1611	1629		0.4				RI,MS
143	γ-eudesmol	1615	1630	tr	0.4				RI,MS
144	1,10-di-*epi*-cubenol	1619	1618					0.1	RI,MS
145	β-eudesmol	1631	1649	0.2	1.5				RI,MS
146	α-acorenol	1628	1632				1.0		RI,MS
147	caryophylla-4(12),8(13)-dien-5-ol[g]	1630	1639		0.2			tr	RI,MS
148	*epi*-α-muurolol	1635	1640			tr	0.7	0.4	RI,MS
149	α-muurolol	1640	1644					0.1	RI,MS
150	α-eudesmol	1636	1652		0.5				RI,MS
151	intermedeol	1639	1666		0.1				RI,MS
152	α-cadinol	1647	1652			tr	1.4	0.4	RI,MS
153	ageratochromene	1655	1658				0.8		RI,MS
154	α-bisabolol	1673	1685	tr	0.4				Std
155	3-oxo-β-ionone	1678	1685				0.9		RI,MS
156	cyperotundone	1688	1695				0.9		RI,MS

157	(2*E*-6*Z*)-farnesol	1709	1698					2.4		RI,MS
158	curcuphenol	1716	1717						0.4	RI,MS
159	(2*E*-6*Z*)-farnesal	1718	1713					1.0		RI,MS
160	(2*E*-6*E*)-farnesal	1737	1740					1.7		RI,MS
161	*n*-tricosane	2300	2300		0.1					Std
	Oil yield (%)			0.01	0.3	0.2	2.0	0.4	1.8	
	Total identified (%)			98.3	99.4	99.3	99.6	76.0	94.3	
	Grouped compounds (%)									
	Monoterpene hydrocarbons				14.9	59.8	0.6	0.6	tr	
	Oxygenated monoterpenes				83.3	11.0	0.3	50.6		
	Sesquiterpene hydrocarbons			97.4	0.2	20.0	5.2		54.7	
	Oxygenated sesquiterpenes				0.4	8.4	0.2	12.1	39.6	
	Phenylpropanoids						84.0			
	Others			0.9	0.6		0.2	12.7		

[a] Components are reported in order of their elution from an HP-5MS capillary column. [b] Retention index experimentally determined using a mixture of C_8-C_{30} of n-alkanes. [c] Retention index taken from Adams (2007) and/or NIST 08 (2008) for an apolar capillary column. [d] Relative percentage values are means of three determinations with a RSD% below 15% for the most abundant components. [e] Analytical data are taken from Pavela *et al*. (Pavela *et al*., 2016). [f] Identification methods: std, based on comparison of RT, RI and MS with those of authentic compounds; MS, based on comparison with WILEY, ADAMS, FFNSC2 and NIST 08 MS databases. [g] traces, % <0.1. [h] Correct isomer not identified.

6.2.2. Inhibition of *T. brucei* proliferation

EOs are complex mixtures of volatile compounds with multi-target actions whose antitrypanosomal effects are largely unknown and barely explored. On this basis, we decided to test the *in vitro* inhibitory effects of a pool of EOs taken from medicinal and aromatic plants growing in Cameroon. Some of them are known for their traditional uses in the treatment of infectious diseases and malaria (Kuete *et al*., 2010; Benelli *et al*., 2017) and in the case of the Neem tree also against *T. b. brucei* (Mbaya *et al*., 2010).

Based on the chemical analysis performed, they exhibited different chemical profiles, being characterized by diverse functionalized groups such as monoterpene hydrocarbons (African cardamom), oxygenated monoterpenes (*A. melegueta* and *D. cinerea*), sesquiterpene hydrocarbons (*A. indica*), sesquiterpene hydrocarbons and oxygenated sesquiterpenes (*E. giganteus*), and phenylpropanoids (*C. anisata*). In this context, the main aim of our work was to identify the chemical scaffolds of possible natural lead compounds against trypanosomiasis.

Testing the EOs obtained from Cameroonian plants, we obtained various degrees of inhibition on *T. brucei* proliferation, varying from not active (*A. melegueta*, *C. anisata* and *D. cinerea*), to moderately active (*A. danielli*, *E. giganteus* and *A. indica*). Notably, the IC_{50} values on *T. brucei* were 7.65, 10.50 and 15.21 μg/mL for the essential oils from *A. danielli*, *E. giganteus* and *A. indica*, respectively (Table 2). Furthermore, the most active oils were also evaluated for growth inhibitory effects on on Balb/3T3 cells as a reference. No effect on mammalian cells was observed with concentrations as high as 100 μg/mL, showing a noteworthy selectivity against *T. brucei* in comparison to mammalian cells, with selectivity indexes above 6.57 in all cases.

The inhibitory effects on *T. brucei* exhibited by the three EOs highlight three classes of active compounds, i.e. monoterpene hydrocarbons (for *A. danielli*), sesquiterpene hydrocarbons (for *A. indica* and *E. giganteus*) (Figure 2). In the case of *E giganteus*, it also contains high amount of oxygenated compounds.

For the monoterpene hydrocarbons, the toxicity against *T. brucei* can be attributed to the high hydrophobicity of this class of compounds, which are able to easily cross the cell membrane causing destabilization of phospholipid bilayer and alteration of its permeability leading to cell damage and death (Petrelli *et al*., 2016; Petrelli *et al*., 2017). Among these compounds, the most abundant was sabinene (43.9%) (Figure 2), which showed an IC_{50} value against *T. brucei* of 5.96 μg/mL, which is close to that of the African cardamom EO (7.65 μg/mL) (Table 2). Another component of this oil with detectable antitrypanosomal activity was β-pinene showing an IC_{50} value of 11.4 μg/mL. The antitrypanosomal activity of sabinene was already reported in a previous

study, although its mechanism of action on the protozoal cell has not been elucidated (Mikus *et al*., 2000).

Table 2. Inhibitory effects of EOs from Cameroonian plants against TC221 and Balb/3T3 cells.

Treatment	IC_{50} (µg/mL)		Selectivity Index (SI)
	***T. b. brucei* (TC221)**	**Balb/3T3**	
Essential Oils			
Aframomum danielli	7.65 ± 1.1	>100	>13.1
Dichrostachys cinerea	>100	-	-
Echinops giganteus	10.50 ± 1.7	>100	>9.52
Azadirachta indica	15.21 ± 0.97	>100	>6.57
Aframomum melegueta	>100	-	-
Clausena anisata	>100	-	-
Pure compounds	**µg/mL (µM)**	**µg/mL (µM)**	
Sabinene	5.96 ± 1.3 (43.8)	>100	>16.7
β-Pinene	11.4 ± 2.6 (83.7)	>100	>8.77
1,8-Cineole	>100	-	
Terpinen-4-ol	>100	-	
(*E*)-Caryophyllene	8.25 ± 1.3 (40.4)	>100	>12.1
Reference drug	**µg/mL (µM)**	**µg/mL (µM)**	
Suramin	0.0286 ± 0.0008 (0.0220)	-	

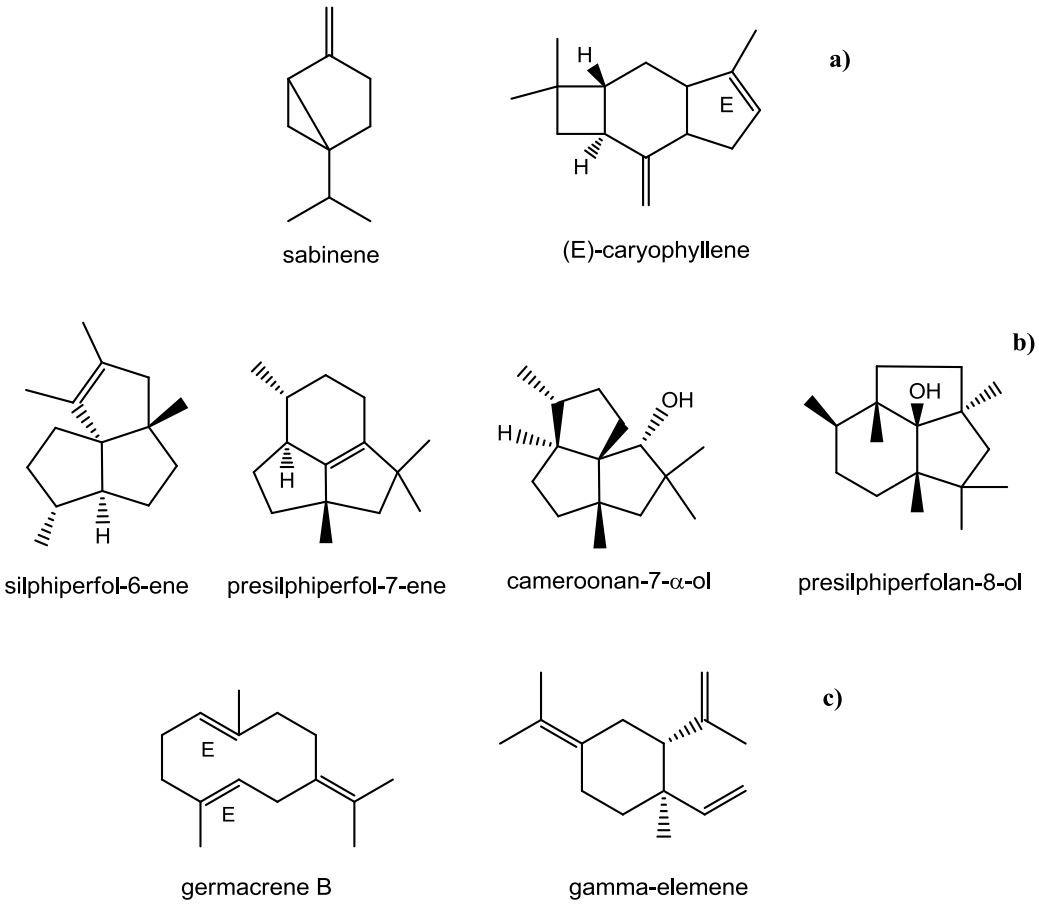

Fig. 2. Chemical structures of the main EO constituents in *Aframomum daniellii* (a), *Echinops giganteus* (b) and *Azadirachta indica* (c).

E. giganteus as well as *A. daniellii* essential oils contained the bicyclic sesquiterpene (*E*)-caryophyllene (Figure 1), which exhibited good inhibitory properties on *T. brucei* (IC_{50} value of 8.25 μg/mL). However, the content of this component is only 6.3% in *E. giganteus* and can therefore not explain the good activity of this essential oil. It is rather tricyclic sesquiterpenes that is the major constituent. This is the first report documenting the antitrypanosomal activity of the tricyclic sesquiterpenes-containing *E. giganteus* essential oil. The latter was a rich source of compounds with an unusual skeleton such as silphiperfol-6-ene, presilphiperfolan-8-ol, presilphiperfol-7-ene and cameroonan-7-α-ol (Figure 2) (Pavela *et al*., 2016). To date these compounds have not been biologically investigated. Previously, the tricyclic sesquiterpene ledol was suggested to be responsible for the trypanocidal properties of *Hagenia abyssinica* (Bruce ex Steud.) J.F.Gmel. EO (Nibret *et al*., 2010). Among the other pure compounds, 1,8-cineole and terpinen-4-ol were inactive against *T. brucei* (IC_{50} > 100 μg/mL) (Table 2) and this also explained the lack of activity for *A. melegueta* and *D. cinerea* essential oils, which are dominated by these compounds.

6.3 Conclusions

In conclusion, our biological investigation on EOs distilled from medicinal and aromatic plants growing in Cameroon demonstrated for the first time that the leaf EO from the neem tree, which showed an IC_{50} value of 15.21 μg/mL, can be a source of sesquiterpenes such as germacrene B and γ-elemene. Since this oil is completely dominated by sesquiterpenes (97.4%), it can be assumed that they are responsible for trypanocidal activity. However, further studies are encouraged in order to clarify their mechanisms of action and *in vivo* efficacy.

6.4 Materials and methods

6.4.1 Plant material

Leaves of *A. indica* were collected during the dry season (January 2017) from a tree in the city of Guidiguis (north of Cameroon), about 70 km from Maroua. The leaves were air-dried in the shadow for one week and kept in papers. Fruits (pods) of *A. melegueta* were collected in a forest near Foumbam (western Cameroon) in December 2016. Once harvested, the seeds were removed from their pods and dried at room temperature over a period of 3 weeks in the absence of sunlight. At the end of the drying process, the seeds were placed into paper bags before hydrodistillation. Leaves of *C. anisata* were collected in the village of Baffou, Menoua Division, Western Cameroon. Leaves of *A. danielli* and fruits of *D. cinerea*, and roots of *E. giganteus* were collected from Bamougoum and Bafoussam's market (Cameroon, Western Region), respectively. The pericarp of *D. cinerea* was removed and the seeds used; the roots of *E. giganteus* were washed with water, and sliced into small pieces. These plant parts were dried at room temperature for one week. The botanical identification of the five species was performed by a taxonomist at the Cameroon National Herbarium (Yaoundé, Cameroon) and by Prof. Filippo Maggi (University of Camerino, Italy), and the voucher specimens were archived with the following codes: 4447 SRFK (*A. indica*), 43117 HNC (*A. melegueta*), 43130 HNC (*A. danielli*), 44242/HNC (*C. anisata*), 42920 HNC (*D. cinerea*) and 23647 SRF (*E. giganteus*). The botanical names were also checked in The Plant List database (www.theplantlist.org).

6.4.2 Isolation of EO

Dry leaves of *A. indica, A. daniellii and C. anisata*, seeds of *A. melegueta* and *D. cinerea,* and roots of *E. giganteus* were cut into small pieces and subjected to hydrodistillation using a Clevenger-type apparatus until no more oil was obtained. The essential oils obtained were dried using Na_2SO_4 and stored at - 20°C in vials sealed with Teflon caps and protected from light before use. The oil yields were calculated on a dry weight basis (%, w/w).

6.4.3 Chemicals

For identification of volatiles, the following analytical standards purchased from Sigma-Aldrich (Milan, Italy) were used: α-pinene, β-pinene, sabinene, 1,8-cineole, camphene, myrcene, α-phellandrene, δ-3-carene, p-cymene, limonene, γ-terpinene, terpinolene, linalool, trans-pinocarveol, terpinen-4-ol, α-terpineol, myrtenal, citronellol, isobornyl acetate, (E)-caryophyllene, α-humulene, (E)-β-ionone, caryophyllene oxide. The reference drug suramin was purchased from Sigma-Aldrich.

6.4.4 GC analysis of EOs

The analytical conditions and instruments used for the separation of Cameroonian EO components were the same of those reported in Chapter 2 paragraph 2.6.8. The EO was diluted 1:100 in *n*-hexane, and then 2 µl of the solution were injected into the GC-MS system. For identification of EO components, co-injection with the authentic standards available in our laboratory (purchased from Sigma-Aldrich, Milan, Italy) was performed, together comparison with of retention indices and mass spectra to those occurring in the ADAMS, NIST 08 and FFNSC2 libraries databases (Adams, 2007; NIST 08, 2008; FFNSC2, 2012). Percentage values of volatile components were the mean of three chromatographic analyses and were determined from the peak areas without the use of correction factors.

6.4.5 *T. brucei* and mammalian cell culture and growth inhibition assay

T. brucei TC221 bloodstream forms and mouse Balb/3T3 fibroblasts (ATCC no CCL-163) were performed as described before in Chapter 2 paragraph 2.6.9, with an adjustment of the seeding density for the mammalian cells. EOs or pure compounds identified from these oils were dissolved in dimethyl sulfoxide (DMSO) and serially diluted with growth medium in white 96-well microtiter plates. 20,000 bloodstream forms of *T. brucei* or Balb/3T3 cells were added to each well in a final volume of 200 µl. IC_{50} values were calculated on log inhibitor *vs*. response curves by non-linear regression using the GraphPad prism 5.04 software.

References

Adams, R.P. (2007). Identification of Essential Oil Components by Gas Chromatography/Mass Spectroscopy; Allured Publishing Co.: Carol Stream, IL, USA.

Adefegha, S.A., Oboh, G., Adefegha, O.M., Henle, T. (2010). Alligator pepper/Grain of paradise (*Aframomum melegueta*) modulates Angiotensin-I converting enzyme activity, lipid profile and oxidative imbalances in a rat model of hypercholesterolemia. *Pathophysiol*. *23*, 191–202.

Adegoke, G.O., Skura, B.J. (1994). Nutritional profile and antimicrobial spectrum of the spice *Aframomum daniellii* K. Schum. *Plant Foods Hum*. *Nutr*. *45*, 175–182.

Agyepong, N., Agyare, C., Adarkwa-Yiadom, M., Gbedema, S.Y. (2014). Phytochemical investigational and anti-microbial activity of Clauseana anisate (Wild), Hook. *Afr*. *J*. *Tradit*. *Complement*. *Altern*. *Med*. *11*, 200-209.

Aworet Samsenny, R.R., Angone, S.A., Mandingou, N.K., Mounanga M.B *et al*. (2015). Study of pharmacological properties of the methanolic extract of Dichrostachys cinerea bark (L.) Wight et Arn (Leguminoseae) in isolated myometrium from pregnant rats. *J*. *Ethnopharmacol*. *169*, 195-199.

Benelli, G., Maggi, F., Petrelli, R., Canale, A. *et al*. (2017). Not ordinary antimalarial drugs: Madagascar plant decoctions potentiating the chloroquine action against Plasmodium parasites. *Ind*. *Crops Prod*. *103*, 19-38.

Bockman, M.R., Kalinda, A.S., Petrelli, R.; De la Mora-Rey, T. *et al*. (2015). Targeting Mycobacterium tuberculosis Biotin Protein Ligase (MtBPL) with Nucleoside-Based Bisubstrate Adenylation Inhibitors. *J*. *Med*. *Chem*. *58*, 7349-7369.

Bohlmann, F., Jakupovic, J. (1980). Neue Sesquiterpen-Kohlenwasserstoffe mit anomalen Kohlenstoffgerüst aus Silphium-arten. *Phytochem*. *19*, 259-265.

Bohlmann, F., Zdero, C., Jakupovic, J., Robinson, H. (1981). Eriolanolides, eudesmanolides and a rearranged sesquiterpene from Eriophyllum species. *Phytochem*. *20*, 2239-2244.

Chakraborty, A., Chowhury, B.K., Bhattacharyya, P. (1995). Clausenol and clausenin—two carbazole alkaloids from Clausena anisate. *Phytochem*. *40*, 295-298.

Dastan, D., Pezhmanmehr, M., Askari, N., Ebrahimi, S.N. (2010). Essential oil compositions of the leaves of Azadirachta indica A. Juss from Iran. *J*. *Essent*. *Oil-Bear*. *Plants 13*, 357-361.

Dua, V.K., Pandey, A.C., Raghavendra, K., Gupta, A. *et al*. (2009). Larvicidal activity of neem oil (Azadirachta indica) formulation against mosquitoes. *Malar*. *J*. *8*, 124.

Dzoyem, J.P., Tchuenguem, R.T., Kuiate, J.R., Teke, G.N. *et al*., (2014). In vitro and in vivo antifungal activities of selected Cameroonian dietary spices. *BMC Complement*. *Altern*. *Med*. *14*, 58.

El-Hawary, S.-S., El-Tantawy, M.E., Rabeh, M.A., Badr, W.K. (2013). Chemical composition and biological activities of essential oils of Azadirachta indica A. Juss. *Int*. *J*. *Appl*. *Res*. *Nat*. *Prod*. *6*, 33-42.

Fankam, A.G., Kuete, V., Voukeng, I.K., Kuiate, J.R. *et al*., (2011) . Antibacterial activities of selected Cameroonian spices and their synergistic effects with antibiotics against multidrug-resistant phenotypes. *BMC Complement*. *Altern*. *Med*. *11*, 104.

FFNSC 2. (2012). Flavors and Fragrances of Natural and Synthetic Compounds. Mass spectral database; Shimadzu Corps: Kyoto, Japan.

Ibrahim, M.A., Mohamed, A., Isah, M.B., Aliyu, A.B. (2014). Anti-trypanosomal activity of African medicinal plants: a review update. *J*. *Ethnopharmacol*. *154*, 26-54.

Igbal, Z., Lateef, M., Jabbar, A., Gilani, A.H. (2010). In vivo anthelmintic activity of *Azadirachta indica* A. Juss seeds against gastrointestinal nematodes of sheep. *Vet*. *Parasitol*. *168*, 342–345.

Ilic, N., Schmidt, B.M., Pouley, A., Raskin, I. (2010). Toxicological evaluation of grains of paradise (*Aframomum melegueta*) [Roscoe] K. Schum. *J*. *Ethnopharmacol*. *127*, 352–356.

Karunamoorthi, K., Hailu, T. (2014). Insect repellent plants traditional usage practices in the Ethiopian malaria epidemic-prone setting: an ethnobotanical survey. *J*. *Ethnobiol*. *Ethnomed*. *10*, 22.

Kuete, V. (2010). Potential of Cameroonian plants and derived products against microbial infections: A review. *Planta Med*. *76*, 1479-1491.

Lamaty, G., Menut, C., Koudou, J., Régnier, P. *et al*. (1993). Aromatic Plants of Tropical Central Africa. XI. Essential Oils of Leaf and Seed of Aframomum melegueta (Roscoe) K. Schum. from Central African Republic. *J*. *Essent*. *Oil Res*. *5*, 81-83.

Mbaya, A.W., Ibrahim, U.I., God, O.T., Ladi, S. (2010). Toxicity and potential anti-trypanosomal activity of ethanolic extract of Azadirachta indica (Meliacea) stem bark: an in vivo and in vitro approach using Trypanosoma brucei. *J*. *Ethnopharmacol*. *128*, 495-500.

Mbaya, A.W.; Ibrahim, U.I., God, O.T., Ladi, S. (2010). Toxicity of potential anti-trypanosomal activity of ethanolic extract of *Azadirachta indica* (Meliacea) stem bark: An in vivo and in vitro approach using *Trypanosoma brucei*. *J*. *Ethnopharmacol*. *128*, 495-500.

Menut, C., Lamaty, G., Amvam Zollo, P.H., Atogho, B.M. *et al*. (1997). Aromatic plants of tropical central Africa. V. volatile components of three zingiberaceae from Cameroon: Aframomum melegueta (roscoe) K. Schum., A. daniellii (hook. f.) K. Schum. and A. sulcatum (oliv. and hanb.) K. Schum. *Flav*. *Fragr*. *J*. *6*, 183-186.

Mikus, J., Harkenthal, M., Steverding, D., Reichling, J. (2000). In vitro effect of essential oils and isolated mono- and sesquiterpenes on Leishmania major and Trypanosoma brucei. *Planta Med*. *66*, 366-368.

Moshi, M.J., Kagaste, G.A.B., Mbwambo, Z.H. (2005). Plants used to treat epilepsy by Tanzanian traditional healers. *J*. *Ethnopharmacol*. *97*, 327-336.

Newman, D.J., Cragg, G.M., Snader, K.M. (2003). Natural product as sources of new drugs over the period 1981-2002. *J*. *Nat*. *Prod*. *66*, 1022-1037.

Nibret, E., Wink, M. (2010). Trypanocidal and antileukaemic effects of the essential oils of Hagenia abyssinica, Leonotis ocymifolia, Moringa stenopetala, and their main individual constituents. *Phytomed*. *17*, 911-920.

NIST 08. (2008). National Institute of Standards and Technology. Mass spectral library (NIST/EPA/NIH); National Institute of Standards and Technology: Gaithersburg MD, USA, 2008.

Noorul, A., Gayathri. Beneficial effects of Neem oil-An updated review. (2016) *J*. *Pharm*. *Sci*. *Res*., *8*, 756–758.

Nour, A.M., Khalid, S.A., Kaiser, M., Brun, R. *et al*. (2009). The antiprotozoal activity of sixteen asteraceae species native to Sudan and bioactivity-guided isolation of xanthanolides from Xanthuim brasilicum. *Planta Med*. *75*, 1363-1368.

Oyebode, O., Kandela, N.B., Chilton, P.J., Lilford, R.J. (2016). Use of traditional medicine in middle-income countries: a WHO-SAGE study. *Health Policy Plan 31*, 984-991.

Pavela, R., Maggi, F., Mbuntcha, H., Woguem, V. *et al*. (2016). Traditional herbal remedies and dietary spices from Cameroon as novel sources of larvicides against against filariasis mosquitoes? *Parasitol*. *Res*. *115*, 4617-4626.

Petrelli, R.; Orsomando, G.; Sorci, L.; Maggi, F. *et al*. (2016). Biological Activities of the Essential Oil from Erigeron floribundus. *Molecules 21*, 1065-1079.

Petrelli, R., Ranjbarian, F., Dall'Acqua, S., Papa, F. (2017). An overlooked horticultural crop, Smyrnium olusatrum, as a potential source of compounds effective against African trypanosomiasis. *Parasitol*. *Int*. *66*, 146-151.

Sawadogo, W.R., Schumacher, M., Teiten, M.-H., Dicato, M. *et al*., (2012) . Traditional West African pharmacopeia, plants and derived compounds for cancer therapy. *Biochem*. *Pharmacol*. *84*, 1225-1240.

Sun, Y.N., No, J.H.,Lee, G.Y., Li, W. *et al*. (2016). Phenolic constituents of medicinal plants with activity against Trypanosoma brucei. *Molecules 21*, 480.

Taber, D.F., Nelson, C.G. (2011). Aliphatic C-H to C-C Conversion: Synthesis of (-)-Cameroonan-7α-ol. *J*. *Org*. *Chem*. *76*, 1874–1882.

Tapanelli, S., Chianese, G., Lucantoni, L., Yerbanga, R.S. *et al*. (2016). Transmission blocking effects of Neem (*Azadirachta indica*) seed kernel limonoids on *Plasmodium berghei* early sporogonic development. *Fitoterapia 114*, 122-126.

Ukeh, D.A., Birkett, M.A., Pickett, J.A., Bowman, A.S. (2009). Repellent activity of alligator pepper, Aframomum melegueta, and ginger, Zingiber officinale, against the maize weevil, Sitophilus zeamais. *Phytochem*. *70*, 751-758.